CAPITAL UNIVERSITY OF SCIENCE AND TECHNOLOGY, ISLAMABAD

Pharmacogenomic Aspects of Inflammatory Biomarkers Inducing Brain Cancer-Glioma for Precision Cancer Medicine

by

Hina Ahsan

A dissertation submitted in partial fulfillment for the degree of Doctor of Philosophy

in the

Faculty of Health and Life Sciences
Department of Bioinformatics and Biosciences

2024

Pharmacogenomic Aspects of Inflammatory Biomarkers Inducing Brain Cancer-Glioma for Precision Cancer Medicine

By

Hina Ahsan

(DBS183002)

Dr. Mohammad S. Mubarak, Professor

Indiana University, Bloomington, USA

(Foreign Evaluator 1)

Dr. Zeliha Selamoğlu, Professor

Nidge Omer Halisdemir University, Türkiye

(Foreign Evaluator 2)

Dr. Shaukat Iqbal Malik

(Research Supervisor)

Dr. Syeda Marriam Bakhtiar

(Head, Department of Bioinformatics and Biosciences)

Dr. Sahar Fazal

(Dean, Faculty of Health and Life Sciences)

DEPARTMENT OF BIOINFORMATICS AND BIOSCIENCES

CAPITAL UNIVERSITY OF SCIENCE AND TECHNOLOGY

ISLAMABAD

2024

I dedicate this dissertation to my family, whose unconditional love, unwavering support, and endless encouragement have been my pillars of strength throughout this challenging journey. Their belief in me and sacrifices made have been the driving force behind my success. I am grateful for their patience, understanding, and constant motivation. This achievement is a testament to their unwavering faith in my abilities. I dedicate this work to them as a token of my deepest appreciation and love.

CAPITAL UNIVERSITY OF SCIENCE & TECHNOLOGY
ISLAMABAD
Expressway, Kahuta Road, Zone-V, Islamabad
Phone:+92-51-111-555-666 Fax: +92-51-4486705
Email: info@cust.edu.pk Website: https://www.cust.edu.pk

CERTIFICATE OF APPROVAL

This is to certify that the research work presented in the dissertation, entitled "**Pharmacogenomic Aspects of Inflammatory Biomarkers Inducing Brain Cancer-Glioma for Precision Cancer Medicine**" was conducted under the supervision of **Dr. Shaukat Iqbal Malik**. No part of this dissertation has been submitted anywhere else for any other degree. This dissertation is submitted to the **Department of Bioinformatics & Biosciences, Capital University of Science and Technology** in partial fulfillment of the requirements for the degree of Doctor in Philosophy in the field of **Management Sciences.** The open defence of the dissertation was conducted on **January 29, 2024**.

Student Name : Hina Ahsan (DBS183002)

The Examination Committee unanimously agrees to award PhD degree in the mentioned field.

Examination Committee :

(a) External Examiner 1: Dr. Tahir Ahmed Baig
Associate Professor
ASAB, NUST, Islamabad

(b) External Examiner 2: Dr. Abdul Rauf
Associate Professor
COMSATS University, Islamabad

(c) Internal Examiner : Dr. Syeda Marriam Bakhtiar
Associate Professor
CUST, Islamabad

Supervisor Name : Dr. Shaukat Iqbal Malik
Professor
CUST, Islamabad

Name of HoD : Dr. Syeda Marriam Bakhtiar
Associate Professor
CUST, Islamabad

Name of Dean : Dr. Sahar Fazal
Professor
CUST, Islamabad

AUTHOR'S DECLARATION

I, **Hina Ahsan** (Registration No. **DBS183002)**, hereby state that my dissertation titled, "**Pharmacogenomic Aspects of Inflammatory Biomarkers Inducing Brain Cancer-Glioma for Precision Cancer Medicine**" is my own work and has not been submitted previously by me for taking any degree from Capital University of Science and Technology, Islamabad or anywhere else in the country/ world.

At any time, if my statement is found to be incorrect even after my graduation, the University has the right to withdraw my PhD Degree.

(Hina Ahsan)

Dated: January, 2024

Registration No : DBS183002

29th Jan 2024

Hina Ahsan

PLAGIARISM UNDERTAKING

I solemnly declare that research work presented in the dissertation titled "**Pharmacogenomic Aspects of Inflammatory Biomarkers Inducing Brain Cancer-Glioma for Precision Cancer Medicine**" is solely my research work with no significant contribution from any other person. Small contribution/ help wherever taken has been duly acknowledged and that complete dissertation has been written by me.

I understand the zero-tolerance policy of the HEC and Capital University of Science and Technology towards plagiarism. Therefore, I as an author of the above titled dissertation declare that no portion of my dissertation has been plagiarized and any material used as reference is properly referred/ cited.

I undertake that if I am found guilty of any formal plagiarism in the above titled dissertation even after award of PhD Degree, the University reserves the right to withdraw/ revoke my PhD degree and that HEC and the University have the right to publish my name on the HEC/ University Website on which names of students are placed who submitted plagiarized dissertation.

(Hina Ahsan)

Dated: January, 2024

Registration No : DBS183002

29th Jan 2024

Hina Ahsan

List of Publications

It is certified that following publication(s) have been made out of the research work that has been carried out for this dissertation:-

1. H. Ahsan and S. I. Malik, "Ngs-Mutational analysis of driver genes and *TGFB1* with tumor suppressive and oncogenic roles in Glioblastoma: An integrated approach with Driver DBV3," genomics (PCGP), vol. 56, no. 04, 2023.
2. H. Ahsan, S. I. Malik, F. A. Shah, H. A. El-Serehy, A. Ullah, and Z. A. Shah, "Celecoxib Suppresses NF-κB p65 (RelA) and TNF*alpha* Expression Signaling in Glioblastoma," Journal of Clinical Medicine, vol. 12, no. 20, p. 6683, 2023..
3. H. Ahsan, M. Asghar, and S. I. Malik, "GCSF, A Diagnostic Marker and Potential Drug Target Candidate in Glioblastoma," 2023
4. H. Ahsan, H. Tanveer, S. I. Malik, "Unravelling Deregulated Signaling Pathways in Glioblastoma(GBM) for targeted Therapies", BICS Conf. CUST, Islamabad, Pakistan, 2023

(Hina Ahsan)

Registration No: DBS183002

Acknowledgement

In the name of Allah, the Most Gracious and the Most Merciful.

I am highly thankful to Almighty **ALLAH** whose bounteous blessing enabled me to complete this research project as well as to write this dissertation. He bestowed us with Holy Quran, which is guidance for the use of reverent, a cure to the diseases and blessing for the believers, and Prophet - **MUHAMMAD** (Peace be upon Him), the most perfect and the best among and of ever born on the surface of earth, who enlightens the hearts of believers in their life. I wish to acknowledge several key figures that contributed much to my research endeavor.

I would like to express my heartfelt gratitude to all those who have contributed to the successful completion of my PhD dissertation. This journey has been a significant milestone in my academic and personal growth, and I am deeply thankful for the support, guidance, and encouragement I have received throughout the process.

First and foremost, I am indebted to my supervisor, Professor Dr. Shaukat Iqbal Malik, for their invaluable mentorship, expertise, and unwavering support. Their guidance and insightful feedback have been instrumental in shaping my research direction, refining my methodology, and elevating the quality of my work. I am truly grateful for their dedication and belief in my potential.

I would like to extent my gratitude towards, Dr. Sahar Fazal. Professor/Dean Faculty of Health & Life Sciences and Dr. Muzaffar Abbas. Professor/Dean Faculty of Pharmacy, CUST, Capital University of Science and Technology, Dr Fawad Ali from Prince Sattam bin Abdul Aziz University Saudi Arabia. I am highly obliged for giving me the best of your assistance by supporting me always whenever I needed help. I have been very lucky for having cooperative lab fellows whose accommodative and friendly behavior made my work less laborious.

I am grateful to my colleagues and fellow researchers from Riphah International University, CEMB University of Punjab and Zhongjing Research and Industrialization Institute of Chinese Medicines China, for their camaraderie, stimulating discussions, and intellectual exchanges. Their support and encouragement have

created a conducive research environment, fostering collaboration and inspiring new ideas. I cherish the friendships and professional connections I have formed during my time as a PhD student.

I would like to acknowledge the funding agencies, foundations, or institutions that have provided financial support for my research. Their support has enabled me to pursue my studies with dedication and focus, and I am deeply grateful for the opportunities they have provided.

I am also indebted to the faculty members of Lund University Sweden, I would like to extend my gratitude towards Professor Muhammad Asghar for technical support and also introduce me in the MEMEG group under group head professor/-Head Staffen.Bensh for fruitful discussion on this project. I am grateful for their assistance and technical support throughout my research journey. Their prompt responses, resources, and services have facilitated the smooth progress of my work.

I am also very grateful to the Tertiary Care Hospitals, Neuro Oncology Departments Pakistan and their associated diagnostics Labs and radiology departments for execution of this project smoothly.

Lastly, I would like to express my heartfelt appreciation to my parents, my family, specially my husband Dr Ahsan ullah Kashif and my lovely kids Eshaal and Raahim and friends for their unwavering love, encouragement, and understanding. Their constant support and belief in my abilities have been a source of motivation and strength during challenging times.

In conclusion, this dissertation would not have been possible without the collective efforts and contributions of all those mentioned above. I am truly grateful for the guidance, support, and opportunities I have received, and I am excited to carry forward the knowledge and experiences gained during my PhD journey into future endeavors.

(Hina Ahsan)

Abstract

The most prevalent and aggressive subtype of intrinsic brain tumors in adults is high grade glioma also called glioblastoma (GBM), which presents a considerable barrier for pharmacological treatment. Even with improvements in surgery, chemotherapy, and radiation, the prognosis for GBM is still dismal, and with a poor survival rate. A thorough investigation employing genomic, transcriptomic, and epigenetic profiling was carried out to address this issue in order to comprehend the molecular pathways and uncover novel therapeutic approaches for GBM. A pharmacogenomics strategy was used in the current study to profile the distinct inflammatory gene expression and in vitro medication responsiveness in high-grade gliomas.In the study cohort over 70 glioma patients were selected and 55 of them were scrutinized on the basis of glioma grades .These patients were then divided into two groups(GFAP-Positive and GFAP-Negative) to explore the cellular and molecular diversity of these tumours. Genome-scale mRNA expression data from 55 studies were merged, including samples from "Tumour Associated Normal Tissue" (TANT) and GBM.

Chemokines, which are well-known for their involvement in several kinds of biological functions,pharmacological functions and pathological circumstances were investigated for their possible role in gliomagenesis. The study emphasised the importance of cytokines and chemotactic substances in the development, angiogenesis, and immune suppression of the both GFAP-Positive and GFAP-Negative glioma groups. In the current study, 11 inflammatory genes (IL-8, IL-1β, IL-6, IL-10, TNF-α, NF-κB p65 (RelA), TGFB1, IL1ra,GCSF,GCSFR and STAT3), have been revealed to stimulate angiogenesis and resist apoptosis in high grade gliomas.

Celecoxib's impact was also evaluated in terms of effectiveness by Inhibition of cellular growth, decreased the expression of TNFα and NF-κB p65 (RelA), and reduction in the viability of the human glioblastoma cell line SF-767 in a dose-dependent manner. The DriverDBV3 database was used to identify driver genes and TGFB1 mutations, highlighting the substantial transcriptional and genomic

heterogeneity of GBM with a focus on 20 clinically significant driver genes linked to several cellular pathways. The research also clarified how neutrophils and tumor-associated macrophages (TAMs) contribute to the development of an inflammatory and immunosuppressive state that is mediated by cytokines/chemokines. The results were verified using a thorough integrated analysis of transcriptome and proteomic profiling, which also involved retrieving information on the RNA sequences of Glioblastoma multiforme from databases maintained by Genome Atlas. Pathway enrichment analysis identified disease-related pathways,e.g, the activation of the JAK/STAT pathway, linked to the progression of GBM.

Additionally, GCSF was the target of "computational docking" investigation utilising the prospective therapeutic candidate Nisin, and the outcomes were validated by invitro analysis, using cytotoxic activity experiments in the human glioblastoma cell line SF-767. The thorough investigation showed that GCSF accelerates the development of gliomas, and their blockage by anticancer bacteriocin peptide Nisin may prevent glioblastoma growth and spread.

The multi-parametric methodology of the current study, which included genomic, transcriptomic, and longitudinal profiling of high-grade gliomas enabled the discovery of significant axis in GBM. The importance of inflammatory hub genes in the development of GBM was further emphasised by gene ontology analysis, database mining, and immunohistochemical confirmation. According to a survival analysis using TCGA GBM data, these strong differentially expressed genes have a significant impact on the prognosis of GBM.

In conclusion, an integrated personalised approach to the profiling of gliomas at various genetic and functional levels offers useful information for pharmacogenomic subgrouping of patients and the creation of tailored treatment plans. In order to identify therapeutic alternatives for particular glioma subpopulations, the study bridges the gap between genetics and functional characteristics.

Contents

List of Figures

List of Tables

Abbreviations

ACKR1	Atypical Chemokine Receptor 1
AGER	Advanced Glycosylation End-product specific Receptor
c-Met	A tyrosine kinase receptor which belongs to the MET (MNNG HOS transforming gene)
CAMLG	Calcium Modulating Ligand
CAR-T cells	Chimeric antigen receptor (CAR) T-cell
CBTRUS	Central Brain Tumor Registry of United States
CCL20	CC chemokine ligand 20
CCL2	C-C Motif Chemokine Ligand 2
CCLE	Cancer Cell Line Encyclopedia
CDKN2A	Cyclin-Dependent Kinase 2A
CDKN2B	Cyclin Dependent Kinase Inhibitor 2B
cDNA	complementary DNA
CDX-110	Celldex Therapeutics' brain cancer vaccine, rindopepimut
CHAC1	Cation Transport Regulator Homolog 1
ChEMBL	Chemical European Molecular Biology Laboratory
CNS	Central Nervous System
CNTNAP3B	Contactin Associated Protein Family Member 3B
COX-2	Cyclo-Oxygenase COX-2
CRP	C-Reactive Protein
CSF-1R	Colony Stimulating Factor 1 Receptor
CSF-1	Colony-Stimulating Factor-1
CTDSP2	Carboxy-terminal domain RNA polymerase II polypeptide A small phosphatase 2

CTLA-4	Cytotoxic T-Lymphocyte Associated Protein 4
CTLs	Cytotoxic T Lymphocytes
CT	Computerized Tomography
CUST	Capital University of Science and Technology
CXCL1	C-X-C motif ligand 1
CXCL2	C-X-C motif ligand 2
CXCL3	Chemokine (C-X-C motif) ligand 3
CXCL8	Interleukin 8, or CXCL8, (C-X-C motif) ligand 8
CXCR2	C-X-C Motif Chemokine Receptor 2
DC	Dendritic Cell
DEGs	Differentially Expressed Genes
DFS	Disease Free Survival
DNA	Deoxyribonucleic acid
dNTP	deoxynucleotide triphosphate
DTT	Dithiothreitol
ECM	Extracellular Matrix
EDN1	Endothelin 1
EGFR	Epidermal Growth Factor Receptor
ELANE	Elastase Neutrophil Expressed
ELISA	Enzyme-linked immunosorbent assay
ENHO gene	Energy Homeostasis Associated gene
FDA	Food and Drug Administration
FDR	False Discovery Rate
GAMs	Glioma-Associated Macrophages
GBM	Glioblastoma Multiforme
GCSFR	granulocyte colony-stimulating factor receptor
GCSF	Granulocyte Colony-Stimulating Factor
GEO-R2	Gene Expression Omnibus R2 package
GEO	Gene Expression Omnibus
GEPIA	Gene Expression Profiling Interactive Analysis
GFAP	Glial Fibrillary Acidic Protein
GNA14	G Protein Subunit Alpha 14

GNA15	G Protein Subunit Alpha 15
GSCs	Glioma Stem Cells
GSTM1	Glutathione S-Transferase M1
GTEX	The Genotype-Tissue Expression
GTF3C1	General Transcription Factor IIIC subunit1
HBEGF	Heparin Binding EGF Like Growth Factor
HGF	Hepatocyte Growth Factor
HNSCC	Head and Neck Squamous Cell Carcinoma
HR	Hazard Ratio
HSF1	Heat Shock Transcription Factor 1
H&E	Hematoxylin and Eosin
ICAM1	Intercellular Adhesion Molecule 1
ICIs	Immune Checkpoint Inhibitors
IDH1	Isocitrate dehydrogenase
IFN-γ	Interferon-gamma
IHC	Immunohistochemistry
IL-1β	Interleukin-1 β
IL-2R	IL-2/4 Receptor
IL-4R	IL-4 Receptor
IL-6	Interleukin-6
IL10	Interleukin-10
IL1Ra	Interleukin-1 receptor antagonist
IL8	Interleukin-8
iNOS	Inducible Nitric Oxide Synthase
IRRGs	Inflammatory Response-Related Genes
KEGG	Kyoto Encyclopedia of Genes and Genomes
LIF	LIF Interleukin 6 Family Cytokine (leukemia inhibitory factor)
LINCS	Library of Integrated Network-Based Cellular Signatures
LPS	Lipopolysaccharides
LRRC37A	Leucine Rich Repeat Containing 37A
MACROH2A1	MacroH2A.1 Histone

MAPKs	Mitogen-activated Protein Kinases
MCODE	Molecular Complex Detection
MCP	Monocyte Chemoattractant Protein
MDM2	Murine Double Minute 2 (Proto-Oncogene)
MDSCs	Myeloid-derived suppressor cells
MDS	Multi-Dimensional Scaling
MELK	Maternal Embryonic Leucine Zipper Kinase
MG/MDMs	Microglia/ Monocyte-Derived Macrophages
MGMT	O6-Methylguanine-DNA Methyltransferase
MHC	Major Histocompatibility Complex
MMP-2	Matrix metalloproteinase-2
MRI	Magnetic Resonance Imaging
MRS	Magnetic Resonance Spectroscopy
mTOR	Mammalian Target of Rapamycin
MTT	Mono-tetrazolium salt
NF-κB	Nuclear factor kappa B
NK	Natural killer cells
NO	Nitric Oxide
NPHP1	Nephrocystin 1
NSCLC	Non-Small Cell Lung Cancer
ODC	Ornithine Decarboxylase
OS9	Osteosarcoma amplified 9 gene
PCA	Principal Component Analysis
PCR	Polymerase Chain Reaction
PGt	Pharmacogenetic
PGx	Pharmacogenomics
PI3K	Phosphatidylinositol-3-kinase
PI3K	Phosphatidylinositol-3-kinase
PIK3CA	Phosphatidylinositol-4, 5-Bisphosphate 3-Kinase Catalytic Subunit Alpha
PIK3R1	Phosphoinositide-3-Kinase Regulatory Subunit 1
PK/PD	pharmacokinetic/pharmacodynamic

PLAUR	Plasminogen Activator Urokinase Receptor
POU2F2	POU Class 2 homeobox 2
PTEN	Phosphatase and tensin homolog
q-q plot	quantile-quantile plot
RARRES1	Retinoic acid receptor responder 1
RELA p-65	p65, is a REL-associated protein involved in NF-κB heterodimer formation nuclear translocation and activation
RHD	Rh Blood Group D
RHD	Rheumatic heart disease
RNase	Ribonucleases
RNA	Ribonucleic acid
ROC Curve	Receiver Operating Characteristics curve
ROS	Reactive Oxygen Species
SFTBP	Surfactant Protein B
SIRPB1	Signal Regulatory Protein Beta 1
SLC24A3	Sodium/potassium/calcium exchanger 3
SLC34A2	Solute Carrier Family 34 member 2
SNPs	Single nucleotide polymorphisms
STAT3	Signal transducer and activator of transcription 3
SVD	Singular Value Decomposition
t-SNE	t-distributed stochastic neighbor embedding
TAMs	Tumor-Associated Macrophages
TANT	Tumor Associated Normal Tissue
TCGA	The Cancer Genome Atlas
TGF β	Transforming Growth Factor-β
TLRs	Toll-like receptors
TME	Tumor Microenvironment
TMZ	Temozolomide
TNF-α	Tumor Necrosis Factor Alpha
TNFAIP6	TNF alpha induced protein 6
TP53	Tumor Protein P53
Tregs	Regulatory T cells

UGT2B17	Uridine di phospho glucuronosyl transferase protein Family 2 Member B17
UMAP	Uniform Manifold Approximation and Projection
VEGF	Vascular Endothelial Growth Factor
VEGF	Vascular Endothelial Growth Factor
WHO	World Health Organization
ZBTB42	Zinc Finger and BTB Domain Containing 42

Symbols

β	Beta
α	Alpha
κ	Kappa
γ	Gamma
ϵ	Epsilon
μ	Mu
λ	Lambda

Chapter 1

Introduction

1.1 Study Background

Cancer describes a group of diseases categorized by abnormal and uncontrollable cell proliferation that has the potential to infiltrate or spread to other parts of the body. It creates a multi-step process that leads to the accumulation of numerous genetic changes [1]. In 2016, approximately 7,046 neuro neoplasms were registered with 459 benign and 6,587 malignant cancers. Around 19.3 million new cancer cases and more than 10 million cancer deaths have been reported in 2020 [2]. According to Pakistan Health Research Council, more than 148,000 new cancer cases are reported each year, and over 100,000 people die from cancer. In Pakistan, brain cancers account for only 2% of all cancer-related deaths [3].

Brain cancers encompass more than a hundred histological sub-groups [4, 5]. Most prevalent brain tumors are gliomas, pituitary adenomas, medulloblastomas, meningiomas ependymomas, schwannomas and central nervous system (CNS) lymphomas. Among them, the most common CNS tumor is glioma, which accounts for 33 percent of all brain tumors [6]. The most prevalent and deadliest brain cancers are the malignant gliomas which originated in the glial cells such as Astrocytes, Oligodendrocytes, and Ependymal cells. These cells regulate and maintain neurons in the brain. Glioma is the most prevalent primary brain cancer with

a pathophysiology that is mostly unclear, while complex genetic anomalies are considered to play role in disease progression.

The diagnosis of CNS tumors has been improved by the 2016 World Health Organization (WHO) classification system that uses molecular information [7]. This system differentiates Low Grade and High Grade glioma subcategories based on if they have mutations in Isocitrate -Dehydrogenase 1 (IDH-1) and the co-deletion of chromosome arms 1p and 19q [8]. However, there is still variability within these subtypes and within each tumor, with different cell populations that have diverse mutations and expression profiles, their malignancy behavior might gets influenced [9]. The detection of more molecular markers of these cell populations could increase the diagnostic precision.

However, there is still variability within these subtypes and within each tumor, with different cell populations that have diverse mutations and expression profiles, their malignancy behavior might gets influenced. The detection of more molecular markers of these cell populations could increase the diagnostic precision. The standards of life of glioma sufferers are influenced by sign and symptoms such as endocrinopathy, edema, fatigue, convulsions, and psychiatric illnesses. According to the National Comprehensive Cancer Network Clinical Practice Guidelines version 3 [10, 11]. The current recommended course of standard treatment for malignant gliomas consists of adjuvant temozolomide chemotherapy, radiation, and maximum surgical resection. The main procedure for surgical guidance is CT/MRI (Computed Tomography/Magnetic Resonance Imaging) (CT/MRI). The diagnosis also depends on the histopathologic and molecular/genetic analysis of gliomas. In South Asian region, Pakistan has the highest incidence of all kinds of gliomas [12]. Previous literature has reported with a median survival time of approximately 11 months, 9% of glioma patients with 2-year survival rate, and no survivors at 3 years in a previous phase I/II trial, glioblastoma (GBM) has emerged as the most common and malignant Grade- IV Astrocytoma, accounting for 14.5% of all central nervous system tumors [13].

Dehydrogenase (IDH) mutations and 1p/19q codeletion are two modern genetic markers that have been used for molecular pathological diagnosis, clinical care,

and prognosis evaluation [14, 15]. Despite the efforts of numerous researchers, only few therapeutic techniques have been evolved which target these markers [16]. Therefore, there is a need to discover new biomarkers which can effectively predict clinical prognosis, therapeutic responses, enhanced sensitivity, precision and reduced costs for glioma, especially glioblastoma (GBM). Recent research has highlighted the critical role of the host inflammatory response in cancer development and prognostics [17]. One of the characteristics of cancer has been associated with inflammation. Tumor progression, angiogenesis, and metastasis are all correlated with inflammation [18, 19]. According to estimates, 15 - 20% of all cancer-related deaths occur as a result of infections or inflammatory reactions [20]. The ongoing, uncontrolled localised and systemic inflammatory responses brought by tissue destruction may have a role in the onset and progression of cancer [21]. Sufficient literature evidence suggests the linkage of Inflammation and cancer pathogenesis, and these studies demonstrate that Immune Cell, specifically those involved in innate immune responses, influenced significantly in the progression of numerous cancer malignancies [22, 23]. Sufficient literature evidence suggests the linkage of Inflammation and cancer pathogenesis, and these studies demonstrate that Immune Cell, specifically those involved in innate immune responses, influenced significantly in the progression of numerous cancer malignancies. In fact, inflammation occurs even before a tumor's malignancy can be detected, resulting in the development of the microenvironment that makes it easier for precancerous lesions to progress towards cancer [24, 25].

The interaction between inflammatory mediators and the tumor micro-environment with their morphological changes has been recognized as a driver of oncogenesis. [26]. Additionally, earlier research suggests that inflammation, which is caused by the cytokine production and an abundance of ROS (Reactive Oxygen Species), can promote the development of higher malignancy by boosting the activities of the adjacent malignant cells [27, 28]. According to Mostofa et al.'s findings, the development of gliomas is strongly correlated with a number of inflammatory mediators, including cytokines, cyclooxygenases, STAT3, NF-κB, and oxidative stress [29].

Glial cell activation, production of inflammatory chemicals and, increased BBB (Blood- Brain Barrier) permeability with associated hallmark of tumor growth contribute towards the invasion of the brain by peripheral immune cells [30]. Microglia are the CNS resident immune cells which initiate process of neuro inflammation [31].

Gliomas associated microglial cells in tumor microenvironment can have at least two sources, i.e., blood-borne macrophages and intrinsic to Brain parenchyma. Macrophage accumulation in brain tumor is facilitated by localized production of chemo-attractants such as Glioma Associated Microglia/Macrophages (GAMs) along with different mediators. Such mediate an essential part in glioma proliferative growth, invasion, and resistance to therapy. Microglia and astrocytes response to neuronal injury is modulated by variation in mediator's expression, alterations in morphological features, and subcellular elements and phagocytosis of cells [32]. Therefore, such changes mark the CNS tissue response to neuro degeneration and damage which results microglial cell activation by producing cytokines, such as interleukin-10 IL-10 (Interleukin-10), IL-1 β (Interleukin-1 β), IL-6(IInterleukin-6), TGF-β (Transforming growth factor) and tumor necrosis factor alpha TNF-α(Tumor necrosis factor alpha).The malignant progression of several cancer types is significantly influenced by inflammatory cytokines [33, 34]. Interleukin (IL1, IL6, and IL8, pro-inflammatory cytokines, are produced and secreted at high levels in human glioblastoma, and the levels of expression are associated with the histopathological grade of the tumors [35, 36]. A mouse model has demonstrated the crucial role that IL-6 plays in the growth of gliomas [37]. An immunosuppressive cytokine called (TGF-β), (Transforming Growth Factor β) which is likewise highly enhanced in High Grade Gliomas, is correlated with an adverse prognosis in the patients of brain cancer e.g. Glioma [38]. According to certain theories, inflammatory cytokines increase tumor invasion, metastasis, angiogenesis, and immune evasion, all of these are contributing factors in tumor malignancy [39, 40].

These cytokines support processes that are essential for the development and spread of cancer, including long-term proliferation, cell migration, apoptosis suppression, and differentiation of tumor cells. It is widely known that the IL-6-STAT3

signaling pathway, along with other inflammatory cytokines such IL1 β, TNF α and IL-23, has been associated with in the progression of cancer in many tumor types, including glioblastoma, which contributes to tumor resistance and recurrence of glioblastoma [41]. Glioblastoma has a high rate of STAT3 activation [42]. The use of "RNAi knockdowns" and "STAT3 inhibitors" has demonstrated that they promotes tumorigenesis in glioblastoma by inhibiting apoptosis[43]. Additionally, it has been noted that when compared to primary glioblastoma, recurrent glioblastoma tumors have higher levels of phosphorylated STAT3 [42]. Furthermore, worse rates of recurrence-free survival and total patient survival were associated with tumors that showed increased nuclear localization of STAT3.

Furthermore, associations between tumor cells and microglia are bi-directional; under the influence of glioma, microglia release various types of molecules that instigate glioma growth, progression, and stimulation of inflammatory cascades. Certainly , Astrocytoma Cells produces the microglia chemo attractant including CSF-1 (colony-stimulating factor-1), G-CSF (granulocyte colony-stimulating factor) and microglia possess the corresponding receptors [44]. Regarding glioma, an elevated expression of inflammatory biomarkers (IL1β, IL6, IL10, IL8, IL1Ra, TGFβ1, TNFα, NF-κB, GCSF, GCSFR, STAT3) has been associated with shorter lifespan in GBM patients participated in 2 Cohort studies. Current research, however, mainly focused on the crucial function of these markers in predicting patient survival and gauging the prognostics of GBM. The diagnostic use of these markers in gliomas and Glioblastoma Multiforme (GBMs) has not been well-established. However, prior research indicates that little is known regarding the associations between IRRGs (Inflammatory Response-Related Genes) and the prognoses of glioma patients.

For many years, intermediate filament proteins have been proved helpful in the diagnosis of tumor due to their tissue- and cell-specific expressions [45]. In 1971, the 50 kDa type III intermediate filament called as GFAP (Glial Fibrillary Acidic Protein) was determined and identified after the dissociation of filaments from fibrous astrocytes. The first reports of elevated GFAP expression in glioblastoma with astrocytoma characteristics appeared a year later, and more reports appeared

after that. GFAP was established as a biomarker for astrocytoma and has a continous in use as a result of numerous research characterizing GFAP expression in glioma subtypes [46]. The first reports of elevated GFAP expression in glioblastoma with astrocytoma characteristics appeared a year. later, and more reports appeared after that. GFAP was established as a biomarker for astrocytoma and has a continous in use as a result of numerous research characterizing GFAP expression in glioma subtypes GFAP is mostly expressed in mature astrocytes in the healthy-state of human brain . Therefore, it is observed that high GFAP expression identifies in more "Differentiated Less Malignant Tumors" measured at clinical as well as in basic experimental conditions. But more recently, in the developing "human brain's radial glia" , "the adult brain's neural stem cells", and the other "Non-Differentiated and Immature central nervous system cells", it has been observed that GFAP is expressed [47]. Since then, GFAP has frequently been utilized to identify glioma cells with stem cell traits and targeting the neural stem cells in order to cause gliomagenesis in animal models [46, 48]. In addition, Non-Neoplastic Astrocytes that, in response, become reactive to tumor growth and do not depict the differentiated state of neoplastic cells have increased GFAP expression [49, 50].

However, High GFAP levels in tumor tissues are not always the direct indicator of a less aggressive and more distinct astrocytoma subtype. According to our most recent research, which assessed the expression of various GFAP isoforms, higher levels of the alternative Splice Variant of GFAP compared to the Canonical Variant of GFAP which are linked to a higher malignant and less differentiated astrocytoma subtype [51, 52]. Inflammatory biomarkers have been demonstrated in the current study to enhance patient classification for treatment and predict survival in brain cancer. The objective of the present study was to describe variations in inflammatory marker expression levels among glioma patients; patients with other grades of glioma, such as grade III and grade IV, to determine the significance and worth of these genes' expression in the diagnosis and prognosis of glioma, with a focus on GBM diagnosis. Pharmacogenomics studies show gene variants impact on the PK/PD of medications. This includes gene polymorphisms that affect drug pharmacology or side effects as well as absorption, distribution, metabolism, and

excretion processes [53]. Clinical precision medicine is significantly influenced by pharmacogenomics, which also helps to foretell therapeutic efficacy and toxicity.

Personalized cancer treatments that use profiling to discover druggable targets are intended to replace inefficient chemotherapy in genomics-driven oncology. Using high-throughput drug screening, this kind of precise medicine connects unique phenotypic characteristics to cell response. Enormous-scale bioinformatics data repositories have been created recently to store the transcriptome reactions to environmental and genetic perturbations as well as disease markers. These databases, including the LINCS (Library of Integrated Network-Based Cellular Signature), CCLE (Cancer Cell Line Encyclopaedia), and ChEMBL (Chemical European Molecular Biology Laboratory), have enabled new computational techniques for drug repositioning by correlating disease signature, Drug Induced expression of gene changes, and cellular response [54]. Traditional treatment only slightly improves survival [55]. Researchers are looking for FDA-approved pharmaceuticals that can be employed as chemotherapy medications due to the growing need for potent anticancer medications [56].

Drug re-purposing, also referred to as drug re-discovery, repositioning of drugs, re-profiling of drugs, and other names [57], is an intriguing approach to managing the re-use of drugs with established formulas, clinical trials, toxicity, post-marketing surveillance safety data, and pharmacokinetics that offer expanded potential for usage. Clinical data and RNA-sequencing data were gathered from open-access databases in order to investigate and characterize the integrated roles of inflammatory genes in glioma. The Gene Expression Omnibus (GEO) database was used to identify genes that were deferentially expressed in normal and glioma tissues. Next, we used information from the TCGA (The Cancer Genome Atlas) to create a predictive signature to forecast clinical outcomes of glioma. Using the GTEX database, the performance of the signature was further verified. Additional analyses included clinical correlation, immunological infiltrates, immunotherapeutic response prediction, and pathway enrichment. In conclusion, we devised a prognostic signature for predicting outcomes in gliomas, and the findings may provide a reliable basis for prognostic assessment and the development of specialized targeted

therapy approaches. In this research, we recommended NISIN as a potential anti-cancer medication for the treatment of glioblastoma include Bacteriocin. In order to propose an eventual benchmark for personalize precision medicine in clinical practice, Pharmacogenomic studies have been conducted in gliomas to demonstrate the effectiveness of temozolomide and celecoxib in chemotherapy due to changes in the expression of inflammatory genes and stimulation of inflammatory cascades.

In conclusion, we devised a prognostic signature for predicting outcomes in gliomas, and the findings may provide a reliable basis for prognostic assessment and the development of specialized targeted therapy approaches. In this research, we recommended NISIN as a potential anticancer medication for the treatment of glioblastoma include Bacteriocin. In order to propose an eventual benchmark for personalize precision medicine in clinical practice, Pharmacogenomic studies have been conducted in gliomas to demonstrate the effectiveness of temozolomide and celecoxib in chemotherapy due to changes in the expression of inflammatory genes and stimulation of inflammatory cascades.

1.2 Gap Analysis

To date, information on the management of brain tumors, such as glioma, in Pakistan remains unexplored, scattered and scarce. It's unfortunate that there is no centralized unified cancer registry and research repository at National level [58, 59], though some of the well reputed institutes maintain cancer data independently [60]. As a result, we lack the data regarding glioma prevalence, its contributing biomarkers involved in disease progression and drug resistance.

Primary studies on glioma incidence and expression studies of inflammatory biomarkers, Interleukin-8, Interleukin-6, Interleukin-10, interleukin-1β, interleukin 1 receptor antagonist, transforming growth factor-β and tumor necrosis factor-α, NF-κB, TNF-α ,GCSF, GCSFR and STAT3 have not been previously conducted in Pakistan at molecular level. Therefore, keeping this in view, there is a challenging need

to better understand the functions and contextual interactions of genetic changes caused by inflammation-induced glioma, as well as to expand the knowledge of oncological precision medicine by using new potential glioma-specific anticancer peptides and bacteriocins instead of conventional chemotherapies to alleviate the adverse effects [61].

1.3 Research Objectives of the Study

In this study, the following core issues has been addressed.

1. To identify the expression of inflammatory biomarkers of glioma in Pakistani population.
   (a) To identify the expression of inflammatory biomarkers (IL-1β, IL-6, IL-8, IL-10, TGF-β, TNF-α, NF-κB and sIL-1Ra) of GFAP positive glioma cases.
   (b) To identify the expression of inflammatory biomarkers (GCSF, GCSFR and STAT3) of GFAP negative glioma cases.
2. To map identified inflammatory gene-expression signatures from Pakistani population with global gene expression signature associated with glioma for optimized precision therapy to prioritize the drug targets.
3. To determine the mutation of significant inflammatory biomarker in glioma.
4. To identify potential anti-cancer peptides or Bacteriocin based drug targets by using an in-silico approach for effective response to personalized drug therapy.

1.4 Significance of the Study

Large-scale gene expression investigation on gliomas of all histological kinds to examine their inflammatory gene expression-based classification can predict Survival

and drug treatment response. This study also intricately highlighted previously undiscovered tumor heterogeneity and identified prognosis-related gene expression differences.

Patients with malignant gliomas have a dismal prognosis despite extensive treatment with chemotherapy, radiotherapy and surgery. Major breakthrough in the molecular genetic assessment of brain tumors, particularly gliomas, have resulted in the identification of various molecular markers that play a vital part in the genesis and malignant transformation of gliomas.

Some of these indicators have been proven to be extremely helpful in histological diagnosis and to forecast survival and therapeutic response. This study identified novel molecular and cellular targets for cancer personalized therapies, paving the way for an Individual-Based Healthcare system delivering improved treatment outcomes with minimal toxicity. Exploring the interaction among inflammatory genes and their associated proteins may help us make more accurate risk assessments and discover biologic targets for therapies to make cancer treatment more bearable for glioma patients.

1.5 Problem Statement

The lack of functional characterization data in glioma pharmacogenomics association research limits our capacity to fully harness a patient's pharmacogenomics information through genotype-guided medication. The functional interpretation of pharmacogenomics complexity could be improved with the use of new experimental and computational methodologies. Understanding tumor molecular characteristics in the form of biomarkers and proving their relationship with drug results will be crucial for diagnosis and tailored treatment. The lack of efficacy and toxicity profile of therapeutic drugs are two main challenges in to improving cancer patient survival and quality of life.

Most anticancer medications only respond in a minority of cases and have a narrow therapeutic index, which frequently result in severe side effects and even death.

Therefore, novel therapeutic approaches that can increase cure rates while minimizing the adverse reactions are urgently required. So far, a glioma inflammatory genes specific profiling has not been done in Pakistani population, which is very crucial step to monitor disease progression, recommend personalized therapy and to develop inflammatory biomarker specific drug targets.

1.6 Research Question

RQ1: Which inflammatory biomarkers are responsible for glioma in Pakistani population?

In this study 11 most prevalent inflammatory biomarkers (IL-1β, IL-6, IL-8, IL-10, TGF-β, TNF-α, NF-κB and sIL-1Ra, GCSF, GCSFR and STAT3) were identified by different aspects in Pakistani population that could be used to determine disease severity and progression, to facilitate histopathological classification of gliomas and personalized therapy.

RQ2: Is there identified inflammatory gene expression signature in Pakistani population similar to globally identified inflammatory gene expression signature responsible for glioma?

The comparison of global inflammatory gene expression profile with context to Pakistani patients' expression profile have been done by analyzing globally available datasets of glioma cases form Cancer repository databases. As a result, high target areas to develop biomarker specific drug had been identified.

RQ3: What are the molecular events (mutations) associated with glioma?

This question had been addressed by the In-silico identification of the mutations associated with the inflammatory biomarker of glioma in globally available glioma datasets with the integration of advanced bioinformatics tools.

RQ4: What are the Pharmacogenomic aspects of prioritized inflammatory biomarkers based on expression due to drug action by integration of In-silico drug docking of potential anti-cancer peptides or Bacteriocin?

This question has been addressed by the potential identification of anti-cancer peptide/Bacteriocin NISIN and exhibited docking with anti-inflammatory biomarker GCSF to block the inflammatory signaling pathway through in silico studies. And also validated by MTT cytotoxicity assay on SF-767 Human Glioblastoma Cell line.

Chapter 2

Literature Review

2.1 Cancer

Cancer is a term that refers to a collection of diseases that are marked by aberrant cell growth and a lack of control over cell proliferation. The formation of a tumor, or neoplasm, often characterizes these diseases. These tumors can either be benign or malignant in nature. While benign tumors do not metastasize or spread to other region of the body, malignant tumors can spread through local, lymphatic, or hematogenous routes. A malignant neoplasm that possesses the ability to metastasize is referred to as cancer. Hanahan and Weinberg (2000) proposed six key abnormalities in cellular physiology which might underpin malignancy development that include growth signals that are self-sustaining, non-responsiveness to anti-growth signals, eluding programmed cell death (apoptosis), dysregulated replication opulent vascularity (angiogenesis) and robust metastatic and tissue invasion as shown in (Figure 2.1) [62]. The biological process by which normally dividing cells develop into cancer has been the subject of extensive research in the biomedical sciences for decades [63]. Although very precise procedures support tumorigenesis, wide variety of general causes, including radiation, chemicals, toxins, bacteria/ viruses, inflammation, and so forth, can triggering the phenomenon.

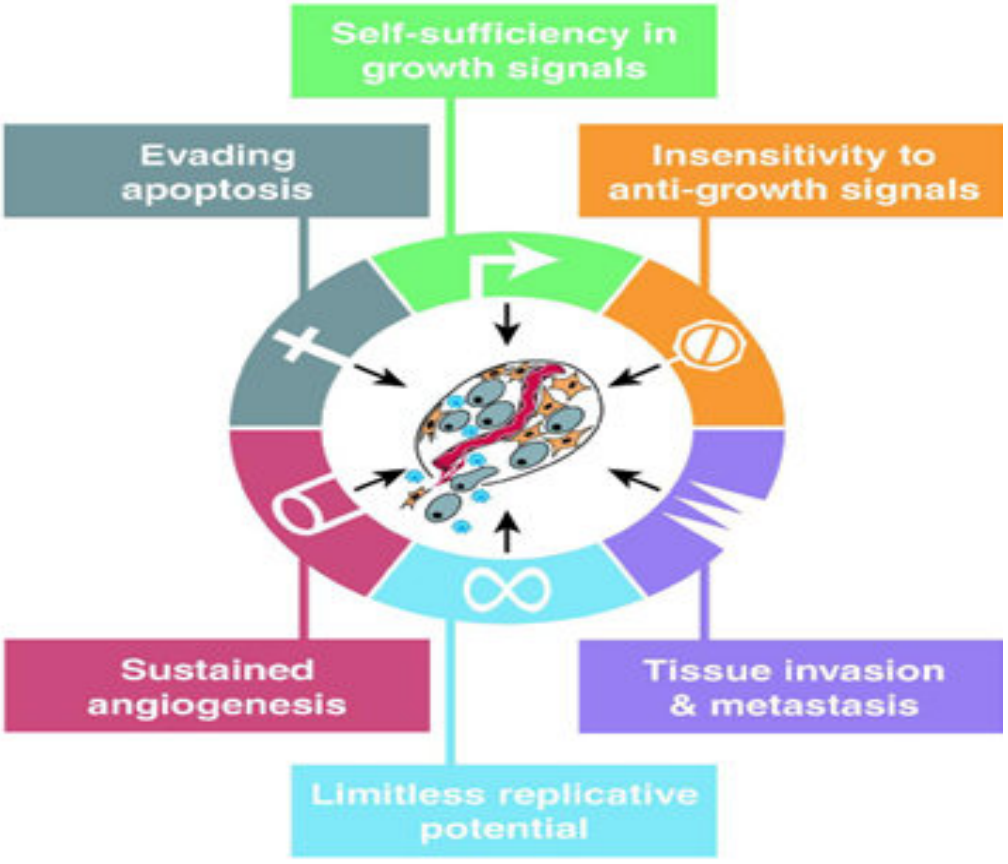

FIGURE 2.1: Hallmarks of cancer [64]

2.1.1 Global Occurrence of Cancer

Cancer is the major contributing cause of mortality and a crucial barrier in extending life expectancy worldwide. According to World Health Organization (WHO), malignant tumor is either first or second leading cause of death under 70 years age in 112 out of 183 nations and remain third or fourth in another 23 countries [2, 65]. Distribution and prevalence of major cancer risk factors directly related to social and economical developments and pose global cancer incidences burden and mortality resulting from population growth and ageing. There has been reported 2-3 fold greater incidence of all types of cancers in developing countries as compared to developed ones. Globocan has also explained the incidence and mortality of different cancers in both genders (Figure 2.2). In 2040 due to demographic shift the worldwide cancer burden is anticipated to riseup to 28.4 million cases which would be 47% high from 2020 [2, 66].

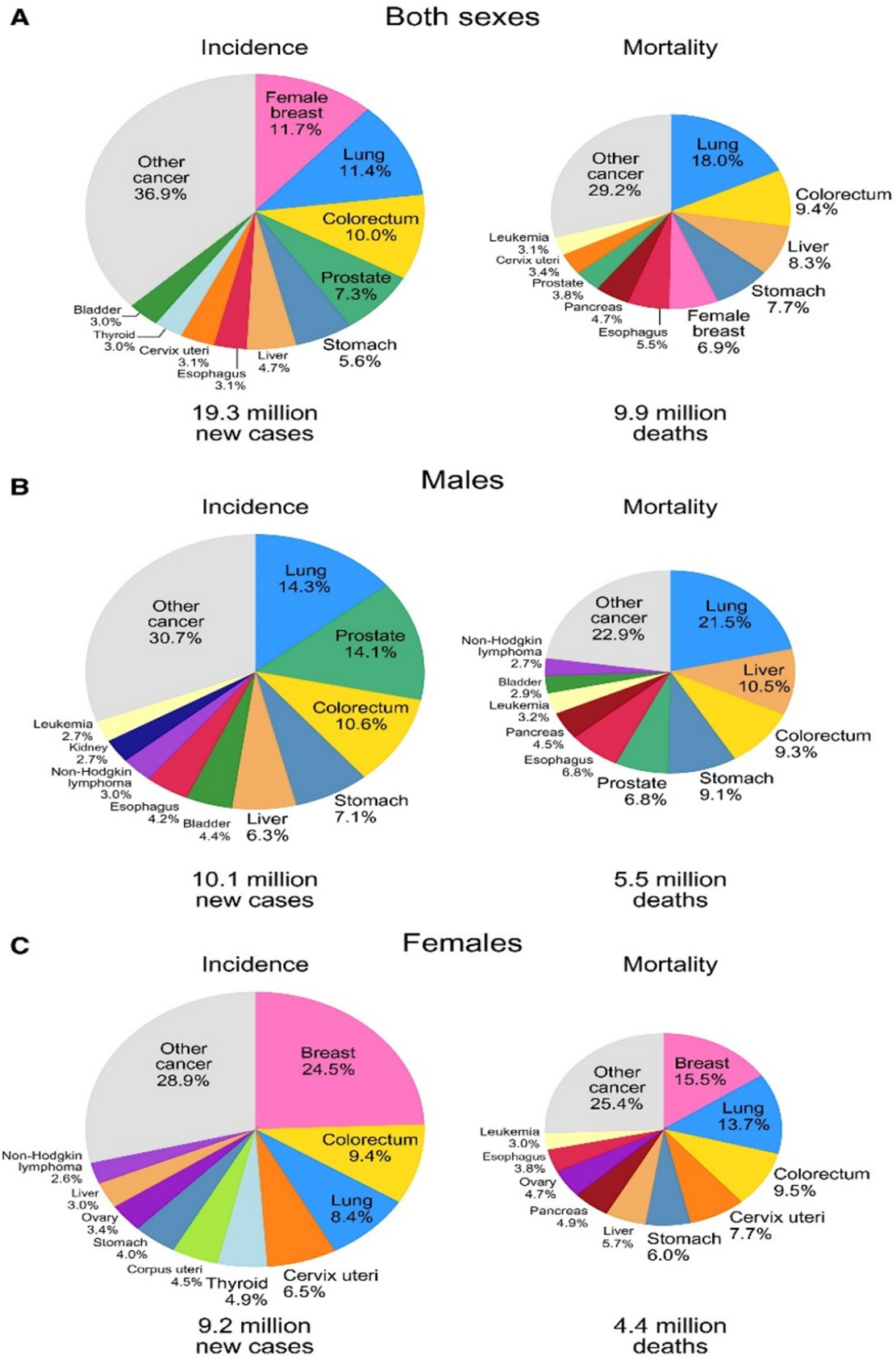

FIGURE 2.2: Top 10 Cancer statistics 2020 by GLOBOCAN [67]

2.2 Brain Cancers

"Brain cancers" differ from other neoplasms, the other brain tumors have constraints of the closed cranial vault, having comparatively limited fatal tumor load, and the failure of metastasis. Brain cancers are the second most prevalent ones in children under the age of 15, after leukemia in terms of occurrence. Intracranial tumors have no known cause, and only a few occurrences of relatively uncommon forms like acoustic neurinoma and neuro fibroma appear to be genetically inherited. Brain cancers are the second most prevalent ones in children under the age of 15, after leukemia in terms of occurrence. Intracranial tumors have no known cause, and only a few occurrences of relatively uncommon forms like acoustic neurinoma and neuro fibroma appear to be genetically inherited. The incidence of brain metastases from a primary tumor in other parts of the body is comparatively limited [68].

Primary and metastatic malignant brain tumors have a high morbidity and a low survival rate for patients. These tumors require complex and multidisciplinary care. WHO classifies primary brain cancer into more than distinct categories based on phenotypic, molecular, and histological characteristics [68]. The Central Brain Tumor Registry of the United States (CBTRUS), which provides the largest population-based data on brain tumors, reported that approximately 70% of initial brain tumors lack cancers. [69]. Among malignant primary brain tumors, gliomas are the most prevalent (80%), followed by other less common subtypes (19%) such as Ependymomas, Schwannomas, Medulloblastomas, Central Nervous System Lymphomas, and Meningiomas. The molecular characterization of primary brain tumors has enabled the development of more targeted therapeutic approaches based on molecular phenotypes [70]. However, the mortality rate from CNS cancers has increased significantly [71]. In 2018, there were 296,851 new cases of brain cancer worldwide, representing 1.6% of all cancer diagnoses [72] . The 5-year survival rate for patients with primary brain tumor depends on the grade and molecular profile of the tumor. While low-grade brain tumors have a 5-year survival rate of more than 90%, high-grade tumors have a very poor prognosis with

less than 5% survival rate [73]. The average overall survival rate for all malignant brain tumors is 36% [74].

2.3 Gliomas and its Classification

Gliomas, the most frequent primary tumors of the spinal cord and brain, exhibit a histological resemblance to normal glial cells and are named accordingly. However, their exact cellular origin remains elusive and could potentially arise from glial or neural precursors, normal glial cells, stem cell, or other types of cells. The traditional diagnostic and classification criteria for gliomas rely on histopathological testing, with the 2007 World Health Organization (WHO) classification categorizing them into several subtypes, including Oligodendroglial tumors, Astrocytic tumors, Ependymal tumors, Oligoastrocytic tumors, Neuronal and mixed Neuronal-Glial tumors including Ganglio-Glioma. This classification encompassed well-defined grade I tumors, forexample Pleomorphic Xanthoastrocytoma, Pilocytic Astrocytomas and Subependymal Giant Cell Astrocytomas, as well as the more commonly observed infiltrating gliomas, including grade II Oligodendrogliomas and Astrocytomas, grade III Anaplastic Oligodendrogliomas, Anaplastic Astrocytomas, Anaplastic Oligoastrocytomas, Anaplastic Ependymomas, and grade IV GBMs [75]. Over the past few decades, extensive study into the biology of gliomas has led to the identification of several critical genetic and molecular mechanisms underlying these tumors. Glioblastoma multiforme and astrocytomas are the most frequent type of brain cancers, while less than 2% of patients have ependymomas and oligodendrogliomas, or medulloblastomas, which could be a separate biologic entity altogether [76]. There is emerging evidence that some viruses, smoking, alcohol usage, drug addiction, or dietary consumption of N-nitroso compounds,and also the use of high frequency radiations, are linked with the initiation of glioma involving inflammation [77]. Gliomas are a clinically, histologically, and genetically diverse category of brain cancers encompassing 80% of cases and 17,000 new ones identified each year [78]. The condition is most common in people between the age of sixty to eighty years of their life span , and

the number of glioma patients is projected to increase as the population ages [79] . Patients with malignant gliomas have a median survival time of fewer then six months; after a year, about 20% of patients are surviving, and after two years, less than 10% are surviving [80].

2.3.1 Astrocytic Tumors

Astrocytic tumors, which originate from glial cells with a star-shaped morphology that perform vital supportive functions for neuronal cells, are the most prevalent types of brain tumors. Glioblastoma, accounting for 34 percent of malignant tumors of the CNS (Central Nervous System), is the more prevalent subtype. Astrocytomas are classified into two groups based on their infiltration patterns. The first group comprises pilocytic astrocytoma, Pleomorphic Xanthoastrocytoma,and subependymal giant cell Astrocytoma) which display a well-defined narrow zone of infiltration. The second group includes low-grade Astrocytomas, Anaplastic Astrocytoma, and Glioblastoma and they have an infiltration zone that is more dispersed. These groups exhibit differences in cellularity, cellular heterogeneity, neovascularization degree, and necrosis presence.

2.3.2 Diffuse Astrocytoma

Diffuse astrocytoma, classified as a grade II tumor by the World Health Organization, is a slow-growing tumor that tends to progress to a more aggressive form, ultimately leading to a fatal outcome. The incidence of astrocytomas is comparable between the genders, and histological analysis reveals that they are hypercellular, with limited pleomorphism, and do not demonstrate mitotic activity. No microvascular growth or necrosis is seen, and the tumor margins are typically ill-defined, with numerous perineuronal satellitosis observations. The median survival rate of patients with diffuse astrocytoma ranges from two to ten (2 - 10) years [81].

2.3.3 Anaplastic-Astrocytoma

Anaplastic Astrocytomas are malignant gliomas classified as grade III tumors by the World Health Organization. These tumors have a strong proliferative capacity and are diffusely infiltrated with localized or distributed patches of anaplasia. Nuclear atypia, hypercellularity, cellular pleomorphism, and microvascular proliferation are frequently seen in anaplastic astrocytomas. The median survival time for patients with anaplastic astrocytoma ranges between 2 and 3 years, which is affected by the time duration for tumor progression to grade IV. With a median age of 41 at diagnosis, the most affected age range is between 40 and 50. The genetic processes involved in the emergence of primary and secondary glioblastomas are depicted in Figure 2.3.

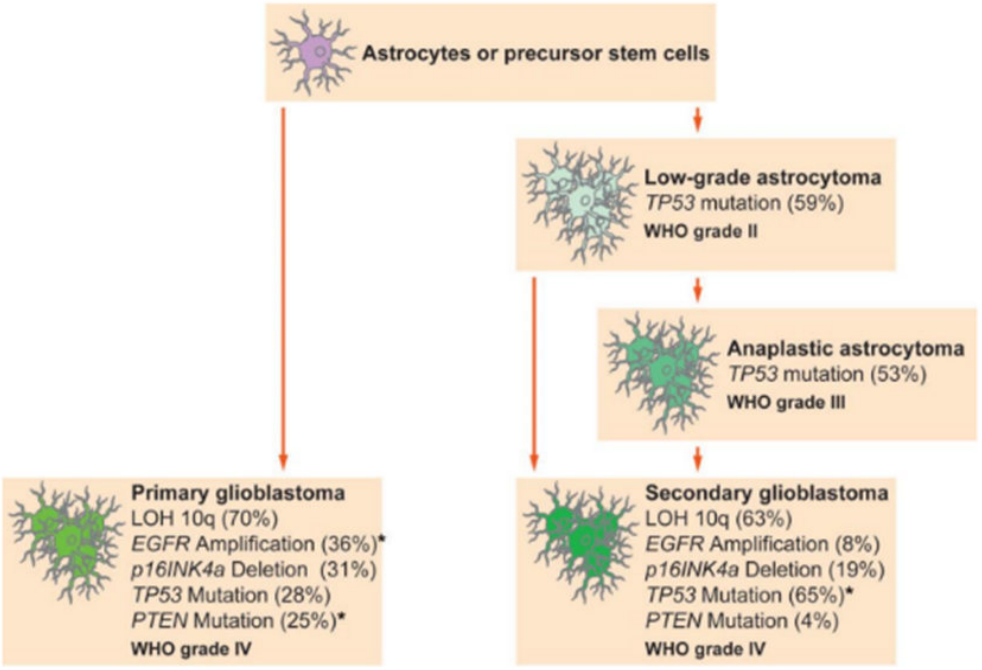

FIGURE 2.3: Glioblastoma genetic pathways are depicted in a flowchart [82]

2.3.4 Glioblastoma Multiform (GBM)

The incidence rate of GBM, a primary brain tumor that is both frequent and deadly, is estimated to be 4-5 new cases per 100,000 population per year [83]. This disease has a poor prognosis, with patients surviving for an average of only

12 months after diagnosis. Although GBM can affect individuals of any age, it is more commonly observed in adults. Due to its highly infiltrative nature, GBM is categorized as a WHO grade IV tumor and is generally found in supratentorial regions with diffuse brain parenchyma infiltration. Prognosis for patients with GBM is poor, with age being a significant prognostic factor. The patients under the age of 50 at the time of diagnosis generally have a favorable prognosis [84].

2.3.5 Oligoastrocytomas

Oligoastrocytomas are tumors that are composed of varying proportions of astrocytes and oligodendrocytes. These tumors were previously diagnosed based on the presence of 25% of any single cell type; however, the current definition includes any mixture of astrocytoma and oligodendroglioma cells. Like oligodendrogliomas and astrocytomas, oligoastrocytomas are divided into low-grade and high-grade (anaplastic) variants based on the, mitotic activity, the degree of cellularity, microvascular proliferation, and necrosis [85].

2.3.5.1 Anaplastic Oligoastrocytomas

Anaplastic oligoastrocytomas are similar to their low-grade counterparts in terms of histological features and supratentorial location with seizures. However, their medical findings are inadequate, with a median survival time of only 1.25 years [86]. The histological-based classification system has been updated over the years and has been useful for clinicians, but it has some limitations that have prompted the recent modification.The histological-based diagnosis technique is susceptible to high interobserver variation which is a serious drawback.Therefore, the diagnostic criteria that separate astrocytoma from oligodendroglioma are better suited for common scenarios,but may be too vague for most tumors, having some mixed feature. The accuracy of histology-based classification can also be affected by inadequate or non-representative tissue sampling [87].

For patients with comparable diagnoses, ranging from weeks to years, conventional classification and grading systems have difficulty providing accurate prognoses.

Some differences can be explained by various clinical factors, such as age factor ,Status of patient performance , and extent of the resection. Nevertheless, when clinical and histopathologic prognostic variables are considered, the significant portions of the survival differences cannot be explained. According to WHO classification system the molecular changes within gliomas have made it possible to improve diagnostic standards, identify prognostic biomarkers, and develop viable targeted therapeutics for molecularly identified glioma subgroups. (Figure 2.4) [88].

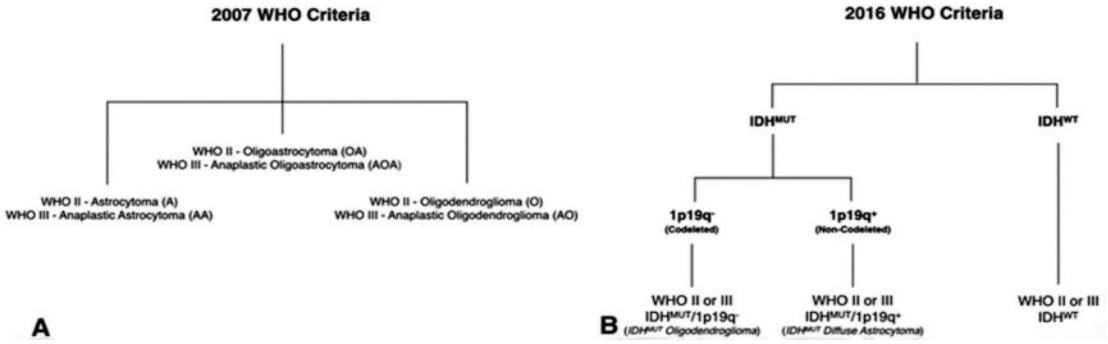

FIGURE 2.4: WHO classification system glioma 2007-2016

2.4 Glioma Diagnosis

The glioma diagnosis is based upon the following testing:

2.4.1 Imaging Modalities

MRI is a non-invasive imaging technique that uses a powerful magnetic field and radiofrequency radiation to generate images of the body's inside organs. It provides high-resolution images of soft tissues, including the brain, and is considered the gold standard for brain tumor imaging. The technique works by detecting the signals generated by the protons in water molecules in the body's tissues. MRI

is a highly effective imaging technique for the diagnosis and monitoring of brain tumors.

2.4.2 Magnetic Resonance Spectroscopy (MRS)

It is used to identify the presence of metabolites via exploring the biochemical spectra that are generated when those chemicals are excited. Through the identification of patterns of change that are correlated with cancer grade, this can offer both diagnostics information and data about the tumor's metabolism. Choline, for instance, is used to evaluate the turnover of cellular membranes, creatinine to gauge energy metabolism, myoinositol to indicate the activation of protein C, lactate to gauge anaerobic metabolism, and lipid to gauge necrosis. It is also helpful in gauging a patient's reaction to cutting-edge treatments that employ a focused molecular approach.

2.4.3 Computerized Tomography (CT)

It is a widely used imaging technique that generates 3-dimensional images of the internal structure of an object using a series of (2- Dimensional X-ray) images captured around a central point of rotation, which are then reconstructed by computer analysis. One advantage of CT over magnetic resonance imaging (MRI) is its ability to provide superior visualization of calcification. In particular, CT scans are recommended for the diagnosis of certain types of tumors, such as oligodendro gliomas and also meningiomas, which frequently exhibit calcification [89].

2.4.4 Pathological Analysis of Malignant Glioma

Despite the crucial roles played by clinical and neuro-imaging approaches, a histologic analysis of tissue samples continues to be the gold standard. A more accurate characterization of the tumor has been made possible by recent developments in molecular profiling, notably the inclusion of a patient's 1p 19q, K27M, H3 and

IDH deletion status into the 2016 WHO classification system, which has aided prognosis and patient care. The most popular histopathologic test for collected tissue is the haematoxylin and eosin (H&E) stained slide. The resulting stain enables the histopathologist to describe the neoplasm's microscopic morphologic characteristics, which are correlated with its biological behavior and prognosis [90]. The most widely used grading standard is the WHO classification system, which is based on the histological appearance of four patient survival-related criteria. The approach distinguishes infiltrated oligodendro gliomas, astrocytomas, and oligoastrocytomas based on morphologic criteria and splits infiltrating gliomas (grades II, III, and IV) from non-infiltrated gliomas (grade I). A final tumor grade is determined by taking into account morphologic characteristics and infiltrative potential [91]. A subpar method for determining the presence of an infiltrating glioma is frozen section diagnostic. Despite the ease with which some characteristics, such as nuclear anaplasia, cellular density, mitotic activity, necrosis and microvascular hyperplasia can be identified, other distinctive diagnostic characteristics are more challenging to identify with certainty and run the risk of introducing artefacts [92].

2.4.5 Immunohistochemistry

It can be used to distinguished between tumor cells from glioblastoma, melanoma, primary central nervous system lymphoma and metastatic carcinoma, using GFAP as a distinguishing protein. The expression of GFAP (Glial fibrillary acidic protein) is specific to astrocytic neoplasms, gametocytes, and gliofibrillary oligodendrocytes of oligodendro gliomas [93].

2.5 Significance of Molecular Pathology in Glioma Classification

The following seven molecular layers and molecular pathology are used to diagnose integrated gliomas as shown in the (Figure 2.5-2.6):

1. Isocitrate dehydrogenase (IDH1) mutations.

2. 1p/19q co-deletion.

3. A thalassemia / mental retardation syndrome −X−linked gene (ATRX) expression

4. TERT promoter mutation/EGFR gene amplification and/or chromosomes 7 gain and 10 loss (+7/−10).

5. CDKN2A/B homozygous deletion on 9p21.

6. Histone H3 K27M/ mutations.

7. Histone H3 G34R/V mutations.

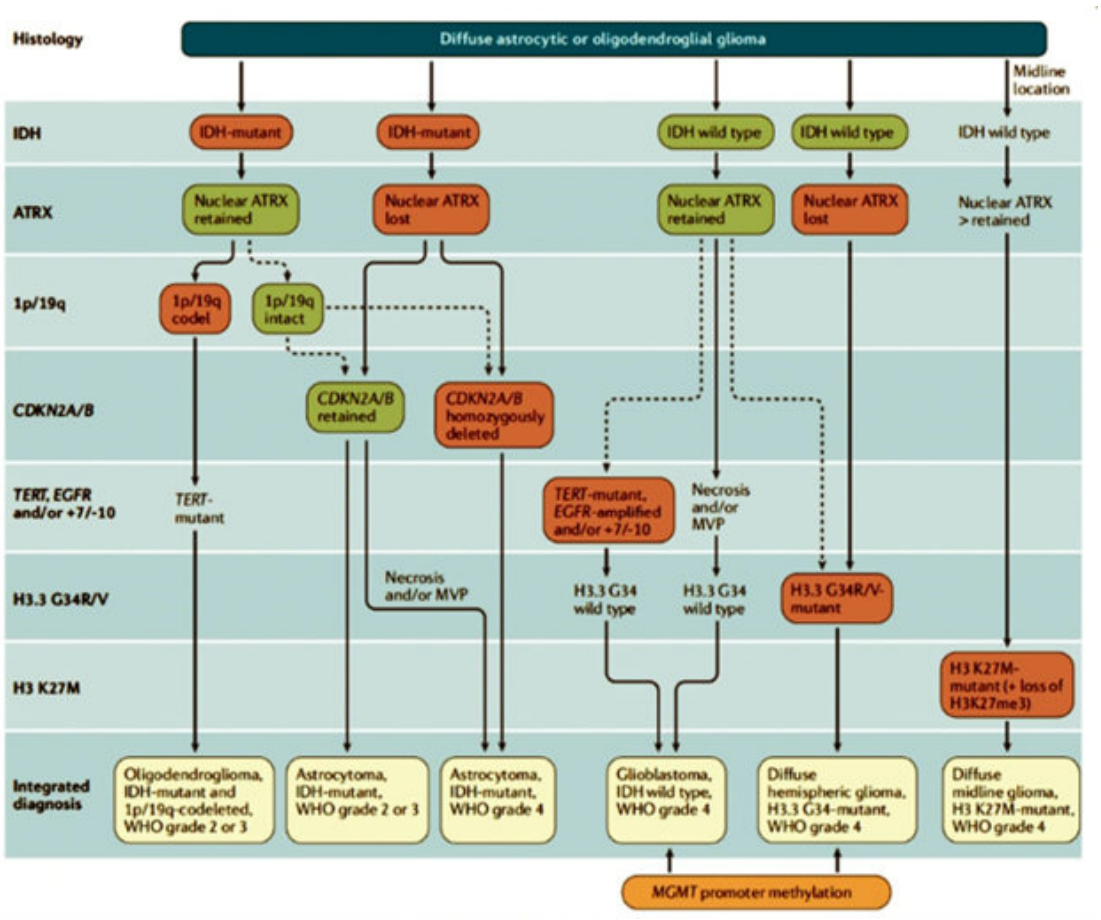

FIGURE 2.5: A seven-layer classification system for diffuse gliomas in adults [94]

In the field of glioma diagnosis, an integrated approach that combines histological features, grading, and molecular information has been adopted, which involves a 7-layered structure. This approach utilizes molecular information to highlight the absence and presence of the most diagnostic alterations for respective tumor types, with green indicating the presence and red indicating the absence of such alterations. As per the WHO classification, gliomas are categorized into different grades, ranging from 2 to 4, based on the increasing degree of malignancy.

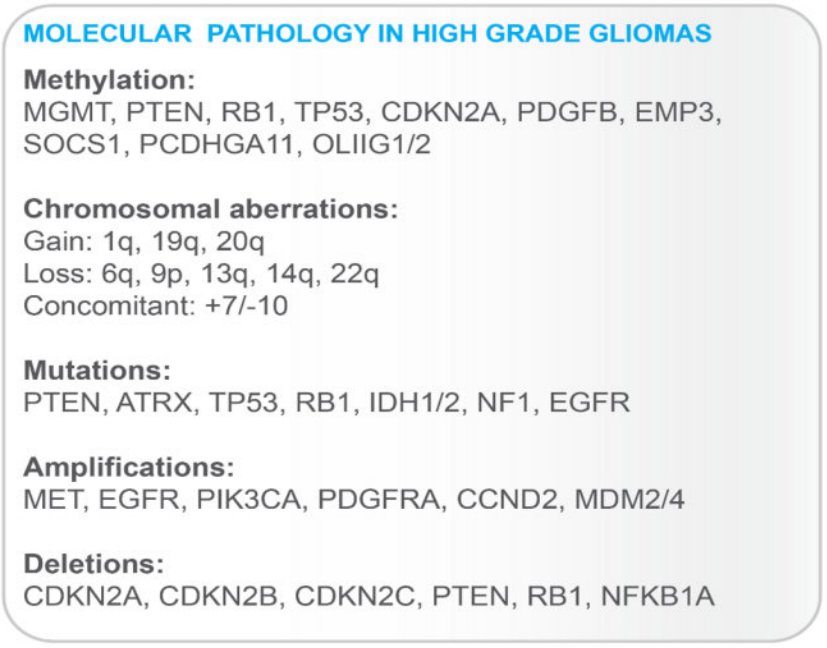

FIGURE 2.6: Molecular Pathology of Glioma [95]

2.6 Prognosis / Prediction

Gliomas are a group of primary brain tumors that are challenging to treat and have a poor prognosis. A variety of prognostic indicators have been identified for these tumors, including histological diagnosis, tumor grade, patient age, race, gender, location of lesion, extent of resection, radiation therapy and chemotherapy. [96]. These indicators have been derived from clinical trials and population registry data. Patients under 50 at diagnosis had a better prognosis than older patients, and patient age has been repeatedly emerged as the most important prognostic factor. This correlation has been observed across age groups and demonstrated

using a Kaplan-Meier curve, where a plot of survival over time reveals a decrease in cumulative survival as patients die. Additionally, the Karnofsky performance scale, a tool used to assess a patient's functional status, has been found to be strongly correlated with survival [97].

Several genetic changes have also been associated with glioma, and studies have investigated their relationship with survival. Scarce literature evidence is available on, like the TP53 mutation, have data, but it's not all that readily apparent. Furthermore, there is considerable variation in response to therapy, and despite the introduction of combined radiotherapy and chemotherapy, the median survival rate for high-grade gliomas remains low at around 46% after one year [98]. Since some of the clinical trials only enrolled patients with higher Karnofsky scores, leaving older patients with lower scores with palliative care only, it is crucial to continuously assess patients to locate and identify deteriorated case scenarios/or the efficacy of treatment regimen.

2.7 Glioma – Therapy

2.7.1 Surgery

Surgery is a crucial part of treating brain tumors, both for diagnosing the condition and for treating intracranial pressure symptoms and improving the prognosis through maximum operative removal of brain tumors. Complete tumor resection has been strongly correlated with improved prognosis [99]. Technological advancements, such as biopsies held with stereotactic volumetric techniques, cortical mapping, and resection with the use of lasers, robotics involvements, and aspirator application, have further improved surgical the outcomes [100]. Along with the patient's medical history and physical examination, a thorough pre-operative assessment employing MRI and CT modalities of imaging is required prior to surgery. Additionally, positron emission tomography scans utilized preoperative procedure to locate particularly active regions and direct the biopsy to these sites. However, complications such as hemorrhage may arise, particularly in vascular lesions like

glioblastoma. A safer and more efficient surgical method is image-guided surgery, which uses MRI and CT scans [101].

2.7.2 Radiotherapy

It plays a critical role in the medical treatment of cancer by targeting the proliferative and inducing apoptosis through various cellular mechanisms such as DNA damage, organelle dysfunction, and membrane rupture. This leads to the formation of free radicals that generate DNA crosslinks and damage nucleotides, ultimately inducing apoptosis. The primary goal of radiotherapy in cancer treatment is to stop the growth and spread of cancer cells while minimizing damage to surrounding normal tissue. In glioma therapy, the objective is to maximize ionizing radiation delivery to the target tissue while minimizing harm to normal brain tissue [102]. Fractionated doses of radiation are commonly used to provide time for tissue recovery, and image-guided techniques can be employed to accurately target the tumor and avoid damage to the surrounding tissue. Patient immobilization is critical for proper targeting, and greater precision can be achieved with stereotactic radiotherapy using a multi-headed cobalt unit known as gamma knife radiation therapy [103].

2.7.3 Chemotherapy

Chemotherapeutic agents exert their effects on inducing cancer cell death through diverse mechanisms.DNA is alkylated by temozolomide, which results in lesions in astrocytoma and GBM.Temozolomide reduces resistance to DNA damage by suppressing MGMT levels. Procarbazine, an important alkylating agent involved in the inhibition of the nucleic acid and protein synthesis, but its use is limited due to side effects such as , nausea, vomiting and rashes [104]. Vincristine is a potent drug that depolymerizes microtubulin formation, leading to cell cycle arrest at mitosis. It shows effect against both High-Grade and Low-Grade gliomas, but shows minimum sensitivity sensitivity against Low-Grade tumors, and its use is associated with neurological toxicity [105].

2.7.4 Immunotherapy

In the context of brain diseases such as glioblastoma, the use of immunotherapy has gained increasing attention. While the brain was historically thought to be devoid of immune surveillance due to the tightly regulated BBB (blood brain barrier) and absence of lymphatics, research has shown that immune surveillance and T cell activation primarily occurs in the meningeal compartment of the central nervous system. Immune checkpoint molecules (CTLA-4 and PD-1) have found to play a crucial role in cancer immunotherapy, with anti-PD-1/PD-L1 and anti-CTLA-4 immune checkpoint inhibitors (ICIs) being extremely effective for malignancies that are aggressive, like Non-Small Cell Lung cancer and advanced Melanoma [106]. Multiple immunological checkpoints are upregulated in the glioblastoma tumor microenvironment (TME), and the proportion of Tregs is enhanced, making ICIs a possible strategy for restoring T cell responses. However, following ICI therapy, GBM tumor can adjust the checkpoint of immune system blockage by upregulated substitute checkpoints such TIM-3. This acquired resistance may be overcome by combination therapy that target numerous checkpoints, such as anti-PD-1 and TIM-3 blocking. Recent research has also identified the inhibitory receptor CD161 as a potential target for immunotherapy, and As indicated in (Figure 2.7), future research studies should explored novel drug targets and combinations of therapies to increase ICI efficacy. [107].

Glioblastoma is an aggressive form of brain cancer that is highly resistant to therapy, making it a challenging disease to treat. Various immunotherapeutic approaches have been developed to target glioblastoma, ICIs myeloid-targeted therapies, dendritic cell (DC) vaccines, peptide vaccines, vaccines used in personalized therapy, and CART cell (Chimeric Antigen Receptor) immunotherapies [107]. To reinstate T cell function with anticancer activity, ICIs work by inhibiting the immunological checkpoints CTLA-4 and PD-1. Myeloid-targeted therapeutics alter pro-tumorigenic immunosuppressive microglia (MG) or MDMs (monocyte-derived macrophages) to become more anti-tumorigenic. Peptide vaccines, DC vaccines, and customized vaccinations train T cells to target tumor neoantigen(s).

In CAR immunotherapies, T cells from the patient or NK-92 cells from a non-patient are genetically modified to express neoantigen-specific CARs, which are then multiplied in vitro and adopted and delivered to the sufferer [107] .Despite the development of these immunotherapeutic approaches, glioblastoma remains highly resistant to treatment, and none of these therapies have been successful in improving treatment outcomes. The major mechanisms of resistance to these immunotherapeutic approaches include intrinsic, adaptive, and iatrogenic mechanisms, which are outlined in the grey boxes. However, many ongoing clinical trials are investigating ways to overcome these resistance mechanisms and improve the effectiveness of immunotherapy for glioblastoma.

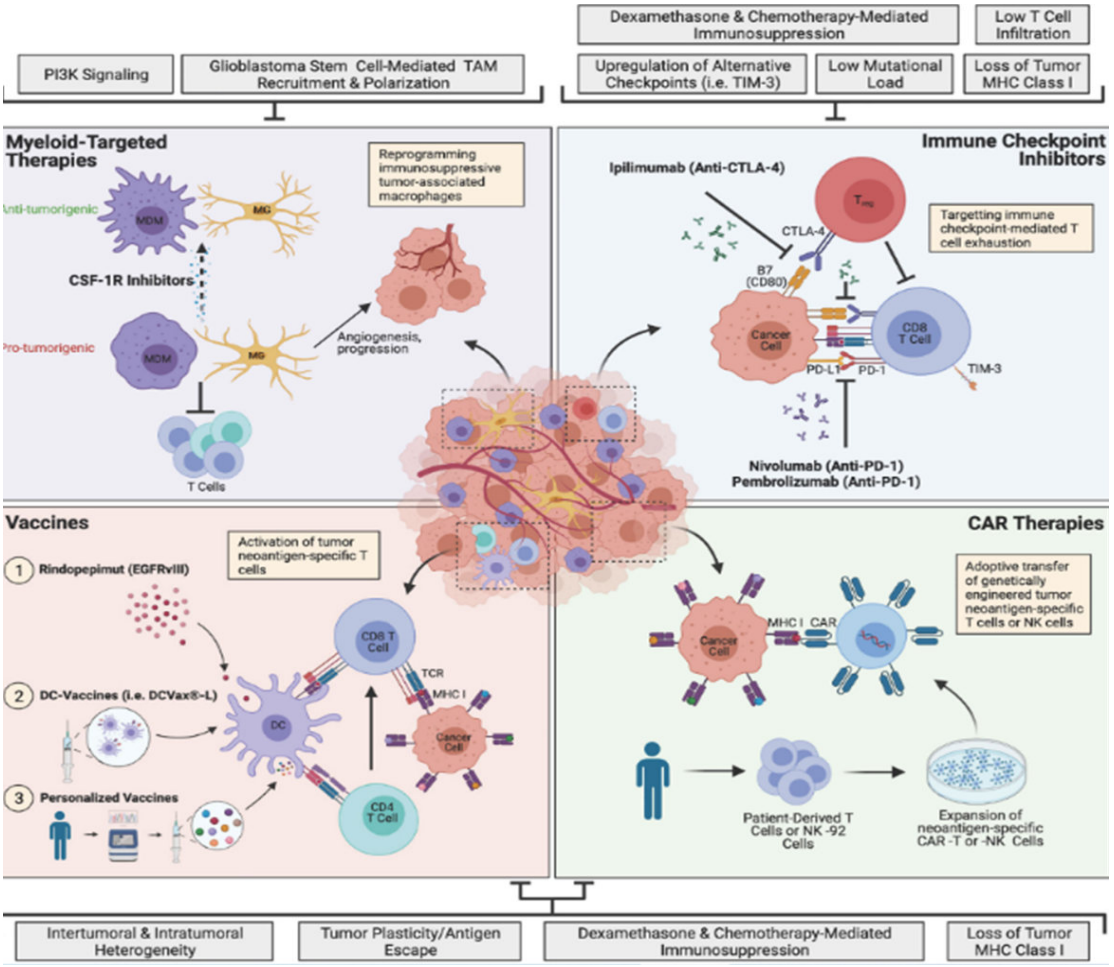

FIGURE 2.7: Landscape of major glioblastoma immunotherapies and mechanisms of resistance [108]

Targeting tumor-associated macrophages (TAMs) in glioblastoma is an important therapeutic strategy. One of the approaches to achieve this is to inhibit the

CSF-1R (colony stimulating factor 1 receptor), a critical receptor for macrophage survival and differentiation [109]. Vaccine-based therapies have emerged as a potential strategy to educate tumor-specific cytotoxic T lymphocytes (CTLs) by presenting tumor neoepitopes that are strongly expressed (Figure 2.7).Direct administration of several peptides that mimic the target tumor's neoepitope(s) is among the simplest ways to make therapeutic vaccinations. However, personalized vaccinations and DC-based vaccines are also being researched as prospective treatments for glioblastoma [110].

2.8 Role of Cytokines and Inflammation in Glioma Tumor Microenvironment

Inflammation is frequently associated with cancer progression and growth. Many variables including viral and bacterial infections, obesity, autoimmune illnesses, tobacco smoking, excessive alcohol intake and asbestos exposure generate tumor-extrinsic inflammation which promotes malignant progression and increases cancer risks [111] . MAPKs(mitogen-activated protein kinases) and transcription factors such as STAT3 and NF-κB are involved in inflammation mediated activation of microglia [112]. which can contribute to the advancement of neurodegenerative and neoplastic diseases [113]. During acute phase of brain injury, microglia switch to the M1 phenotype and release chemical messengers like ROS (Reactive Oxygen Species), nitric oxide (NO), excitatory amino acids and pro-inflammatory cytokines such as IL-6, IL-1 and TNFα [114]. IL-6 is a potent cytokine that was first recognized for its ability to promote T cell proliferation and activation, B cell differentiation, and the modulation of acute-phase responses. The IL-6 binds to signal transducer receptor (IL6ST) which dimerizes activating the JAK/STAT pathway [115], which induces the classical pathway and trans-signaling. The IL-6-STAT3 signaling pathway, along with other inflammatory cytokines like IL1β and TNFα, has been implicated in tumor progression in a variety of tumor including glioma and contributing to tumor recurrence and resistance. TNFα stimulates the expression of IL-6 during this inflammatory response. IL-6 then controls

the inflammatory response by suppressing the expression of various other anti-inflammatory cytokines while increasing the expression of inflammatory cytokines such as IL-1β [116]. Up regulation of IL-6 expression has been associated with poor patient survival in gliomas and IL-6 excision has been shown in a mouse model to prevent glioma formation [117]. Furthermore, by establishing an inflammatory environment, IL6 promotes the survival and proliferation of glioma stem cells (GSCs). IL-1β promotes glioma growth by activating the p38 MAPK pathway and increasing IL-6 levels [118].

After inflammasome-mediated activation, IL-1β is the only cytokine that is processed by caspase-1. Innate immune cells, such as antigen-presenting cells activated by IL-1 signaling, and CD4+ T cells are polarized towards Th17 and Th1 cells [119]. As a consequence, IL-1β plays a significant role in the resolution of acute inflammation and the initiation of adaptive anti-proliferative responses. Nevertheless, IL-1β produced as a result of chronic inflammation promotes tumor growth. It promotes metastasis employing various types of mechanisms. It also encourages the proliferation of myeloid-derived suppressor cells. The pharmacological inhibitors of IL-1 signaling could be used as a therapeutic intervention for IL-1 associated tumor development [120]. IL-1α and IL-1β bind to IL-1R1 and IL-1R2 which are expressed by Dendritic cells T cells, monocytes, polymorphonuclear leukocytes, B cells and macrophages. IL-1Ra and IL-1R2 antagonism, therefore, modulates IL-1 signaling and hence diminish IL-1 mediated inflammation [121] .Thus, innate pro-inflammatory cytokines such as IL-1, IL-6 and TNF-α, are essential for the resolution of acute inflammation. However, chronic inflammation, associated hyper expression of innate cytokines promote tumor formation by prolonged NF-κB activation and MAPK activation. These cytokines also induce antiapoptotic and pro-tumorigenic proteins expression [122].

Cytokines are a class of specialized proteins involved in the regulation of innate and adaptive immune cell functions in response to various antigens, including microbial invasions. They play a critical role in inflammatory and immune responses by promoting lymphocyte growth and differentiation and activating cytotoxic effector cells. Additionally, they are essential for haemopoiesis and have therapeutic

applications in stimulating or inhibiting inflammation [123].

The transcription factors STAT3 and NF-κB play important roles in glioblastoma progression and are activated by various cytokines. STAT3 is constitutively active in GBM and mediates the effects of interferon and interleukin-6 cytokine families through the JAK-STAT pathway. Similarly, NF-κB is activated by cytokines such as VEGF, TNF-α, and IL-1, and promotes pro-inflammatory target gene expression. TNF-α also activates NF-κB through TNFR1, leading to anti-apoptotic responses [124]. A20, which is a negative regulator of NF-kB, show expression at lower levels in GBM and is associated with TMZ resistance. The expression of various cytokines by glioma cells can have both positive and negative effects on tumor growth, proliferation, migration,invasion, neo angiogenesis, and immune cell infiltration. Figure 2.8 depicting the inflammatory markers and cytokines infiltr

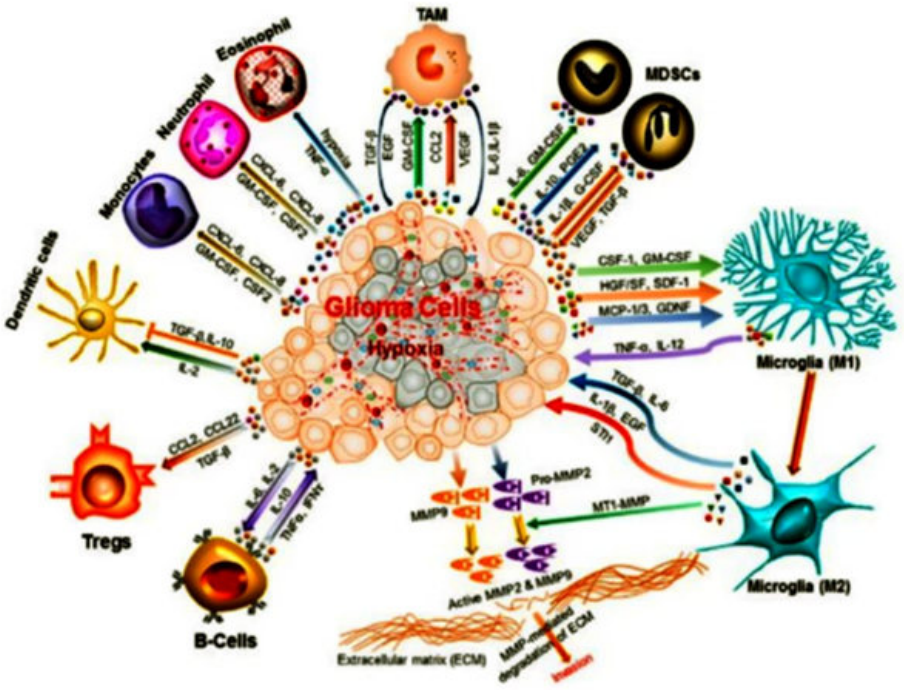

FIGURE 2.8: Inflammatory markers and cytokines infiltrations in Glioma microenvironment [125]

2.9 Microglia

Microglia are myeloid cells that reside in the Central Nervous System and perform a vital role in inflammatory reactions, as well as injury and repair. Microglia are

drawn to gliomas and polarized into cancer-nourishing cells that assist in angiogenesis, invasion, and matrix remodeling and adaptive immune suppression. Even though the signaling pathways and key regulators that enable classical inflammatory response are well characterized, the transcriptional and signaling circuits that underline alternate microglia activation are insufficiently recognized [126]. CNS immune system is significantly influenced by microglia cells, which act as macrophages that are localized to tissue in the brain [127]. These cells significantly influence brain development and the homeostasis of the neural environment by phagocytosing apoptotic cells and promoting neurogenesis, synapse formation, and the growth of axon [128, 129]. Additionally, microglia cells are important members of the first line of defense and take part in immune surveillance [130].

2.9.1 Microglial and/ Macrophage Activation and Polarizations (during resting stage)

Sedentary microglia cells actively monitor their environs via highly mobile pseudopodial extensions on their bodies. The microglia that are resident in the tissue become active resulting in a variety of pathological events, including wounds, viral infections, bacterial infections, or damage of the tissue. Microglia are suitable as antigen-presenting cells because they express co-stimulatory molecules and high levels of (Major Histocompatibility Complex II) MHC II molecules when activated [131]. Microglia serves as a direct mediator between the adaptive and innate immune systems in this way. Additionally, they produce TNF-α, a pro-inflammatory protein that facilitates the invasion of peripheral macrophages. The entire myeloid cell population then causes an immediate inflammatory response. Microglia and macrophages are cells that play a vital role in the immune response of CNS. These cells use a variety of immunological pattern recognition receptors to recognise immunogenic antigens including lipopolysaccharides (LPS), which is followed by pathogen removal by phagocytosis. The activation of microglia/macrophages leads to the expression of redox molecules, scavenger receptors, and inducible nitric oxide synthase (iNOS), resulted in the production of high levels of nitric oxide. This

metabolic state is associated with the pro-inflammatory, M 1-like a ctivated phenotype of macrophages/ microglia. However, microglia/macrophage activation is a dynamic process that is tightly regulated. Through the secretion of immune-regulating substances and anti-inflammatory substances, A polarity change to an anti-inflammatory M 2-like p henotype f ollows t he p ro-inflammatory re sponse of M1-like microglia/macrophages, which inhibits immunological responses, prevents tissue damage, and promotes the process of healing [132].

Multiple markers, such as CD206, CD204, and CD163, are expressed by M2-polarized macrophages and microglia.The IL-4 and IL-13 produced by T helper cells (TH) stimulate the M2a subtype primarily. The TGF-β (Transforming growth factor), IL-2 receptor (IL-2R), and CCL15, CCL17, CCL24 are among the anti-inflammatory cytokines and chemokines that are expressed as a result of the binding of IL-4R (IL-4 receptor), which activates the STAT6 transcription factor. Additionally, the M1-specific NF-κB signaling is silenced as a result of IL-4R signaling. In contrast to (M2a) microglia and macrophages, the (M2b) subtype is activated by immunological complexes, TLRs (Toll-like receptors), or inhibitors of the IL1 receptor (IL1R). These receptors' downstream signaling triggers the release of IL1, IL6, IL10, TNF-α and CCL1 which regulates the immune system by activating TH2 and regulatory T cells (Tregs). Finally, exposure to anti-inflammatory cytokines including IL10, TGF-β, and glucocorticoids causes the (M2c) phenotype to become active. The response to IL10 involves the phosphorylation of the STAT3 transcription factor, leading to the transcription of various molecules, including TGF-β, FIZZ1, and PPAR-γ, resulting in an anti-inflammatory microenvironment. Versican, Pentraxin 3, and Antitrypsin expression are markers for the (M2c) phenotype and promote the formation of extracellular matrix and tissue remodeling [133].

2.9.2 Role of Microglia / Macrophages in Glioma Microenvironment

Discrimination between pro-inflammatory (M1-polarized) and anti-inflammatory (M2-polarized) GAMs is challenging. Nevertheless, CD40, CD74, and MHC II are associated with M1-polarized GAMs, whereas CD204, CD163, CD206, FIZZ1, ARG1, and pSTAT3 are attributed to M2-polarized GAMs. Anti-inflammatory M2 GAMs with CD204+ and CD163+ are linked to high grade tumor and shorter patient survival in gliomas. Glioma cell-derived factors, such as TGF-β and M-CSF, contribute to M2-like GAM polarization by promoting the up regulation of several M2 markers [134]. The activation of microglia/macrophages is either focused on the conventional, pro-inflammatory M1-like phenotype or on the alternatively activated anti-inflammatory M2-like phenotype depending on the particular stimuli. As shown in figure 2.9, glioma cells attract GAMs and cause an M2-like polarization, which encourages tumor growth and invasion. Chemo attractants, such as MCP-1, MCP-3, and SDF-1, secreted by glioma cells promote GAM infiltration. Furthermore, GM-CSF, EGF, and EGFR/MAPK signaling also play an essential role in microglia recruitment and polarization. Even in the context of brain tumors, these findings offer a helpful foundation for further characterizing GAM polarization [135].

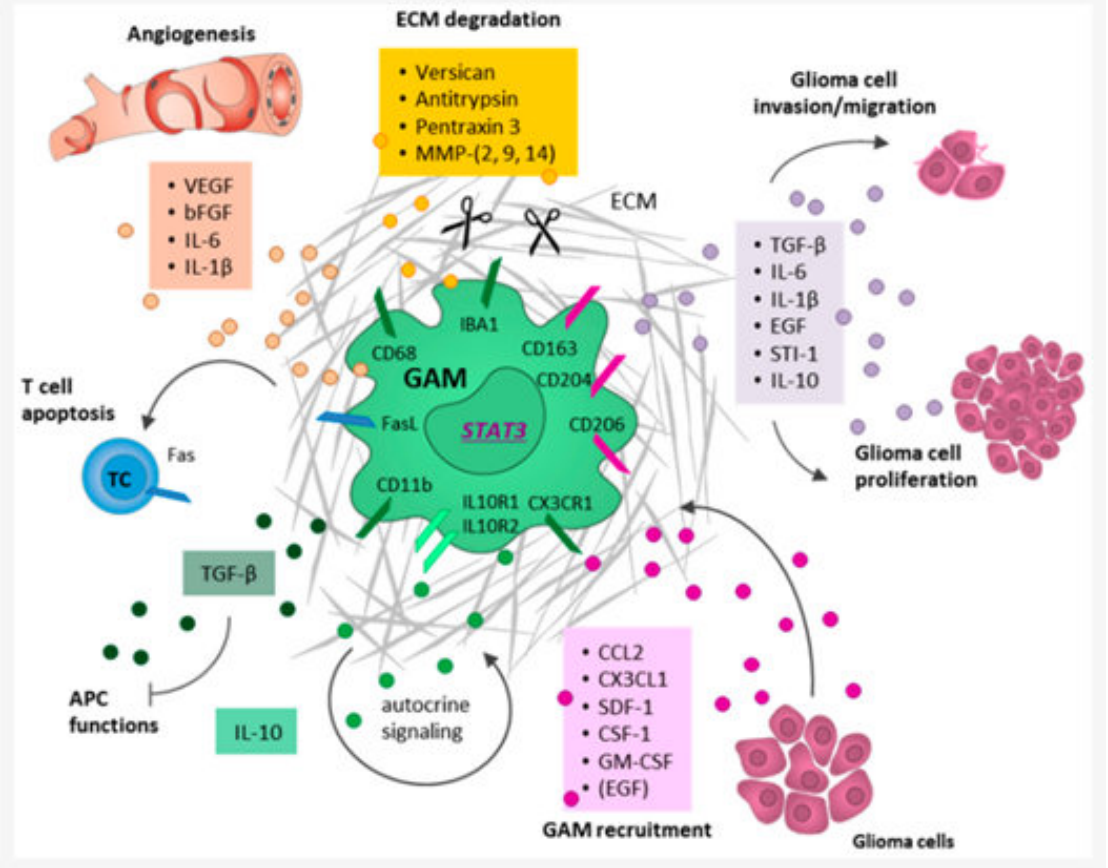

FIGURE 2.9: GAMs' involvement in the development of a tumor microenvironment that promotes tumor growth [136]

2.9.3 Interaction between Gliomas and Macrophages

GAMs interface evolve together with malignant tumor cells closely in the tumor microenvironment.GAMs significantly contribute to tumor development, cell relocation, and invasion after active tumor cellular-mediated recruitment and polarization into the (M2-pro-tumorigenic) like phenotype. Additionally, they contribute in the depletion of extracellular matrix, promote neoangiogenesis, and support an immune-suppressive microenvironment. In vitro and in vivo, astrocytoma and glioblastoma cells release the (MCP)-1 (monocyte chemoattractant protein) one of the most significant chemo attractants known to attract GAMs [137]. In addition, motility of GBM and transformation into the M2-like phenotype are encouraged by M-CSF (CSF-1), which is released by glioma cells. In addition to inducing GAM invasion in vitro, the cytokine GM-CSF released by glioma cells also inhibits GAM-Dependent invasion in an organotypical brain slice model. EGF has

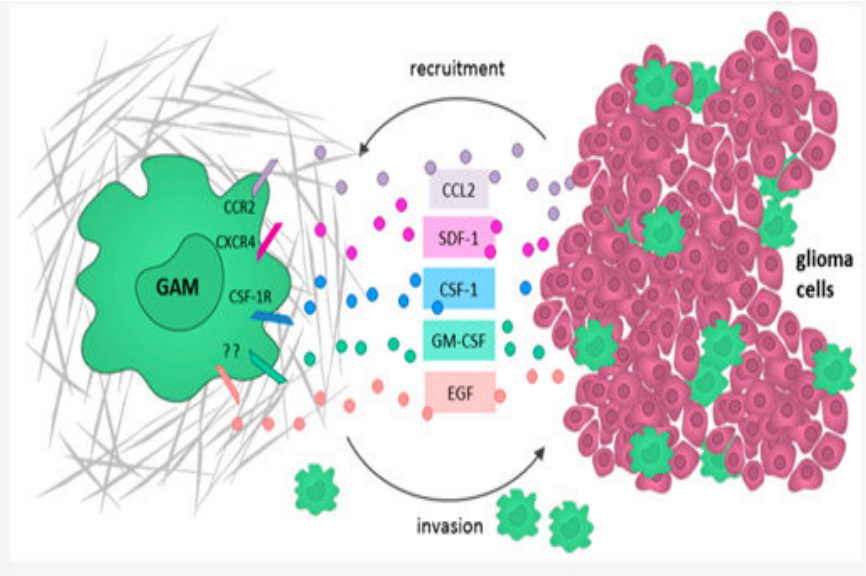

FIGURE 2.10: GAMs (glioma-associated microglia/macrophages) recruitment by glioma cells [140]

also been discovered to act as a paracrine motility factor that attracts microglia to the location of the lesion [138]. The production of the pro-inflammatory cytokines IL-1β and TNF-α is decreased when the EGFR/ MAPK signaling in microglia is inhibited, according to in vivo animal models. Multiple glioma cell-derived chemokines, including SDF-1 (CXCL12), MCP-1 (CCL2), EGF, M-CSF (CSF-1) and GM-CSF, work together to recruit GAMs and then cause their M2 polarization (Figure 2.10). Therefore, inhibiting these ligands or their associated receptors may provide potential targets for new treatments [139].

2.9.4 GAMs Activate TME Immunosuppressive and Promote Glioma Cell Invasion

GAMs are known to promote invasion of glioma cells and contribute to an immunosuppressive TME. TGF-β, STI-1(stress-inducible protein-1) , IL6, IL1, and EGF are a few GAM-derived factors that have been found to induce glioma cell invasion. TGF-β superfamily members 1-3, which are produced by glioma cells and are increased in glioma tissues have been extensively studied and are among these substances classified as immunosuppressive cytokines [141]. Particularly, it has been shown that TGF-β2 derived from MMP-2 is induced to develop by

GAM,a type of enzyme that, in vitro, makes glioma cells more aggressive. Furthermore, astrocytoma aggression and an unfavourable outcome for GBM patients are strongly correlated with MMP-2 expression. [142].

Both soluble substances and direct interactions between cells are used by M2-polarized GAMs to carry out their immunosuppressive activities. Low levels of the M1-associated pro-inflammatory cytokines TNF-α, IFN-γ, IL-2, and IL-12, as well as high levels of the M2-associated anti-inflammatory cytokines TGF-β, IL-6, and IL-10, were discovered in the tissues of gliomas, pointing to an immunosuppressive TME. It was determined that glioma cells and GAMs were the primary sources of these cytokines. TGF-β secretion increased when glioma cells and microglia monocultures were co-cultured. Reduced phagocytic activity is brought about by the down regulation of MHC II molecules, co-stimulatory moleculesCD86 and CD80 and MHC II molecules in GAMs as a result of the subsequent TGF-β signaling [143].

Similar to TGF-β, IL-10 also contributes to an immunosuppressive TME by preventing the proliferation of T cells, antigen-presenting cells, and Tregs. Increased IL-10 expression levels are linked to malignancy in gliomas. In human GBM, GAMs are thought to be the primary source of IL-10. It has been demonstrated that tumor-derived GAMs exhibit increased STAT3 signaling compared to healthy microglia/macrophages when it comes to IL-10 transcription. A worse prognosis for glioma patients and elevated tumor grade have both been linked to activated pSTAT3 expression. Additionally, conditioned media produced from glioma cells can boost microglia cells' STAT3 activity, which in turn causes them to secrete more of the anti-inflammatory M2-like cytokines IL-6 & IL-10. Together, these findings pointout the STAT3 targeting as promising therapeutic strategy [133].

2.10 Signaling Pathways in Glioma

The signaling pathways implicated in glioma have been extensively studied due to their critical role in promoting tumor growth and progression. Genetic alterations

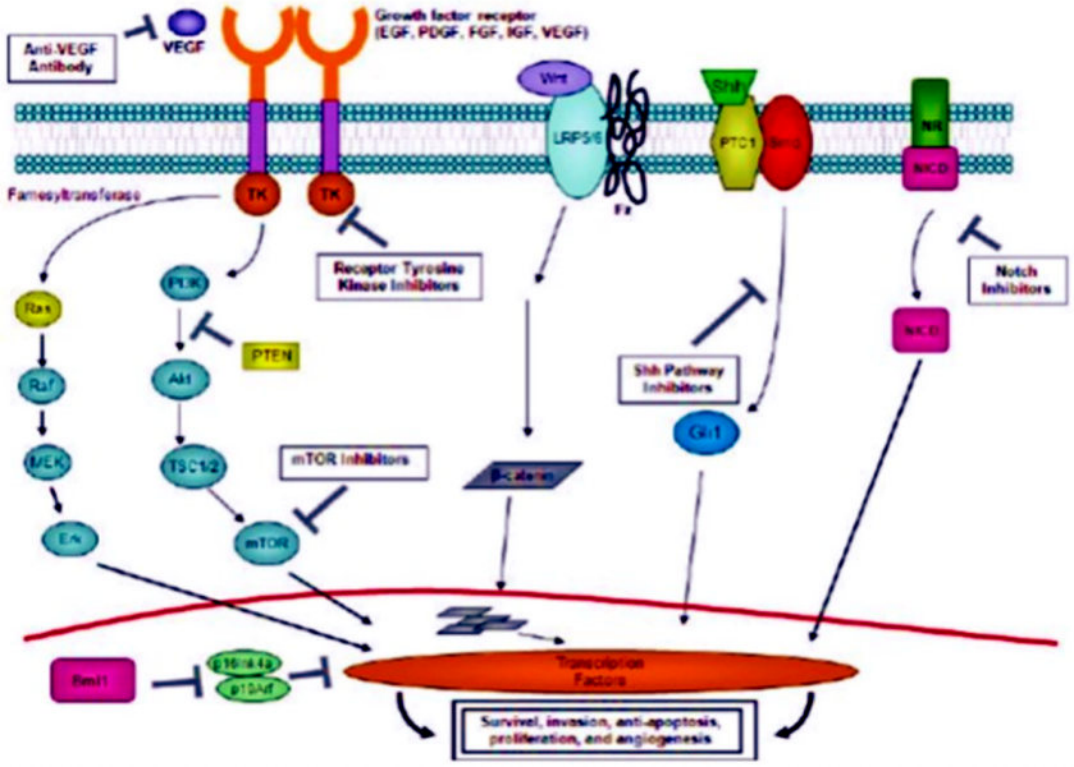

FIGURE 2.11: Important signaling pathways in gliomas [145]

identified in human GBM samples have highlighted the importance of certain onco-pathways [144], such as EGFR amplification and downstream activation of STAT3 (signal transducer and activator of transcription) in glioblastoma cells shown in (Figure 2.11), While these pathways have been the focus of current GBM drug trials, other pathways such as (JAK/STAT) and (NF-κB), which are significantly elevated in various types of human malignancies, hold enormous potential for the creation of more efficient, molecularly tailored GBM treatments.

Cancer research has focused on JAK2/STAT3 Signaling because it is essential for the development and survival of several kind of human malignancies. To inhibit the transition of healthy cells into cancerous ones, STAT3 activity must be strictly controlled since it affects the transcription of genes involved in apoptotic cell cycle. The majority of human neoplasms, however, exhibit abnormal STAT3 activity, which shows the breakdown of endogenous regulatory mechanisms. The tyrosine phosphorylation status of STAT3 in GBMs demonstrates that it is constitutively active [146]. In individuals with anaplastic astrogliomas, phosphorylated STAT3 is associated with a poor prognosis [147]. IL-6 cytokines have a strong relationship

with GBMs because of their ability to activate STAT3. All tumors examined to date had high levels of IL-6, one of the most frequently dysregulated cytokines in cancer [148]. In GBMs, the protein inhibitor of activated STAT3 (PIAS3), a negative regulator of activated STAT3, is produced at extremely low levels, which supports constitutive STAT3 signaling and cell growth, according to a recent study. These results imply that STAT3 suppression in antigen-presenting cells can enhance the T-cell-mediated antitumor immune response in glioma. However, STAT3's function in glioma genesis is complicated and might be influenced by the tumor's mutational profile [149].

In GBM, the Wnt, vascular endothelial growth factor (VEGF), TGF β, EGFR, NF-κB, CDKN2A, (PI3K)/AKT (phosphatidylinositol-3-kinase) and mTOR (mammalian target of rapamycin) pathways have been found to be altered or upregulated, possibly contributing to the disease progression and aggressive tumor behavior. The cellular differentiation, polarity, proliferation, motility, and stem cells activity are all significantly influenced by the canonical Wnt pathway. This pathway's increased activity has been connected to GBM development, aggressiveness, and invasive potential as well as resistance to chemotherapy and radiation therapy [150]. The tyrosine kinase receptor EGFR controls cell proliferation, migration, adhesion, differentiation, and death. TGF-β, an inflammatory pathway that normally promotes tumor suppression, mediates malignant characteristics in cancer cells. A crucial regulator of both healthy and pathological angiogenic response is VEGF. and considered as powerful stimulant of endothelial cell development [151]. An essential component of immunity, inflammation, cancer, and nervous system health is the protein transcription factor NF-κB. Oncogenic NF-κB mutations typically promote tumor growth and invasion, decrease apoptosis, and create drug resistance. Cellular quiescence, proliferation, cancer, and longevity are all governed by the mTOR and PI3K/AKT pathway. This pathway is overexpressed in a number of cancer forms, including glioblastoma multiforme, and is triggered by a number of growth factors, including members of the human EGFR family and the PDGFR family. AKT promotes cell survival, deactivates cell cycle inhibitors, and increases cell cycle proteins, all of which have an impact on cellular proliferation. It also drives protein synthesis and cell growth. There is potential for the

development of targeted therapeutics for glioblastoma that could enhance clinical outcomes for patients given the number of disrupted signaling pathways [152].

The NF-κB signaling system is aberrantly constitutively activated in GBM, which encourages oncogenesis by promoting Apoptotic suppression, tumor proliferation, invasion and therapeutic resistance. The p65-p50 heterodimer, which binds to NF-κB sites in target genes to control gene transcription, is the most prevalent type of NF-κB protein dimer. NF-κB dimers are inactive in non-stimulated cells because they bind to three cytoplasmic inhibitory factors, (IκB$-\alpha$), (IκB-β) and(IκB-ϵ), preventing nuclear localization and transfer. NF-κB dimers, on the other hand, bind to κB-sites in the nuclear regulatory areas of genes that are involved in numerous biological processes. NF-κB supports the functions of neurons as well as processes linked to synapse development and plasticity. Notably, research has revealed that in 81% of GBM cases, the NF-κB p65 subunit is overexpressed [153].

By preventing IκB kinase breakdown, the flavonoid a mentoflavone, wh ich can penetrate the blood-brain barrier, blocks the NF-κb pathway. This substance decreases the viability and growth of GBM cells, causing a sub-G1 population to appear that indicates apoptosis [154].

A fundamental genetic program for instruction is the Wnt signaling pathway that supports GBM's capacity for growth, aggression, and invasion. According to recent studies, Wnt activation-causing mutations in the adenomatous polyposis coli gene occur in roughly 13% of cases of GBM and have a mutation frequency of approximately 14.5 percent. Furthermore, elevated canonical Wnt pathway activity, which results in cancer stem cells from differentiated cells, causes GBM resistance to chemotherapy and radiation therapy [155].

The PI3K/AKT/mTOR intracellular signaling system controls cell growth, metabolism, and proliferation. Three categories of PI3K inhibitors exist: dual PI3K/mTOR, isoform-selective, and pan-PI3K. With a frequency of 4 to 27%, PIK3CA expresses p110α, a subunit of the catalytic pathway of class IA PI3K that is commonly altered in GBM [156]. In GBM cells, PIK3CA significantly k nockdown decreased migration, cell survival and invasion by decreasing AKT and FAK activation.

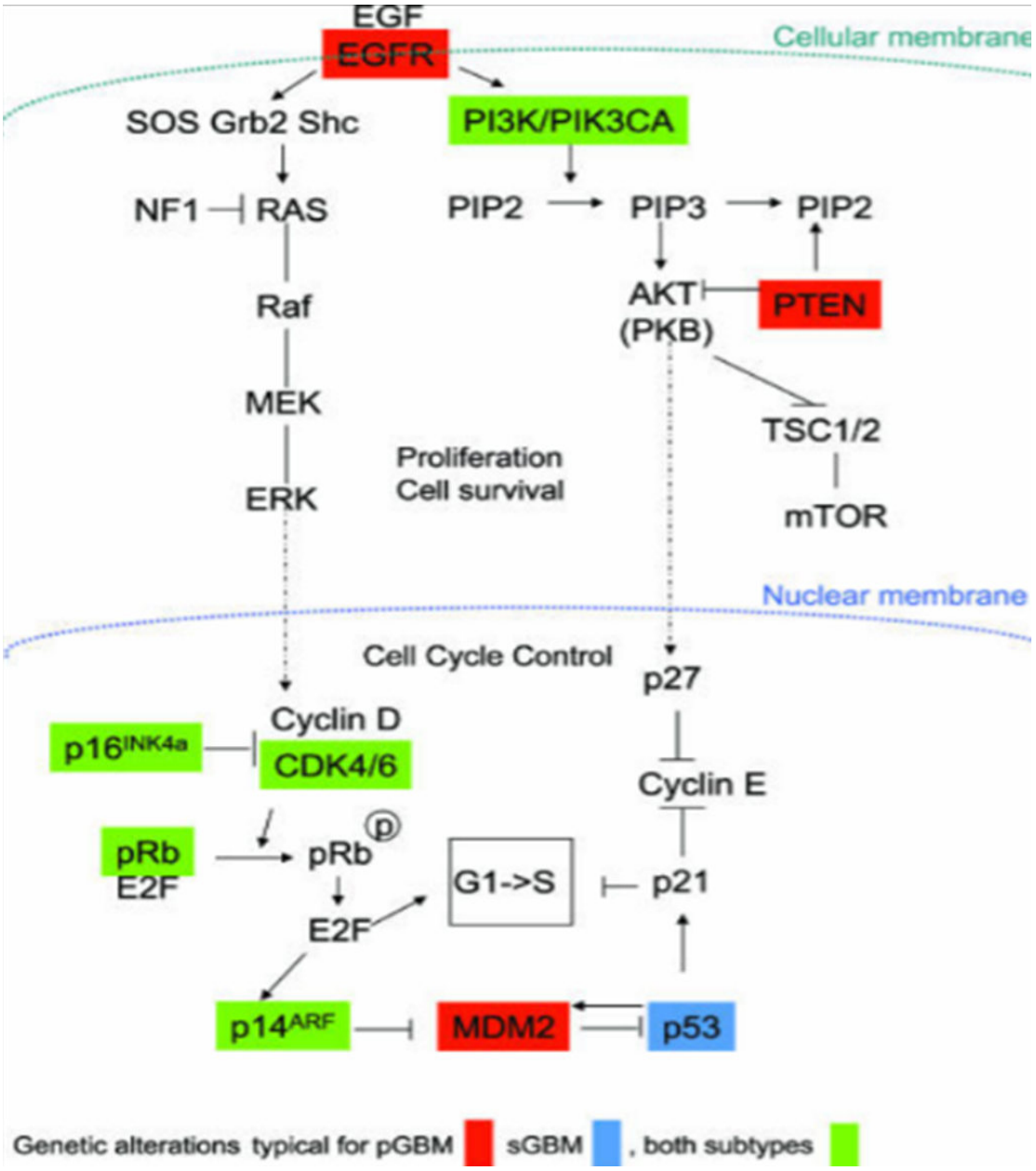

FIGURE 2.12: Major signaling involved in the pathogenesis of glioblastoma [158]

MTOR, a member of the PI3K-related kinases, regulates various growth signals by phosphorylating the immediate substrates (Figure 2.12). It is found that in previous studies more than 90 percent of glioblastomas, the mTOR signaling pathway is hyperactivated [157].

The HGF (Hepatocyte Growth Factor), the ligand of the c-Met receptor tyrosine kinase (RTK), is expressed on the surfaces of many different cells. Through the

stimulation of numerous signaling pathways, aberrant activation of the (HGF/c-Met) axis in cancer cells, which is intimately associated to mutations of c-Met gene, overexpression, promotes tumor growth, amplification, and its progression [159]. C-Met overexpression is present in about 37% of GBM patients. The mechanism of resistance that facilitate GBM invasion in xenografts model also involves c-Met. Clinical trials have been conducted on a number of c-Met-targeting medications, including Onartuzumab, a monoclonal antibody that specifically binds c-Met [160].

Changes in FGFR expression in astrocytes may promote malignant transformation and the development of GBM as a result of the stimulation of mitogenic response, migration-prone, and antiapoptotic responses. Fisogatinib is a FGFR4 gene inhibitor that has shown strong activity and selectivity, which led to significant anti-tumor efficacy in clinical trials [161]. In addition to causing tumor growth, activation of the BRAF gene in human neural stem and progenitor cells also causes oncogene-induced senescence in some low-grade brain tumors [162]. In contrast, adult diffusely developing tumors with a poor prognosis are also found to have BRAF gene changes. BRAF inhibitors that target the BRAFV600E mutation, such as (Dabrafenib and Vemurafenib), have made substantial progress in the treatment of malignant melanoma. Given the existence of the V600E mutation, BRAF inhibition is currently a therapeutic option for a limited cohort of patients with recurrent glioblastoma multiforme [163].

2.11 Importance of Inflammatory Molecular Bio Markers in Glioma Diagnosis and Therapy

Several inflammatory biomarkers have been studied in gliomas, including TNF-α, and TGF-β,C-reactive protein (CRP),and IL-6 among others. Elevated levels of these biomarkers associated with poorer prognosis and shorter survival in glioma patients. For example, high levels of (CRP) shown to be an independent predictor of poor prognosis in glioblastoma patients.

In addition to prognosis,expression of inflammatory biomarkers can also predict treatment selection. For example, the presence of high levels of TGF-β has been associated with resistance to anti-angiogenic therapy, which is commonly used in glioblastoma treatment. In contrast, the presence of elevated levels of IL-6 has been associated with better response to certain immunotherapies, such as checkpoint inhibitors.

Overall, the use of inflammatory biomarkers in glioma diagnosis and therapy is still in the early stages of development, and more research is needed to fully understand their clinical utility. However, the potential for these biomarkers to provide additional information to guide treatment selection and improve patient outcomes makes them a promising area of investigation in neuro-oncology[164].

2.12 Tissue Expression Profiling in Glioma

Transcriptional analysis of tissue expression profile is a crucial step in the discovery and development of new drugs. Its effects on numerous facets of drug discovery, including target identification, target validation, chemical selection and verification, pharmacogenomics aspects, biomarker creation, evaluation of clinical trial, and toxicology are extensive. Standardized processes and a single array platform are essential for maximizing the use of the invested resources. This makes sure that sizable species-specific databases are produced, which makes it easier and more secure to compare data sets from various trials.

Transcriptional profiling can identify a large number of differentially regulated transcripts across a series of samples. Housekeeping genes are likely to be unregulated genes and may not be transcribing proteins critical to the particular processes in biology are being studied. The localization of expression of genes inside the tissue can be determined with great value by fractionation, aiding in identifying the native protein translated from a novel gene or in identifying specific regions for natural or targeted deletion of genes of interest. The precise comparative expression pattern of individual genes or gene families connected to particular biological mechanisms and pathways can be studied using bioinformatics methods

[165].

High-throughput genomic technologies extensively used to comprehend the mechanisms involved in the genesis of disease processes. Gene expression profiling with microarrays can identify differentially expressed genes, aiding in the discovery of diagnostic molecular markers [166]. Immunohistochemistry (IHC) is another method to identify molecular markers that can determine the grade of gliomas appropriately,by determine those patients who have a better chance of surviving or who might benefit from chemotherapy . For instance, GFAP immunostaining yields supplementary information for diagnostic and prognostic evaluation of human astrocytomas. However, in contrast to the tumor samples in different datasets, the number of normal control samples in public gene expression databases is disproportionately small [167].

Overall, the study of the precise relative expression pattern of single gene or number of gene families is associated with specific biological mechanisms and pathways is made possible by tissue expression profiling through transcriptional analysis and high-throughput genomic technologies, which also aid in the identification of diagnostic molecular markers.

2.13 Impact of Expression Profiling in Personalized Medicine

Gene expression profiling stands at the forefront of advancement in personalize medicine, specially in the field of precision oncology, bestowing a rational approach in glioma. Predictive diagnostic and prognostic molecular markers are increasingly being used to supplement histopathological classification of gliomas. Furthermore, extensive molecular profiling investigations have indicated that various types of gliomas have distinct genetic and epigenetic abnormalities that can be used to classify tumors [168].

2.14 Pharmacogenomics and Glioma

The high rate of clinical development medication failure is a significant contributor to the unfavorable perceptions of the pharmaceutical industry's low productivity. The costliest studies are in phase III, and nearly half of all medications that reach this stage fail because of insufficient efficacy or toxicity problems. Furthermore, drugs that make it to the market can show unexpected variations in efficacy and safety. The use of pharmacogenomics (PGx) profiling technologies can facilitate to identify inter-individual differences in drug treatment response [169]. This includes oligonucleotide microarrays, which can investigate mRNA levels, and DNA single nucleotide polymorphisms (SNPs), commonly referred to as pharmacogenetic (PGt) analysis. PGx can also involve the analysis of mRNA processing, microRNA levels, and DNA insertions, deletions, rearrangements, and copy number. Although other profiling methods provide a more comprehensive understanding of drug treatment at the molecular level, only oligonucleotide microarrays and SNP profiling technologies are currently feasible on a large scale [170]. By deriving a characteristic signature from the differentially expressed genes for each pharmacological medication of a specific cell type, PGx can be used to predict responsiveness or outcome.

Pharmacogenomics helps patients with oligodendrogliomas understand chemotherapy response. The use of pharmacogenomics can identify genetic markers that differentiate responder from non-responder patient groups and the ones most likely to experience a negative medication reaction. Although the standard of care chemotherapies is now nonspecific, the rapidly advancing understanding of GBM genetics has enabled unparalleled pharmacogenomic investigations, and highly targeted and safer effective treatments are soon to be available [171]. Y chromosome, 1p, 6q, 9p, 10p, 10q, 13q, 14q, 15q, 17p, 18q, 19q, 22q, and other chromosomes have all shown common regions of loss, according to recent comprehensive genetic screenings of GBM. In addition, GBM has shown gains in gene expression brought on by genetic changes, such as whole-chromosome duplication, intrachromosomal allele amplification, extrachromosomal amplification, and activating mutations.

GBMs may have at least four DNA repair pathways that may eliminated, including Nucleotide Excision Repair, Mismatch Repair,Base Excision Repair, and direct reversal of lesions in recombination. Methylation of promoter CpG islands, which shown in gliomas, may lead to loss of MGMT expression.

Recent genome-wide association studies have provided additional insights into the genetic abnormalities of GBM. Gene expression profiles of gliomas may be a better predictor of survival than histology. Using automated network-based approaches with TCGA data, discovered a new driver candidate gene AGAP2/CENTG1 that can activate the PI3K pathway. It is being investigated how to discover medicines that focus on some of these oncogenic events using gene delivery technologies such viral vectors, nanoparticle structures, expression plasmids, and liposomal preparations, Comprehending the full scope of the molecular pathways behind the genetic anomalies in GBMs [172].

2.14.1 Pharmacogenomic Aspects of Anti- Cancer Peptides and Bacteriocins

Gene expression signatures provide administrative tools to address the demand for personalised medicine of glioma patients including future therapeutic applications of anti-cancer peptides and Bacteriocin. A modern concept of personalized medicine to treat various cancers is mainly focused on anti-cancer peptides and Bacteriocin the potential use of Bacteriocin in cancer therapy is due to their inhibitory effects on DNA synthesis complexes and membrane proteins, which cause cytotoxicity or apoptosis of tumor cells. These are antimicrobial peptides produced by a wide range of bacteria. In order to overcome chemotherapeutic drug resistance, Bacteriocin have robust tissue penetration capacity with efficient potential uptakes by cancer cells synergized with intrinsic activity [173].

Bacteriocin exhibit immune-modulatory role and dampen the PAMPs (pathogen-associated molecular patterns) associated inflammatory effects by regulating cytokines levels. They play key role by up- regulating anti-inflammatory cytokines expression and mitigating proinflammatory cytokines by regulating the activation

of certain pathways, such as nuclear factor kappa-B (NF-κB) signaling pathways during microglial activation in glioma [174].

Cationic peptides have unique properties that make it possible for them to cause the death of tumor cells, making them increasingly recognised as promising anti-cancer drugs. Pyocin, colicin, pediocin, and microcin are some of the bacteriocins that have been reported with antitumor activities. Furthermore, modified bacteriocins have been claimed to treat effectively glioblastoma xenograft mouse model [175]. Wide range of *in-silico* and Computational approaches can augment anticancer peptides and Bacteriocin based drug discovery to downregulated certain inflammatory culprit markers responsible for cancer onset, progression, metastasis, immune evasion, and drug resistance [176].

2.14.2 NISIN: An Anticancer Peptide/ Bacteriocin

The gram-positive bacterium *Lactococcus lactis* naturally produces the 34-amino acid polycyclic antimicrobial peptide known as NISIN during fermentation. It is effective against both Gram-Positive and Gram-Negative bacteria, which makes it a promising target for use in pharmaceuticals, veterinary, and health care products, in addition to its role as a food preservative. The Food and Drug Administration (FDA) and WHO both approved NISIN for use in humans in 1969 and 1988, respectively. The FDA has recognized NISIN as a safe option. NISIN consumption per individual in the US is thought to range between 0.94 to 2.24 mg per day [177].

Despite the fact that bacteriocins like NISIN have been in use for several years to prevent germs from growing on food, they have only lately been studied to inhibit the growth of cancer cells or trigger apoptosis. Apoptosis is a procedure that gets rid of surplus or old cells, but since cancer cells are resistant to it, it's important to formulate new drugs that can trigger apoptosis in cancer cells. The earlier investigation focused at NISIN's impact on an astrocytoma cell line's proliferation and apoptosis (SW1088). [175].

In head and neck squamous cell carcinoma (HNSCC) cells, NISIN preferentially induces apoptosis, arrests the cell cycle, and decreases cell proliferation as compared

to primary keratinocytes. In vivo, NISIN also inhibits the growth of HNSCC tumors. The interaction of NISIN with the cellular membrane alters the integrity of the membrane and creates transient holes, which in turn mediates reorganization of phospholipid and permits an inflow of ions [178]. Specifically, cation transport regulator homolog 1 (CHAC1), a proapoptotic cation transport regulator, as well as a concurrent extracellular calcium influx are how NISIN causes these effects on HNSCC. However, CHAC1 is not required for these effects to occur. These findings collectively imply that NISIN may be a viable cancer treatment agent, and further investigations are warranted to explore its potential as a therapeutic agent [179].

2.15 Drug Repurposing in Glioma and NSAIDS

The field of drug repurposing in neuro oncology has been shown promising role, with several commonly used medications such as statins or NSAIDs being investigated for their potential impact on glioma survival through various biological mechanisms, including targeting of the mevalonate or cyclooxygenase pathways. However, prior studies investigating the use of these medications in glioblastoma patients have yielded inconclusive results, with some indicating improved survival while others showed no improvment [180]. The cyclo-oxygenase (COX)-2 enzyme is essential for the metabolism of arachidonic acid, which produces prostaglandins. Prostaglandin production and COX-2 expression have been linked to carcinogenesis and tumor progression, and other brain disorders. It has been demonstrated that eicosanoid biosynthesis inhibitors increase astrocytic differentiation and reduce proliferation in glioblastoma cells [181]. Previous studies have shown that selective (COX-2 Inhibitors), such as celecoxib, exhibits growth-inhibitory effects and induce apoptosis in a variety of cancer cell lines, which has sparked a lot of interest in them as safe and efficient anticancer treatments. Additionally, *in vitro* analysis were performed to investigate the possible impact of the selective (COX-2 Inhibitor) on the growth, migration, and suppression of COX-2 expression in glioma cells [182].

Chapter 3

Research Methodology

3.1 Reagents and Chemicals

DNA Extraction Kit, RNA extraction kit, DTT, cDNA synthesis kit, agarose, RNase-Zap, DEPC treated PCR water, PCR master mix, Real Time PCR Master Mix Kit, RNA Later, DNA Loading dye, 100 bp DNA ladder, ethidium bromide, ultra-pure distilled water, cell culture grade, ethanol, isopropanol, TAE, Taq-1.5 U (Ferments), Sense and Antisense primers (0.5 μmolperl), MgCl2 (50 mmolperl), d.NTP (0.2 mmolperl), and DNA-template (1. μg). ELISA- Kit (AB.CAM), polystyrene plates, typically in 96-well plates, Primary and/or Secondary Detection Antibody, Analyte/Antigen, Coating Antibody/Antigen, Buffer, Wash, and Substrate/Chromogen. IHC reagents (Deionized and distilled water, Xylene, Ethanol, anhydrous denatured, histological grade (100, 95, 80, and 70%), Hematoxylin solution, Tacha's Bluing solution: for bluing hematoxylin Stained Nuclei, Wash Buffers: follow vendor recommendations. Antigen Retrieval Buffer, Depends on specific antigen retrieval method: for HIAR e.g. 10X Antigen Decloaker (Bio.care, Pacheco, C.A, U.S.A) diluted 1:10 with deionized water,0.1% TBS-Tween,3% hydrogen peroxide (for blocking endogenous peroxidase); Use peroxidase blocking solution to reduce background staining (Bio.care, Pacheco, C.A, U.S.A),Slides with adhesives for tissue retention, Western blott

(AB.CAM), lysis- buffers, NP-40 buffer, RIPA-buffer (radio immunoprecipitation-assay- buffer), Tris-HCl, Laemmli.2X.buffer/loading-buffer, Running-buffer (Tris-Glycine/SDS), Transfer.buffer (wet), Transfer buffer (semi-dry), Blocking-buffer (3–5%) milk or BSA (bovine serum albumin),Antibodies.

3.1.1 Consumables

2mL screw cap tubes, Real time PCR plates, PCR tubes, Falcon tubes, DNA/RNA free tubes, P10, P100, P1000 tips boxes RNase, DNase free, petri plates, ependrof tubes, PCR tubes, blotting paper.

3.2 Design Procedure and Ethical Statement

This study was a retrospective cross-sectional series to include patients diagnosed with brain tumor in Pakistan. This study was intended to collect clinical data from selected age group for glial brain tumors including histopathological findings, which would determine the national prevalence and incidence of these tumors. Tissue samples from surgically resected glioma tumors were compared to matched samples for other diseases (ODC) by gender and age.The Capital University of Science and Technology (CUST), Islamabad, Pakistan, granted approval for the study,which followed the Declaration of Helsinki's guidelines (Ref: BI&BS/ERC/19-2 and September 23, 2019). 55 glioma patients (mean age, 35 years) who underwent brain surgery between January 2018 and December 2021 had their biopsy samples collected from various surgery departments of public sector tertiary care hospitals in Pakistan. 55 glioma patients (mean age, 35 years) who underwent brain surgery between January 2018 and December 2021 had their biopsy samples. The Clinical data and patients MRI scans were collected from tertiary care settings of Neuro departments Pakistan. Patient's glioma sample was collected against written informed agreement to participate in the study along with patient information. Follow-up data were collected using medical records and patient follow-up visits.

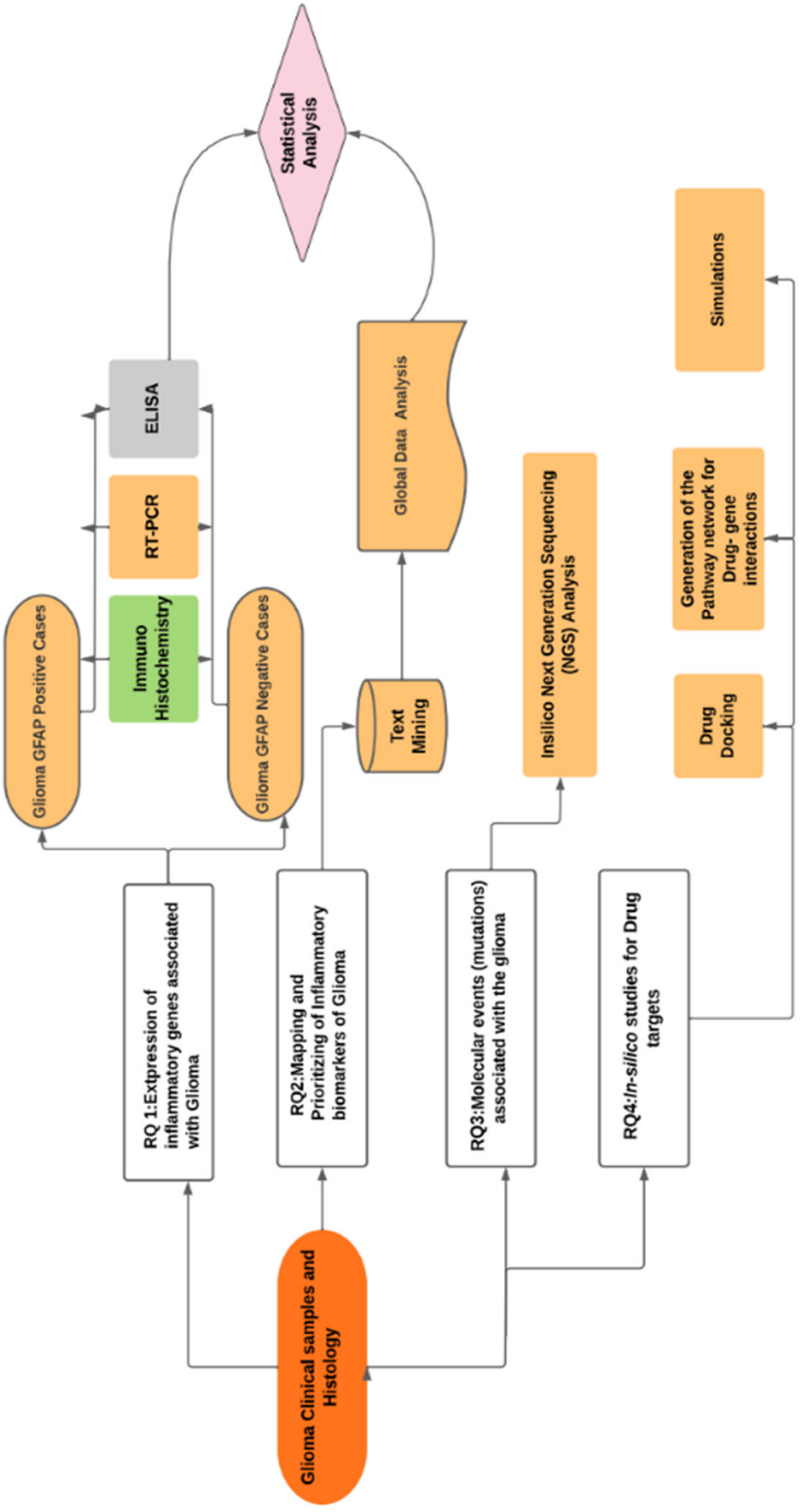

FIGURE 3.1: Flow chart of methodology

3.2.1 Inclusion Criteria

The inclusion criteria for the sampling of disease cohort (glioma patients) were considered as follows:

1. Newly diagnosed glioma tissue biopsies confirmed on the basis of Immunohistochemical and radiological findings
2. Histopathological verified diagnosis according to 2016 WHO classification
3. Eligible ages for Study including the patients with: 18 years and older (Adult, older Adult)
4. Gender eligible for current Study: All
5. Control Biopsies = Tumor Associated Normal Tissue (TANT) minimum ≈ 10
6. Sampling Method: Non-Probability Sample
7. Chemotherapy status Both type of glioma patients whether underwent chemotherapy or not

3.2.2 Exclusion Criteria

- Presence of Brain cancers other than glioma
- Gliomatosis cerebri
- Patient's glioma size less than 2 cm^3
  - Ages less than 18 years
- Impact of complex comorbidity leading to systemic disorder in the study.
- • Second primary malignancy (With the exception of treated basal cell carcinoma of the skin, in situ cervical cancer, past malignancy treated more than 5 years before to enrolment without recurrence, or T1 vocal cord cancer in remission.)

- Any types of body cancer metastasized to brain
- Pregnancy

3.3 Wet Lab Analysis

Expression profiling of inflammatory genes **(IL-1β, IL-6, IL-8, IL-10, TGF-β, TNF-α, NF-κB and sIL-1Ra, GCSF, GCSFR and STAT3)** had been done by quantification techniques and were also compared by globally available datasets of glioma cases through integration of advanced bioinformatics tools.

3.3.1 MRI Imaging

Each patient underwent an intraoperative MRI scan for trajectory planning on a 3 Tesla MRI scanner (Siemens AG Healthcare, Erlangen) for the diagnosis and confirmations of glioma grades under the following circumstances: The specs are 260mm x 260mm FoV, 1.03mm3 voxel size, and 256x256 image matrix [183].

3.3.2 Patients Clinical Samples

3.3.2.1 Tissue Samples Specifications

The samples were initially obtained from patients primarily from the affected brain regions, specifically the frontal and temporal sites of the primary tumor, through surgical resections. The collection of tumor tissue samples was conducted by considering variations in cellularity and the presence of necrotic areas in patients with glioblastoma multiforme (GBM). Tumor-associated normal tissues (TANT) were typically obtained from the region adjacent to the tumor mass [184, 185]. The minimum weight required for processing, as per internal guidelines, includes "125" mg of tumor tissue and "50" mg of adjacent normal tissue. Volumetric measurement was utilized to assess the size of GBM tumor samples. The tissue

specimens were sectioned into small fragments, (approximately 1-2 mm^3 in size), through the utilization of a sterile scalpel. These fragments were subsequently subjected to preservation techniques involving formalin fixation and later paraffin embedding (FFPE) for the purpose of histopathological examination and immunohistochemistry. Additionally, the tissue fragments were appropriately stored at ultra-low temperatures (–80^{o}C) in order to maintain the integrity of nucleic acids and proteins and prevent degradation [186, 187].

Human glioma tumor samples (total = 55) were collected of patients undergoing tumor resection. None of the study subjects had received any radiotherapy or chemotherapy prior to sample collection. The samples were preserved in RNA later at 4^{o}C for 1-3 days and later on were stored at –80^{o}C. Another portion of the excised tissue was fixed in formaldehyde solution and embedded in paraffin for histological evaluation [188]. Classification of all tumor samples were ensured as per recommendations of WHO malignant tumor grade types [189].

3.4 RQ1: Expression of Inflammatory Genes Associated with Glioma

3.4.1 Histopathological & Immunohistochemically Confirmation of Glioma

The glioma samples to be investigated in this research work will consist of human 55 biopsies obtained during brain cancer resection procedures. After the Resection process,A distinct section of the resected tissue was preserved in formaldehyde solutions, samples were dehydrated and embedded in paraffin blocks for histological evaluation. FFPE blocks was mounted in microtome and sliced into 4 μm thick slices. At last, the slices were rehydrated followed by hematoxylin and eosin staining. Hematoxylin and eosin-stained slices underwent light microscopic examination to confirm the histological diagnosis [190]. All the samples were diagnosed by histopathologist as glioma, according to WHO classification system of

brain tumors. The expression of Glial fibrillary acidic protein (GFAP) through Immunohistochemical staining using FFPE tumor blocks were carried out.Sliced tissue slices were deparaffinized in xylene for this purpose and hydrated by soaking in ethanol. Sections were placed in epitope retrieval solution for antigen retrieval and incubating them with combinations of GFAP antibodies [191, 192].

3.4.2 Screening of Clinical Samples

The glioma samples were screened on the basis of expression of Glial fibrillary acidic protein GFAP through immune histochemistry. Two cohorts were differentiated on the bases of GFAP-positive and GFAP-negative, to analyze the expressed of inflammatory genes in the respective cohorts.

3.4.3 RNA Isolation and cDNA Synthesis

Total RNA was isolated using triazole method. First the sample was homogenized by homogenizer and the manual RNA extraction was carried out through triazole method. Subsequently, cDNA was synthesized through reverse transcription with oligo dT primers using Super Script II. Synthesized cDNA was quantified on nanodrop spectrophotometer [193].

Table 3.1: Primers

Genes	**Forward Primer**	**Reverse Primer**
IL-8	AAG AGA GCT CTG TCT GGA CC	GAT ATT CTC TTG GCC CTT GG
IL-6	ACT CAC CTC TTC AGA ACG AAT TG	CCA TCT TTG GAA GGT TCA GGT TG
IL-1β	AGC TAC GAA TCT CCG ACC AC	CGT TAT CCC ATG TGT CGA AGA A
IL-10	TGC CTA ACA TGC TTC GAG ATC TCC G	TTA GAG GGA GGT CAG GGA AAA CAG C

Genes	**Forward Primer**	**Reverse Primer**
sIL-1Ra	GGC CTC CGC AGT CAC CTA ATC ACT CT	TAC TAC TCG TCC TCC TGG AAG TAG AA
TGF-β	CAA TTC CTG GCG ATA CCT CAG	GCA CAA CTC CGG TGA CAT CAA
TNF-α	CCT CTC TCT AAT CAG CCC TCT G	GAG GAC CTG GGA GTA GAT GAG
NF-κB p65	AGG CAA GGA ATA ATG CTG TCC TG	ATC ATT CTC TAG TGT CTG GTT GG
GCSF	GTG CCA CCT ACA AGC TGT GC	AAA GGC CGC TAT GGA GTT GG
GCSFR	AAG AGC CCC CTT ACC CAC TAC ACC ATC TT	TGC TGT GAG CTG GGT CTG GGA CAC TT
STAT3	CAT ATG CGG CCA GCA AAG AA	ATA CCT GCT CTG AAG AAA CT
β actin	CAT GTA CGT TGC TAT CCA GGC	CTC CTT AAT GTC ACG CAC GAT
GAPDH	GAA GGT GAA GGT CGG AGT C	GAA GAT GGT GAT GGG ATT TC

IL-1β,IL-6,TNF-α,βactin https://www.ncbi.nlm.nih.gov/pmc/

IL-8 https://www.ncbi.nlm.nih.gov/pmc/

GAPDH https://acsjournals.onlinelibrary.wiley.com/doi/pdf/

IL-10 https://www.ncbi.nlm.nih.gov/pmc/articles/

NF-κB p65 https://www.ncbi.nlm.nih.gov/pmc/

sIL-1Ra https://arthritis-research.biomedcentral.com/articles/

TGF-β https://www.mdpi.com/2072-6694/

GCSF,GCSFR https://www.nature.com/articles/

STAT3 https://bmcmedgenet.biomedcentral.com/articles/

3.4.4 Quantitative RT-PCR (QRT-PCR) Validation

The resulting total cDNA will be amplified through polymerase chain reaction against gene-specific primers using "SYBR Green master mix". Reaction for all sample were performed in triplicate using a PCR protocol. For each primer set, Log-Linearity of the amplification curve will be ascertained down to the range of picograms for cDNA. Specificity of PCR products were confirmed by agarose gel electrophoresis and melting curve analysis [150]. The house keeping gene GAPDH was used to normalize cDNA amount to the crossing point. Expression profiling of inflammatory genes (**IL-1β, IL-6, IL-8, IL-10, TGF-β, TNF-α, NF-κB and sIL-1Ra**) had been done in GFAP-positive glioma samples and for genes (**GCSF, GCSFR and STAT3**) in GFAP negative glioma samples by quantification techniques qRTPCR [194].

3.4.5 Enzyme-linked Immunosorbent Assay

ELISA (Enzyme-linked Immunosorbent Assays) were performed according to manufacturer's instructions. Total protein was extracted from glioma samples stored in RIPA buffer using protein extraction kit. Corresponding proteins expression of eleven mediators such as **IL-1β, IL-6, IL-8, IL-10, TGF-β, TNF-α, NF-κB and sIL-1Ra** and **GCSF, GCSFR and STAT3** were quantified respectively from GFAP positive glioma pts group and GFAP negative pts group respectively, through their respective ELISA kits. On an ELISA reader, absorbance was measured. Experiments were carried out in three replicates[195].

The known concentrations of inflammatory genes were added to the ELISA plate. The OD values obtained from the standards were used to plot a calibration curve, which interpolates protein concentrations based on their OD values. Blank correction was used to correct for background noise, and OD values obtained for each well of the ELISA plate at 450 nm as per the guidlines. Sample processing involved

homogenization of glioblastoma tissue samples, extracting proteins of interest, incubation, washing, detection, and substrate addition. The specific details of the ELISA test procedure was followed by specific kit and manufacturer's instructions (Abcam Elisa kits USA).Using the appropriate ELISA MAXTM Deluxe Set in accordance with the manufacturer's guidelines, cytokine levels were assessed.

3.4.5.1 Statistical Analysis

Statistical analysis of generated data from RT PCR and ELISA was presented as ± standard deviation. Data were analysed using one-way ANOVA and t test followed by appropriate analysis by GraphPad Prism software 9.0 depending upon the selection of cohorts for DEGs in glioma patients.The p values less than 0.05 were regarded as statistically significant. The degree of normality evaluation employed the D'Agostino & Pearson test.

3.4.6 In Vitro Study of Inflammatory Genes in SF-767 Human Glioblastoma Cell Line SF-767

3.4.6.1 Cell Line and Culture Conditions

Monolayers of the human glioma cell line SF-767 were grown in in IMDM (Iscove's Modified Dulbecco's Medium) with "foetal bovine serum" (FBS 10%), 1% Glutamine, 100 IU per mL penicillin, and 100 g per mL streptomycin combination. Cell cultures were subcultured three times weekly and kept at 37°C in a humidified 5% CO2 environment. Utilizing cell cultures at low passages, each assay using glioma cell lines was carried out separately in triplicate [196].

3.4.6.2 MTT Cellular Proliferation Assay

The antiproliferative impact of the therapy was assessed using the MTT assay (Roche Diagnostic GmbH, Basel, Switzerland). This method was used alongside other assays (RT-qPCR and ELISA or techniques) to investigate the influence of

inflammatory processes on cell viability. The Yellow Tetrazolium Salt MTT[3-(4,5-dimethylthiazol-2-yl)-2, (5-diphenyl- tetrazolium -bromide)] can only be broken down into purple formazan crystals by metabolically active cells. Three repetitions of 10000 cells/well in 200 μL medium were used to seed the 96-well culture plates.In each well About (10. μL) of MTT reagents were added following each treatment, and the plates were then incubated at 37°C for 4 hours. A spectrophotometer set at $\lambda = 595$ nm was used to measure the optical density (OD) after the cells had been lysed with 100 μL of solubilization buffer. Results are given as percentages compare to the control [197]. The mean values acquired from the cell viability studies were statistically compared using the Student's t-test in Microsoft Excel with one-tailed distributions. The analysis of variance (ANOVA) and t-test were used to examine the significance of differences between study groups. Statistics were judged significant for values with $p < 0.05$. Results are demonstrated as the MSD (Mean Standard Deviation)for all data. Each study was carried out in triplicate.

3.5 RQ2: Mapping and Prioritizing of Inflammatory Biomarkers of Glioma

3.5.1 Text Mining

Mapping of candidate genes was done by text mining system. Global inflammatory genes associated with glioma were extracted for comparison with local biomarkers through text mining-based web services. Since 2010 until the present, the Core Mine platform (https://www.coremine.com) and PubMed has been used for the massive biological data integration of glioma associated inflammatory genes, their analysis, and the identification of underlying mechanisms involved in disease progression. This platform was employed as a query-based analysis method for glioma therapeutic targets and diagnostic gene markers. It was also used to obtain all the inflammatory gene names discovered in the literature that was already available and pertinent to the search topic [198]. The term "glioma" was searched, and the

results were used to screen all the inflammatory genes related to the term. For the following stage of the research, the globally acquired differential gene set was further intersected with the gene set discovered using text mining.

3.5.2 Transcriptomic Profiling

"The Cancer-Genome-Atlas" (TCGA), Gene Expression Profiling, Interactive Analyses GEPIA2, Genome Tissues Expression Database (GTEx), and Microarray gene database GEO were used with the integration of c-Bioconductors R packages with servers, i.e., [199], to investigate the differentially expressed genes (DEGs) in glioma patients.

3.5.2.1 Data Acquisition Extract

In current study we collected 620 glioma cases from four public datasets in the current study in order to make comparative meta-analysis with tissue biopsy samples. The Cancer-Genome-Atlas (TCGA), Genome Tissues Expression database (GTEx), gene expression profiling and Interactive Analyses GEPIA2, and other bioinformatics tools and databases were used to conduct the studies (http://gepia.cancer-pku.cn). We obtained RNA Sequencing Expression Data for 207 healthy brain tissues and 163 glioblastoma patients from TCGA and GTEx, respectively. Includes 252 samples of the microarray dataset from the GEO database. We used GEPIA2 to validate the differential analysis of the expression of "IL-1β, IL-6, IL-8, IL-10, TGF-β, TNF-α, NF-κB, sIL-1Ra, GCSF, GCSFR, and STAT3," as an indicator of the degree of DEG expression, we plotted the results using a boxplot with log2 of transcript count per million. To calculate p-values, Log2FC— Cutoff was used. The q-value cutoff was set at 0.01 and the log2FC— Cutoff value was modified to 1.

3.5.2.2 Microarray and RNA-Seq Data Screening and Normalization of Inflammatory DEG for Transcriptomic Analysis

To investigate the (DEG) (Differentially Expressed Inflammatory Genes) in patients of glioma, we collected 252 cases of glioma from the (Dataset.GSE16011) microarray database (www.ncbi.nlm.nih.gov/geo./query/acc.cgiacc= GSE16011) profile of gene expression of GSE16011 was downloaded from (GEO- database). Based on Agilent GPL8542 platform (Affymetrix-GeneChip-Human Genome-U133-Plus-2.0 Array).Genes that express deferentially in High-Grade and Low-Grade gliomas are found by GEO2R. RNA-sequencing data from (GBM) samples (dataset ID: TCGA-GBM) and htseq counts were also downloaded from the "TCGA" database (https://www.cancer.gov/) are included in the other validation sets. The dataset included 5 samples of paracancer tissue (brain tissue that is positioned next to malignant tissue) and 156 samples of glioma tissue. We used the integrated online programmes UALCAN and iDEP 0.9330, hosted at http://ge-lab.org-idep/, for data pre-processing and log transformation of normalized expression values. When it comes to parameter selections, we selected a |log2.FC| (cutoff of 1) and a q-value cutoff of 0.01 as well as log2(TPM + 1) transformed expression data for plotting, TCGA tumors compared to TCGA normal, and GTEx normal for matched normal data in plotting. For the examination of differential gene expression, we also applied the ANOVA statistical technique. TPM normalization for gene expression analysis was utilized by UALCAN and GEPIA2. DEGs were found using the DESeq2 method and the microarray data set (a minimum fold-change of 2 and a false discovery rate (FDR) cut-off of 0.05). This reduced the false positive rate and false discovery rate. Additionally, among the DEGs, 11 inflammatory genes with substantially differential expression and greater connection were chosen as hub genes.

3.5.3 Protein Interactions & Gene Enrichment Ontology

The g: Profiler and David servers were used for gene ontology investigations [200, 201]. GO was used to find important signaling pathways and biological components

of differentially expressed genes. PPIs (protein-protein interactions) were used to investigate variations in biological function. STRING.v.10 and Metascape were employed to identify the source gene's intrinsic interactions [202]. In addition, information about the GBM target genes' activities was obtained from a number of databases, including PubMed, CTD, OMIM and PubMed, [203]. To illustrate the network used to look into the significance of sources (DEGs) and targets proteins in patients with glioblastoma ,Cytoscape version 3.6 software and Gene-MANIA and were used. [204, 205].

3.5.4 Integration of Modelling and Pathway Enrichment

With statistically significant p-values 0.05, we used the Shiny GO Tool and Fun-Rich Tool version 3.1.3 to examine the route enrichment of DEGs [206, 207]. Using the Reactome, "Kyoto Encyclopedia of Genes and Genomes" "KEGG", and "Wiki pathways", putative biomarkers were curated and mapped [208]. The biological and signaling pathways of potential biomarkers were put back together using the PathVisio3tool [209].

3.5.5 Analysis of Infiltrative Immune Cells

To investigate the Infiltration of different Immune Cells and their clinical impact, the immune cell correlation study of mostly involved DEG from two groups GFAP-positive and GFAP-negative groups in high grade gliomas were carried out using the immunede-conv package in R and the CIBERSORT.x approach via the TIMER-2.0 server. After configuring batch correction, starting "Bulk-mode," and selecting the (quantile- normalization-process), sample data were purity-corrected as needed. Then, correlations with a Spearman's (p value,0.05) were shown. The Wilcoxon rank-sum test was used to evaluate the differences between the two groupings [210].

3.5.6 Survival Analysis

Based on the optimal cut-off, we divided GBM samples into high and low GBM classes using the R package surv Misc and the gepia-2 software. The relationship between the expression of the GBM-associated genes under investigation and A log-rank test, a Kaplan-Meier analysis, and a survival package were used to study survival . A p-value of 0.05 or less was deemed to indicate statistical significance [211].

3.6 RQ3: Molecular Events (Mutations) Associated With the Glioma

3.6.1 Next Generation Sequencing (NGS) Analysis

3.6.1.1 Data Collection

The TCGA database had 163 tumor samples and 207 normal samples in the glioblastoma data. We only used samples for which data for the Driver dbV3 database contained the four genomic platforms of expression of RNA, mutation in genes, CNV, and gene fusion.Recent TCGA RNA and exome sequencing data were downloaded via the GDC data portal (https://portal.gdc/.cancer.gov/), and they were pre-processed using the Driver DBV3 portal.This portal includes the TCGA 2BED tool, for Methylation data from fire-hose (https://gdac.broad-institute.org/), for TCGA R package, "TCGA bio links" and CGC, which was collected from COSMIC (cancer.sanger.ac .uk/census) and the NCG 6.0 database, was used to define cancer-related genes. These pairs' mutation and CNV data were obtained through the data portal. Using the Pathway Mapper database, the representing genes of eleven traditional Pan-cancer signaling cascades/pathway were obtained [212]. In the DriverDBv3 online datahub, at least seven algorithms (or 50 percent of all algorithms) predicted the driver genes that were the subject of this investigation [213].

3.6.1.2 Screening and identification of Driver Genes by Mutational Analysis

Eight computational techniques were used by DriverDBV3 to locate cancer driver genes. All mutations are used to identify driver genes by four approaches that are based on mutation frequencies: MutsigCV, OncodriverFM, Simon, and ActiveDriver. The sub-network based approaches were implemented using MEMo, Dendrix, MDPFinder, and NetBox. The DriverDBv3 database's 15 well-known driver geneX prediction methods were then utilised to determine the 80 driver genes. Genes identified as driver genes by more than seven-algorithms are what we refer to as driver genes [214].

3.6.1.3 DNA-Level Differences and Mutation Annotation

In our study, the glioblastoma driver gene TGFB1 and 10 genes associated with pathways involved in oncogenesis were evaluated for DNA-level alterations like CNV, gene mutation, and fusion of genes. For each subtype, a thorough investigation of the prevalence of DNA changes and the number of samples with DNA changes was conducted. All mutations were mapped to well-known databases, and a variety of bioinformatics tools are displayed in the Annotation module to estimate the functional effects of these changes [215]. DriverDBV3 uses data gathered from numerous databases, including NHL.BI GO ESP, 1000-genomes, db-SNP, COSMIC, ClinVar (http://www.ncbi.nlm.nih.gov/clinvar/), NHGRI GWAS catalogue, HGMD-PUBLIC, and OMIM (http://omim.org/), to annotate known variations.We used SnpEff and VEP to predict the impact of each mutation, including , stop gained/lost, on synonymous coding, and frame-shift. Also, we assigned a Driver Score of 7 to each mutation based on the 7 algorithms that classify the mutation as harmful.

3.6.1.4 Analysis of the Genomic Landscape Mutations

The mutations of DEG (GCSF) were examined using the cBioportal database and the Active Driver DB, a human proteo-genomics database [216]. These are used to visualize and analyze multimodal cancer genetics as well as find protein post-translational modification (PTM) sites. Based on the TCGA database, cBioPortal was used to evaluate gene modifications, a list of gene types, the relationship between gene mutations and a patient's prognosis for developing GBM. The threshold for significance was fixed at 0.05 [217].

3.7 RQ4: In-silico Studies for Drug Targets

3.7.1 Utilizing the NISIN Bacteriocin Peptide Complex for Molecular Drug Docking

3.7.1.1 Visualization and Retrieval of Experimentally Reported NISIN

The target protein, GCSF (PDB: 5GW9), was provided with its crystal structure by the Protein-Data-Bank (www.rcsb.com). The Uniprot database was used to retrieve the sequence. [218]. Using the Chimaera algorithm, water molecules and heteroatoms were removed from the PDB data.

The potential anticancer NISIN bacteriocin peptide (PDB: 1WCO) was also acquired from the Protein-Data-Bank (www.rcsb.com) [219]. The protein and drug library was developed using the Molecular Operating Environment (MOE) program. Prior to energy minimization, proteins and ligands were given hydrogen atoms using the protonate 3D method in MOE to get them ready for docking. After minimization of energy, more unbounded structures were eliminated using the AMBER99 force field. The best seven configurations were selected using the force field refining technique. Protein-protein docking analyses of putative bacteriocins and the proteins that interact with them were validated using ClusPro

[220]. UCSF Chimaera was used to assess and display the docking data [220, 221] (www.cgl.ucsf.edu/chimera/download.html).

3.7.1.2 Evaluation and Validation of Models

The Procheck tool was used to confirm the overall structural geometry and stereochemical precision of the protein structure [222]. Using the Ramachandran plot statistics, the model's stability was assessed, and the validity of the residues was established. For the Ramachandran plot and Z-score analysis, four high-resolution GCSF structures with PDB ID 5GW9 were chosen [223]. As an approach to comprehend the stability and adaptability of the docked model, NMA, or normal mode analysis, was also applied. The iMod approach was used to calculate the stability level. Along with the elastic network model, deformability, eigenvalue, and covariance matrices were created [224].

3.7.1.3 Cytotoxicity Assay

The MTT test was used to calculate the cell viability percentage. A 96-well culture plate with 1×10^3 SF-767 glioblastoma cells was used, and the cells were treated to Nisin. It was used as a anti-inflammatory and an apoptotic agents, at different concentrations (1, 5, 10, 30, 60, and 100 μg/mL) during 48 hours at 37^{o}C. The cellular fraction was first labelled with MTT solution (5 mg/mL in PBS) for 4 hours before being solubilized in 50 μL of dimethyl sulfoxide (DMSO). The supernatant was then discarded. The plate also contained cells that had received PBS treatment as a negative control. The absorbance was then calculated at 570 nm using 620 nm as a reference [175].

Chapter 4

Results

4.1 Epidemiological Findings of Gliomas Patients in Pakistani Population

There were 70 patients diagnosed with different Grades of glioma by Histopathological testing during study period 2018–2021. Clinical data and sampling were done form tertiary care hospitals of Pakistan. It was estimated that approximately more than 70% cases were diffuse gliomas. In this study total 55 patients having High Grade-gliomas (Grade-III and Grade-IV) were scrutinized. And about half of these patients had Grade-4 tumor as per specified by WHO (World Health Organization). The average age of the participants were 50 $\pm$ 13 years. Most frequently affected site was frontal, temporal and parital region Of frontal lobe and spinal cord and were observed in 38.2%, 50.9% and 10.9% respectively as shown in table 4.1. When cases were stratified on the basis of histological subtypes, highly cellular tumor with increased nuclear and cellular pleomorphism, and endothelial proliferation were identified as most frequently diagnosed group of glial tumors in our cohorts (n = 55). Glioblastoma was the most common malignant tumors, with a proportion of 74.5% with (n = 41). The other most frequent histological subtype of diffuse gliomas were Grade-III (n = 14). The other type of glial tumors including Grade-I and Grade-II gliomas were excluded from the study. Through statistical analysis it was observed that There was no significant difference in ages of both the gender (P = 0.457). Nor did we record a significant difference in tumor site with respect to gender (P = 2.06). Gender was significantly associated with grade of tumor (P = 0.016) with nearly three-quarter males and females diagnosed with Grade-IV tumors. Proportion of diffuse glioma was more in males as compared to females as shown in bar chart (Figure 4.1). Males had significantly higher average tumor grade as compare to females (P = 0.05).

TABLE 4.1: Comparative clinical demographical and epidemiological variables

		Count	**Frequency** %
Gender	Male	40	72.7%
	Female	15	27.3%
Age	less than 18yrs	0	0.0%
	18yrs-45yrs	38	69.1%
	46yrs-55yrs	12	21.8%
	56yrs and above	5	9.1%
WHO Glioma Grades			
	Grade-III	14	25.5%
	Grade-IV	41	74.5%
GFAP expression	GFAP Positive	33	60.0%
	GFAP Negative	22	40.0%
Ethnicity	Asian	55	100.0%
MRI status	Yes	55	100.0%
Histo-pathologic diagnosis	yes	55	100.0%
Site_of_resection_or_biopsy	Frontal	21	38.2%
	Temporal	28	50.9%
	Parital	6	10.9%

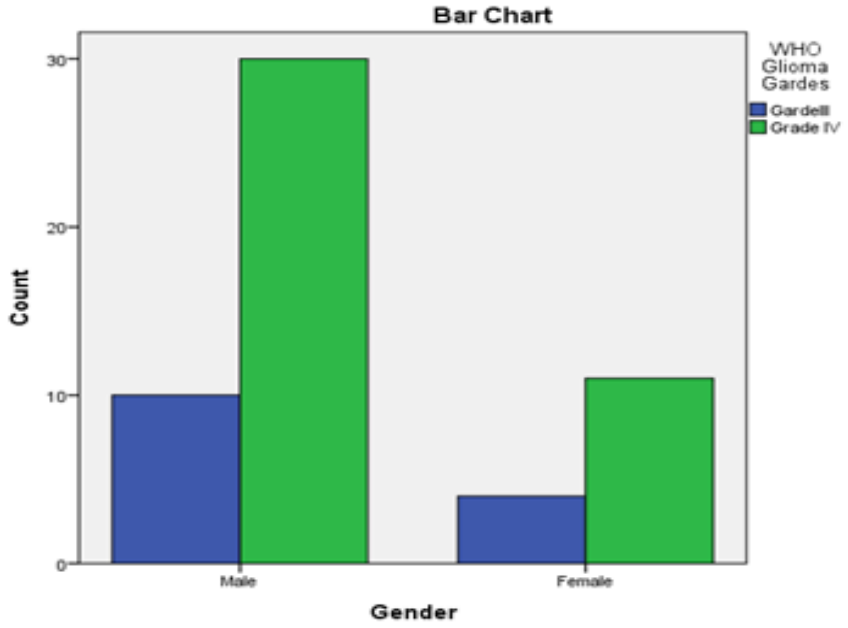

FIGURE 4.1: Descriptive frequencies in between gender and tumor Grades of glioma patients

Depicting the higher frequencies of Grade-IV in both male and female by considering P = 0.05 significant through chi-square test, and also males are significantly higher in number than females diagnosed with Grade-IV glioma.

4.2 Expression of Inflammatory Genes Associated with Glioma

Patients Clinical Samples Wet Lab Analysis

4.2.1 Gene Expression Signatures in Distinct Spatial regions of High Grade Gliomas by MRI and Histopathology

High grade Glioma tumor were characterized by Magnetic resonance imaging of axial slide of (T1-weighted MRI) after contrast administration with small areas of patchy enhancement and (T2-weighted FLAIR), obtained prior to stereotactic brain biopsy show a predominantly enhancing lesion within the left lobe with associated edema in (Figure 4.2A - 4.2B). Histopathology findings indicated that the HE staining of high grade Glioma tissues had evident atypia and deeper staining as compared to adjacent tumor associated normal tissues which showed agglomeration of less tumor cells around the periphery of necrotic regions, together with some mitotic activity and vascular growth (Figure 4.2C). While (Figure 4.2D) showed a high proliferation index, localized necrosis, hyperchromatic tumor cells in a parallel fashion, and dense cellularity at 40X magnification power. Nonetheless, there may be instances in which combinations of many lineages contribute to the tumor burden.

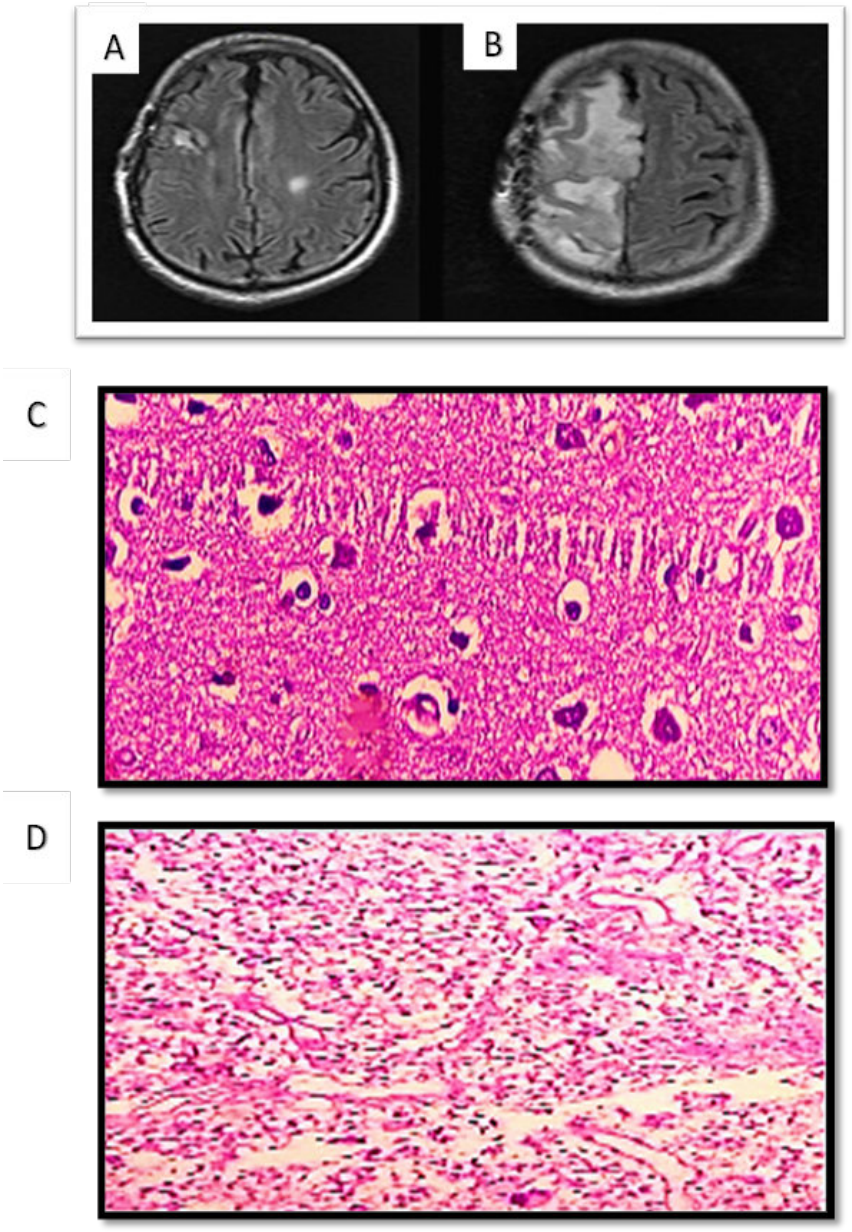

FIGURE 4.2: Gene expression signature in high grade Gliomas by MRI and histopathology

A)" Representative axial slices of T1-weighted MRI after contrast administration with small areas of patchy enhancement. B) T2-weighted FLAIR obtained prior to stereotactic brain biopsy show a predominantly enhancing lesion within the left lobe with associated edema. C) Histopathology image of TANT depicting the agglomeration of lesser tumor cells around the periphery of necrotic regions, together with some enhanced mitotic activity and vascular growth. D) H&E staining also shows the arrangement of small hyperchromatic tumor cells in a parallel fashion,

which resembles the arrangement in neuronal tumors. The images were retrieved using 40X magnification power."

4.2.2 Immunohistochemical Confirmation for Diagnosis and Grading of Positive GFAP Expression in High Grade Gliomas

Within the recruitment period, we included 55 patients with single first-ever diagnosed space-occupying lesions in the brain. Table 4.1 depicts the baseline characteristics of the study population. It also characterizes the entity of the lesions that was reached after a full diagnostic workup, including histology in almost all cases.

Thirty-three of the 55 included patients had positive GFAP expression. In view of the MRI imaging data and the clinical progression all the cases were diagnosed as having glioma. Fourteen patients had a lower grade Glioma (WHO III n = 14), and 19 patients had GBM. In our study, the Radiological findings based on 'contrast-enhanced computer tomography' (CT) revealed that the maximum cases of glial tumors were metastasisized (Grade-IV) as compared to non-enhancing Grade-(III). In the present study, glial tumors were widely reactive for GFAP (Figure 4.3A). In GBM patients, GFAP expressions were significantly correlated with tumor volume while considering p = 0.001. We compared histopathology images of GFAP positive in Grade-III and Grade-IV glioma cases and found that the 14 cases of glioma Grade-III showed less expression of GFAP as compared to Grade-IV showed high expression of GFAP it is found direct proportional to the number of cells after quantification of cell count by ImageJ as shown in figure 4.3B. Although GFAP expression is considered to decrease with higher tumor grade, specific GFAP isoforms have been detected in increased amounts, as the abundance of GFAP-δ isoform has been identified in glioblastoma cells using immunohistochemistry. GFAP expression in tissue biopsy (Figure 4.3B) were significantly higher in GBM patients compared to all other diagnostic entities ($p < 0.001$). This diagnosis was immunohistochemically proven in 33 GFAP–positive glioma cases (Figure

4.3C). ROC analysis provided a comparable diagnostic accuracy and determine the classification of Glioma grades by discriminating GFAP -positive and GFAP -negative for optimal chemotherapy. ROC analysis provided a cut-off point of $\geq$0.01 μg/L for an optimized differentiation between GFAP -positive and GFAP -negative subjects [AUC 0.789 (95%CI 0.675–0.903). The fourfold panel revealed a sensitivity of 70% to 95% to differentiate glioma cases from other diagnoses (Figure 4.3D) and Table 4.2.

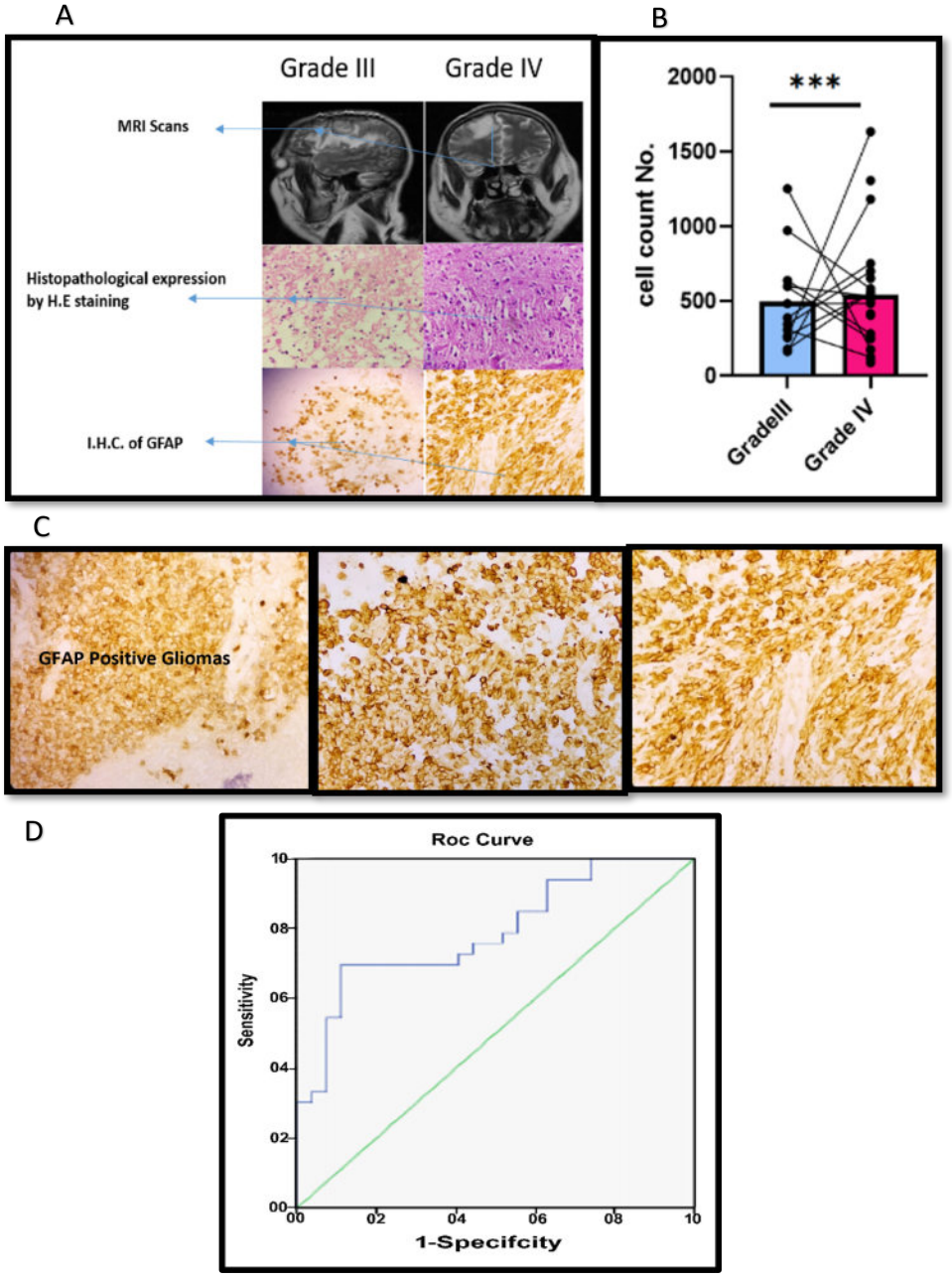

FIGURE 4.3: Immunohistochemical Confirmation of Positive GFAP expression in high Grade-gliomas

TABLE 4.2: ROC analysis provided a cut-off point of ≥0.01 μg/L for an optimized differentiation between GFAP-positive and GFAP-negative subjects [AUC 0.789 (95 %CI 0.675–0.903)]

Area Under the Curve

Test Result Variable(s): cell Count GFAP Positive Glioma

			Asymptotic 95% Confidence Interval	
Area	**Std. Error**[a]	**Asymptotic Sig.**[b]	**Lower Bound**	**Upper Bound**
.789	.058	.000	.675	.903

a. Under the nonparametric assumption

b. Null hypothesis: true area = 0.5

Table 4.2 ROC analysis provided a cut-off point of ≥0.01 μg/L for an optimized differentiation between GFAP -positive and GFAP -negative subjects [AUC 0.789 (95 %CI 0.675–0.903)].

A) MRI scan obtained prior to stereotactic brain biopsy show a predominantly enhancing lesion within the left lobe with associated edema in Grade-III and Grade-IV glioma patients. Histopathology image of Grade-III and Grade-IV glioma patient depicting the agglomeration of tumor cells around the periphery of necrotic regions, together with enhanced mitotic activity and vascular growth. H&E staining also shows the arrangement of small hyperchromatic tumor cells in a parallel fashion, which resembles the arrangement in neuronal tumors. The images were retrieved using 40X magnification power. B) Box plots showing different GFAP expressions based upon cell count in glioma Grade-III and Grade-IV at significance level p = 0.05. C) IHC staining revealing glial fibrillary acidic protein positivity in gliomas. The images were retrieved using 40X magnification power. D) Receiver operating characteristics (ROC) analysis displaying sensitivity and specificity for GFAP-positive glioma cases.

4.2.3 Quantitative Expression of Inflammatory Genes in GFAP Positive Glioma

To evaluate the potential role of IL-1β, IL-6, IL-8, IL-10, TGF-β, and TNF-α, NF-κB and sIL-1Ra in glioma, we quantified the expression of all mentioned inflammatory genes by Real Time PCR. In all genes mRNA and protein expression was significantly increased in glioma biopsy samples. We examined the gene

expression of targeted genes among glioma specimen sections within tumor and tumor-associated normal tissue (TANT). Tumor-associated normal tissue is obtained from the vicinity of the tumor site and serves as a comparison or control tissue for studying various aspects of tumor biology, including gene expression, signaling pathways, and cellular interactions. In the current study it is obtained from the region adjacent to the tumor mass.

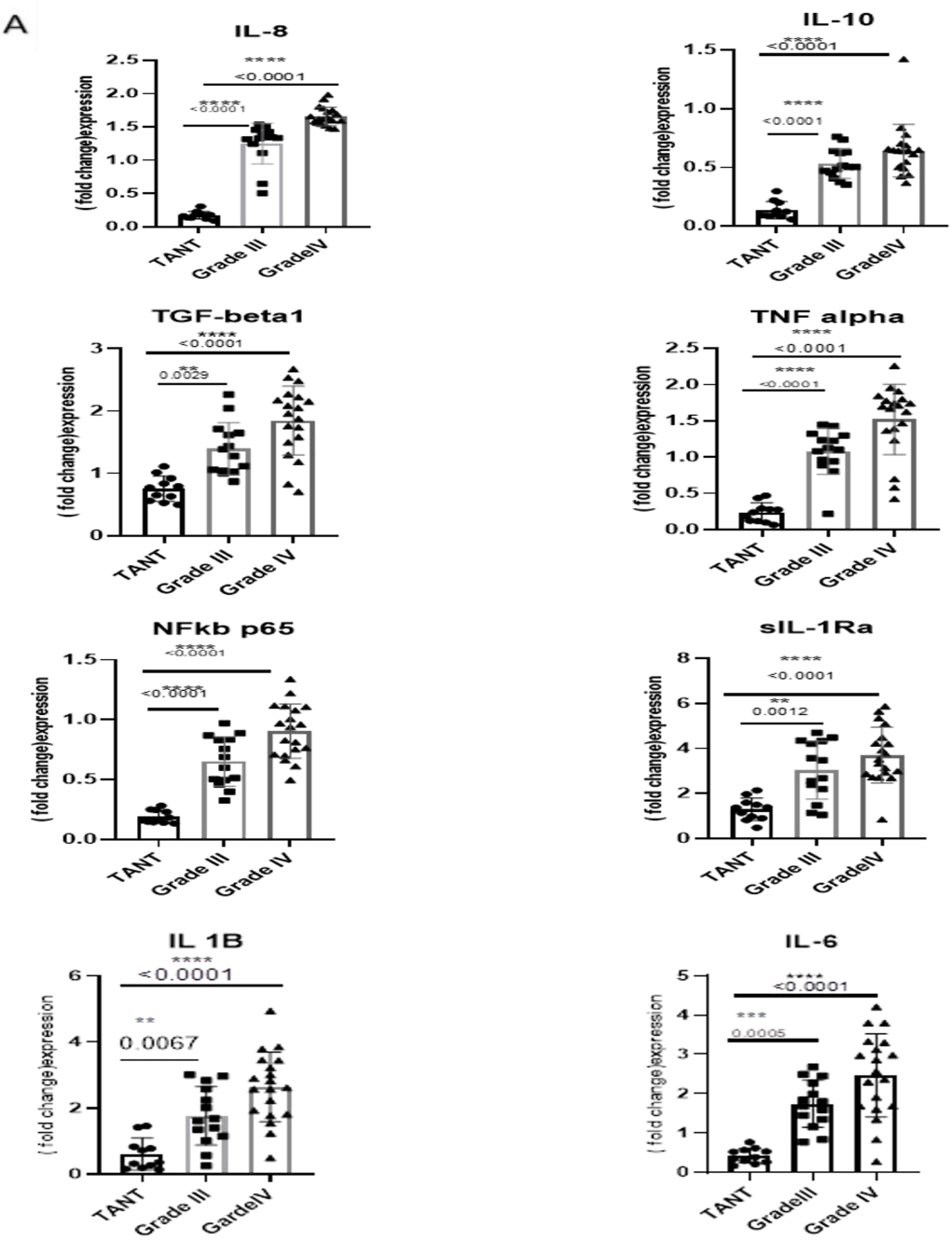

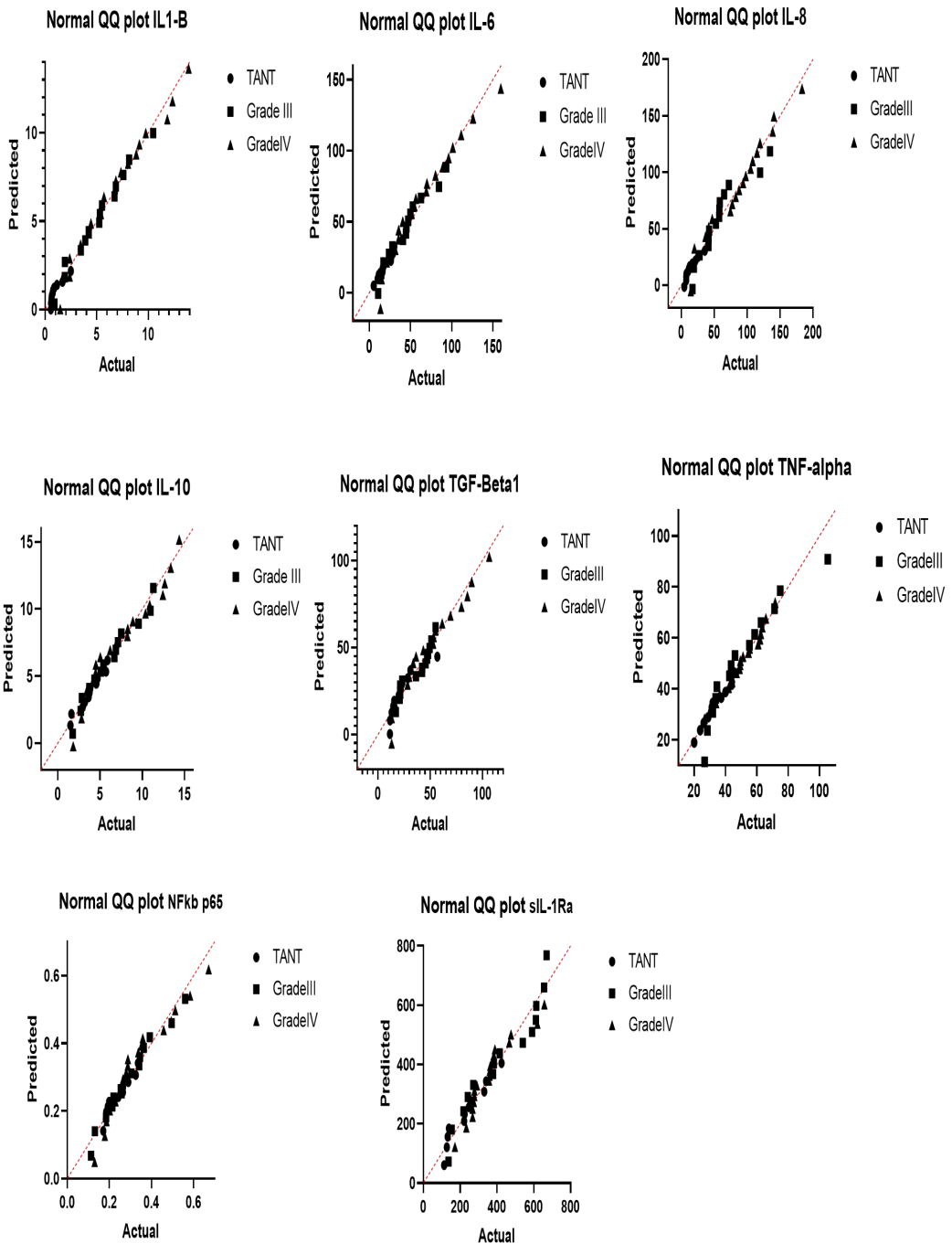

FIGURE 4.4: Quantification expression of inflammatory genes of GFAP-positive glioma patients by RT-PCR

A) Elevated expression levels of the 8 candidate reference genes (IL-1β, IL-6, IL-8,

IL-10, TGF-β, TNF-α, NF-κB and IL-1Ra) in biopsy tissue of glioma through RT-PCR.B) The values of three biological replicates are shown, indicating a univariate normality test. The graphs were plotted with the Graph Pad Prism 9 software by considering significance level p = 0.05.

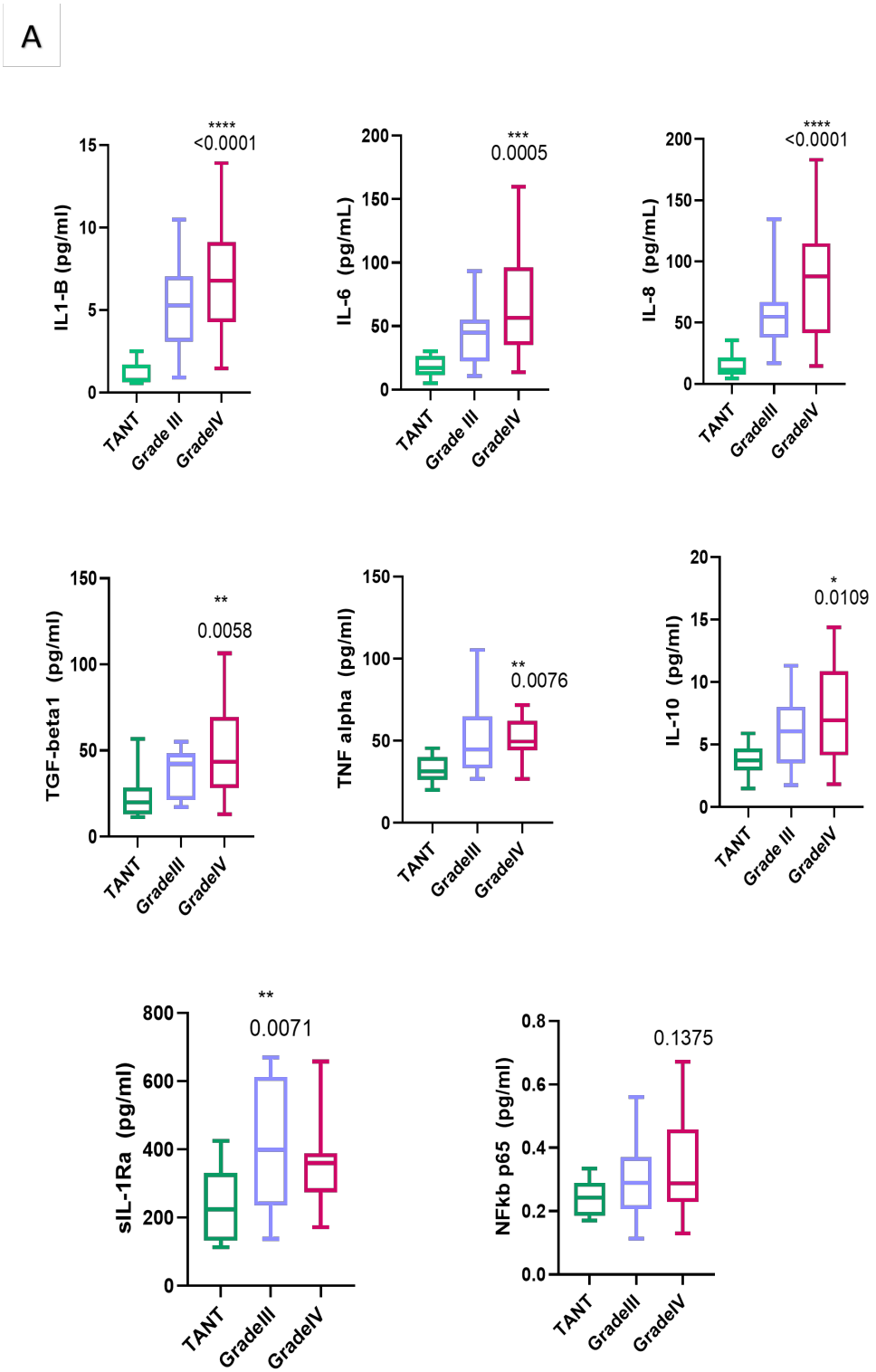

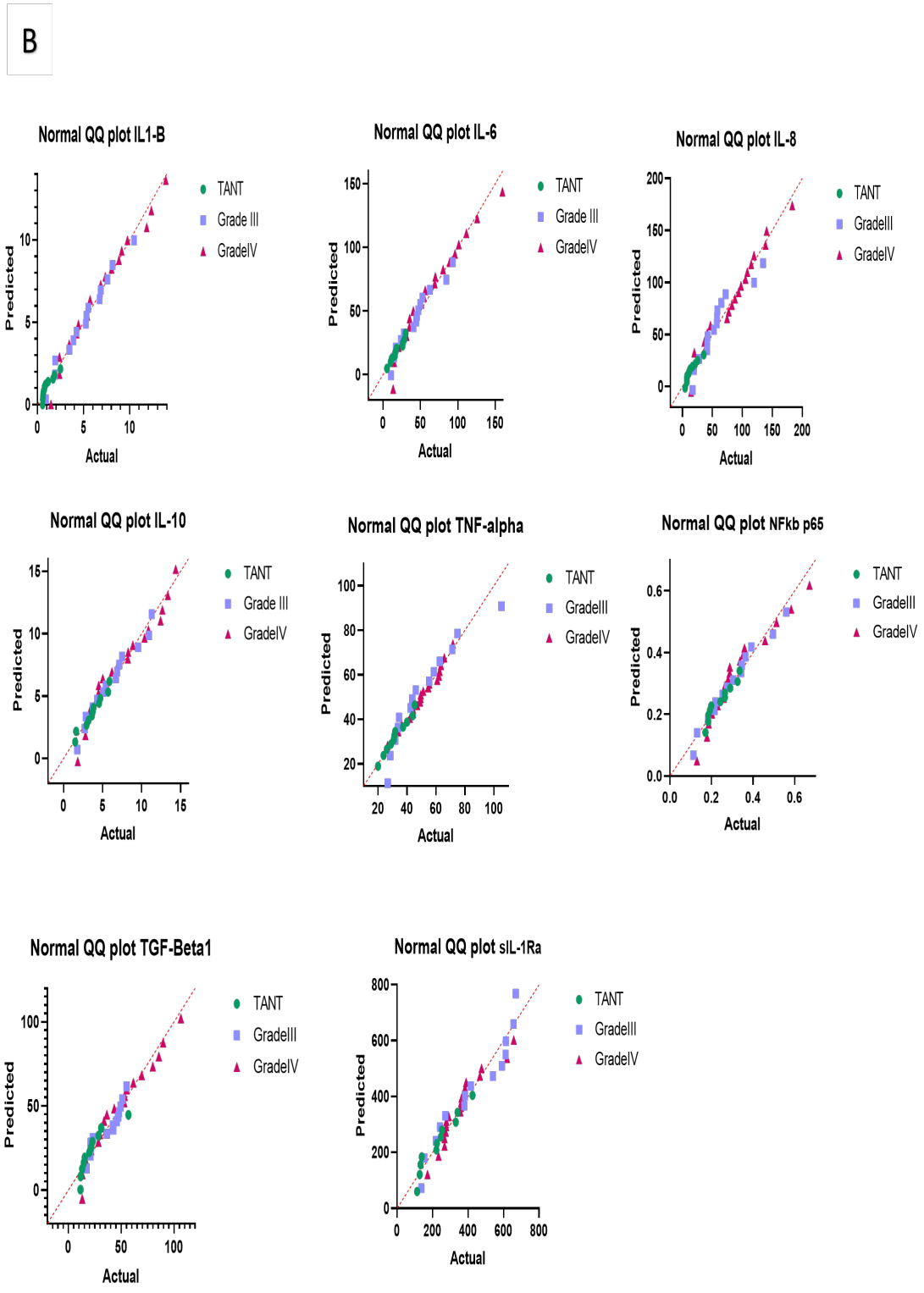

FIGURE 4.5: Quantification expression of inflammatory genes in GFAP-positive glioma patients by Enzyme-Linked Immunosorbent Assay

A) Elevated expression levels of the 8 candidate reference genes (IL-1β, IL-6, IL-8, IL-10, TGF-β, TNF-α, NF-κB and IL-1Ra) in biopsy tissue of glioma through

ELISA. B) Enzyme-Linked Immunosorbent Assay validated the expression of DEGs in glioma patients with univariate normalization. The graphs were plotted with the Graph Pad Prism 9 software by considering significance level p = 0.05.

4.2.3.1 Expression Profiling Through Heat Map Clustering, PCA, UMAP and T-SNE of inflammatory genes

Heat map and clustering by expression profile similarity demonstrated that all tumor samples clustered similarly, showing that the expression profile within a tumor specimen is preserved across the specimen. This shows that the significant variation in gene expression occurs across samples of various grades of the tumor, followed by samples of the same grade, and finally, within a specific sample. Average linkage and correlation distance in 8 rows and 43 columns were grouped. Heat maps showed that tumor cells have high expression of genes (GBM, red in color) as compared to tumor associated normal tissue (TANT, green in color) in respect to color range from green to red brown according to normalized Z-score scale ranges from 0 to 100 (Figure 4.6A). Heat map clustering showed that tumor cells have high expression of genes (GBM, red in color) as compared to tumor associated normal tissue (TANT, green in color) in respect to color range from green (TANT) to red brown according to Z-score scale -2 to 2 (Figure 4.6B). Principal component analysis (PCA) showed overall separation between the TANT (green), Grade-III (yellow) and Grade-IV (brown) of patient samples. Rows are subjected to unit variance scaling, and SVD (Single Value Decomposition) with imputation is employed to determine the major components. Principal components 1, 2 and 3 which account for 68%, 8% and 7% of the total variance, are displayed on the X, Y and Z axes, respectively (Figure 4.6C) and uniform manifold approximation and projection (UMAP) also showed separation between control and diseased samples, specifically the TANT (green color cluster), Grade-III (yellow color cluster) and Grade-IV (red brown) were clustered separately. More over the both grades of glioma showed a dispersed pattern of distribution with others patient group neighboring cluster and the TANT group showed very low variation, suggesting a high degree of heterogeneity among patients (Figure 4.6D). T-SNE scatter plot of the

samples depicts the clustering patterns of the samples according to the expression of genes. The transverse ordinates represent the principal components; the yellow and brown color in the graph represent the samples, and the green color represent the TANT showing wide heterogeneity among the samples (figure 4.6E).

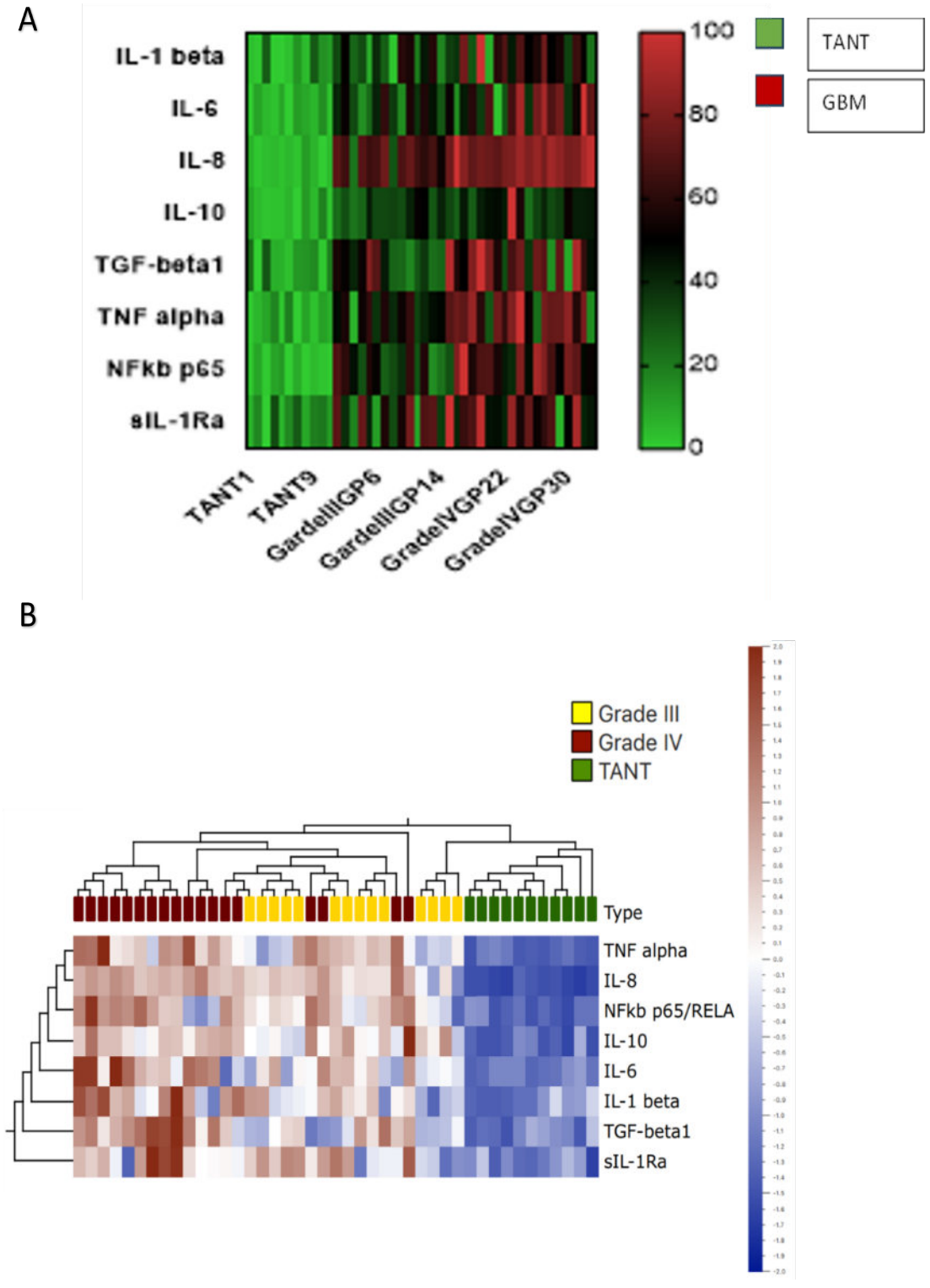

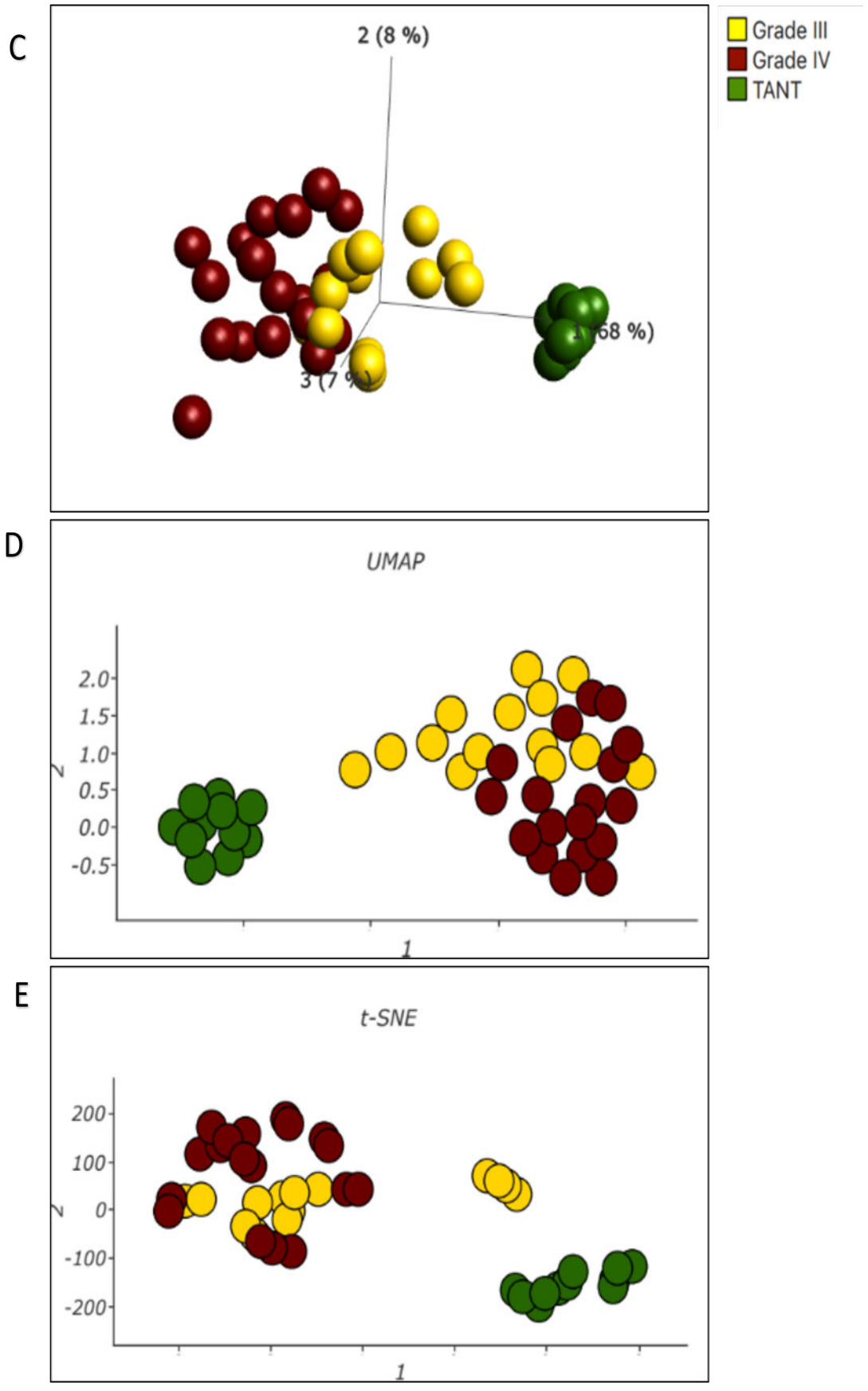

FIGURE 4.6: Expression of glioma patients through Heat Map Clustering, PCA, UMAP & T-SNE of inflammatory genes.

A) Heat Map clustering of glioma samples based on eight differentially expressed genes with the highest coefficient of variation across all samples. Rows are centered; unit variance scaling is applied to rows. Both rows and columns are clustered using correlation distance and average linkage. Heat maps colored from green to red brown according to normalized Z-score displayed on color scale 0 to 100. B) Heat Map clustering of glioma samples based on 8 candidate reference expressed genes with the highest coefficient of variation across all samples also consistent with the clustering Rows are centered; unit variance scaling is applied to rows. Both rows and columns are clustered using correlation distance and average linkage. Heat maps colored from green (TANT) to red brown (GBM) according to scale. C) Unit variance scaling is applied to calculate principal components. X, Y and Z axis show principal component 1, 2 and 3 principal component 3 that explain 68%, 8% and 7% of the total variance. D) Uniform manifold approximation and projection (UMAP) analysis showed separate clusters in between TANT, Grade-III and Grade-IV.E) T-SNE scatter plot of the samples depicts the clustering patterns of the samples according to the expression of genes. In the diagram, the transverse ordinates represent the principal components; the yellow and brown color in the graph represent the samples, and the green color represent the TANT.

4.2.4 Quantitative Expression of Inflammatory Genes in GFAP Negative High Grade Glioma (Glioblastoma) Patients

In the current study GCSF was used to investigate the GFAP marker in the GBM samples, as the expression of GCSF is correlated with the GFAP reported in the previous literature. To evaluate the potential role of **GCSF, GCSFR** and **STAT3** in high grade Glioma (glioblastoma), we quantified the expression of all mentioned inflammatory genes by Real Time PCR. In all genes mRNA and protein expression was significantly increased in glioblastoma biopsy samples. We examined the gene expression of targeted genes among glioblastoma specimen sections within tumor and tumor-associated normal tissue (TANT). All tissue samples were

initially cut from four regions of the specimen, but samples with sufficient RNA quality and quantity was subjected to RT-PCR analysis of gene expression (Figure 4.7A). **GCSF, GCSFR** and **STAT3** exhibited increased expression in tumor tissue biopsy samples. These data are also consistent with ELISA findings (Figure 4.8A). The values of three biological replicates are shown, indicating a univariate normality test both in RT-PCR and ELISA (Figure 4.7B - 4.8B).However these findings reveled inverse proportion with the expression of GFAP. **GCSF, GCSFR** and **STAT3** exhibited increased expression in tumor tissue biopsy samples.

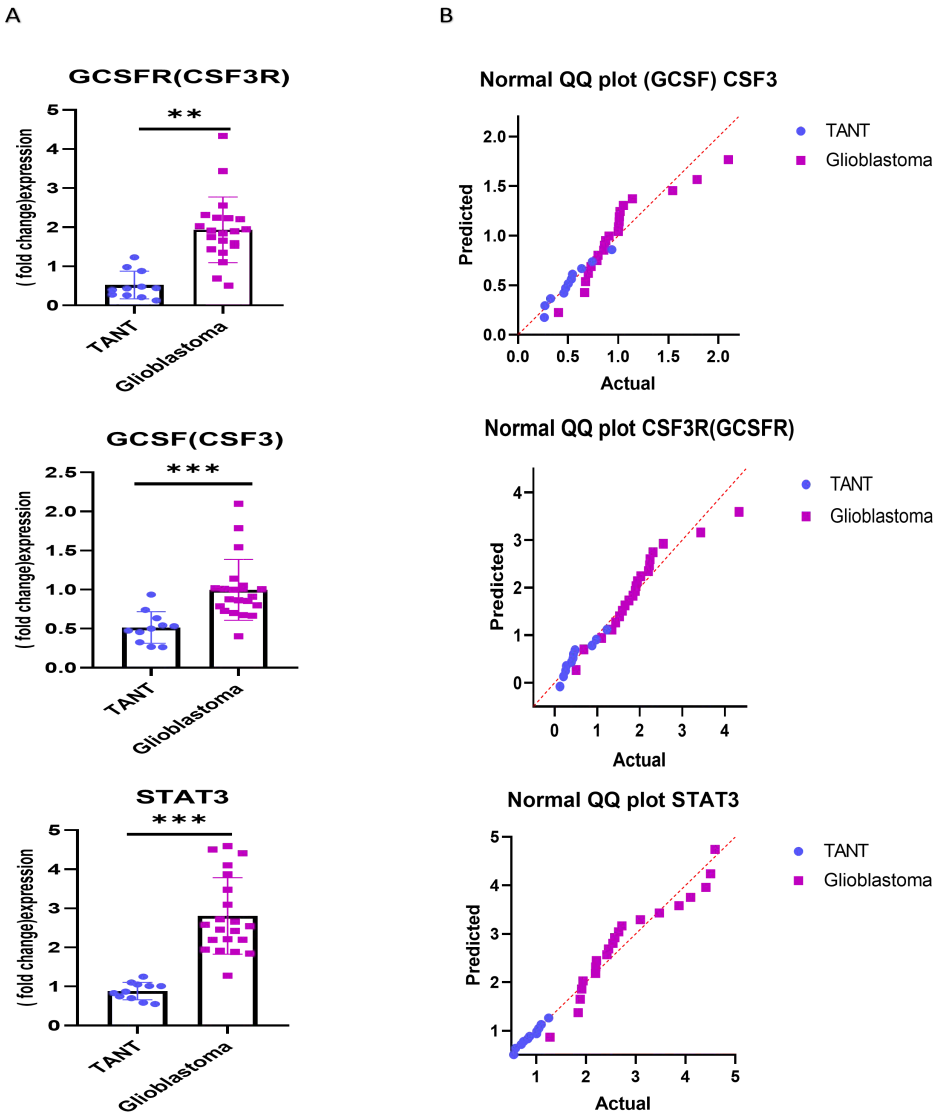

FIGURE 4.7: Quantitative expression of inflammatory genes in GFAP negative high grade glioma (glioblastoma) through RT-PCR

A) Expression levels of the 3 candidate reference genes (**GCSF, GCSFR** and

STAT3) in biopsy tissue of glioblastoma through RT-PCR. B) The values of three biological replicates are shown, indicating a univariate normality test. The graphs were plotted with the Graph Pad Prism 9 software.

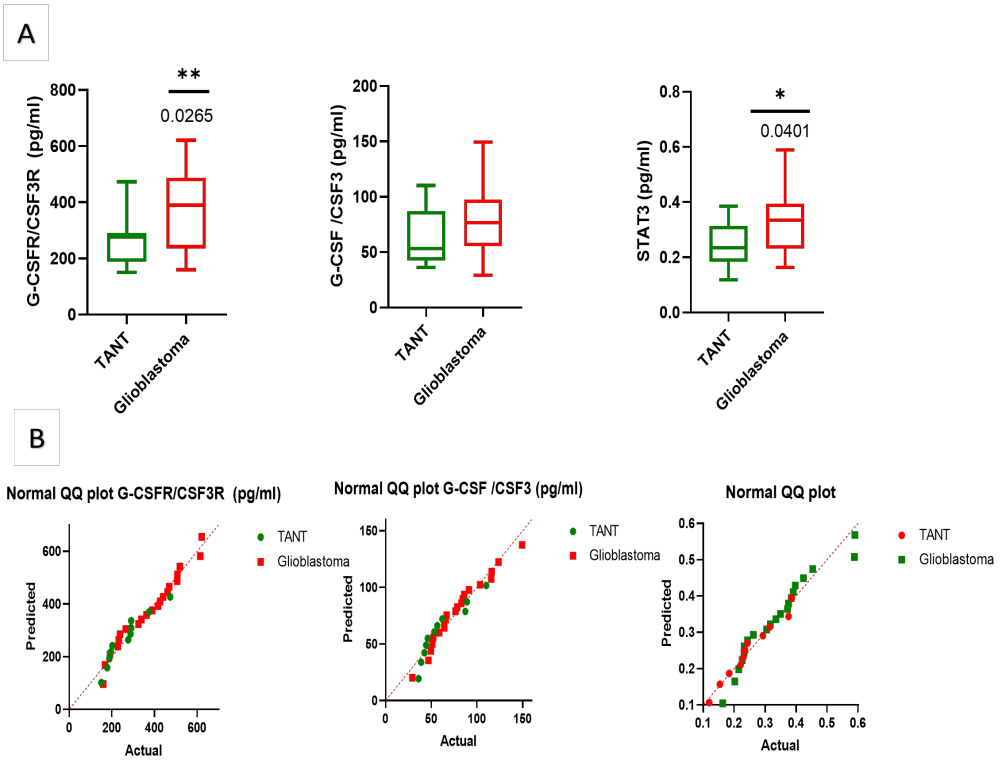

FIGURE 4.8: Quantitative expression of inflammatory genes in GFAP negative high grade glioma (glioblastoma) through ELISA

A) Expression levels of the candidate reference genes (GCSF, GCSFR and STAT3) in biopsy tissue of glioblastoma through ELISA. B) The values of three biological replicates are shown, indicating a univariate normality test. The graphs were plotted with the Graph Pad Prism 9 software.

4.2.4.1 Expression through heat-map clustering their correlation PCA and UMAP in Glioblastoma

Heat map and clustering by expression profile similarity demonstrated that all tumor samples clustered similarly, showing that the expression profile within a tumor specimen is preserved across the specimen. This shows that the significant variation in gene expression occurs across samples of various grades of the tumor, followed by samples of the same grade, and finally, within a specific sample. Average linkage and correlation distance in 3 rows and 32 columns were grouped.

Heat maps showed that tumor cells have high expression of genes as compared to tumor associated normal tissue in respect to color range from blue to red brown according to Z-score scale −1 to 1 (Figure 4.9A) and similar pattern also observed in that tumor cells have high expression of genes as compared to tumor associated normal tissue in respect to color range from green to red brown according to the scale range 0-100 (Figure 4.9B).Principal component analysis (PCA) showed overall separation between the TANT(C) and GBM (GB) patient samples. Rows are subjected to unit variance scaling, and SVD with imputation is employed to determine the major components. Principal components 1 and 2, which account for 77% and 19% of the total variance, are displayed on the X and Y axes, respectively (Figure 4.9C) and uniform manifold approximation and projection (UMAP) also showed separation between control and diseased samples, specifically the TANT (marked as C) and GBM (marked as GB) were clustered separately. More over the GB showed a dispersed pattern of distribution with others patient group neighboring cluster and the C group showed very low variation, suggesting a high degree of heterogeneity among patients (Figure 4.9D). The expression of GCSF and its receptor was confirmed by the receiver operating characteristic (ROC) curves for each of our predictive schemes in the categorization of patients based on their IV malignancy and was also employed to classify glioblastoma based on the combination of three distinct feature types: histopathology , expression, and magnetic resonance imaging characteristics Similarly, the GCSF and GCSFR cut-off point was determined for which accuracy measures were derived from cross-tabulations (Figure 4.9E).

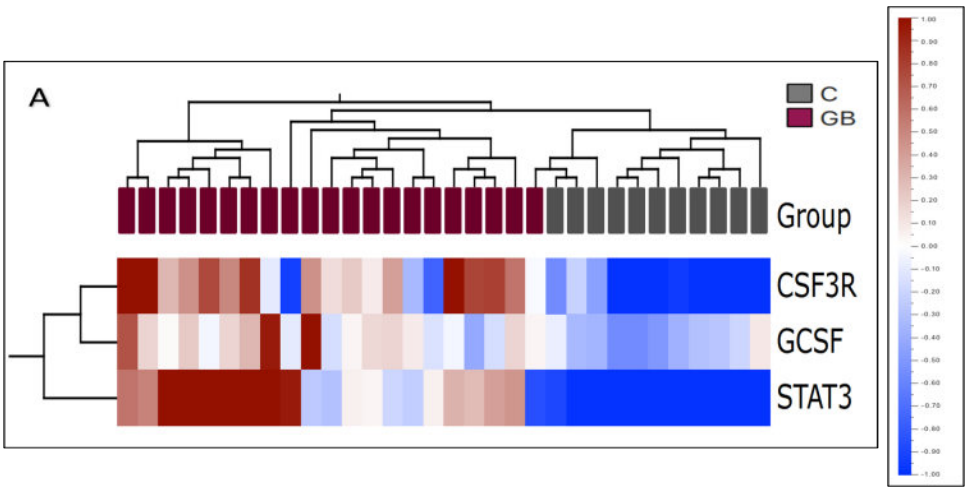

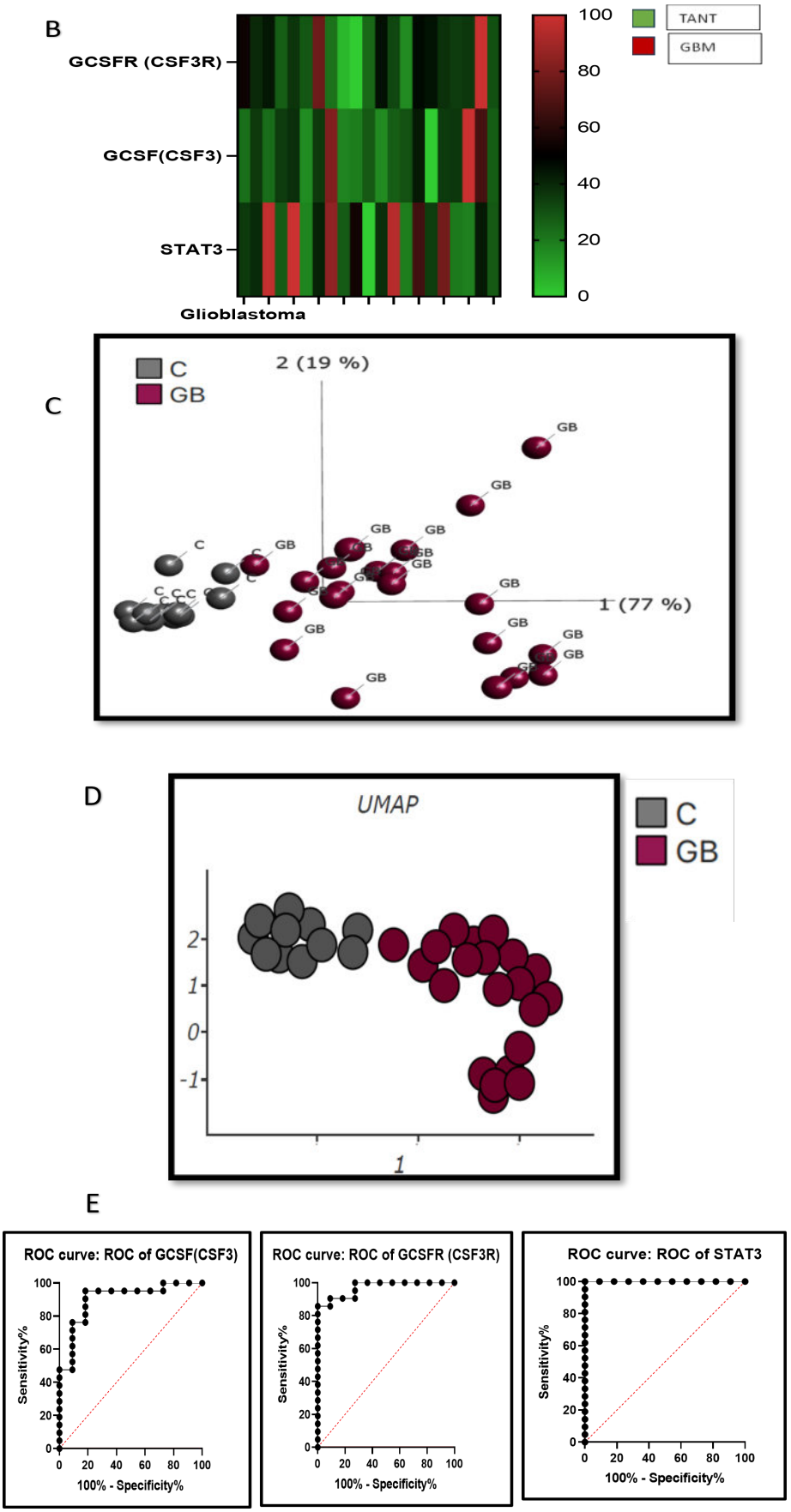

FIGURE 4.9: Expression of High-grade glioma patients (Glioblastoma) through Heat Map Clustering their correlation, PCA and UMAP in of inflammatory genes

A) Heat Map and hierarchical grouping of glioblastoma samples based on three differentially expressed genes with the highest coefficient of variation across all samples. Rows are centered; unit variance scaling is applied to rows. Both rows and columns are clustered using correlation distance and average linkage. Heat maps colored from blue to red brown according to Z-score scale -1 to 1, representing TANT gray in color and GBM red in color B) Heat Map of glioma samples based on 3 candidate reference expressed genes with the highest coefficient of variation across all samples also consistent with the clustering Rows are centered; unit variance scaling is applied to rows. Both rows and columns are clustered using correlation distance and average linkage. Heat maps colored from green to red brown according to scale 0 - 100. C) Unit variance scaling is applied to calculate principal components. X and Y axis show principal component 1 and principal component 2 that explain 77% and 19% of the total variance. D) Uniform manifold approximation and projection (UMAP) analysis showed separate clusters in between C and GB. However, suggesting a high degree of heterogeneity for the tumor brain in individual patients of glioblastoma. E) ROC curves show specificity of GCSF and GCSFR in the prognosis of glioblastoma.

4.3 Expression of Inflammatory Genes on Cancer Cell Line Human Glioblastoma SF-767

In vitro expression study of NF-κB p65 (RelA) and TNFα in SF-767 Glioblastoma cell line after treated with Temozolomide and Celecoxib

In the current study the expression of NF-κB p65 (RelA) and TNFα have been investigated with the effect of chemotherapeutic drug (Temozolomide) and NSAID (Celecoxib) by using human glioblastoma cell line SF-767 to study the NF-κB signaling pathway. From the 8 panel inflammatory genes of GFAP positive GBM group, NF-κB p65 (RelA) was selected to further investigate the effect and expression through invitro studies, as NF-κB p65 (RelA) is a transcription factor that regulates the expression of many cytokines proinflammatory genes (TNFα)

and inflammatory genes (IL-1β, IL-6, IL-8, IL-10 and TGF-β) in tumor microenvironment and progression of GBM as already reported in the previous literature.

Treatment with Celecoxib and temozolomide impact on glioblastoma cells

The TMZ (temozolomide) treatment effects on the glioblastoma SF-767 cell line were evaluated for 48 hours at concentrations of 10, 50, 100, 150, and 200 μM. The SF-767 cell line was exposed to TMZ 10 μM, and following the treatment, the cells were inhibited by 33.1%. A higher TMZ concentration (200 μM) was more lethal, resulting in 89% of the GBM cells dying following the treatment. Similarly, after being treated for 48 hours with 10 μM of Celecoxib, 12.8% of the cells died. In contrast, after being treated for 48 hours with 200 μM of Celecoxib, 75% of the cells died (Figure 4.10A). The findings demonstrated that as treatment concentration and duration increased, cell viability declined. The MTT (3-[4,5-dimethylthiazol-2-yl]-2,5 diphenyl tetrazolium bromide) experiment demonstrated that a larger dose of TMZ had a greater cytotoxic impact, as shown in figure 4.10A.

Moreover, the expression of inflammatory biomarkers NF-κB p65 (RelA) and TNFα was studied after treatment with temozolomide and Celecoxib. A quantitative RT-PCR analysis was performed in SF-767 cell line treated temozolomide with three concentrations (50 μM, 100 μM and 150 μM) to assess the mRNA expression level of inflammatory genes (NF-κB p65 (RelA) and TNFα). Pro-inflammatory genes were significantly elevated in the stress groups after stimulation with IL-1 beta, a potent stimulator of the inflammatory responses. The cells were treated for 48hrs. Compared to the stress group, the TMZ did not significantly reduce the expression of NF-κB p65 (RelA) and TNFα of the Glioblastoma SF-767 cell line in a dose-dependent manner (Figure 4.10B - 4.10C). Furthermore, the mRNA expression level of NF-κB p65 (RelA) and TNFα in the Celecoxib-treated SF-767 cell line was studied at a similar concentration as TMZ. Compared to the stress group, Celecoxib significantly reduced the expression of NF-κB p65 (RelA) and TNFα of the Glioblastoma SF-767 cell line in a dose-dependent manner (Figure 4.10D-4.10E).

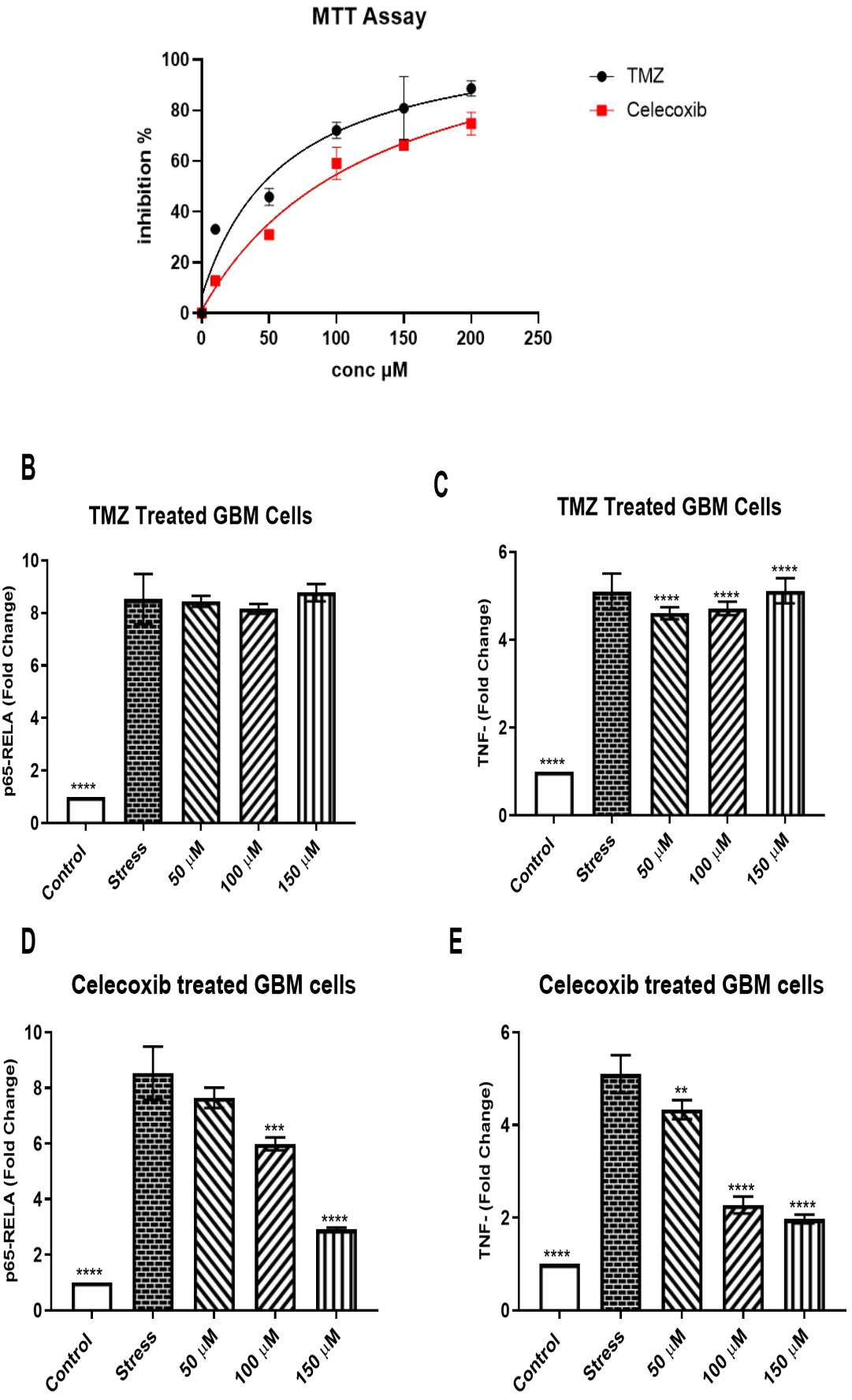

FIGURE 4.10: Cytotoxicity is evaluated using the MTT proliferation test

The ratio of GBM cells that were inhibited after being treated for 48 hours with TMZ and Celecoxib at various doses.

(A) Black and red curve TMZ and Celecoxib in a dose-dependent manner. Increasing the concentration of any of these drugs makes the cytotoxic response more potent. (B) The mean and standard deviation of three independent experiments are used to illustrate the quantitative analysis of MTT. When compared to the untreated control, $^{*}p<0.05$ and $^{**}p<0.01$ are significant. Quantitative RT-PCR analysis of mRNA expression levels of inflammatory marker NF-κB p65 (RelA) in Glioblastoma SF-767 cell line treated with TMZ at 50 μM,100 μM and 150 μM. The GAPDH gene was used as the internal control to normalize the data. IL-1B was used as stress to trigger an inflammatory cascade. The mRNA expression of genes was computed in fold change compared to the control .The data are presented as the mean $\pm$ SD of the triplicate tests compared with the control group ($P \leq 0.05$ for each). (C) similarly, mRNA expression levels of inflammatory marker TNFα in the Glioblastoma SF-767 cell line treated with TMZ at 50 μM ,100 μM and 150 μM.(D) Quantitative RT-PCR analysis of mRNA expression levels of NF-κB p65 (RelA) in Glioblastoma SF-767 cell line treated with celecoxib at 50 μM ,100 μM and 150 μM. The GAPDH gene was used as the internal control to normalize the data. (E) Similarly, mRNA expression levels of TNFα in the Glioblastoma SF-767 cell line treated with celecoxib at 50 μM, 100 μM and 150 μM.

4.4 Mapping and Prioritizing of Inflammatory Biomarkers of Glioma

Mapping and Data Mining

Literature data from PubMed and Core mine

Literature data is retrieved using PubMed database for group I(Glioma), group II (Glioblastoma)with applying filter of Text Availability as 'Abstracts' and Publication dates as '10 years'. Total 18792 results were obtained for group I + II. These terms were co-occurring in the abstracts and full text of the published articles .Coremine extract keywords from medical literature. Coremine was used to decrease the redundancy of results of RapidMiner and to avoid the biasness. Glioma

and Glioblastoma keywords were obtained with their frequency of occurrence for group I and II respectively. From the results of Coremine we found Glioma' (disease) (73360 articles), Glioma' (disease) (55630 connections) And Glioblastoma' (disease) (50897 articles) in the year between from 2014-2022. The other associations related to glioma with different nodes for example, Disease, drugs, symptoms, molecular functions and cellular components etc. are also shown in the figure 4.11.

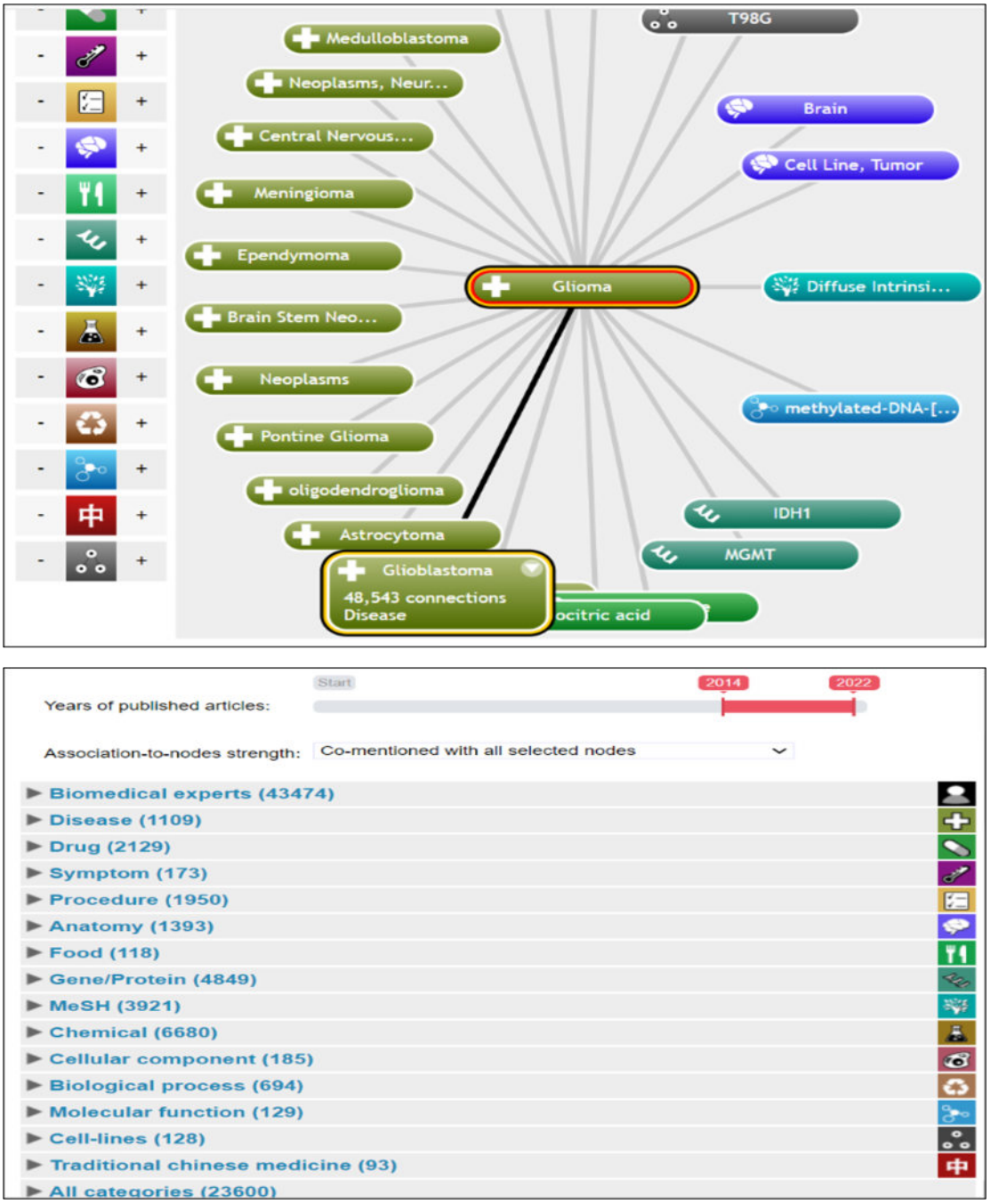

FIGURE 4.11: Data Mining using PubMed and Coremine.

Selected data for all the two groups (Glioma, Glioblastoma) then visualized using Coremine plugin of preferred layout view.

4.5 Global Microarray Bioinformatics Analysis

4.5.1 Microarray Analysis and Normalization of Driver Inflammatory Genes (IL-1β, IL-6, IL- 8, IL-10, TGF-β, TNF-α, NF-κB p65, IL1Ra) of High Grade Glioma Tumorigenesis

We obtained 252 samples of High grade gliomas-related Affymetrix (CELL format) cDNA dataset GSE16011. AffyBatch has 712 $\times$ 712, 1164 $\times$ 1164, 1050 $\times$ 1050, and 732 $\times$ 732 array sizes. DEGs were detected by applying the GEO2R online analysis tool, setting adjust P-value ≤ 0.05 and $|\text{logFC}| \geq 2$ as selection criteria. In this analysis total samples consisting of 85 grade-III and 159 Grade-IV and 8 healthy controls. The analysis of 17527 genes analyzed through GEO2-R package identified 7394 expressed genes in healthy control vs grade-III, 8805 differentially expressed genes in healthy control vs Grade-IV and 8831, differentially expressed genes in Grade-III vs Grade-IV samples. There were 3412 up regulated and 3981 down regulated genes in healthy control vs. Grade-III glioma patients (Figure 4.12A). Similarly, 4381 and 4423 genes were upregulated and downregulated genes in healthy control vs Grade-IV respectively among 8805 genes (Figure 4.12B). In case of Grade-III vs Grade-IV, 5285 genes found to be upregulated and 3546 downregulated (Figure 4.12C). As shown in figure 4.12D-4.12E-4.12F, the mean difference plot of same DEGs has been highlighted. The density estimation of data is shown by the histograms representing expression after normalization. The array distributions have similar shapes and ranges, indicating that the data is of good quality. The right-hand distribution of the array reveals a high background level (Figure 4.12G). Mean-Variance relationship of Expression Data shows strong mean-variance trend in present data. In the (figure 4.12H), each point represents a gene. The blue line represents constant variance and red line highlights removal

of drop trend in mean-variance trend approximation of normalized data. Limma Venn diagram analysis was used to explore and download the overlapped genes between multiple contrasts. The analysis identified 4734 differentially expressed genes having p-value less than 0.05 in three categories. We first investigated the degree of overlap between DEGs of each signature.

Of the 4734 total DEGs, 3149 (96.6%) were common to each signature. In group 1 (healthy control vs Grade-III) 158 (3.33%) and in group2 (healthy control vs Grade-IV) 558 (11.78%) and in group 3 (Grade-III vs Grade-IV) 2992 (63.20%) were differentially expressed. while 3247 genes were common between two groups healthy control vs Grade-III and healthy control vs Grade-IV, and 839 were common between healthy control vs Grade-III and Grade-III vs Grade-IV and similarly 1850 were unique in between healthy control vs Grade-IV and Grade-III vs Grade-IV all groups (Figure 4.12I). However, the 8 driver Inflammatory genes (IL-1β, IL-6, IL- 8, IL-10, TGF-β, TNF-α, NF-κB, IL1Ra showed significant p value in particular 3 groups as shown in table 4.3. Specifically, these DEGs suggesting that transcriptomic-wide changes are more prominent during late phases of neoplastic progression.

Moderated t-statistic quantile-quantile (q-q) plot was used to analyze the quantiles of data samples against the theoretical quantiles of a Student's t distribution to validate Limma test results. As shown in (figure 4.12J), the points lie along a straight line, meaning that the values for moderated t-statistic computed during the test follow their theoretically predicted distribution. In (figure 4.12K), UMAP plot shows uniform manifold approximation and dimension reduction in order to visualize significant relationship among the samples. The nearest neighborhood considered significant in the plot. Specifically, the UMAP function was used with 15 nearest neighbors explaining the greatest degree of variance among healthy control, Grade-III and Grade-IV corrected high grade glioma meta-datasets. Plot densities have been highlighted using R Limma to view the distribution of values among three categorizations to validate normalization as UMAP analysis.

TABLE 4.3: Differentially expressed inflammatory genes (IL-1β, IL-6, IL- 8, IL-10, TGF-β, TNF-α, NF-κB, IL1Ra) of High grade Glioma in Microarray Dataset Analysis

		Control Vs Glioma Garde III				**Control Vs Glioma Garde IV**			**Glioma Garde III Vs Glioma Garde IV**							
ID		log2 (fold change)	minus Log10 (P value)	log2 Exp	log2 FC		log2 (fold change)	minus log10 (P value)		log2 Exp	log2 FC		log2 (fold change)	minus log10 (P value)		log2 Exp	log2 FC
4790_at	Nfκ B	-0.677	4.894	8.481	-0.677	4790_at	0.853	7.538	4790_at	8.481	0.853	4790_at	-0.176	2.796	4790_at	8.481	-0.176
7040_at	TGFB	-0.846	2.256	6.924	-0.846	7040_at	1.425	5.58	7040_at	6.924	1.425	7040_at	-0.578	6.52	7040_at	6.924	-0.578
3553_at	IL1B	-	-	-	-	3553_at	1.271	3.064	3553_at	7.465	1.271	3553_at	-0.548	3.939	3553_at	7.465	-0.548
3586_at	IL10	-	-	-	-	3586_at	-	-	3586_at	-	-	3586_at	-	-	3586_at	-	-
3569_at	IL6	-	-	-	-	3569_at	-	-	3569_at	-	-	3569_at	-0.794	6.586	3569_at	6.042	-0.794
7124_at	TNF α	-	-	-	-	7124_at	-	-	7124_at	-	-	7124_at	-	-	7124_at	-	-
3557_at	ILRa	-	-	-	-	3557_at	-	-	3557_at	-	-	3557_at	-0.103	4.088	3557_at	5.113	-0.103
3576_at	IL8	-	-	-	-	3576_at	2.649	4.342	3576_at	6.653	2.649	3576_at	-1.675	10.833	3576_at	6.653	-1.675

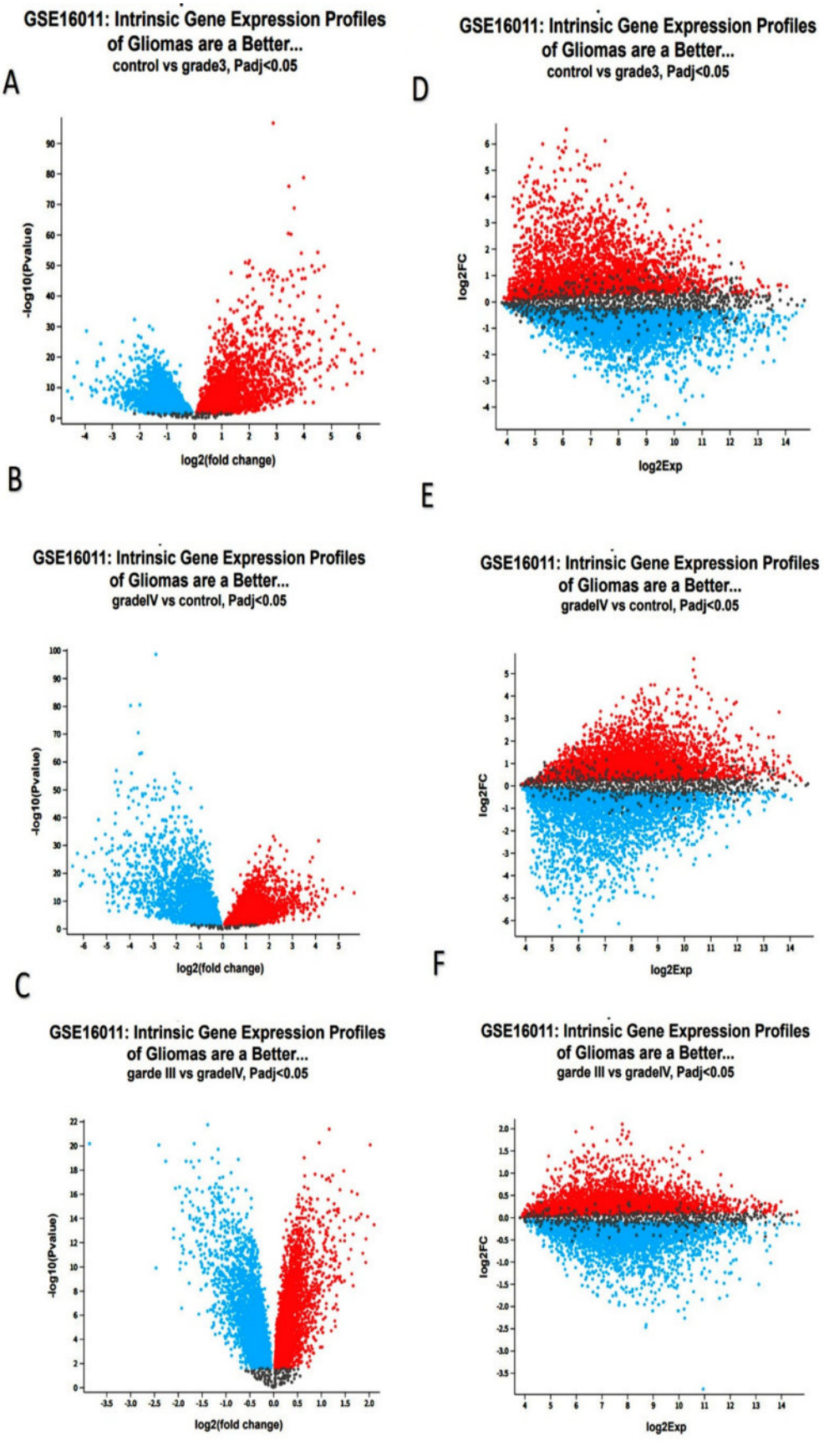
GSE16011: Intrinsic Gene Expression Profiles of Gliomas are a Better...
control vs grade3, Padj<0.05
A
-log10(Pvalue)
log2(fold change)
B
GSE16011: Intrinsic Gene Expression Profiles of Gliomas are a Better...
control vs grade3, Padj<0.05
D
log2FC
log2Exp
E
GSE16011: Intrinsic Gene Expression Profiles of Gliomas are a Better...
gradeIV vs control, Padj<0.05
-log10(Pvalue)
log2(fold change)
C
GSE16011: Intrinsic Gene Expression Profiles of Gliomas are a Better...
gradeIV vs control, Padj<0.05
log2FC
log2Exp
F
GSE16011: Intrinsic Gene Expression Profiles of Gliomas are a Better...
garde III vs gradeIV, Padj<0.05
-log10(Pvalue)
log2(fold change)
GSE16011: Intrinsic Gene Expression Profiles of Gliomas are a Better...
garde III vs gradeIV, Padj<0.05
log2FC
log2Exp

G

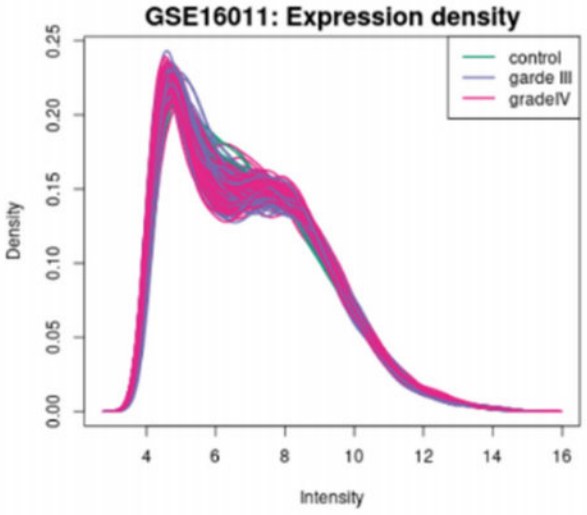
GSE16011: Expression density
control
garde III
gradeIV
Density
0.00
0.05
0.10
0.15
0.20
0.25
4
6
8
10
12
14
16
Intensity

H

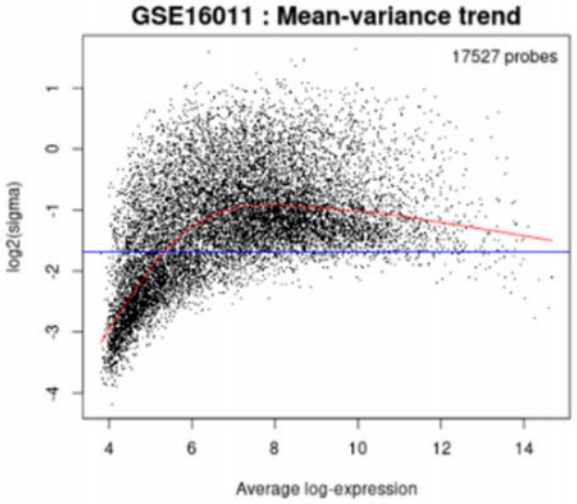
GSE16011 : Mean-variance trend
17527 probes
log2(sigma)
1
0
-1
-2
-3
-4
4
6
8
10
12
14
Average log-expression

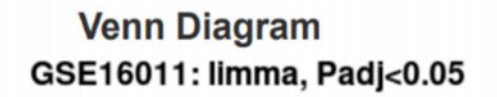
Venn Diagram
GSE16011: limma, Padj<0.05

I

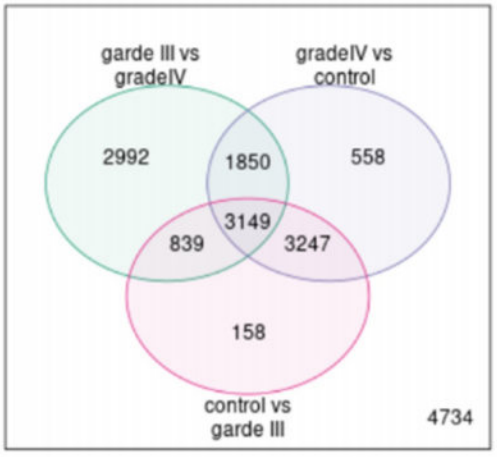
garde III vs gradeIV
gradeIV vs control
2992
1850
558
3149
839
3247
158
control vs garde III
4734

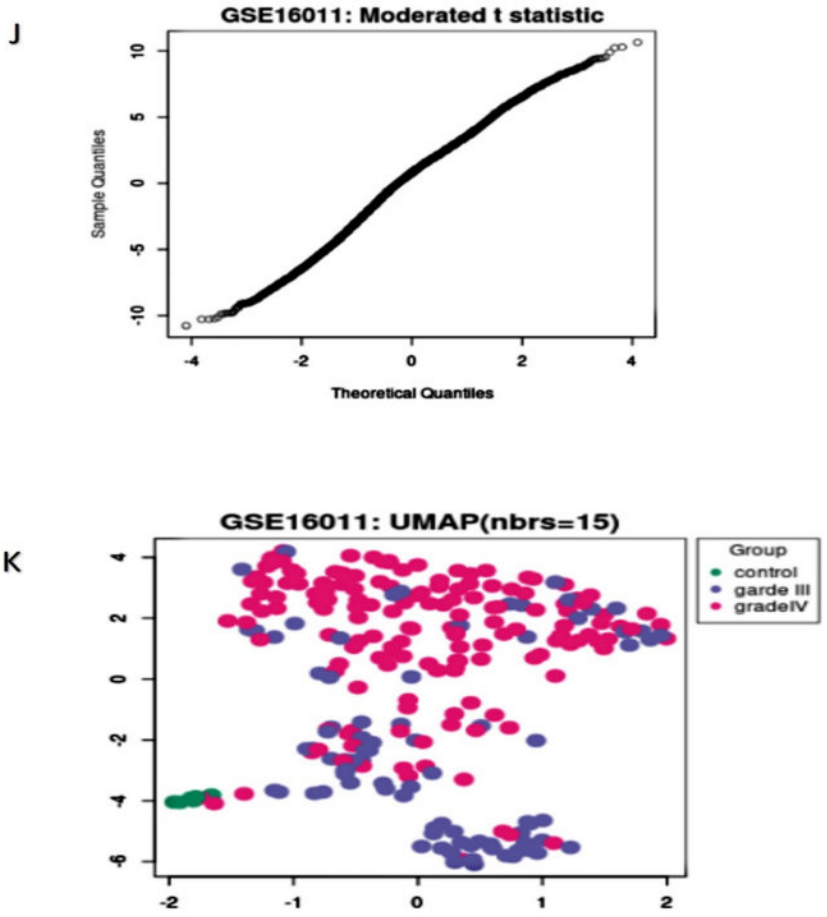

FIGURE 4.12: Microarray analysis and Normalization of driver inflammatory genes of High grade glioma tumorigenesis

A-B-C) Differentially expressed gene of glioma showed all upregulated and down-regulated genes in the three groups control vs. Grade-III glioma, healthy control vs Grade-IV and Grade-III vs Grade-IV and were selected by volcano plot filtering (fold change ≥ 1 and P-value ≤ 0.05). D-E-F) the mean difference plot of same DEGs has been highlighted and displayed log2 fold change versus average log2 expression values to visualized differentially expressed genes. G) The histogram shows the density of the data analyzed. Normally, the proportions of the clusters have comparable shapes. Significant levels of background shifted the intensities of the different arrays toward the right. H) Mean-Variance relationship of Expression Data shows strong mean-variance trend. I). Limma Venn diagram analysis was used to explore and download the overlapped genes between multiple contrasts. The analysis identified 4734 differentially expressed genes having p-value less than

0.05 in three categories (healthy control vs Grade-III), (healthy control vs Grade-IV) and (Grade-III vs Grade-IV). J) Moderated t-statistic quantile-quantile (q-q) plot was used to analyze the quantiles of data samples against the theoretical quantiles of a Student's t distribution to validate Limma test results. K) UMAP plot shows uniform manifold approximation and dimension reduction in order to visualize significant relationship among the samples.

4.5.2 Global RNA-Seq Bioinformatics Analysis

Expression analysis through UALCAN and IDEP

We obtained another datasets comprised of 156 samples of High grade gliomas and 5 samples of normal tissue for RNA- seq analysis through UALCAN, setting adjust P-value < 0.05 and $|\text{logFC}| \geq 2$ as selection criteria (transcript per million). The gene expression analysis provided information about relative Differential expression levels of the gene (IL-1β, IL-6, IL-8, IL-10, TGF-β, TNF-α, NF-κB, IL1Ra) in normal versus tumor samples of glioblastoma (GBM). The inflammatory genes IL-8, IL-10, TGF-β, and NF-κB were upregulated while IL-1β, IL-6, IL1Ra and TNF-α, were showed down regulation of expression as illustrated in (Figure 4.13A). For each tumor subgroup, the box-whisker plots present interquartile ranges (IQRs), including minimum, 1^{st} quartile, median, 3^{rd} quartile, and maximum values. Similarly the expression of inflammatory genes were also consistent to the RNA- seq data obtained from TCGA data base comprised of 163 GBM tissue and 5 normal tissue analyzed by IDEP analyzing tool as shown in (Figure 4.13B). With FDR <0.01 and fold change >2 as cutoffs, we used DESeq2 to identify DEGs. The whole transcriptome was built via the assembled reads obtained from the alignment files. The expression was determined in the form of fragments per kilo base of transcript per million mapped reads (FPKM). Read count and FPKM values were calculated for each assembled gene/transcript. The two group types up samples control and down samples control have differential transcription profiles, with identified DEGs. The 3 inflammatory genes (IL-8, IL-10, TGF-β) were shown up regulation in up sample control while the four genes

(IL-1β, IL-6, IL1Ra and TNF-α) were downregulated shown in down sample control as illustrated in Venn diagram in (Figure 4.13C).Furthermore, the gene count of all samples was used in the differential-expression-related analyses as the preferred input.

The preprocessed results of all disease samples (green color density curve) showed comparative similarity as compared to control sample (red color density curve) and were graphically presented as a read count bar plot in terms of expression and a distribution of a density plot of transformed data (Figure 4.13D). Using a threshold of false discovery rate (FDR) <0.1 and fold-change >2. The MA plot (Figure 4.13E) and the interactive MA plot (Figure 4.13F) show that inflammatory genes leads to significant transcriptomic response. The up and down-regulated genes are then subjected to enrichment analysis based on the hyper geometric distribution. The heat map of DEGs were derived from both the comparisons and divided in to two cluster groups' (representing blue and yellow bar) disease disease sample groups (red in color) and control sample group (green in color) through K-mean as shown in Figure 4.13G.

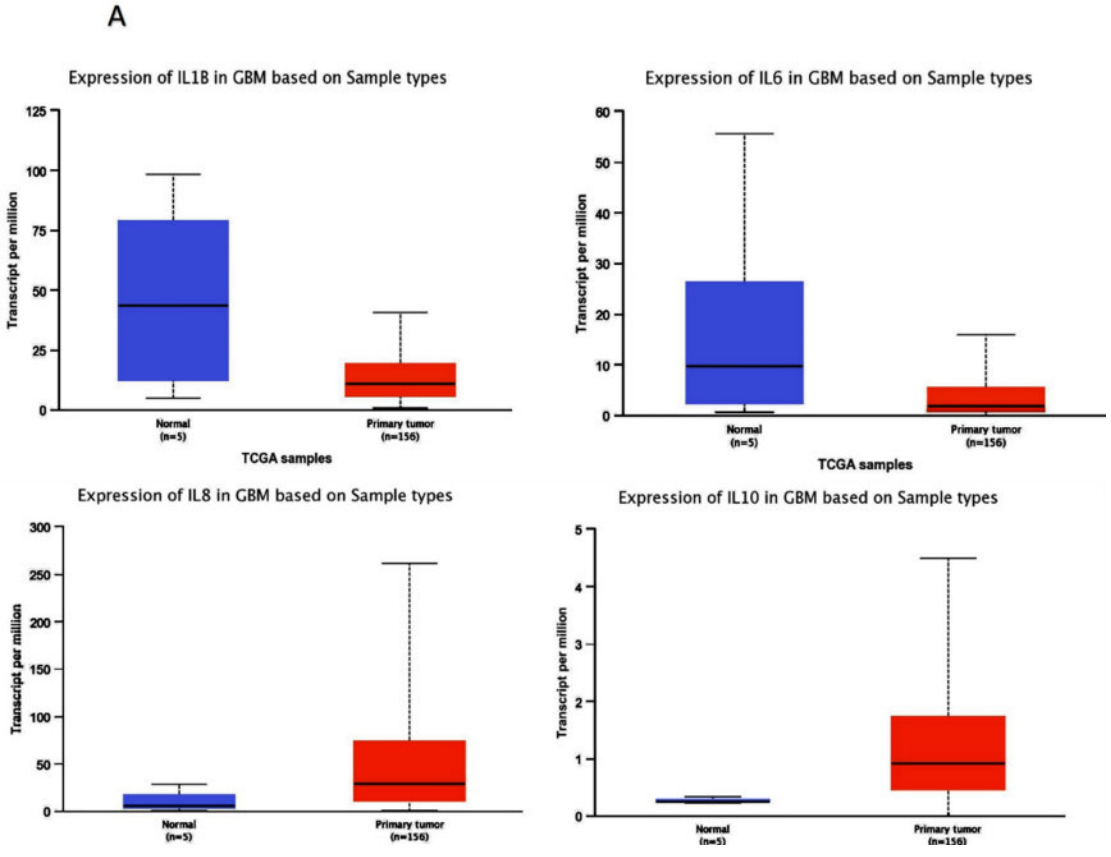

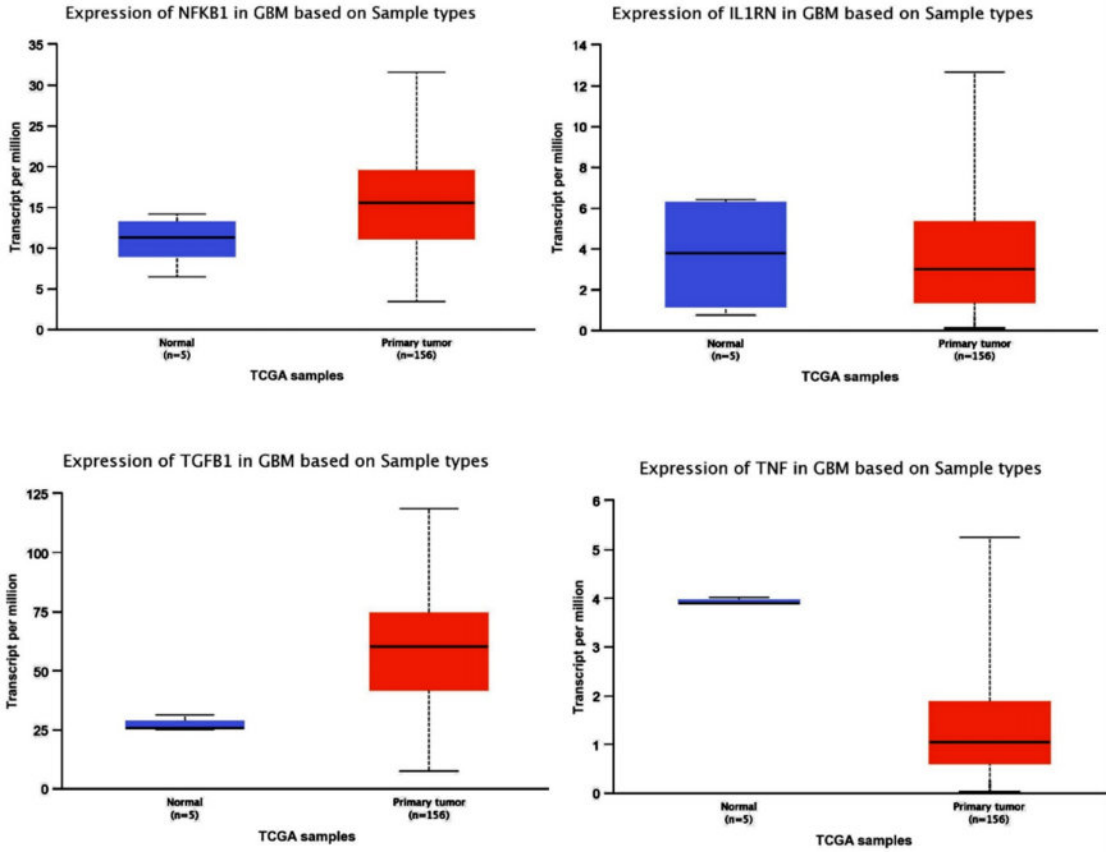
Expression of NFKB1 in GBM based on Sample types
Transcript per million
Normal (n=5)
Primary tumor (n=156)
TCGA samples
Expression of IL1RN in GBM based on Sample types
Transcript per million
Normal (n=5)
Primary tumor (n=156)
TCGA samples
Expression of TGFB1 in GBM based on Sample types
Transcript per million
Normal (n=5)
Primary tumor (n=156)
TCGA samples
Expression of TNF in GBM based on Sample types
Transcript per million
Normal (n=5)
Primary tumor (n=156)
TCGA samples

B

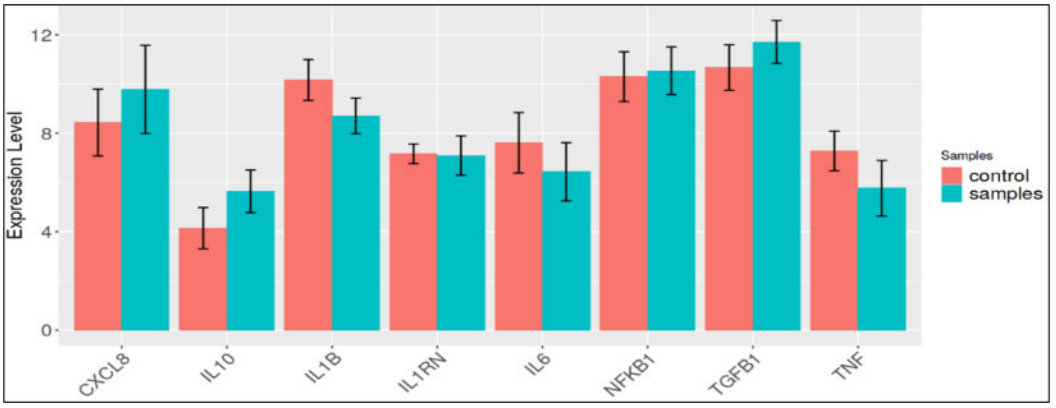
Expression Level
Samples
control
samples
CXCL8
IL10
IL1B
IL1RN
IL6
NFKB1
TGFB1
TNF

C

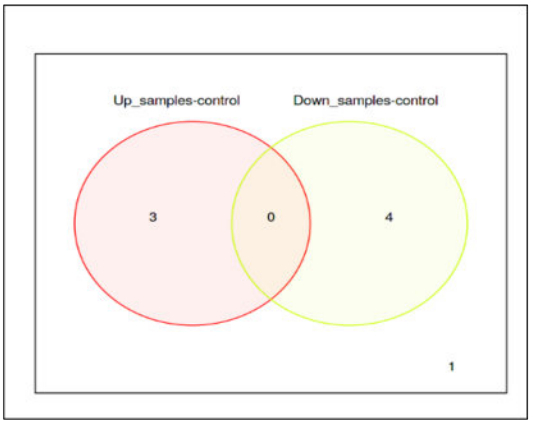
Up_samples-control
Down_samples-control
3
0
4
1

D

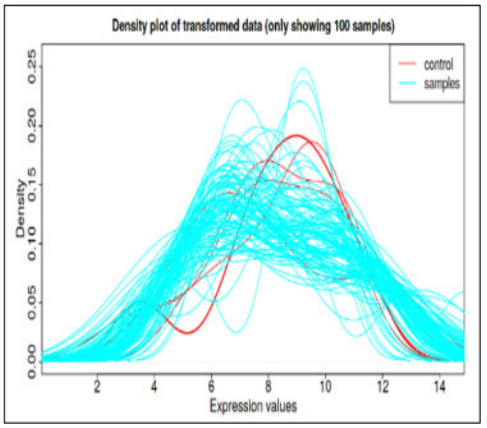
Density plot of transformed data (only showing 100 samples)
control
samples
Density
Expression values

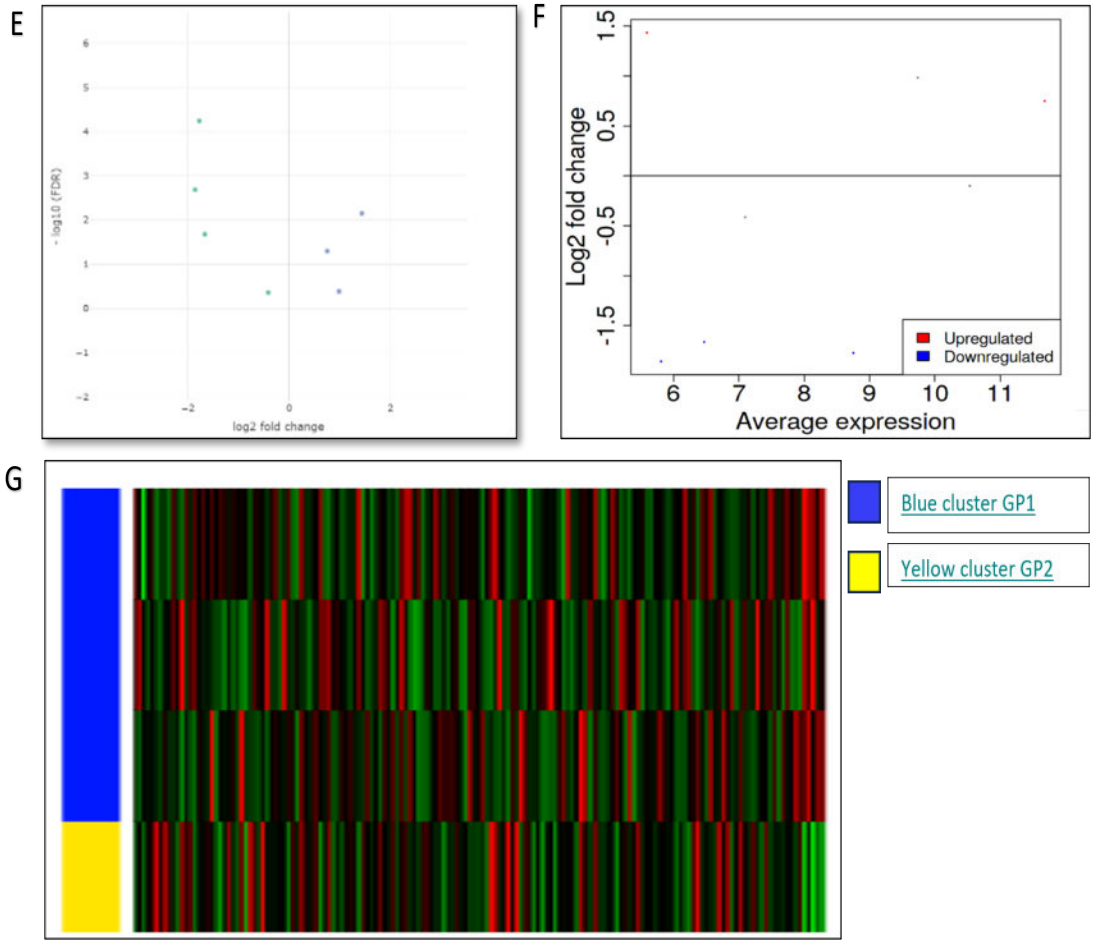

FIGURE 4.13: Global RNA-seq expression analysis.

A) Box-whisker plots showing the expression of inflammatory genes (IL-1β, IL-6, IL- 8, IL-10, TGF-β, TNF-α, NF-κB, IL1Ra) in glioblastoma samples (GBM).B) Bar chart showing Differential expression of (IL-1β, IL-6, IL- 8, IL-10, TGF-β, TNF-α, NF-κB, IL1Ra) in normal and GBM samples. C) Venn Diagram showed the overlap between down regulated and up regulated inflammatory genes GBM samples. D) The GBM samples (green color density curve) showed comparative similarity as compared to control sample (red color density curve) and were graphically presented as a read count bar plot in terms of expression and a distribution of a density plot of transformed data. E-F) The MA plot and interactive MA plots for deferentially expressed genes between control and GBM showed up regulation and down regulation. G) K-means heat map with 2 different set of clusters (yellow and blue) of identified module by iDEP servers for deferentially expressed genes between control (Green color) and GBM (Red).

4.5.3 Principle Component Analysis and T-SNE

PCA plot using the first and second principal components is shown in (Figure. 4.14A). There is a clear difference of expression between the disease samples (GBM) and the control samples groups. The samples from the control group clustered the upper portion of the graph. The samples from the GBM group clustered on the opposite side. The first principal component that explains 45% of the variance and second principal component that explains 16% of the variance Plot using multidimensional scaling (MDS), and t-SNE (Figure 4.14B). This also showed a similar distribution of the samples and were considered significant for pathway enrichment analysis by treating the loadings of the principal components as expression values. The differential expression analysis via DEseq2 revealed up- and downregulated inflammatory genes among the control and glioblastoma (GBM) groups used in the study.

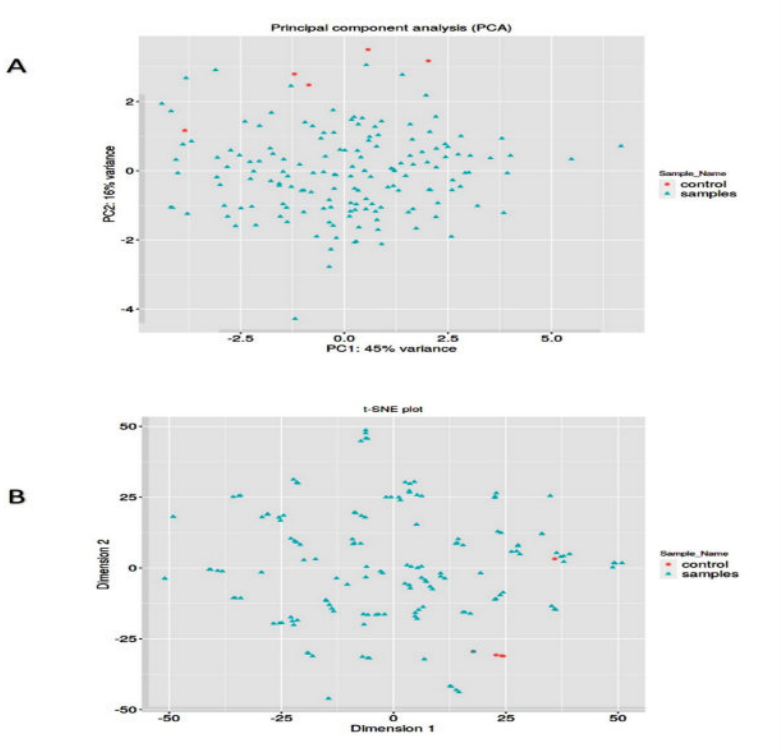

FIGURE 4.14: **PCA and T-SNE analyses.**

A) PCA indicate the substantial differential expression among control and disease (GBM) sample groups, with the PC1 with 45% variance and PC2 with 16% variance and was consistent with the cluster distribution in T-SNE plot analysis by

K-means in B.

4.6 Differentially Expressed Inflammatory Genes Validation

To validate the inflammatory gene expression across 163 human brain tumor samples compared to 207 normal matches, we used the GEPIA webserver. To validate the inflammatory gene expression across 163 human brain tumor samples compared to 207 normal matches, we used the GEPIA webserver. The expression was compared on the basis of grade classification. Through GEPIA the normal tissue data was used from the GTEx project to provide a reliable baseline for comparison. Inflammatory genes expression between tumors, their matched normal, and data from the GTEX database were compared.

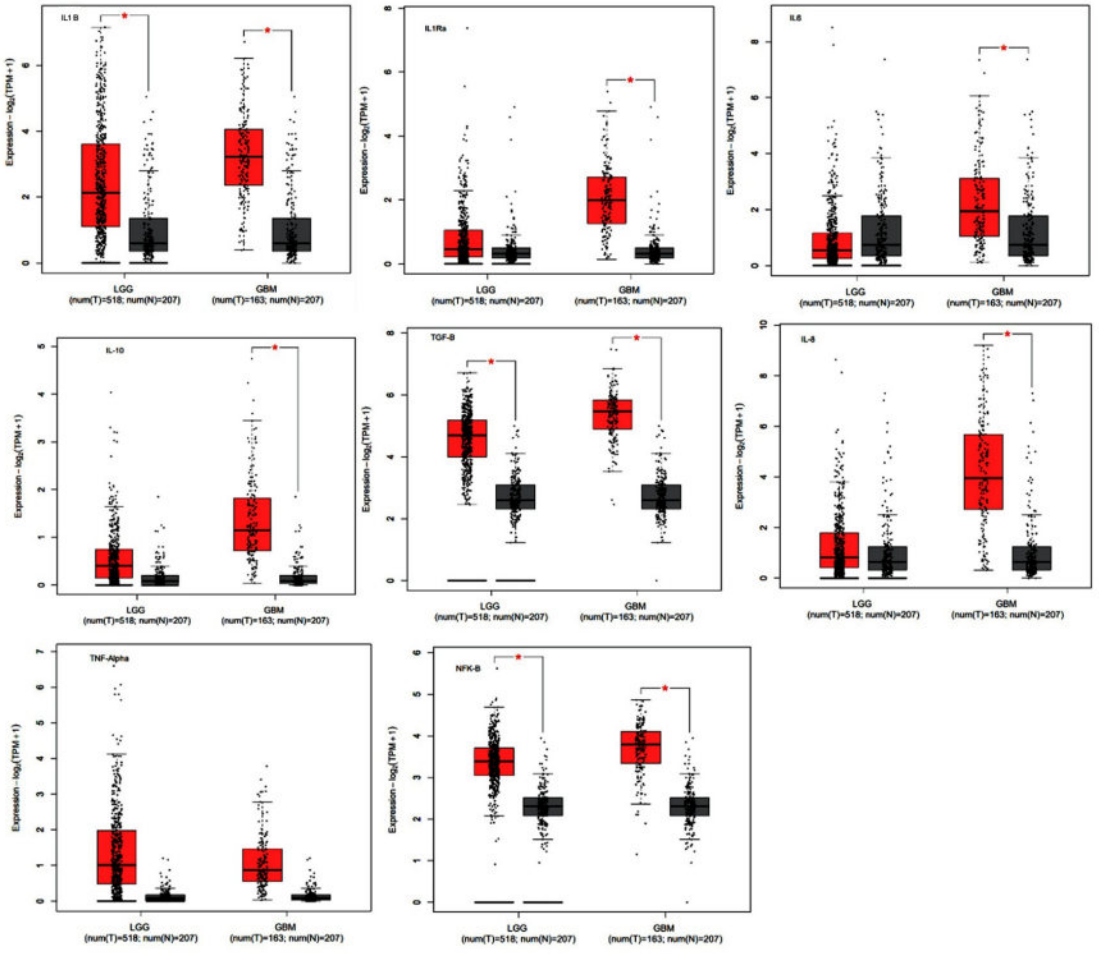

FIGURE 4.15: Differentially expressed inflammatory genes validation

Tissue gene expression validation of 8 inflammatory genes according to the GEPIA2 showed significant ($^*p < 0.01$) differential expression between LGG, GBM and normal tissue. The cut-off value for log2FC (fold change) was 1. We used a p-value threshold of 0.01 and a jitter size of 4. TPM is an acronym for transcripts per million.

To validate the global relevance of our data GBM patients, we performed a comprehensive integrated analysis of respective genes (IL-1β, IL-6, IL- 8, IL-10, TGF-β, TNF-α, NF-κB, IL1Ra) by retrieving GBM microarray data and RNA-sequence data from genome atlas databases. Using GEPIA2, TCGA, and GTEX integrated platform with the integration of R, we discovered that the expression of IL-1β, IL-6, IL- 8, IL-10, TGF-β, TNF-α, NF-κB, IL1Ra were found higher in GBM samples (n=163) However, IL6 showed down expression in low grade Glioma samples (n=518) compared to normal brain tissues (n=207). The expression was considered according to log2FC (fold change) as shown in (Figure 4.15).

4.7 Independent Prognostic Analysis and Clinical Correlation Analysis

We analyzed the correlation of overall survival (OS) and disease free survival (DFS) with elevated expression among the 8 inflammatory genes (IL-1β, IL-6, IL- 8, IL-10, TGF-β, TNF-α, NF-κB, IL1Ra).In GBM patients, the higher expression of IL8, correlated with poor OS .Based on TCGA data in Gepia2, the prognosis analysis demonstrated that GBM patients with high IL- 8 expression had inferior OS ($p = 0.049$; HR: 1.4; 95% CI) in comparison to patients who had low IL8 expression. Whereas this association was not present for other 7 genes with elevated expression i.e. IL-1β ($p = 0.46$; HR: 1.1; 95% CI); IL1Ra ($p = 0.41$; HR: 1.2; 95% CI); IL-8 ($p = 0.15$; HR: 1.3; 95% CI); IL-10 ($p = 0.26$; HR: 1.2; 95% CI); TGF-β($p = 0.42$; HR: 1.2; 95% CI); TNF-α($p = 0.66$; HR: 1.1; 95% CI); NF-κB($p = 0.49$; HR: 1.1; 95% CI) as shown in (Figure 4.16A).

In addition, the increased IL-6 and TGF-β expression exhibited poor Disease free survival(DFS) in GBM patients ($p = 0.0077$; HR: 1.8; 95% CI) and ($p = 0.048$; HR: 1.5; 95% CI) respectively, but does not show significant correlation for IL-1β

(p = 0.16; HR: 1.3; 95% CI); IL1Ra (p = 0.41; HR: 1.2; 95% CI); IL-6 (p = 0.074; HR: 1.4; 95% CI); IL-10 (p = 0.16; HR: 1.3; 95% CI); TNF-α(p = 0.5; HR: 0.86; 95% CI); NF-κB(p = 0.49; HR: 1.1; 95% CI) of GBM Patients as shown in (Figure 4.16B). The results demonstrated that the high IL- 8 expression had significant correlation with poor prognosis of OS in TCGA dataset for GBM patients, while IL- 8 did not display significant correlation with DFS from TCGA dataset for GBM patients, whereas IL-6 and TGF-β expression had significant correlation with DFS from TCGA dataset for GBM patients.

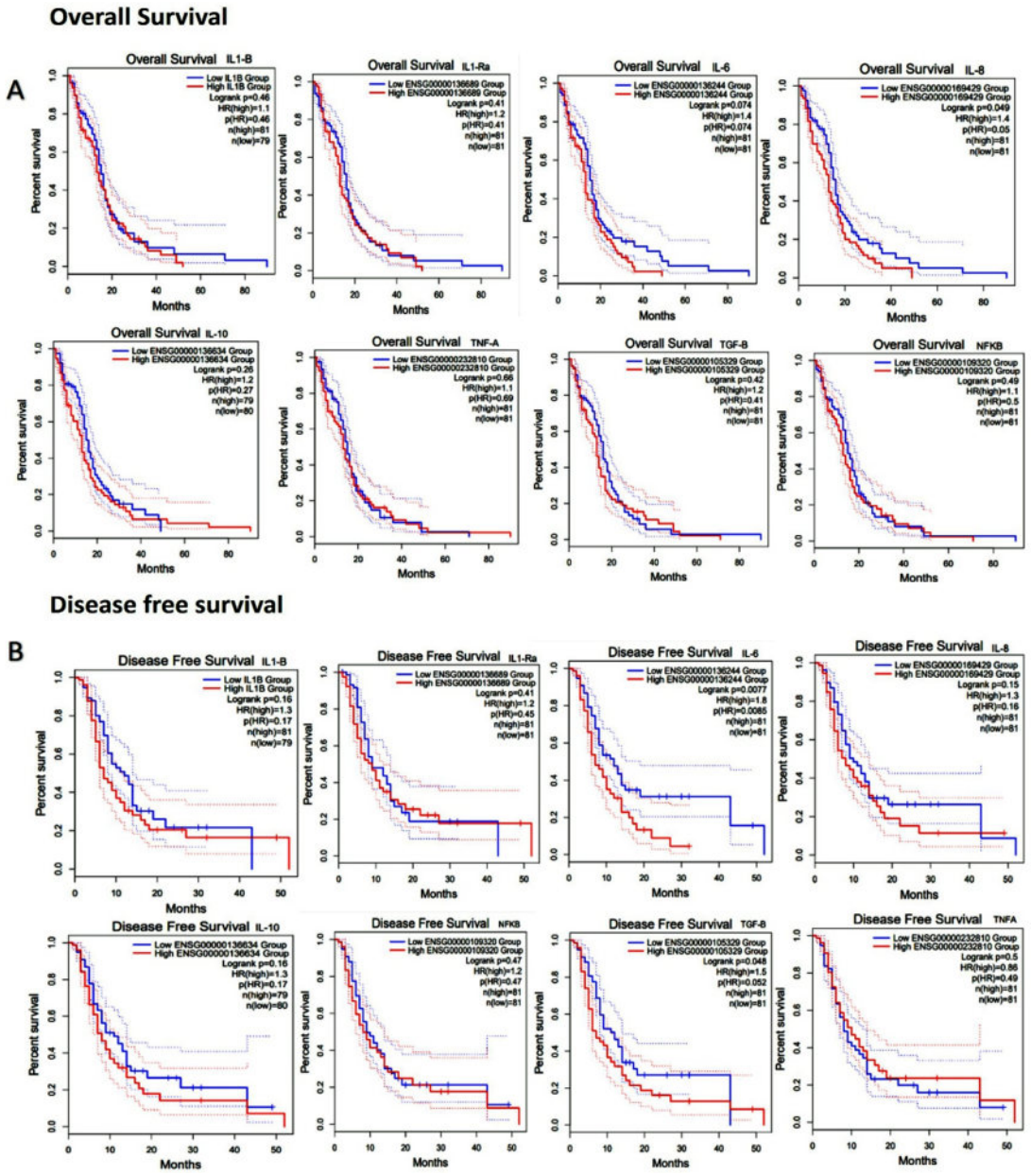

FIGURE 4.16: The relationship with expression of inflammatory genes and prognosis in GBM

A) Kaplan-Meier curves of overall survival (OS) showed the high IL-8 expression had significant correlation with poor prognosis of OS. B) In Disease free survival (DFS) in GBM patients, the increased IL-6 and TGF-β expression exhibited poor Disease free survival (DFS) in GBM patients. Whereas the blue line indicates low expression group, the red line indicates high expression group, dashed line indicates 95% CI and HR, Hazard ratio.

The results demonstrated that the high IL- 8 expression had significant correlation with poor prognosis of OS in TCGA dataset for GBM patients, while IL- 8 did not display significant correlation with DFS from TCGA dataset for GBM patients, whereas IL-6 and TGF-β expression had significant correlation with DFS from TCGA dataset for GBM patients.

4.8 Variegated Expression and Prognostic Value of GCSF, GCSFR, and STAT3

To investigate the global relevance of our GBM patient's data, we performed a comprehensive integrated analysis of transcriptomic and proteomic profiling of respective genes by retrieving GBM RNA-sequence data from genome atlas databases. Using the GEPIA2, TCGA, and GTEX integrated platform with the integration of R, we discovered that the expression of GCSFR and STAT3 were higher in GBM samples (n = 163) compared to normal brain tissues (n = 207) (Figure 4.17A). However, GCSF expression was not significant, similar to our finding where GCSF expression was higher in GBM samples but difference did not reached to log2FC (fold change). To study the link between the differential expression of GCSF, GCSFR, and STAT3 genes and GBM patient prognosis, we assessed the correlation between differential expression and overall survival with GEPIA2. It demonstrated that patients with a high expression of GCSF, GCSFR and STAT3 had a lower overall survival (Figure 4.17B). The survival heat map of hazard ratio Log10 (HR) indicated the prognostic impacts of GCSF, GCSFR and STAT3 and compared the survival contribution of GCSF, GCSFR and STAT3 by using

Mantel-Cox test. The hazard ratio values for GCSF, GCSFR, and STAT3 were 2.3, 1.5 and 1.2, respectively (Figure 4.17C). The correlation between GCSF (CSF3) and GCSFR (CSF3R) was analyzed, and highly correlate in glioblastoma patients with an optimum cut-off median at significance level p = 0.05. The high correlation between GCSF (CSF3) and GCSFR (CSF3R) was considered significant and positive, with R-value of 0.37 (Figure 4.17D), which demonstrated a positive correlation between OS and variation of expression. These results suggest that differential expression of GCSF, GCSFR and STAT3 impart a critical role in the prognosis of patients with GBM and may prove an appropriate survival predictor in these patients.

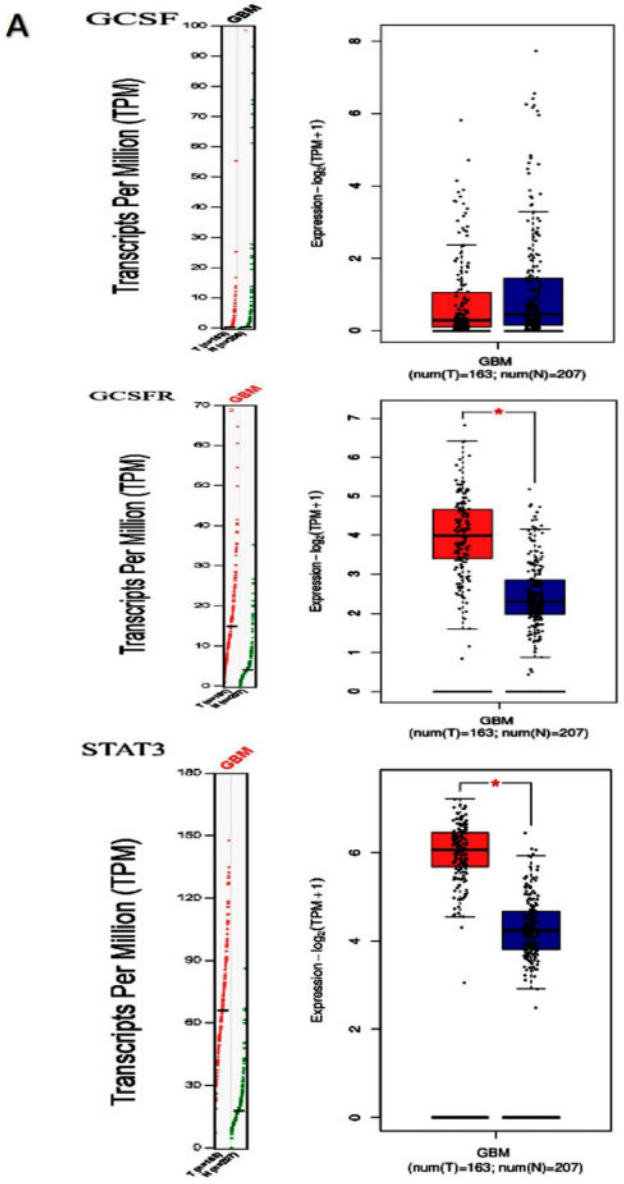

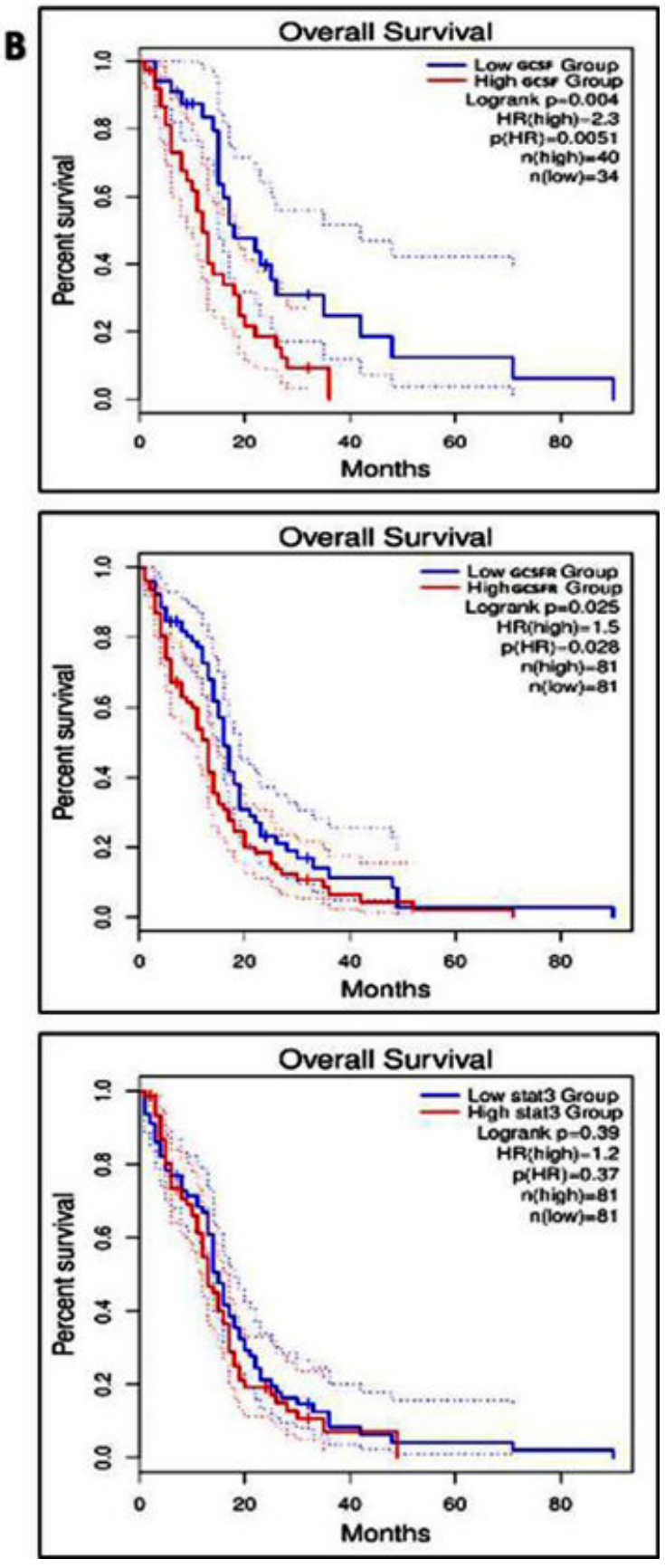
B
Overall Survival
Low gcsf Group
High gcsf Group
Logrank p=0.004
HR(high)=2.3
p(HR)=0.0051
n(high)=40
n(low)=34
Percent survival
Months
Overall Survival
Low gcsfr Group
High gcsfr Group
Logrank p=0.025
HR(high)=1.5
p(HR)=0.028
n(high)=81
n(low)=81
Percent survival
Months
Overall Survival
Low stat3 Group
High stat3 Group
Logrank p=0.39
HR(high)=1.2
p(HR)=0.37
n(high)=81
n(low)=81
Percent survival
Months

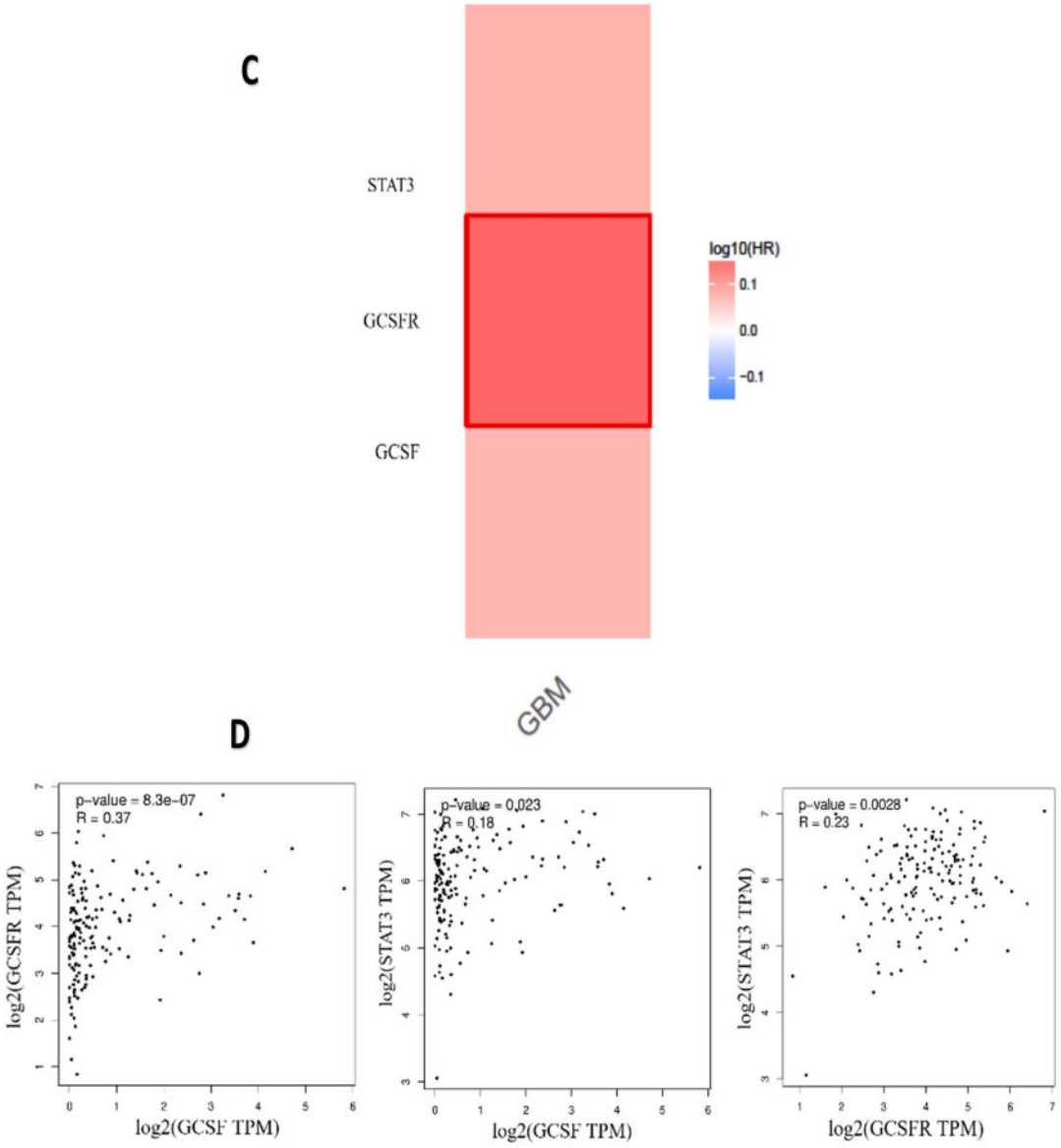

FIGURE 4.17: GCSF, GCSFR and STAT3 expression, survival analysis, heatmap and their correlation in glioblastoma

A) Tissue gene expression according to the GEPIA2, TCGA and GTEX databases. GCSFR, GCSF, and STAT3 show significant (*p $<$ 0.01) differential expression between GBM and normal tissue. The cut-off value for log2FC (fold change) was 1. We used a p-value threshold of 0.01 and a jitter size of 4. TPM is an acronym for transcripts per million. B) Using the GEPIA2, TCGA, and GTEX platforms, Kaplan-Meier survival graphs were generated. The overall survival curve of several malignant tissues was investigated between a high expression group (red line) and a low expression group (blue line) of GCSFR, GCSF, and STAT3, using p = 0.01

as the threshold for statistical significance. C) The survival heat map of hazard ratio (HR) indicates the prognostic impacts of highly significant expressed genes, e.g. GCSF log10 (HR) = 2.3, GCSFR log10 (HR) = 1.5 and STAT3 log10 (HR) = 1.2. D) The correlation analysis of GCSF, GCSFR, and STAT3 has been depicted. GCSF and GCSFR revealed a high correlation with an R-value of 0.37.

4.9 Protein Interactions and Gene Enrichment Ontology of Inflammatory Genes

The biological roles of inflammatory genes (IL-1β, IL-6, IL-8, IL-10, TGF-β, TNF-α, NF-κB, IL1Ra, GCSF, GCSFR and STAT3) and the aforementioned co-expressed genes were investigated using Metascape and g profiler (Figure 4.18A). The enrichment background is comprised of all genes in the genome. Terms with a minimum count of 3, p-value < 0.01, and an enrichment factor > 1.5 (Enrichment factor is the ratio of observed numbers to the expected counts by chance) were retrieved and clustered based on their association similarities. Furthermore, p-values are determined using the cumulative hyper geometric distribution. In contrast, q-values are determined using the Benjamini-Hochberg process to account for multiple tests when performing hierarchical cluster analysis on the enriched terms. Kappa scores are taken as the similarity metric, and sub-trees with a similarity > 0.30 are considered clusters. The term having the highest statistical significance is selected to represent the cluster resulting in the inactivation of GCSF signaling at Log10 p = -9.30 and Log10 q = 5.01 (Figure 4.18B). The most frequent terms are shown in the bar chart representing the p-value of immune system process, signaling and response to stimulus in response of GCSF, GCSFR, and STAT3 (Figure 4.18C). In addition, a network map of the enriched terms with log p-values was constructed showing all genes in different color nodes (Figure 4.18D). An enrichment study of protein-protein interactions of respective genes was performed using the following databases: STRING, BioGrid, OmniPath, and InWeb IM. Only physical interactions in STRING (physical score > 0.132) and BioGrid have been used. The resulting network comprises the subset of proteins interacting

physically with at least one other component. The Molecular Complex Detection (MCODE) algorithm has been applied to identify densely connected network components (Fig.4.18E- 4.18F). MCODE1 was associated with inactivation of CSF3 (GCSF) signaling, signaling by CSF3 (GCSF), and JAK/STAT signaling pathway and prostaglandin signaling. However, the Gene Ontology analysis of DEGs showed significant enriched terms (p-value < 0.05) of all inflammatory genes in two groups (GFAP positive and GFAP negative). To further analyze the relationship between gene and disease, the function of the gene and its regulation, subtypes, and cellular processes play key roles in understanding of its biology and the dysregulation of different biological processes causing GBM. The GFAP –positive group of genes (IL-1β, IL-6, IL- 8, IL-10, TGF-β, TNF-α, NF-κB, IL1Ra) and GFAP-negative group of genes (GCSF, GCSFR and STAT3) were further examined to estimate the molecular mechanism involved in glioblastoma. This analysis highlighted the genes and pathways in the molecular and biological functions and other signaling components of gene with significant Log p-value (Figure 4.18G-4.18H). We evaluated the regulatory network and functionally related genes using the Gene MANIA database for both groups of genes. We identified twenty genes with the highest correlation for each group. For GFAP-positive groups, which were, Platelet factor 4 (PF4) , Chemokine (C-C motif) ligand 8 (CCL8), C-X-C Motif Chemokine Ligand 10(CXCL10), C-C Motif Chemokine Ligand 2 (CCL2), Heparin Binding EGF Like Growth Factor (HBEGF), Atypical Chemokine Receptor 1 (ACKR1), G Protein Subunit Alpha 14 (GNA14), MacroH2A.1 Histone (MACROH2A1) , G Protein Subunit Alpha 15 (GNA15), Plasminogen Activator, Urokinase Receptor (PLAUR), Intercellular Adhesion Molecule 1(ICAM1), Chemokine (C-X-C motif) ligand 3(CXCL3), (interleukin 8, or CXCL8, (C-X-C motif) ligand 8 (CXCL8), CXCR1, (C-X-C motif) ligand 2(CXCL2) , (C-X-C motif) ligand 1 (CXCL1), Interleukin 6 (IL6), Interleukin 1B (IL1B), CC chemokine ligand 20 (CCL20), C-X-C Motif Chemokine Receptor 2(CXCR2), Matrix Metallopeptidase 13 MMP13 as shown in (Figure 4.18I).

Similarly For GFAP-negative group of genes which were GCSFR, elastase neutrophil expressed (ELANE), Interleukin 6 (IL6), interleukin 6 signal transducer

(IL6ST), POU Class 2 homeobox 2 (POU2F2), heat shock transcription factor 1 (HSF1), surfactant protein B (SFTBP), C-X-C motif chemokine ligand 3 (CXCL3), TNF alpha induced protein 6 (TNFAIP6), heparin binding EGF like growth factor (HBEGF), advanced glycosylation end-product specific receptor (AGER), endothelin 1 (EDN1), RELA proto-oncogene, NF-kB subunit (RELA), C-C motif chemokine ligand 2 (CCL2), LIF interleukin 6 family cytokine (LIF), retinoic acid receptor responder 1 (RARRES1), nephrocystin 1 (NPHP1), calcium modulating ligand (CAMLG), general transcription factor IIIC subunit1 (GTF3C1), solute carrier family 34 member 2 (SLC34A2). The different modes of orientation of gene –gene network show the different functions of genes, including physical interaction at about 77.64%. The group of genes which shows physical interaction with each other are GCSFR, GCSF, ELANE, TNFAIP6, AGER, RELA, IL6, IL6ST, LIF, CCL2 and similarly the other gene functions are co-expression 8.01%, predicted 5.37%, colocalization 3.63%, genetic alteration 2.87%, pathway 1.88%, shared protein domain 0.60%, and pfam 0.21% (Figure 4.18J).

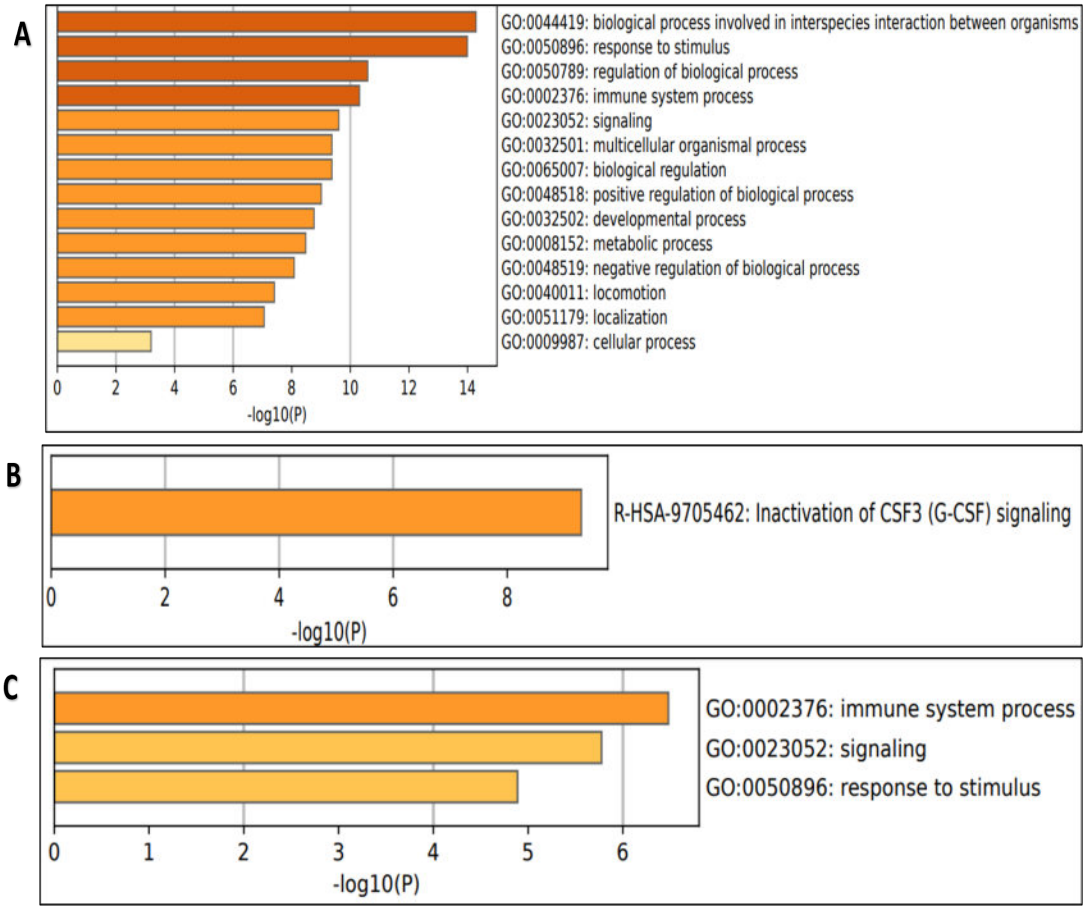

D

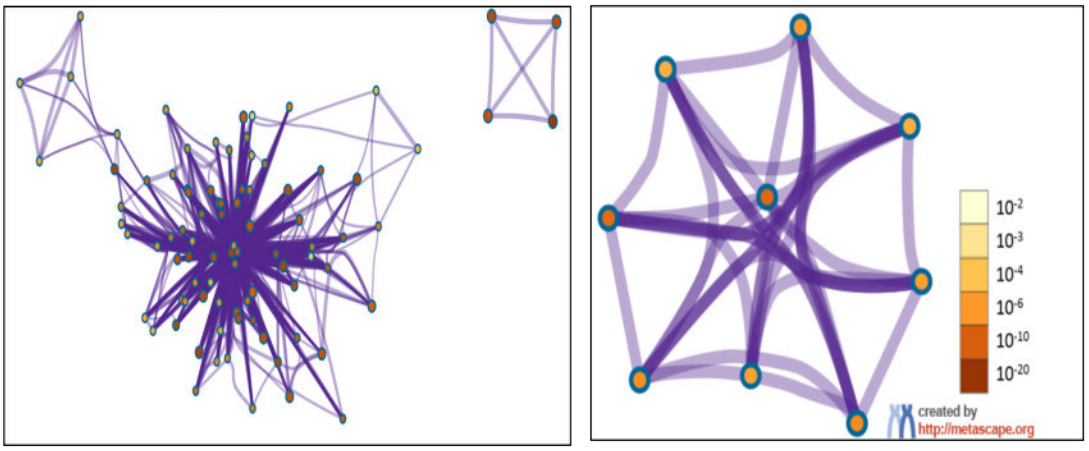

E

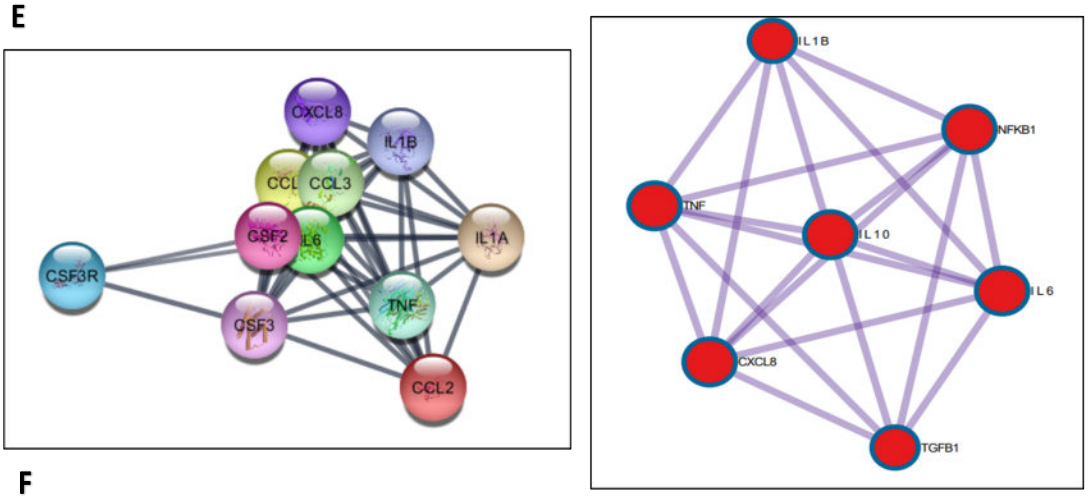

F

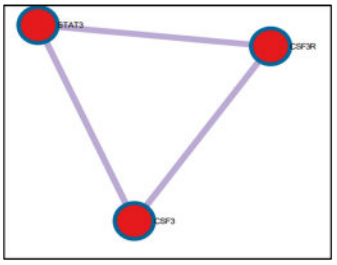

GO	Description	Log10(P)	Color	MCODE	GO	Description	Log10(P)
R-HSA-9705462	Inactivation of CSF3 (G-CSF) signaling	-9.3		MCODE_1	R-HSA-9705462	Inactivation of CSF3 (G-CSF) signaling	-9.3
R-HSA-9674555	Signaling by CSF3 (G-CSF)	-9.1		MCODE_1	R-HSA-9674555	Signaling by CSF3 (G-CSF)	-9.1
hsa04630	JAK-STAT signaling pathway	-6.8		MCODE_1	hsa04630	JAK-STAT signaling pathway	-6.8

GO	Description	Log10(P)	Color	MCODE	GO	Description	Log10(P)
hsa05142	Chagas disease	-17.4		MCODE_1	hsa05142	Chagas disease	-17.4
hsa05146	Amoebiasis	-17.4		MCODE_1	hsa05146	Amoebiasis	-17.4
WP5088	Prostaglandin signaling	-17.1		MCODE_1	WP5088	Prostaglandin signaling	-17.1

G

GFAP – positive group of inflammatory genes (IL-1β, IL-6, IL- 8, IL-10, TGF-β, TNF-α, NF-κB, IL1Ra)

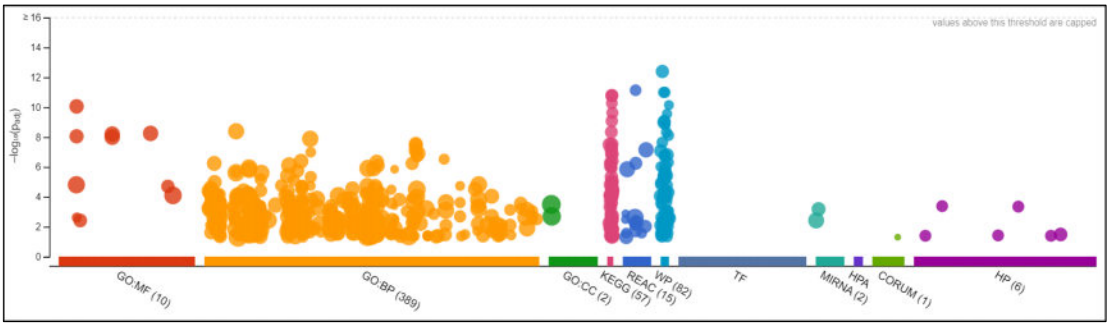

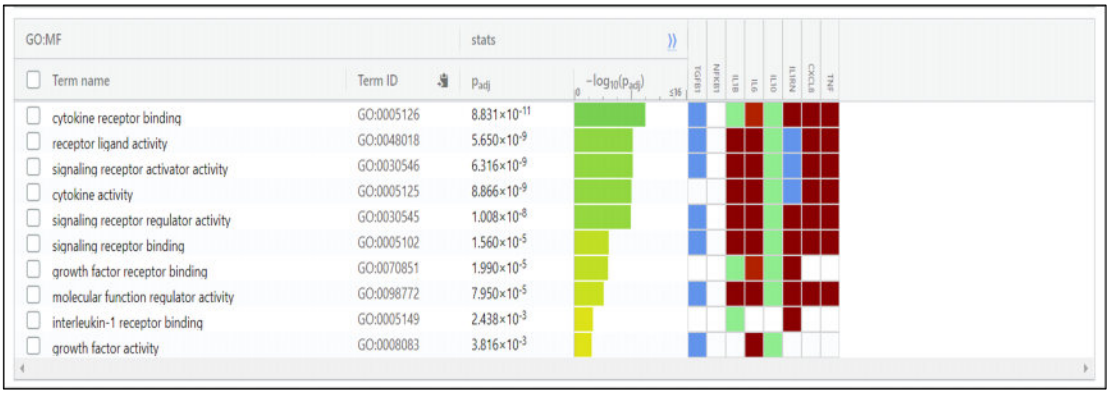

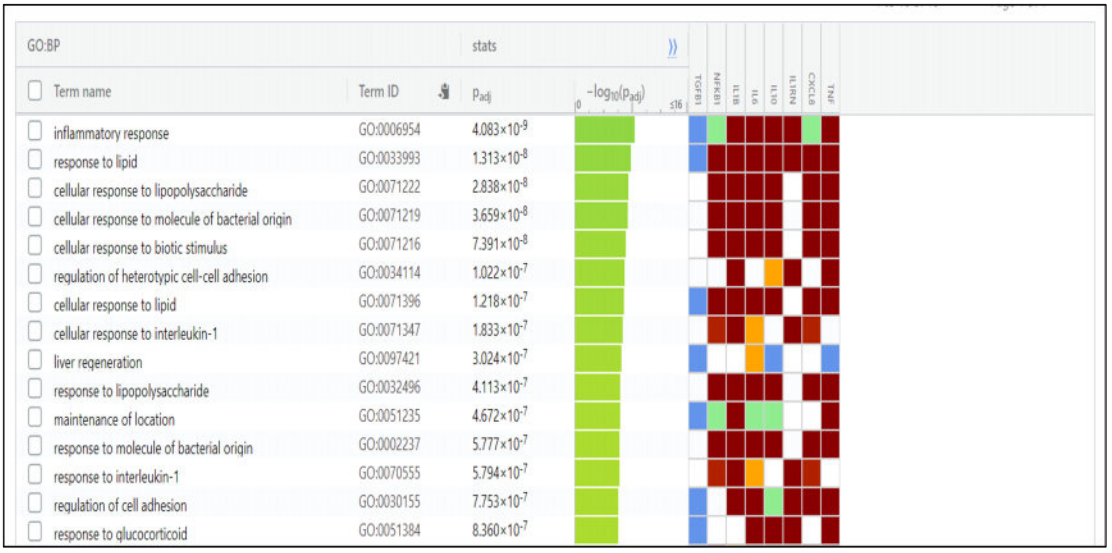

H **GFAP – negative group of inflammatory genes (GCSF, GCSFR and STAT3)**

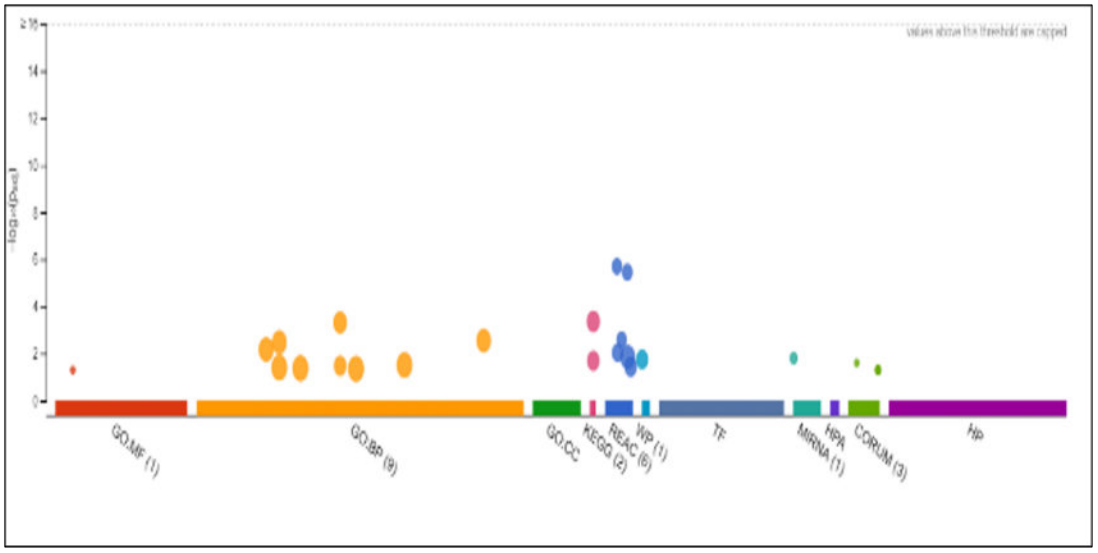

GO:MF

Term name	Term ID	p_{adj}	$-\log_{10}(p_{adj})$	CSF3	CSF3R	STAT3
granulocyte colony-stimulating factor receptor binding	GO:0005130	4.988×10^{-2}				

GO:BP

Term name	Term ID	p_{adj}	$-\log_{10}(p_{adj})$	CSF3	CSF3R	STAT3
regulation of myeloid cell differentiation	GO:0045637	4.769×10^{-4}				
regulation of hemopoiesis	GO:1903706	2.790×10^{-3}				
myeloid cell differentiation	GO:0030099	3.314×10^{-3}				
cytokine-mediated signaling pathway	GO:0019221	6.681×10^{-3}				
cellular response to cytokine stimulus	GO:0071345	3.075×10^{-2}				
positive regulation of myeloid cell differentiation	GO:0045639	3.292×10^{-2}				
hemopoiesis	GO:0030097	3.894×10^{-2}				
response to cytokine	GO:0034097	4.187×10^{-2}				
hematopoietic or lymphoid organ development	GO:0048534	4.424×10^{-2}				

KEGG

Term name	Term ID	p_{adj}	$-\log_{10}(p_{adj})$	CSF3	CSF3R	STAT3
JAK-STAT signaling pathway	KEGG:04630	4.309×10^{-4}				
Hematopoietic cell lineage	KEGG:04640	2.013×10^{-2}				

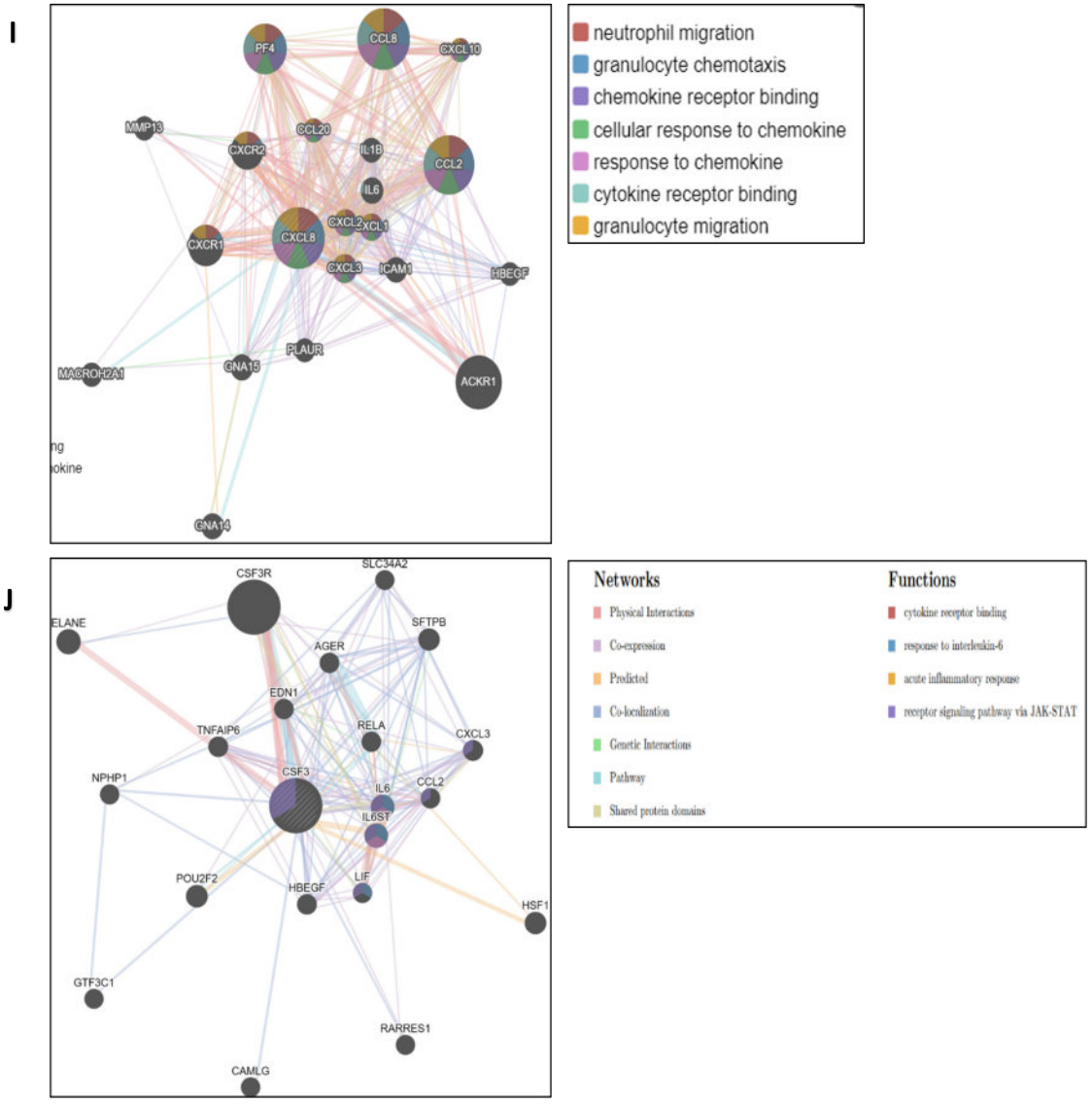

FIGURE 4.18: The PPI and Gene enrichment analysis of inflammatory genes in GBM patients

A) Top clusters for inflammatory genes (IL-1β, IL-6, IL- 8, IL-10, TGF-β, TNF-α, NF-κB and IL1Ra. B) (Biological responses and signaling) at p-value in log base-10. B) Top 1 cluster for GCSF (CSF3) gene (inactivation of signaling) at p-value in log base-10. C) Bar chart of the first three enriched terms for CSF3. D) Enriched terms network: Color by cluster ID, wherein nodes share the same cluster-ID are often adjacent and colored by p-value, where terms with more genes are more likely to have a significant p-value. E-F) PPI network Identification of significantly connected inflammatory genes and Identification of enriched term net graph MCODE component. G-H) Significant p-values summary of GO analysis of

DEGs (GFAP-positive group and GFAP negative group) suggest essential molecular functions and comprise the crucial GO categories evaluated according to the levels of DEGs enrichment. I-J) In GBM patients, the GeneMANIA database reported 20 genes significantly associated genes of both group through gene-gene networks. Differential mode of the orientation of gene-gene network showing different functions of genes.

4.10 Pathway Enrichment Analysis and Associated Mechanisms

The volcano plot was implemented with interactivity and customization for associated pathways related to inflammatory genes of GFAP positive group group in the current study to investigate the detailed effect of these inflammatory genes in the initiation of inflammatory response during progression of GBM tumor. It showed the log of the FDR versus the enrichment ratio for all the functional categories highlighting the degree by which the significant categories stand out from the background .The size and color of the dot was proportional to the number of overlapping (for ORA) or leading edge genes (for GSEA) of the category. The significantly enriched categories were labeled, and the labels are positioned automatically by a force field-based algorithm at startup (Figure 4.19A).For analysis pathway databases were used. For the WikiPathways and KEGG databases, the overlapping/leading edge genes were highlighted in inflammatory cascade, and the input scores for the genes were also used to specify a color gradient for the leading edge genes when GSEA is run against the WikiPathways database (Figure 4.19B). TNF signaling pathway, TNF induce NFKB signaling, MAPK signaling pathway, Toll like receptor signaling pathway and pathway in cancers were significant. For GFAP - negative group, the GCSF, GCSFR, and STAT3 genes were analyzed through fold chain enrichment analysis using shiny GO (http://bioinformatics.sdstate.edu/go/), which identified five critical enriched pathways, as shown in (Figure 4.19C). The essential pathway regulated by the DEGs is JAK/STAT signaling, along with

the association of hematopoietic cell lineage, cytokine-cytokine receptor interaction, and PI3K-AKT signaling pathway. The activation of STAT3 pathway is crucial to carcinogenesis and immune evasion. Various potential upstream and downstream regulatory mechanisms and development of the immunological milieu are transcriptionally upregulated by STAT3 activation. The equilibrium of cytokines stimulates the infiltration of immunosuppressive immune cell types, such as myeloid-derived suppressor cells (MDSCs), regulatory T cells (Tregs), and tumor-associated macrophages/microglia (TAMs). These cytokines promote STAT3 signaling within immune cell populations to induce immunosuppressive macrophage polarization, diminish antigen presentation, and suppress T cell activation. KEGG pathway indicates the genes involved in GBM progression showing significant fold chain enrichment of 3.5 −log10 (FDR) in JAK/STAT signaling pathway. Therefore, we examined GCSF role in the associated pathways in GBM to highlight aberrant signal transduction cascades and potential drug targets especially in the critical JAK/STAT pathway (Figure 4.19D).

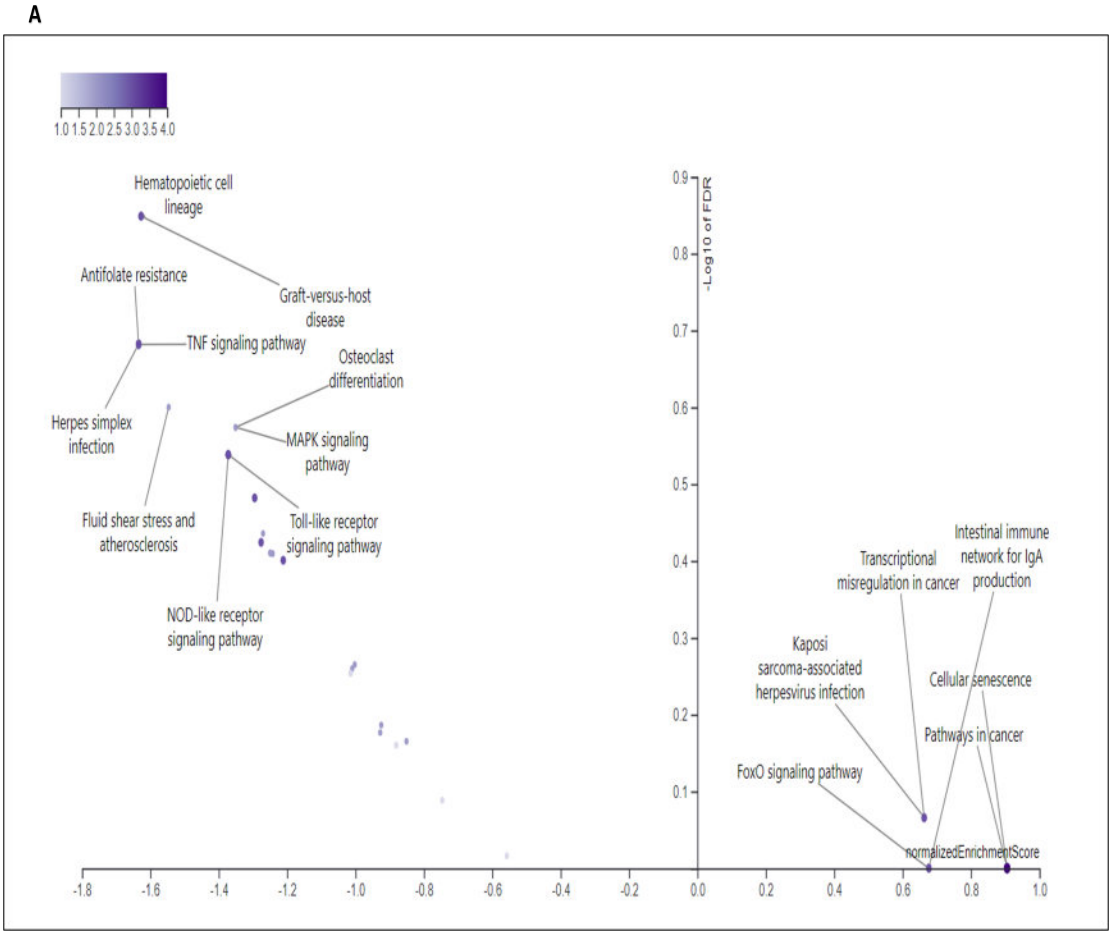

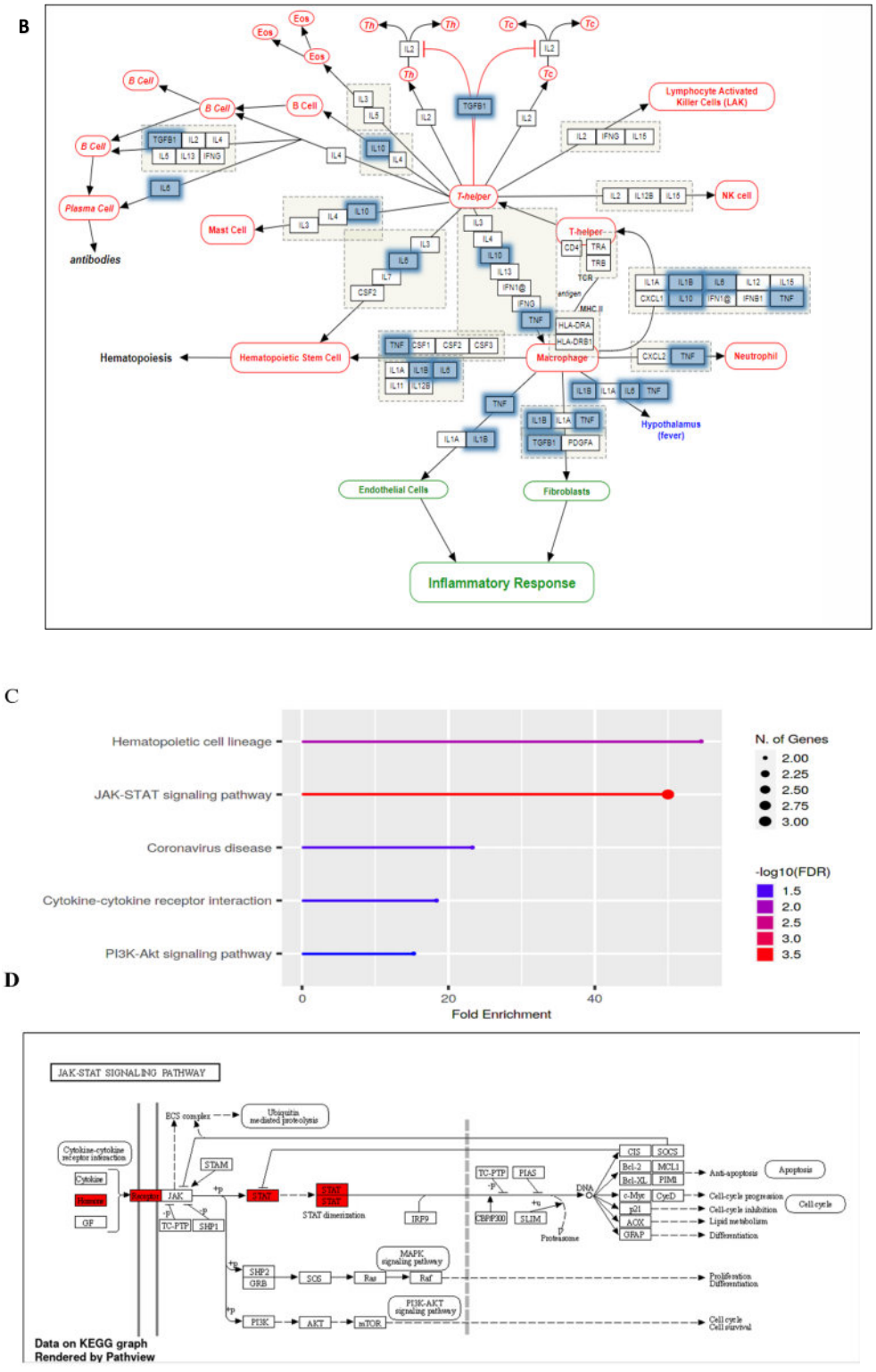

FIGURE 4.19: Pathway enrichment analysis

A) Customizable volcano plot for significant associated pathways. B) Highlighted overlapping/leading edge genes in inflammatory cascade associated with different pathways. C) Highlighting the percentage of DEGs in the biological pathway using the shiny GO tool. D) KEGG

and Wiki Pathways have been employed to map the pathways. Color codes are applied to explain the involvement of DEGs and their associated mechanism in the pathway model.

4.11 Immune Infiltration in GBM

Associations and Correlation between Levels of immune cell infiltration and expression from GFAP Positive group

GBM tumor progression and patient's outcome can be significantly influenced by the correlation between the GBM cells and the immune system in the tumor microenvironment. The immune cells are responsible in the activation of signaling pathways because of both the pro-tumorigenic and anti-tumorigenic effects as reported in previous literature. TGFB , TNFα and NF-κB p65 (RelA) are the three important signaling molecules, involved in the inflammation, proliferation, cell differentiations and immunosuppression. TGFβ1 plays a drastic role in the progression and angiogenesis of GBM via interacting chemokines and macrophages in the tumor microenvironment. To determine the levels of TGFβ1 gene expression and immune infiltration correlated with GBM, we employed the TIMER web server with the integration of TIMER, CIBERSORT, and MCPCOUNTER. TGFβ1 expression levels were discovered to positively associated with B cells (Rho = 0.428, p = 1.77e-07), CD4+ (Rho = 0.328, p = 9.07e-05), Macro phage \Monocyte (Rho = 0.407, p =7.95e-07), Macro phage (Rho = 0.466, p = 9.31e-09), Treg Cell (Rho=0.261, p=2.06e-03), Neutrophil (Rho = 0.338, p = 5.34e-05) Myeloid Dendritic cell (Rho=0.624, p=3.54e-16) and NK cell resting (Rho = 0.168, p = 4.96e-02) infiltration levels in GBM as shown in (Figure 4.20A).

We also used the TIMER web server with the integration of EPIC, CELL, CIBERSORT and QUANTISEQ, TIMER to visualize the correlation between TNFα and NF-κB p65 (RelA) gene expression levels and immune infiltration levels in GBM. TNFα is the pro-inflammatory cytokines that play a crucial role in the inflammation, immune response, promote tumor cell growth and invasion in GBM. We found that the expression levels of TNFα were positively correlated with B cells (Rho = 0.251, p = 2.04e-03) , CD8 + T cells (Rho = 0.174, p = 4.26e-02), CD4+ (Rho = 0.262, p = 2.00e-03), Monocyte (Rho = 0.245, p = 3.96e-03), Macrophage (Rho = 0.242, p = 4.34e-03), Myeloid Dendritic cell (Rho = 0.232, p = 6.27e-03),

and NK cell (Rho = 0.329, p = 8.74e-05), infiltration levels in GBM and TNFα was also negatively correlated with Treg Cell (Rho = -0.262, p = 2.00e-03), (Figure 4.20B). Similarly, NF-κB p65 (RelA) were positively correlated with, CD4+ (Rho = 0.173, p = 4.35e-02), Treg Cell (Rho = 0.2, p = 1.90e-02), Myeloid Dendritic cell (Rho = 0.366, p = 1.12e-05), B cells (Rho = 0.173, p = 4.37e-02), Macrophage M0 (Rho = 0.187, p = 2.84e-02), NK cell (Rho = 0.245, p = 3.98e-03), and Neutrophil (Rho = 0.478, p = 3.46e-09).NF-κB p65 (RelA) was also negatively correlated with CD8 + T cells (Rho = -0.283, p = 7.99e-04) and Macrophage M2 (Rho = -0.213, p = 1.24e-02), as shown in (Figure 4.20C).

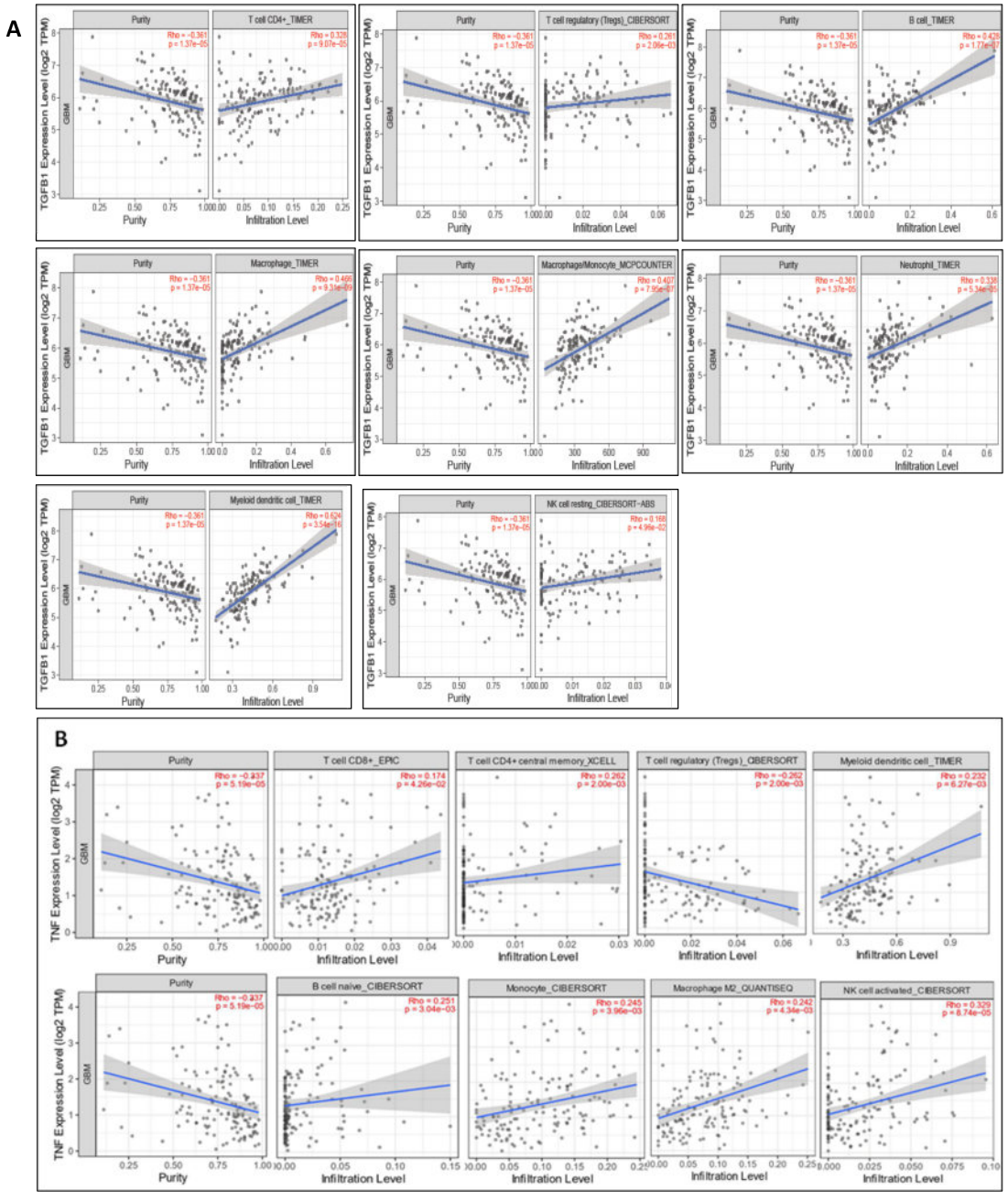

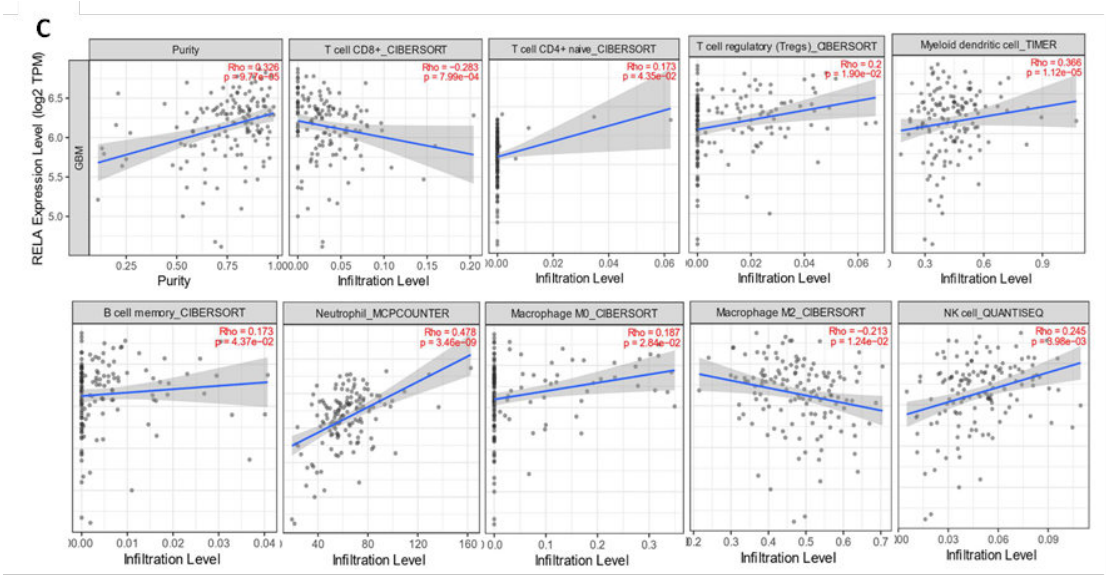

FIGURE 4.20: Relationships between TGFβ1, TNFα and NF-κB p65 (RelA) expression levels and immune cell infiltration levels in GBM

A) Correlation between the abundance of immune cells and the expression of TGFβ1 at significant p-value ≤ 0.05. B) Correlation between the abundance of immune cells and the expression of TNFα at significant p-value ≤ 0.05. C) Correlation between the abundance of immune cells and the expression of NF-κB p65 (RelA) at significant p-value ≤ 0.05.

4.12 Differential Abundances of Infiltrative Immune Cells and Their Correlation with GCSF from GFAP Negative Group

In the current study GCSF expression was analysed for immune infilteration in GBM. Previous studies reported that immune infiltration is often associated with developing a favorable tumor microenvironment for oncogenesis. The TIMER database was used in the current investigation to examine the correlation between GCSF transcriptomic expression and immune infiltration. Using the CIBERSORTx algorithm, the relative proportions of 9 kinds of infiltrative immune cells with significant differences in GBM were obtained, including T cells CD4, Tregs, B cell memory, neutrophil, monocyte, myeloid dendritic cell, NK cell resting, mast

cells and eosinophils which were differentially expressed. These correlations suggest that differential GCSF expression is a characteristic of multiple gene signatures associated with pro-tumor immune environments in GBM patients. The expression of GCSF was positively correlated with B cells (Rho = 0.191, p = 2.53e−02), CD4+T cells (Rho = 0.184, p = 3.11e−02), Tregs (Rho = 0.315, p = 1.74e−04), neutrophils (Rho=0.269, p=1.47e−03), monocyte (Rho = 0.191, p = 2.52e−02), Myeloid dendritic cell (Rho=0.304, p=3.03e−04), NK cell resting (Rho = 0.336, p = 6.09e−05), mast cells resting (Rho = 0.17, p = 4.64e−02) and eosinophils (Rho = 0.326, p = 1.00e−04) as shown in Figure 4.21.

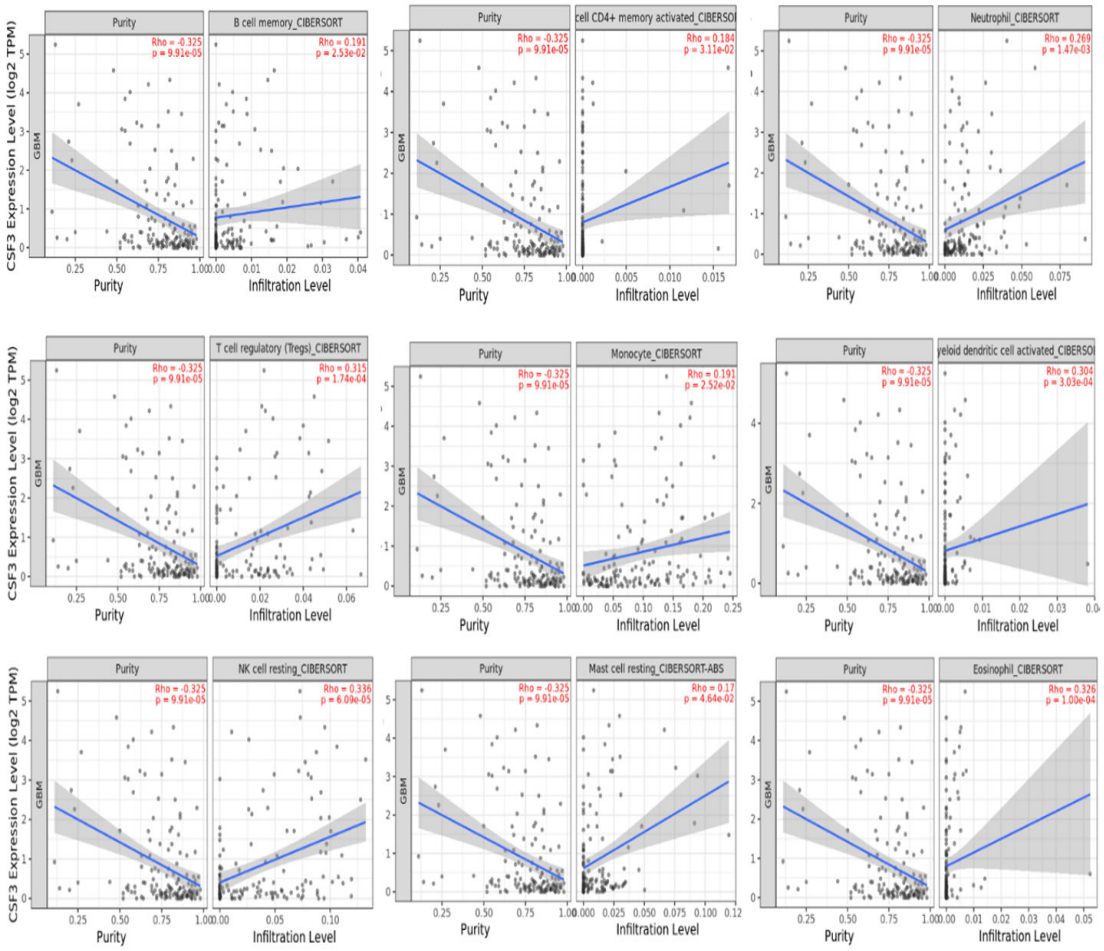

FIGURE 4.21: Correlation between GCSF expressions with 09 immune infiltration levels using algorithms CIBERSOFT.

The association between GCSF and immune infiltrating cells shows a positive differential infiltrative correlation with a significant p-value ≤ 0.05.

4.13 Molecular Events (Mutations) Associated with the Glioma

Insilico Next Generation Sequencing (NGS) Analysis

4.13.1 Identification of Driver Genes in Glioblastoma Network and Functional Analysis

The GBM summary network (Figure 4.22A) showed the relationship between driver genes and miRNA drivers in glioblastoma. Driver genes have a variety of characteristics and colour-coded nodes identify them. As yellow nodes identify MicroRNA (miRNA) drivers. These nodes are joined by lines to depict the protein-protein interactions (PPIs) in the STRING database and synergistic effects, which are defined as situations in which the hazard ratio (HR) of two genes is larger than 1.5 times that of each gene. Moreover, miRTar Base keeps track of how miRNAs and genes interact (Figure 4.22B). We predicted the driver genes of glioblastoma samples in the TCGA database using the DriverDBV3 online database, as shown in table 4.4, in order to better understand the molecular characteristics of glioblastoma. Our top 20 driver genes are Epidermal Growth Factor Receptor (EGFR), Phosphatidylinositol-4,5-Bisphosphate 3-Kinase Catalytic Subunit Alpha (PIK3CA), Isocitrate Dehydrogenase (NADP(+)) 1 (IDH1), Tumor Protein P53 (TP53), Phosphatase and tensin homolog (PTEN), Rh Blood Group D (RHD), Phosphoinositide-3-Kinase Regulatory Subunit 1 (PIK3R1), leucine rich repeat containing 37A (LRRC37A), Glutathione S-Transferase M1(GSTM1), Signal Regulatory Protein Beta 1(SIRPβ1), Sodium/potassium/calcium exchanger 3(SLC24A3), Major Histocompatibility Complex, Class II, DR Beta 5 (HLA-DRB5), osteosarcoma amplified 9(OS9), Carboxy-terminal domain RNA polymerase II polypeptide A small phosphatase 2 (CTDSP2), Maternal Embryonic Leucine Zipper Kinase (MELK), Zinc Finger And BTB Domain Containing 42 (ZBTB42), UDP Glucuronosyltransferase Family 2 Member β17 (UGT2β17), Energy Homeostasis Associated (ENHO), Cyclin Dependent Kinase Inhibitor 2B

(CDKN2B) and contactin associated protein family member 3B (CNTNAP3B). We employed DriverDBV3 having more than seven algorithms to predict driver genes simultaneously to improve the accuracy of our results. Through network analysis, 80 driver genes were expressed, and the top 20 driver genes of glioblastoma were screened for gene ontology based upon significant log values of biological process ERBB2 signalling pathway, regulation of cyclin-dependent proteins, regulation of cyclin-dependent proteins kinases, positive regulation of production of miR and negative regulation of mitotic cell cycle (Figure 4.22C-4.22D). The twelve gene set collections from seven public database KEGG, PID, Biocarta, Recatome, MsigDB, miRTar, and miRWalk are used in the pathway analysis. The significant genes at KEGG were PIK3CA, PIK3R1, TP53, EGFR, PTEN, CDKN2A and CNTNAP3B at –log10 (p-value) (Figure 4.22E). Similarly cellular functional analysis showed phosphatidylinositol 3-kinase complex, cytoplasmic part region of cytosol, cytoplasm and apical plasma membrane shown highest log values (Figure 4.22F). Lastly the molecular functions of driver genes of GBM also shown significant log10 values in respect to natural killer cell lectin-like receptor, insulin substrate insulin binding and cyclin dependent protein serine threonine in (Figure 4.22G).

TABLE 4.4: Top 20 driver genes of glioblastoma summary table

Cancer	**Gene**	**CGC**	**NCG6.0**	**Mutation**	**CNV**	**Methylation**
GBM	EGFR	1	1	12	1	0
GBM	IDH1	1	1	7	0	0
GBM	PIK3CA	1	1	9	0	0
GBM	PIK3R1	1	1	9	0	0
GBM	PTEN	1	1	11	0	0
GBM	TP53	1	1	12	0	0
GBM	RHD	0	0	0	-1	0
GBM	LRRC37A	0	0	0	1	0
GBM	GSTM1	0	0	0	-1	0
GBM	SIRPβ1	0	1	0	1	0
GBM	SLC24A3	0	0	0	1	0

Cancer	Gene	CGC	NCG6.0	Mutation	CNV	Methylation
GBM	HLA-DRB5	0	0	0	1	0
GBM	CTDSP2	0	0	0	1	0
GBM	OS9	0	0	0	1	0
GBM	MELK	0	0	0	-1	0
GBM	ZBTB42	0	0	0	-1	0
GBM	UGT2β17	0	0	0	-1	0
GBM	ENHO	0	0	0	-1	0
GBM	CDKN2B	0	1	0	-1	0
GBM	CNTNAP3B	0	0	0	-1	0

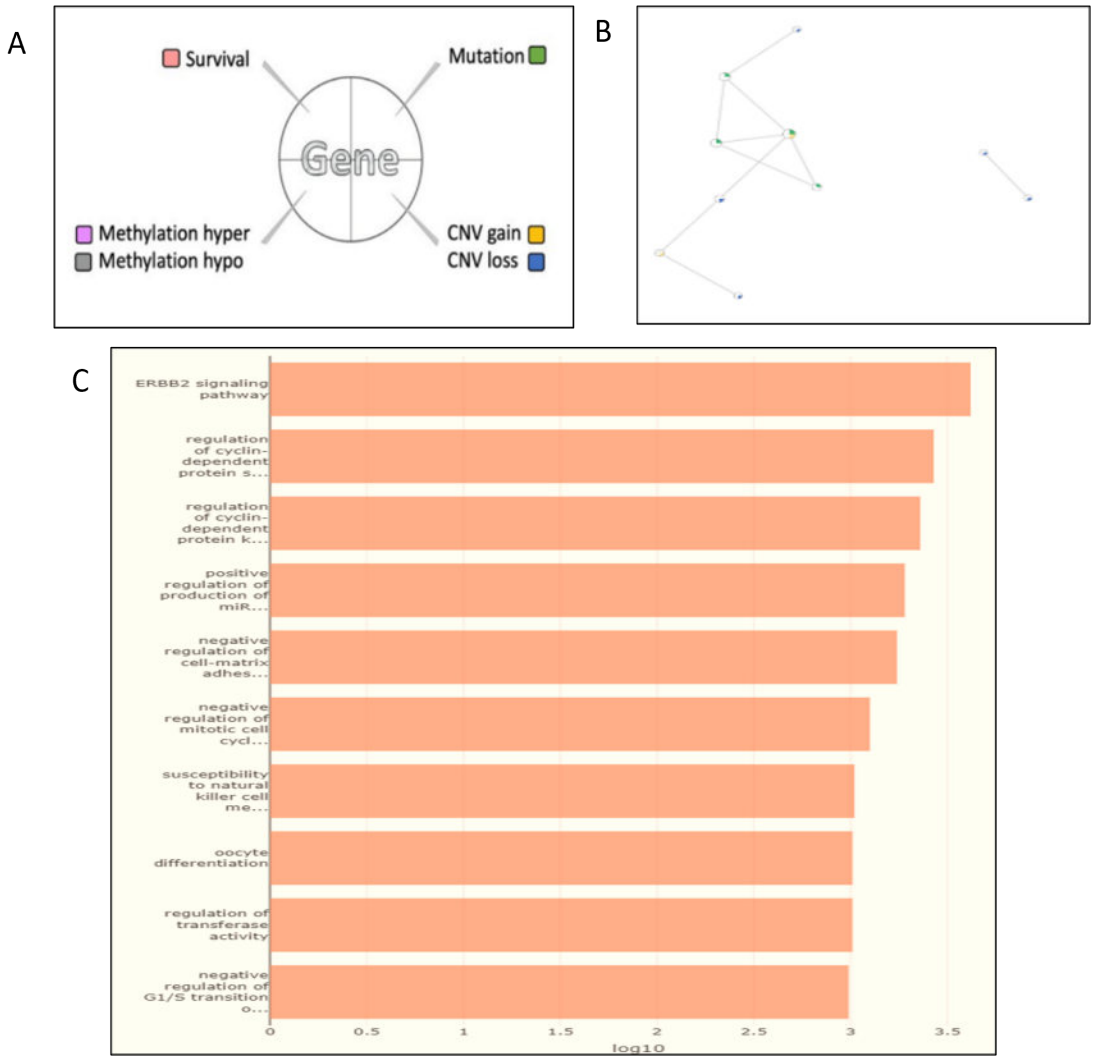

A) The glioblastoma network presents the relationships between driver genes and miRNA drivers in a specific cancer type. B) In the Summary panel, a network

D

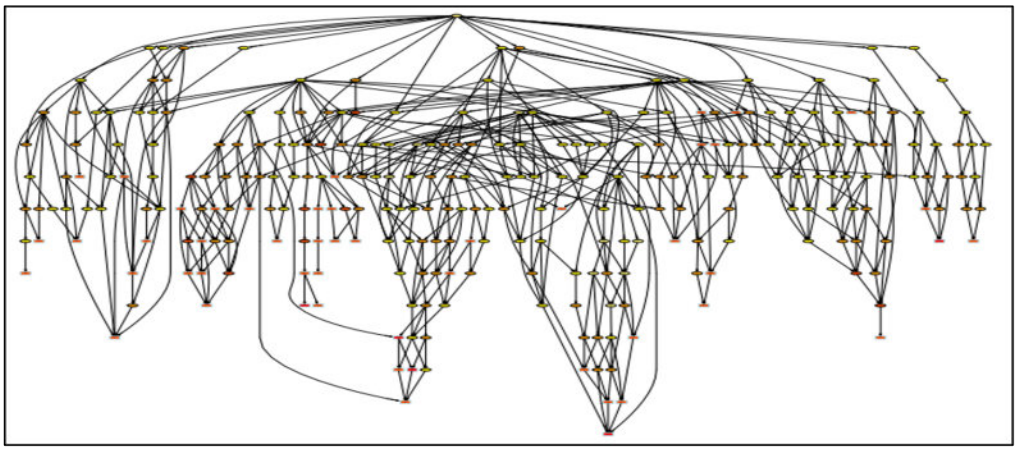

E

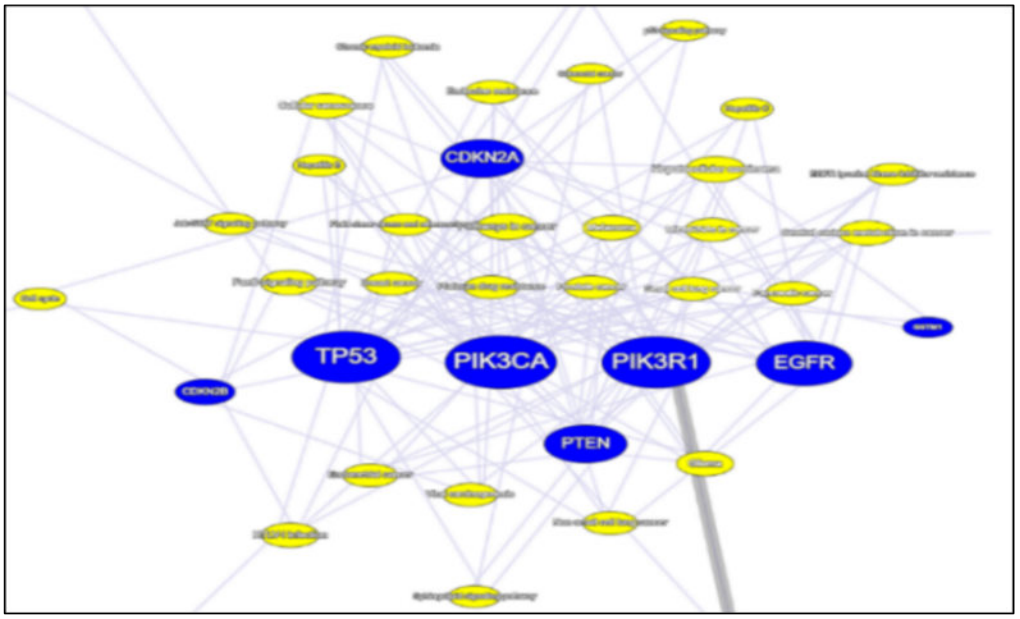
CDKN2A
TP53
PIK3CA
PIK3R1
EGFR
PTEN

F

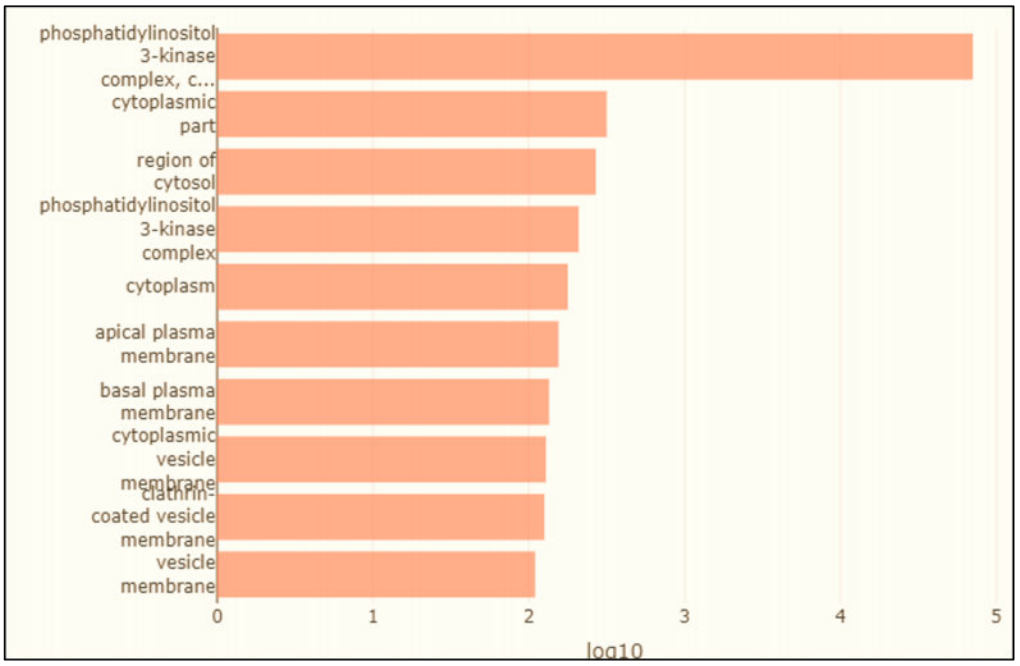
phosphatidylinositol 3-kinase complex, c...
cytoplasmic part
region of cytosol
phosphatidylinositol 3-kinase complex
cytoplasm
apical plasma membrane
basal plasma membrane
cytoplasmic vesicle membrane
clathrin-coated vesicle membrane
vesicle membrane
0
1
2
3
4
5
log10

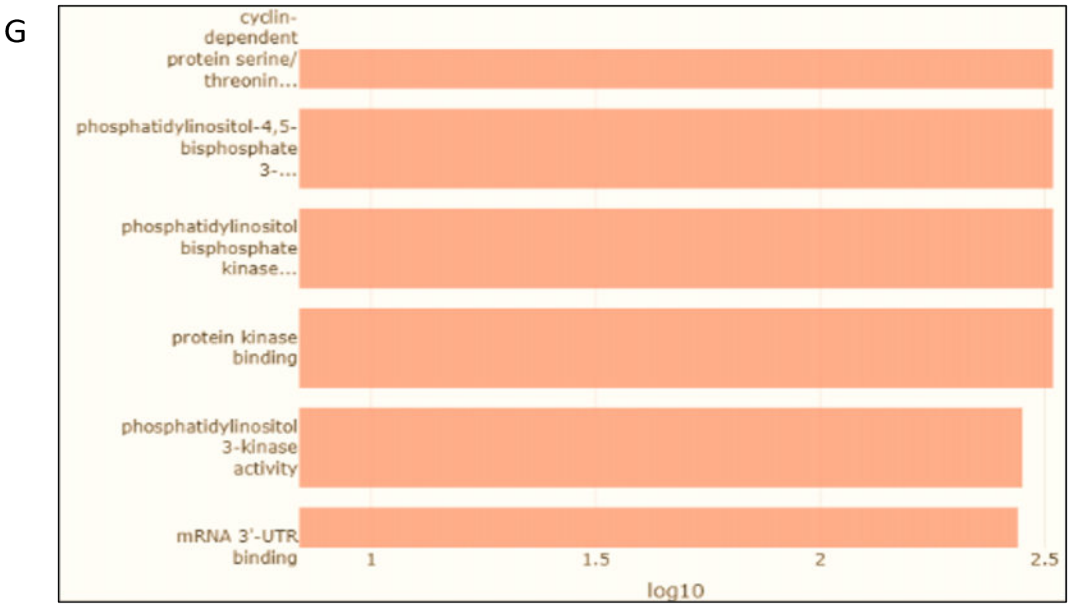

FIGURE 4.22: Analysis of the driver genes in glioblastoma.

shows the drivers for mutation, CNV, methylation, and miRNA, each represented by a different colour grid in the node. Protein-protein interactions between nodes make up the string database's interactions. Determining which two genes' hazard ratios (HR) are larger than 1.5 for each gene. C-D-F-G) With a statistically significant value of Log10 P = 0.05, the functional annotation section provides gene ontology of functional analysis of driver genes in biological, cellular, and molecular processes. E) The Pathway section contains 12 gene set collections collected from 7 open-access databases: at -log10 for KEGG (p-value).

4.13.2 The Mutational and Survival Analysis of Driver Genes

The current in silico studies have shown that glioblastoma has many driver gene mutations. To more clearly establish the impact of driver genes on the prognosis of glioblastoma patients, we analyzed the driver gene mutations in the erroneous modifications of commonly altered genes and essential cancer genes in many signaling pathways. The bar graph depicted the top 30 major mutation drivers as determined by multiple computational tools, including the new tools CoMET, Mutex, and DriverML (Figure 4.23A). It was observed that the change frequency

of driver genes EGFR, TP53, PTEN, PIK3CA, PIK3R1, IDH1 were more significant, and we discovered these driver genes had a higher proportion of mutations. This graphic shows the relationships between the top 30 mutation driver genes and cancer patients with the integration of tools as shown in figure 4.23B-4.23C.

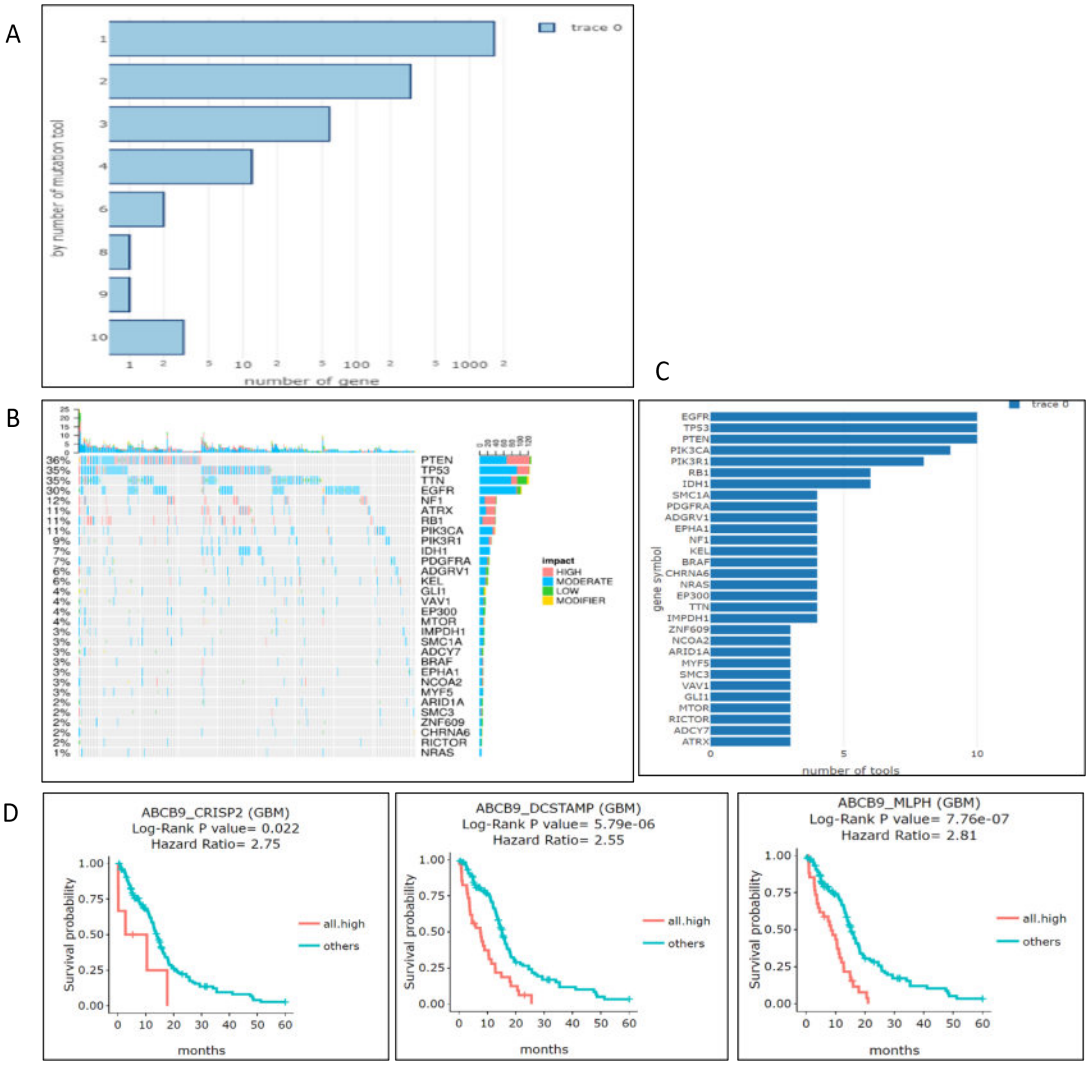

FIGURE 4.23: Mutational and survival Analysis of the driver genes in glioblastoma

A) The plot indicates defined mutation driver numbers by a different number of computational tools according to the mutation summary table. B) Using cancer patient samples on the x-axis and the top 30 genes on the y-axis, this graphic shows the relationships between the top 30 mutation driver genes and cancer patients. C) This plot shows the top 30 genes on the y-axis and the number of tools by which they are defined on x-axis. D) This section includes all gene pairs with HR fold change greater than 1.5 in both directions. The patients are divided into

groups depending on the patients' levels of gene expression for each gene pair. The hazard ratios for CRISP2, DCSTAMP, and MLPH were 2.75, 2.55, and 2.81 respectively. The survival probabilities of the patient groups are then contrasted throughout the months, as demonstrated in the plots with a significant p-value of 0.05.

The impact of driver gene mutations on the prognosis of GBM patients was then examined. Based on whether the driver gene had a mutation, CNV, or gene fusion, we separated the samples of each subtype into an altered group and a non-altered group. Our investigation discovered that CRISP2, DCSTAMP, and MLPH had a poor survival effect and a substantial hazard ratio. The orange and green nodes indicate the survival genes with HR $>$ 1. For each synergistic survival event, Kaplan-Meier plots were generated using the comparison of all high against others and four expression-based groups (all high, low/high, high/low, and all low). The hazard ratio values for CRISP2, DCSTAMP, and MLPH were 2.75, 2.55, and 2.81, respectively, as shown in Figure 4.23D.

4.13.2.1 CNV, MET and miRNA-Define Dysregulation Features of Protein-Coding Drivers and Locus Enrichment Analysis of Glioblastoma

In order to analyse the aberrant shifts and changes in gene expression and to define CNV and methylation dysregulation events, IGC, DIGGIT, and methylmix were used to identify CNV dysregulation events. Whereas the ELMER and methylation mix were used to identify methylation dysregulation incidents to analyze the aberrant shifts and changes in gene expression and define CNV and methylation dysregulation events by driverDBV3. As a result, this aligns CNV and methylation computational algorithms and interpretations of abnormal miRNA regulation with negative correlation coefficients between miRNA and driver genes. Using a heat map, we identify the top 30 drivers, CNV and methylation panels which also showed these novel traits in a similar way (Figure 4.24A). Similarly percentage bar charts showed significant gain in percentage of genes are EGFR (81%), LANCL2 (79%), SEC61G (78%), VOPP1 (77%), NIPSNAP2 (73%), MRPS17

(73%), ZNF713 (73%), PSPH (73%), SUMF2 (72%) and the genes with the significant loss functions were CDKN2A (71%), CDKN2B (70%), MTAP (67%), KLHL9 (60%), MLLT3 (54%) and TUSC1(50%) as shown in (Figure 4.24B). The most significant regions with identified CNV events were 1,3,4,6,7,9,12,13,14,15,17,20,22 and Y, as indicated in locus enrichment, which were also carried out to comprehend those regions that include CNV/differentially methylated events (Figure 4.24C).

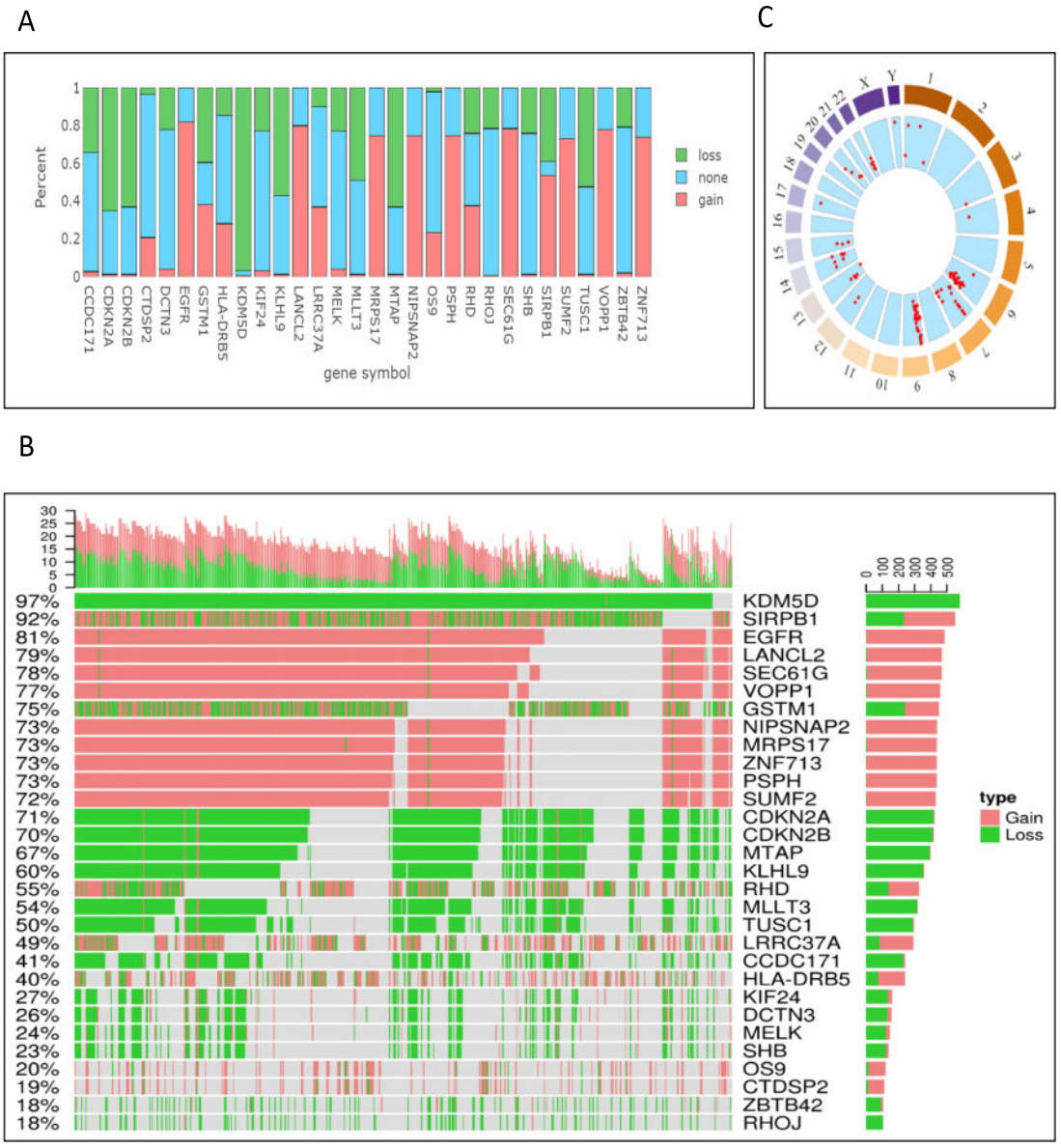

FIGURE 4.24: CNV, MET and miRNA-define dysregulation features in GBM.

A) The top 30 CNV drivers are shown on a Heat Map in the CNV panel. B) A percentage bar chart in the CNV panel displays the sample proportions for the

top 30 CNV drivers. C) Based on the locus enrichment analysis's findings, a circle graph in the CNV panel highlights the driver's loci on each chromosome with a red dot.

4.13.2.2 Mutational Analysis of DEG from GFAP-Positive Group of Glioblastoma

In the current study TGFβ1 is used for Insilco mutational analysis by using TCGA datasets of glioblastoma to investigate and compare the possible factors causing differential expression. As in this study the quantitative expression profiling revealed the upregulation of TGFβ1 in GBM biopsies samples from GFAP positive group. Similarly, the pathway enrichment analysis and immune infiltrations also provided significant association of TGFβ1 with other signaling pathways involved in glioblastoma. It is reported in the literature that TGFβ1 is acting as multifunctional cytokine and plays an important role in the interaction of other cytokines, chemokines, macrophages and signaling molecules involved in inflammatory cascade of glioblastoma. There are two distinct functions of TGFβ1 responsible for progression of GBM. In the early stage of GBM it may act as tumor suppressor by inhibiting proliferation and promoting differentiation. How ever in later stage it can be changed into pro-tumorigenic activity by facilitating cells invasion, metastasis, and immunosuppression.

Differential expression of TGFβ1 in pan-cancer and GBM biopsy samples due to mutations

Differential expression of the TGFβ1 gene concerning various cancer types is visualized using the Gene Summary analysis (Figure 4.25A). The Differential Expression (DE) indicated Red block in GBM. The boxplots show the expression patterns across all cancer types for TGFβ1.

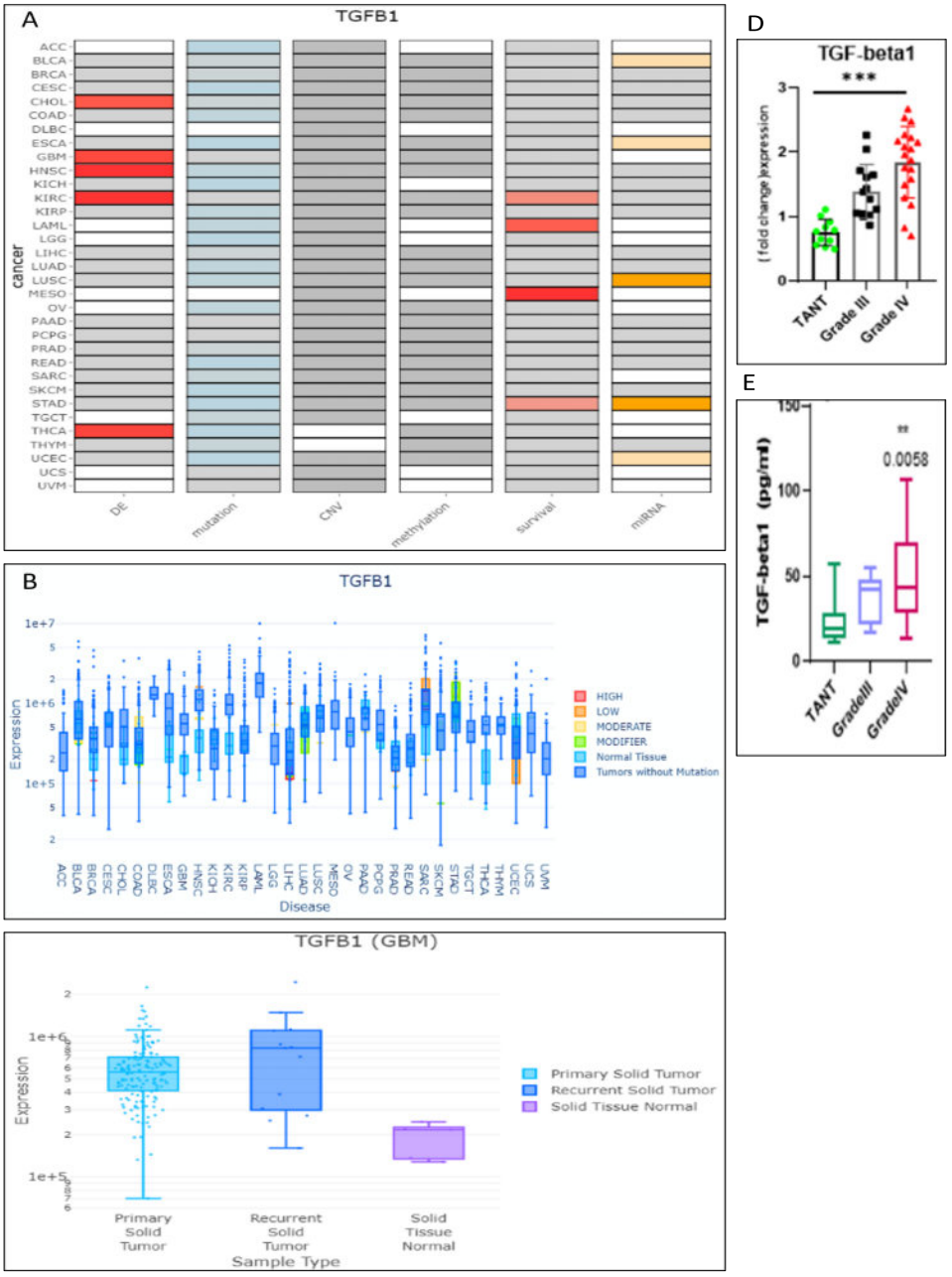

FIGURE 4.25: Differential expression of TGFβ1 in pan-cancer and in GBM GFAP-Positive biopsy samples due to mutations

A) Multi-omics characteristics in the major cancer types are shown in a summary graph for TGFβ1. B) A percentage bar chart in the CNV panel represents the top 30 CNV drivers sample proportions. C) TGFβ1 expression shown in Solid Tissue Normal was 2.1655e+5, Primary Solid Tumor was P=5.5846e+5 and expression of TGFβ1 shown in Recurrent Solid Tumor was 8.2995e+5. D) Expression levels of TGFβ1 in biopsy tissue of GBM through RT-PCR. The graphs were plotted with the Graph Pad Prism 9 software. E) Enzyme-Linked Immunosorbent Assay

validated the expression of DEGs in GBM patients. The expression is grouped by mutation class, showing the expression of TGFβ1 in GBM in between 1e+5 to 1e+6 (Figure 4.25B). The distribution of expression inside each GBM tumor type is shown in detail by the plot in a similar way. TGFβ1 expression shown in Normal Solid Tissue was 2.1655e+5, Primary Solid Tumor was P=5.5846e+5 and expression of TGFβ1 shown in Recurrent Solid Tumor was 8.2995e+5 (Figure 4.25C). To evaluate the mutational status of TGFβ1 in GBM, we quantified the expression of TGFβ1, and it was observed that protein expression was significantly increased in high grade Glioma biopsy samples. We also examined the gene expression of targeted gene among Grade-III and Grade-IV (GBM) specimen sections within the tumor and tumor-associated normal tissue (TANT). All tissue samples were initially cut from four specimen regions, but samples with sufficient RNA quality and quantity were subjected to RT-PCR gene expression analysis (Figure 4.25D). These data are consistent with ELISA findings (Figure 4.25E).

4.13.2.3 CNV, MET and miRNA-Define Dysregulation Features of TGFβ1 of GBM

The gene mutation function provides visualizations to illustrate mutation statistics corresponding to protein regions and exons in multiple cancer types. The gene mutation function provides visualizations to illustrate mutation statistics corresponding to protein regions and exons in multiple cancer types. This heat map displays the frequency of TGFβ1 mutations at various protein locations in various cancer types (Figure 4.26A). The mutation rate is calculated as the sample count divided by the mutation count and is shown by a colour scale. (Mutation rate = mutation count/sample count). The heat map shows mutations in 3 samples, protein- region 156- 176, for 2nd sample the at protein- region 176- 195 and 3rd sample, at protein- region 332-351(Figure 4.26B). The bar chart also showed the mutation rate of the TGFβ1 and its protein positions for GBM. The green colour bar showed a low mutation rate at protein- region (156- 176, 0.00295237), with the mutation rate; 2.95-03, the red color bar showed high mutation rate at protein- region (176- 195, 0.00318139) with mutation Rate:3.18-03 while blue

color bar showed moderate mutation rate at protein- region 332- 351, 0.00307135 at mutation rate 0.003 (Figure 4.26C). The Gene CNV function uses bioinformatics algorithms to visualize the copy number gain or loss of a user-selected gene across various cancer types. The Gene CNV function uses bioinformatics algorithms to visualize the copy number gain. The scatter plot displays the relationship between CNV value and gene expression (y-axis) (x-axis). The expression levels are shown in the left boxplot, and the CNV values for each type of CNV are shown in the bottom boxplot. TheTGFβ1 showed 638.2k median expression copy number gain while the segment mean ranges from 0.489 at 0 to 0.5. Similarly, the TGFβ1 showed 320.7k median expression copy number loss while the segment mean ranges from median -0.66 at -1 to -0.5. While TheTGFβ1 showed 580.4k expression copy number none while the segment mean ranges from 0.0480 (Figure 4.26D). The expression levels are shown in the left boxplot, and the CNV values for each type of CNV are shown in the bottom boxplot. TheTGFβ1 showed 638.2k median expression copy number gain while the segment mean ranges from 0.489 at 0 to 0.5. Similarly, the TGFβ1 showed 320.7k median expression copy number loss while the segment mean ranges from median -0.66 at -1 to -0.5. While TheTGFβ1 showed 580.4k expression copy number none while the segment mean ranges from 0.0480. The relationship between gene expression and beta value is similarly shown in the "Methylation" section. In order to demonstrate a detailed view of the methylation distribution and correlation in GBM, this graph combines a scatter plot and boxplot. The value of TGFβ1 in the GBM data set considers as usual, having the value 0.0353K, Cor =-0.136 while p=0.13 as shown in (Figure 4.26E). The gene miRNA network depicts the relationships between a TGFβ1 and miRNAs. Table 4.5 lists details for seven miRNA genes. Twelve prediction tools or experimental validations that miRTarBase recorded contributed to defining the interactions. Predicted relations are shown as dotted lines, while validated relations are shown as solid lines. Lists details for seven miRNA genes. Twelve prediction tools or experimental validations that miRTarBase recorded contributed to defining the interactions. Predicted relations are shown as dotted lines, while validated relations are shown as solid lines. A minimum of six, eight, or ten tools can further filter the predicted relations by driverDBV3 (Figure 4.26F).

Table 4.5: Gene-miRNA of Glioblastoma Table

	Mirbase mat_id	**Gene Symbol**	**Ensg**	**Validated**	**No. of Tool**	**Pearson Cor**	**Pearson pv**	**Spearman Cor**	**Spearman pv**	**Kendall Cor**	**Kendall pv**
BLCA	hsa- miR- 93-5p	TGFβ1	ENSG 00000 105329	1	0	-0.243	7.07 E-07	-0.32	5.13 E-11	-0.215	1.03 E-10
ESCA	hsa- miR- 93-5p	TGFβ1	ENSG 00000 105329	1	0	-0.24	2.20 E-03	-0.314	5.40 E-05	-0.207	1.01 E-04
LUSC	hsa- miR- 17-5p	TGFβ1	ENSG 00000 105329	1	0	-0.274	1.22 E-09	-0.368	1.05 E-16	-0.254	1.49 E-16
LUSC	hsa- miR- 93-5p	TGFβ1	ENSG 00000 105329	1	0	-0.298	3.24 E-11	-0.334	9.75 E-14	-0.228	1.07 E-13
STAD	hsa- miR- 17-5p	TGFβ1	ENSG 00000 105329	1	0	-0.271	1.11 E-07	-0.388	7.76 E-15	-0.26	7.46 E-14
STAD	hsa- miR- 93-5p	TGFβ1	ENSG 00000 105329	1	0	-0.35	3.83 E-12	-0.457	0.00E+00	-0.31	4.88 E-19
UCEC	hsa- miR- 93-5p	TGFβ1	ENSG 00000 105329	1	0	-0.205	1.73 E-06	-0.328	7.59 E-15	-0.224	1.01 E-14

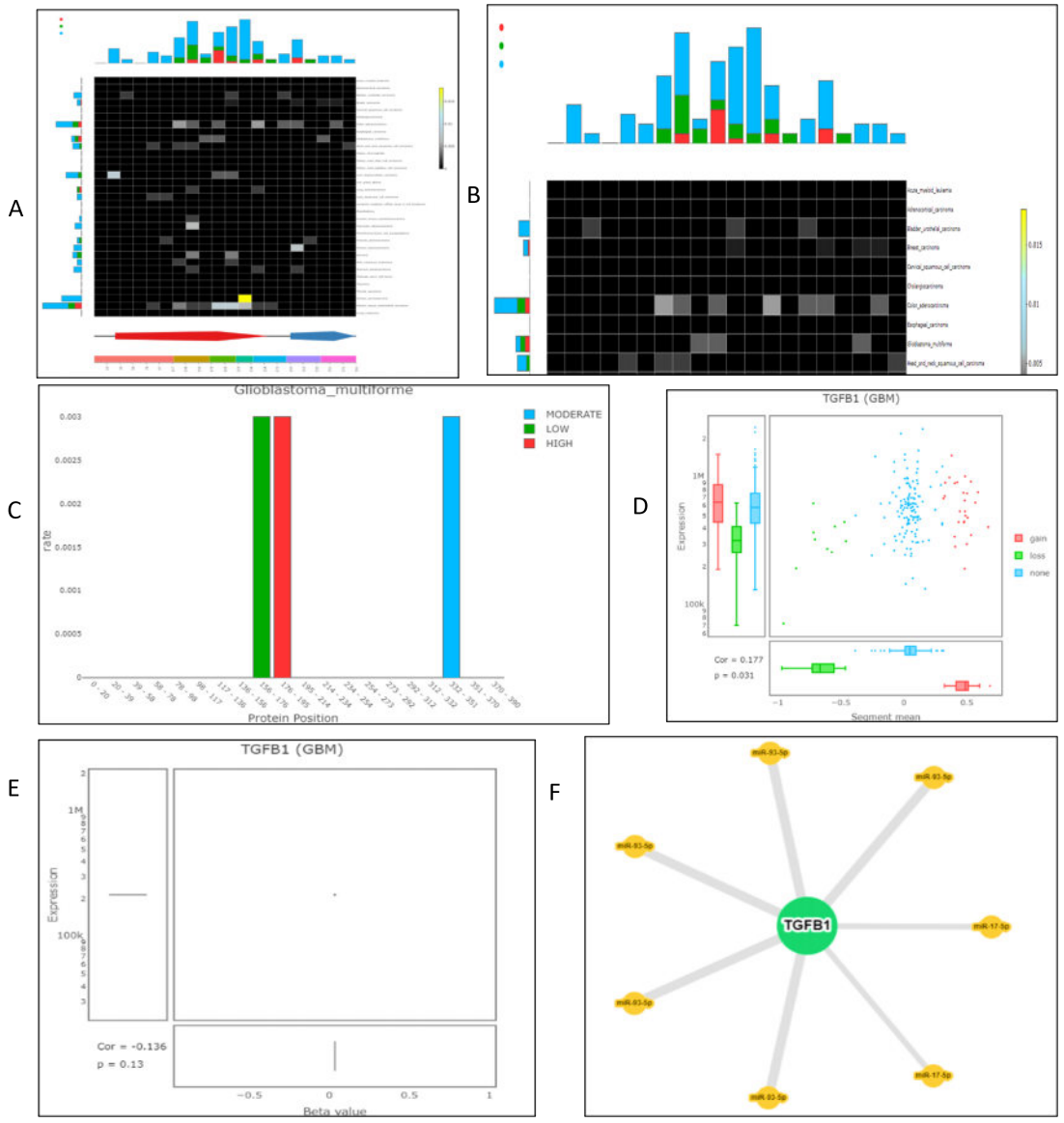

FIGURE 4.26: CNV, MET and miRNA-define dysregulation features of TGFβ1 of GBM

A) The heat map indicates the mutation rate of TGFβ1 at different protein positions in several cancer types. B) The heat map shows mutations in 3 samples. The mutation rate =0.00295237 at protein-region 156-176. For the 2nd sample, the mutation rate =0.00318139 at protein- region 176- 195; for the 3rd sample, the mutation rate =0.00307135 at protein- region 332-351. C) The bar chart also showed the mutation rate of the TGFβ1 and its protein positions for GBM. The green colour bar showed a low mutation rate at protein- region 156- 176, and the red colour bar showed a high mutation rate at protein- region 176- 195, while the blue colour bar showed a moderate mutation rate at protein- region 332- 351.D)

This graph combines a scatter plot and boxplot to demonstrate a thorough picture of the CNV distribution and correlation in GBM. E) The gene methylation function provides visualizations of the methylation pattern of TGFβ1 across GBM. F) The gene miRNA function provides visualizations illustrating the relations between TGFβ1 and miRNAs across GBM.

4.13.2.4 Mutational Analysis of DEG From GFAP-Negative Group of Glioblastoma

It is explored from the current analysis, that GCSF (CSF3) showed differential expression from global datasets and found elevated expression in GFAP negative group of GBM biopsies. Therefore, in order to determine the possible contributing factors, the in silico mutational analysis has been done to investigate genomic landscape alteration and frequency changes of GCSF in GBM.

Genomic Landscape Alteration and Frequency Changes of GCSF in GBM Patients

We explored the potential mechanism of GCSF (CSF3), GCSFR (CSF3R) and STAT3 in the pathogenesis of GBM from the dataset of patient samples of the TCGA Pan-Cancer Atlas database with the respective genetic alterations of GCSF (CSF3) 1.7%, GSCFR (CSF3R) 2.1% and STAT3 1.7% respectively (Figure 4.27A). According to the TCGA database, 4.73% of glioblastoma genes were found to be altered, with the following frequencies: mutation 0.51% , amplification 0.84%, deep deletion 0.34%, mRNA high 1.86%, mRNA low 1.0%, and multiple alteration 0.17% (Figure 4.27B). The comparison between the number of mutation counts and a fraction of the copy number alterations in the genome shows the frequency of GCSF family genes mutation in GBM patient samples with significant positive Pearson and Spearman correlation which is R = 0.77 and R = 0.18 respectively. Each dot highlights the number of samples. In the case of each sample the fraction of the genome which altered with the number of mutations present (Figure 4.27C) . We also used the cBioPortal and GEPIA2 database to examine frequency changes of GCSF mRNA expression (mRNA expression z-scores relative to diploid samples (RNASeqV2 RSEM)) including, shallow deletions, diploid, gain and amplifications upregulation of missense mutation.

The findings suggest the median value ranges from -0.39 to -0.16 as low-level gain,

diploid copy numbers between -0.36 and 0.5 and included gain. The majority of them also showed few amplifications ranging from -0.37 to -0.24. However, shallow deletion showed a significant rise from -0.36 to 0.73 (Figure 4.27D). The graphical summary depicts the position and frequency of all mutations within the framework of Pfam protein domains encoded by the canonical gene isoform, as well as specific mutation positions. The length of the line linking the mutation annotations to the protein indicates the number of mutation-bearing samples. Germline frameshift mutations at hotspot (L194R) codons 100 and 207aa, associated with elevated IL6 expression, represent the majority of GCSF mutations (Figure 4.27E). The shared exclusivity study showed that distribution of cell cycle control was likely to occur in GBM through principal component analysis of GBM tumor cells in the brain. To investigate the optimal gene combination to compare GBM with normal brain tissue, the combined expression levels of three validated genes (GCSF, GCSFR, and STAT3) were examined using PCA dimensionality reduction. According to Figure 4.27F, the three-dimensional space represented by the three variance components (PC1, PC2 and PC3) attributed to the expression values of these three genes revealed a remarkable demarcation between 163 GBM and 207 healthy controls. The source data plot portraying the logarithmic (log) p-values for each protein reveals that the PCA-based component represents nearly all differential expressions (red Dots), keeping the GBM projection scale range from 0.5 to 1.5 as shown in Figure 4.27G.

A) Illustrates genetic alteration of GCSF 1.7%, GSCFR 2.1% and STAT3 1.7% B) Alteration frequency in glioblastoma multiform depicts the percentage of mRNA low expression, high expression, deep deletion, amplification and mutation. C) The comparison between the number of mutation counts and a fraction of the copy number alterations in the genome shows a positive Pearson and Spearman correlation with a significant p-value < 0.05. D) GCSF gene amplification versus mRNA expression in GBM shows putative copy number alteration of diploid and shallow deletion according to GISTIC (Genomic Identification of Significant Targets in Cancer). E) Distribution of GCSF mutations in GBM cancer across protein domains at hotspot (L194R) codons 100 and 207aa associated with elevated expression of IL6. F) The scatterplot distribution of the first three principal components of PCA from the protein expression data differentiates between normal and malignant tissues used for PC analysis. The green dots represent the normal

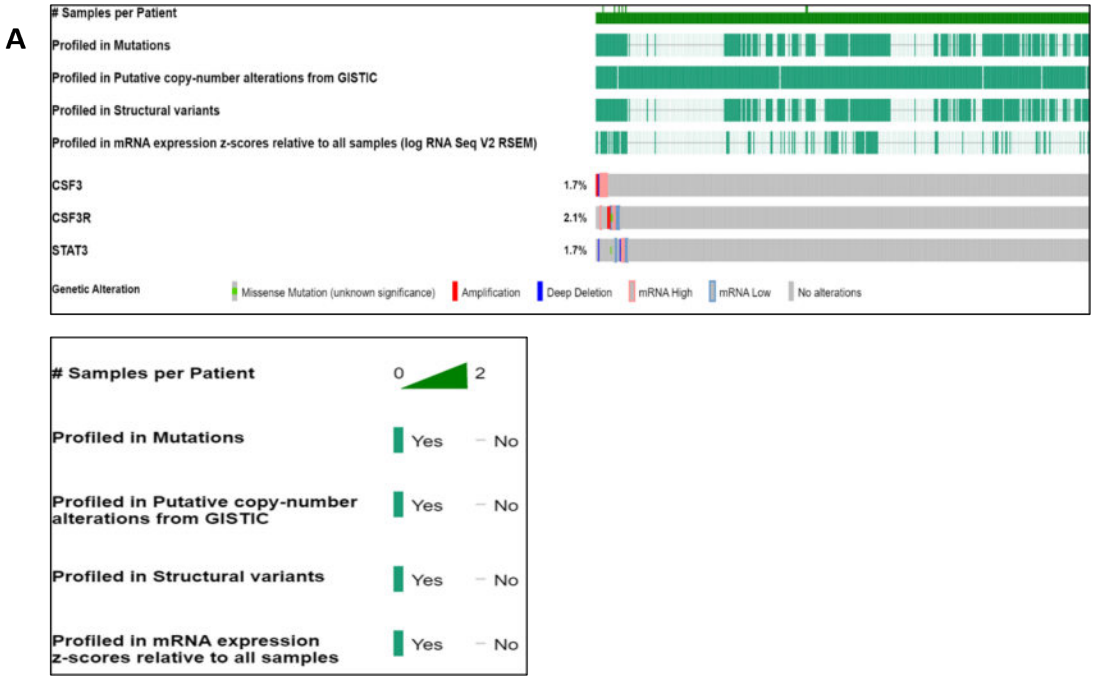

tissues, whereas the blue dots indicate tumors between (+) and (-) coordinates. G) 2D plot also depicts the logarithmic log p-values for each protein on the x-axis and the y-axis showing GBM (red Dots) projection between scales 0.5 to 1.5 of value.

4.14 In-Silico Studies for Drug Targets

4.14.1 Utilizing the Nisin Bacteriocin Peptide Complex for Molecular Drug Docking

Molecular Docking of Anticancer Bacteriocins and Validation by MTT Assay

The crystal structure of C163, a backbone circularized GCSF of the model, was improved and used for further investigation. Various structure validation programmes evaluate the generated model proteins, including stereochemical quality and geometrical conformations assessments. The Ramachandran plot computations were conducted using the PROCHECK software and revealed that 93.3% of residues were located in the most desirable zone, 5.9% in the permissible region, and 0.7% in the prescribed region of model protein (Figure 4.28A). In addition, the Rama favoured region for the crystal structure of C163 was shown to be 93.3% for 5GW9. MOE software was used to dock anticancer bacteriocins peptide against GCSF in glioblastoma against a specific binding pocket. All complexes were

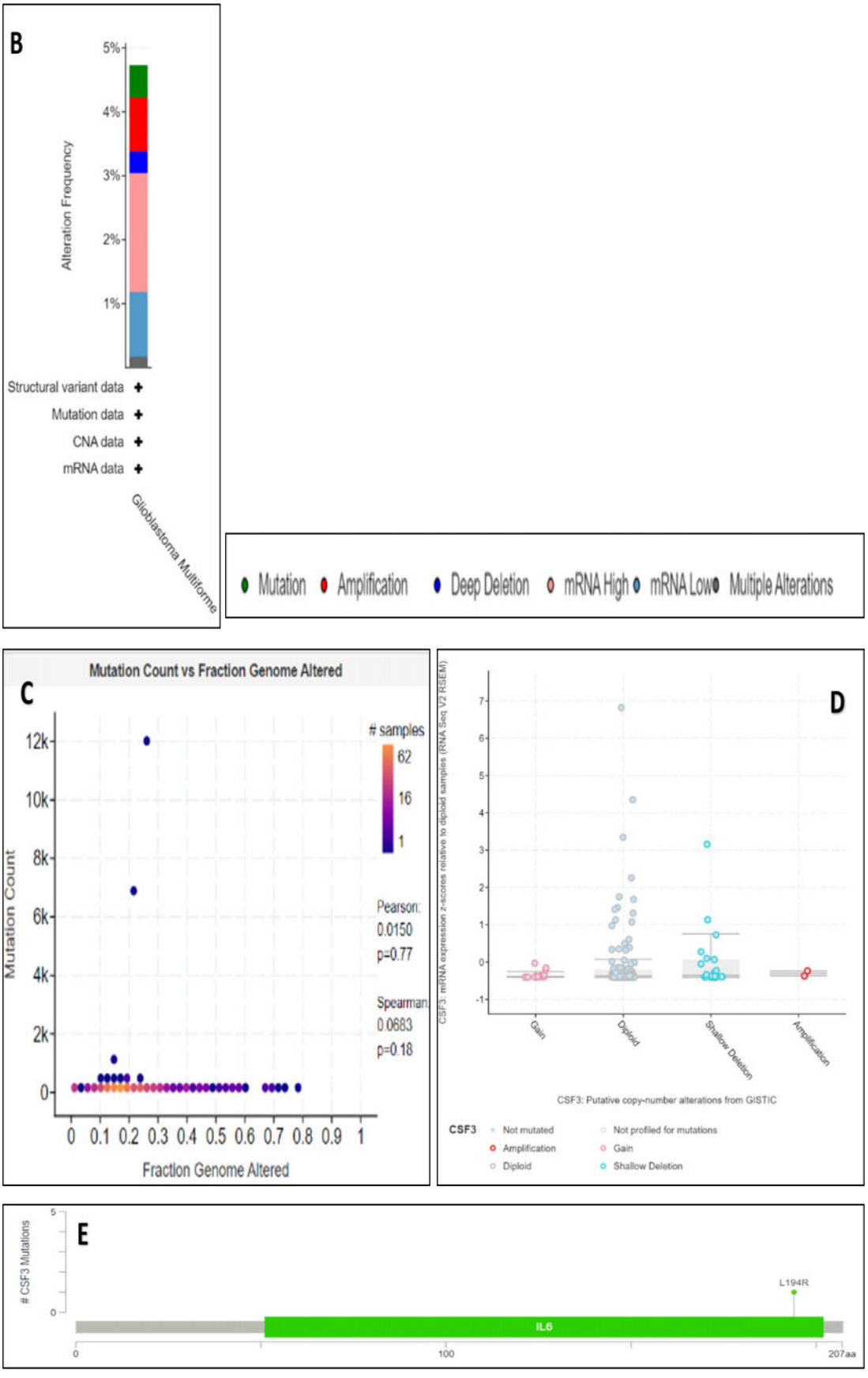
B
5%
4%
3%
2%
1%
Alteration Frequency
Structural variant data
Mutation data
CNA data
mRNA data
Glioblastoma Multiforme
Mutation
Amplification
Deep Deletion
mRNA High
mRNA Low
Multiple Alterations
C
Mutation Count vs Fraction Genome Altered
samples
62
16
1
Pearson:
0.0150
p=0.77
Spearman:
0.0683
p=0.18
Mutation Count
12k
10k
8k
6k
4k
2k
0
0 0.1 0.2 0.3 0.4 0.5 0.6 0.7 0.8 0.9 1
Fraction Genome Altered
D
CSF3: mRNA expression z-scores relative to diploid samples (RNA Seq V2 RSEM)
Gain
Diploid
Shallow Deletion
Amplification
CSF3: Putative copy-number alterations from GISTIC
CSF3
Not mutated
Amplification
Diploid
Not profiled for mutations
Gain
Shallow Deletion
E
CSF3 Mutations
L194R
IL6
0
100
207aa

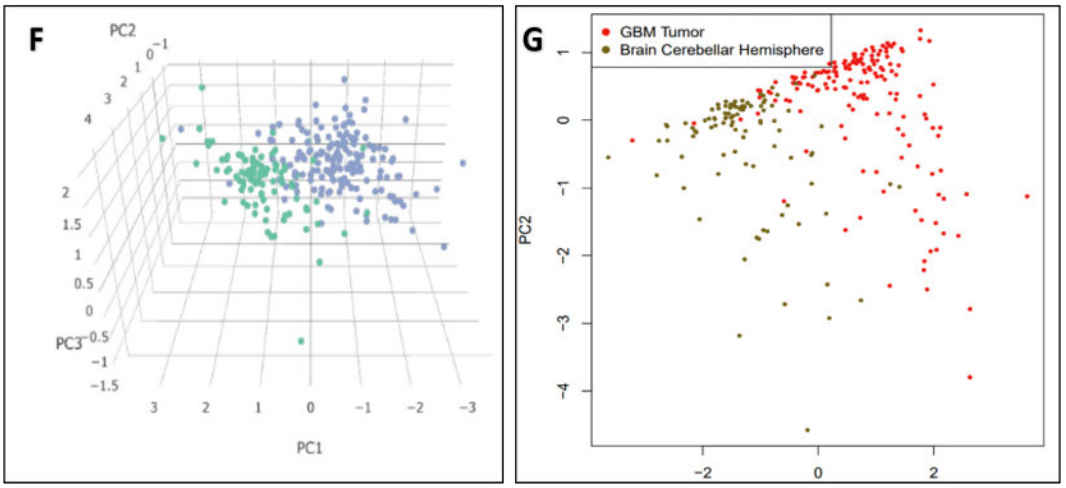

FIGURE 4.27: Genome landscape alterations of GCSF in GBM patients

grouped based on non-covalent interaction strength, the energy function score (S-Score), hydrogen bonding, and maximal accommodation with the binding pocket (Figure 4.28B). Among 33 docked clusters, 7 were selected for interaction analysis based on highest levels of hydrogen bonding, vander Waals interaction, and other hydrophobic interactions with binding pocket residues. Cluster 0 had the lowest energy-weighted score of -554.7 kcal/mol with a total 413 members, Moreover, the visualization of the docking results reported 3 hydrophobic interactions with Ser β156, Glu 46 and Arg 170 residues of cluster 0. Furthermore, cluster1 had a score of -538.1 kcal/mol and their visualization revealed the 8 hydrophobic interactions with the Glu A124, Gln A120, Thr A116, Gly B88, Phe B84, Glu A123, Gln β135 and Thr β134 residues (Figure 4.28C$-$4.28D). The stability and the quality of the docked model was examined by dynamic simulation through deformability and B-factor as shown in (Figure 4.28E). The results indicated an insignificant hinge and an intermediate RMS for the B-factor, as the experimental B-factor taken from corresponding PDB field and calculated from NMA is obtained by multiplying NMA mobility 8pi2 (Figure 4.28F).

Deformability is a measure of the ability of a given molecule to deform at each of its residues. This is mainly observed in the form of "highest peaks" that can be derived from high deformability regions. The minor deformability was observed in the docked NISIN complex as the complex has some peaks of approximate value 0.8 - 1.0 deformability index. A low likelihood of deformation was suggested for the anticipated homology model (Figure 4.28G). The covariance matrix provides

how residues in the complex are correlated; the higher the correlation, the better is the complex. The red coloration indicates a good correlation between residues, white coloration depicts no correlation, while blue indicates anticorrelations. The Nisin docked complex suggests a good correlation with a few anticorrelations in the majority (Figure 4.28H) represented the above-mentioned results. The dose-dependent cytotoxicity of Nisin against SF-767 cells and normal cell line CHO was evaluated using MTT assay and determined by statistical analysis. Nisin, a compound with anti-inflammatory properties, was investigated for its potential to disrupt cell membrane integrity, induce apoptosis, and increase resistance to apoptosis in cancer cells.

In this study the proliferation of SF-767 cell was significantly inhibited showed 78.15% inhibition at 100 μg/mL while at 1 μg/mL was 16.70 %. At 48 hrs the IC50 value of Nisin for SF-767 was 30.65 μg/mL found. Whereas the results show that Nisin has lesser cytotoxicity in a normal cell line CHO with an IC50 value of 110.4 μg/mL as compared to glioblastoma cell line SF-767 as shown in Figure 4.28I.

A

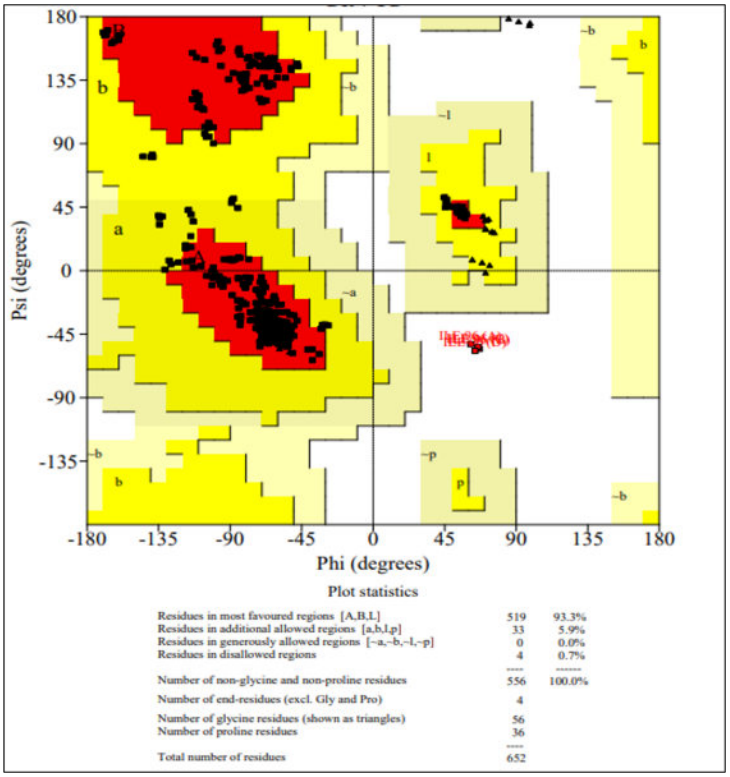

A) Ramachandran plot statistics for modelled protein GCSF. B) The best scoring docked complexes for target receptors 3D Docked pocket. It also demonstrates

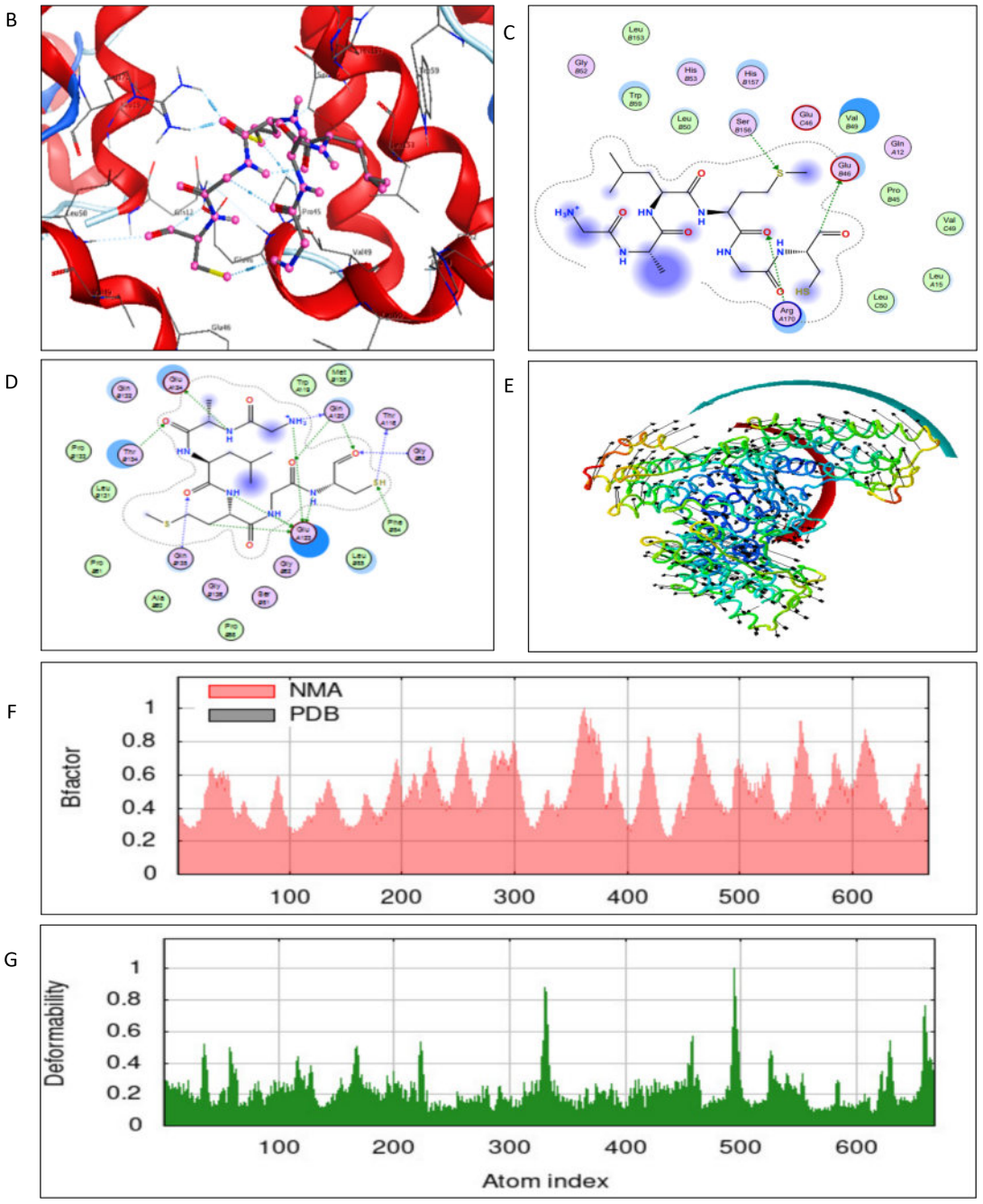

our ligand's overlaid 3D interaction with the active region of the receptor protein GCSF. The ligand molecule is shown in marine blue, the amino acid residues are shown in grey blue, and the protein structure is shown in red. C) 2D interactions of 1WCO with 5GW9 reported 3 hydrophobic interactions with Ser β156, Glu46 and Arg 170 residues of cluster 0. D) 2D interactions of 1WCO with 5GW9 reported revealed the 8 hydrophobic interactions with the Glu A124, Gln A120, Thr A116, Gly B88, Phe B84, Glu A123, Gln β135 and Thr β134 residues of cluster 1.E) Molecular dynamics simulations of the complex generated between our drug and

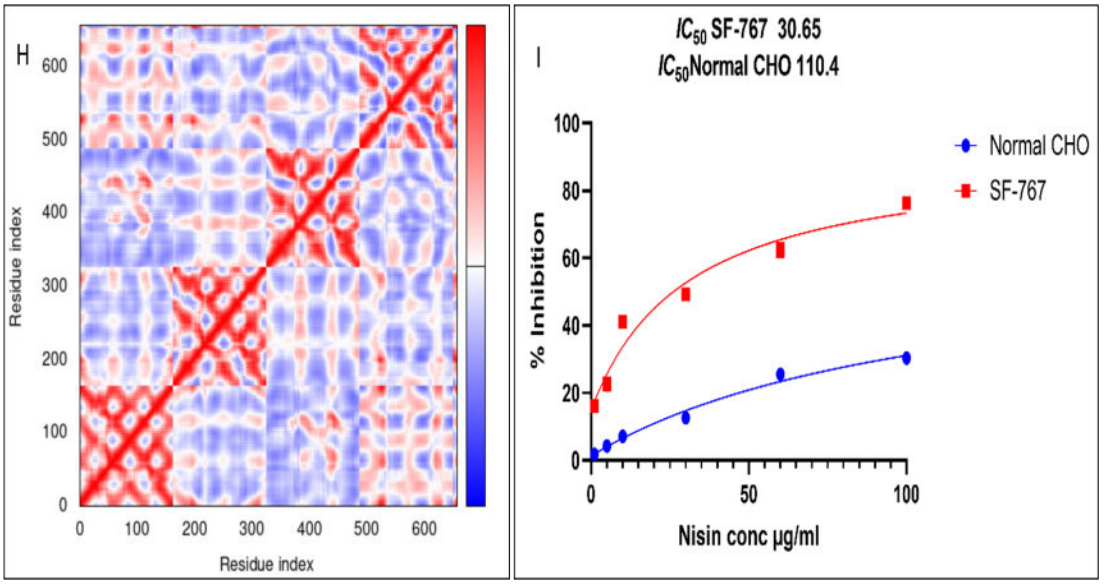

FIGURE 4.28: Molecular Docking of Anticancer Bacteriocins Nisin

receptor, which represents the docked molecule orientation F-G) represents outputs of NMA study deformability and B-factor plot graph. H) represents residue index co-variance heat Map for the Dock modelled GCSF-Nisin. I) The effects of Nisin on % inhibition as determined by MTT assay. Blue curve represents normal CHO and Red curve show SF-767 Cancer Cell lines whcih were incubated for 48 h with different concentrations of Nisin.

Chapter 5

Discussion

This study significantly contributes to the scant amount of knowledge on the broad range of brain tumors in Pakistan . Using the extensive dataset made available by The TCGA (Cancer-Genome-Atlas), this study is the first to compare the clinicopathological characteristics of diffuse gliomas in the wider community. In affluent nations like the US, Canada, Australia,France and the United Kingdom, the prevalence of Central Nervous System (CNS) tumors is higher where as Ethiopia and the "Republic of Congo", two African nations, show significantly lower incidence rates. [225]. Variable incidence rates have been observed in Asian countries including India, Afghanistan, China, and Iran [226]. These findings underscore the evident geographical heterogeneity in the incidence of CNS tumor . The absence of a population-based national cancer registry impedes the understanding of epidemiological diversity of this tumor type. To outline the clinicopathological range of CNS tumors in our community, descriptive research was conducted. The outcomes of diffuse gliomas were compared to the global (TCGA) data that was readily available.

In current study, most of the CNS tumors were located in the cerebrum. The temporal region was the most common site (50.9%), followed by the parietal region (10.9%) and the frontal lobe (38.2%). This finding is in consistent with the other studies, which have reported the temporal region as the most common site of CNS tumors [227].

In Pakistan, glial tumors are the most prevalent type of neoplasm, comprising 41% of all primary CNS tumor cases[228]. Meningeal tumors were the second most common type, with 27.7% of cases. Many studies have reported that gliomas account for 40–67% of primary CNS tumors and meningeal tumors account for 9–27% [229].

Glioblastoma-multiforme (GBM) was the most prevalent histological subtype of glioma with 74.5% of cases in the current study. According to a prior study from Karachi, oligodendrogliomas were the most prevalent histological glioma subtype [230]. This might be brought on by varying environmental circumstances and genetic composition.More investigation is required to comprehend the variation in the most common histological subtype of glioma in different populations. GBMs account for 31.1% of all diffuse gliomas in Pakistan, making them the second most common brain tumor after oligodendrogliomas. Among the primary CNS tumors, pilocytic astrocytoma made up 5.8% among 25 cases in the previous studies of Pakistani population. The pilocytic astrocytoma was observed to lack an IDH mutation and was not categorized as a diffuse glioma [231].

The grade of a CNS tumor is an important prognostic factor. Grade-IV tumors are the most aggressive type of CNS tumor. They have the worst prognosis. In this study, Grade-IV tumors were diagnosed more frequently than Grade-III tumors. Other studies have also shown that "Grade-IV "tumors are the most prevalent grade of malignancies of Central Nervous System [232].Gliomas are aggressive and challenging to treat because of their invasive nature. Understanding the pathways that trigger glioma invasion is crucial to develop new anti-invasive treatment strategies.

Previous research in Pakistan has not examined the predictive value of GFAP (Glial Fibrillary Acidic Protein) staining for GBM survival. Parameters of GFAP stain in Glioblastoma Cells and clinical evidence have been found to be strongly correlated. We determined a cutoff that is clinically applicable.Glioblastoma Survival, Overall Survival (OS), and Long-Term Survival have independent correlations with GFAP staining levels of "greater" than or "equal" to 75% . [233].Investigations

on lipids in the cerebral tissues of people with multiple sclerosis provide the majority of the clinical evidence for GFAP staining[234]. Our findings highlight its prognostic significance in GBM. Astrocytes are differentiated by the existence of GFAP. It is a peculiar structural protein that was discovered and described by Dr. Eng in 1969. GFAP is an intermediate filament (IF) III protein.It is essential for glial cells' cytoskeletal structure, preserving their Mechanical Strength, supporting nearby neurons, and supporting the blood-brain-barrier. [235]. Among the 10 isoforms of GFAP, GFAP-α is predominantly found in the different regions of brain and contributing parts of spinal cord [236]. GFAP-δ, also known as GFAP-ϵ primarily expressing by Astrocytes in the subventricular-zone [237]. The gene encoding GFAP is localized to "human-chromosome-17q21". It harbor mutations in certain disease states including Alexander's disease, and glioma-like tumors [238].

Lower GFAP expression has been seen in giant cell gliomas in earlier research [239]. In astrocytomas, previous studies noted a gradual reduction of GFAP expression along with invasive malignancy [240]. Genome-wide GBM sequencing did not identify somatic mutations in GFAP [241].

Low proliferating potential was shown to be present in GFAP-positive tumor cells by Takeuchi.*et.al* [233, 242]. "Berendsen" and Van Bodegraven.et.al., emphasized the Differential Expression of GFAP which did not consistently align with the degree of astrocytoma malignancy [243].As a predictive diagnostic for glial tumors, GFAP staining may have some clinical relevance. The potential clinical effects of GFAP-δ which was linked to increased tumor invasiveness in cerebral astrocytoma, were discussed by Brehar.*et.al* [244]. These findings are consistent with our study revealing an association between the percentage of GFAP stain in the cells of Glioblastoma and Patient Survival. Higher GFAP values in GBM tissues were strongly correlated with poorer outcomes. GFAP demonstrated a robust association with overall survival and long-term survival [245]. The observations were independent of important confounding factors such as Age, Preoperative KPS (Karnofsky Performance Status), Extent of surgery, IDH1-mutations, and MGMT-Methylation Status. This correlation was confirmed through univariate, multivariate, and survival analyses. The observed association between

GFAP stained molecules and survival of GBM patients may indicate acute cellular membrane deterioration in GBM tissue [246]. Previously reported data showed that decrease in GFAP expression [247], may be due to increased cellular mitotic rate. Our study employed a GFAP staining for "quantification" and "proportional expression". The present results warrant validation in a large prospective series.Previous research explored the effect of GFAP affect on the migration of cells and motility[248]. Such studies have yielded somewhat inconsistent results. Some studies have associated GFAP expression with higher velocities of cell migration [249]. Many findings have reported the lower migration velocities [250, 251]. It is important to note that the GFAP depletion's impact on cell activity might not only depend on the specific isoform. It is also affected by the cellular context and surroundings[252]. Intermediate filament (IF) network can modulate microtubule organization and cell polarity, promoting migration persistence [253, 254]. However, it is unclear whether the Absence of GFAP-α or the Dominance of GFAP-δ regulating the directional migration. Moreover, , ECM (Extracellular matrix) composition and structure are examples of extrinsic variables that may affect migration and invasion. [255].

Multiple studies have reported an increasing dominance of GFAP-δ in Grade-IV glioma tumors [250, 256, 257]. This finding has been supported in our current study (Fig. 4.4 and 4.5). Brehar *et al.* found that patients with highly invasive tumors exhibited higher percentages of GFAP δ-positive cells [258]. Glioma tumors are known for their high heterogeneity. It exists not only between patients but also at the single-cell level within a tumor [259, 260]. A single tumor likely consists of a mixture of cells with varying GFAP $\delta/\ \alpha$ ratios. Diverse behaviors may result from these diverse cell groups. In case of grade IV glioma,It is conceivable that a greater number of cells with a high GFAP $\delta/\ \alpha$ ratio support the infiltration of the brain parenchyma and subsequent relapse after therapy. Further research is needed to understand the exact mechanism responsible for the shift in GFAP-Isoform expression in Grade-IV tumors [261]. The splicing machinery is dysregulated, which increases the aggressive nature of gliomas [262].In Grade-IV gliomas, hypoxia is thought to be a major initiator of glioma infiltration. [263]. Our study elucidates

the intricate relationship between GFAP isoforms, cytokines/chemokine expression, and glioma invasion. These findings hold great promise for the development of targeted therapeutic interventions against GFAP-positive glioma tumors.

GBM is characterized by the presence of various Cytokines, including tumor necrosis factor-alpha (TNF-α), interleukins (IL1 β, IL6, IL8, IL10), NF-κB p65 (RelA) and TGFB1. All of them play crucial roles in triggering the inflammatory cycle within the tumor microenvironment. These factors promote carcinogenesis by preventing growth inhibition, inducing metastasis and angiogenesis, and sustaining the cancer cell stemness [264, 265]. IL-1 β was found to be overexpressed in glioblastoma patient samples. IL-1 β induces glioma cell migration.Glycerol-3-Phosphate- Dehydrogenase (GPD2) is phosphorylated by IL-1 β, which also stimulates the Phosphatidylinositol-3-kinase (PI3K) Pathway .This pathway supports tumor cell survival and growth [266]. It upregulates pro-inflammatory cascades at the mRNA level [267]. The interaction between Ras and IL-1 β/ TNF α was shown to enhance IL-8/IL-6 cytokine hypersecretion. It leads toward the activation of p38 MAPK signaling pathway in GBM cell lines [268]. In vitro studies have demonstrated that IL-6 stimulates the release of Vascular- Endothelial-Growth-Factor (VEGF) and has a significant impact on activation of JAK/STAT3 pathway [269].

The focus of current GBM research lies in exploring the role of inflammatory genes (cytokines/chemokines) to promote tumor cell growth and angiogenesis. We conducted a comparative analysis of gene expression for 11 inflammatory genes and their corresponding receptors. Tumor-associated normal brain tissue was used as a reference. IL6, TGFB1, and IL8 (CXCL8) were overexpressed in GFAP-positive GBM samples, according to the distinct gene expression patterns of chemokine/cytokines and their associated receptors. These genes regulate proliferation of cells, cell communication, and cellular component movement (Figure 4.4, 4.5). When compared to global gene expression datasets, CXCL8 overexpression in GBM was consistently reported (Figure 4.13, 4.15). Our investigation showed a significant increase in CXCL8 expression in GBM. The expression of its receptor (both mRNA and protein) remained relatively stable in Diffuse-Astrocytoma (Low-Grade Astrocytoma) and Glioblastoma (High-Grade -Astrocytoma). The findings indicate

a potential association of IL8 (CXCL8) with the aggressiveness of tumor and its involvement in cell proliferation pathways. IL8 is a active member of the (C-X-C) Chemokine family. It was identified initially as a neutrophil chemo-attractant with inflammatory activity [270]. It also serves as a potent angiogenic factor in tumorigenesis and metastasis [271, 272]. Despite its recognized angiogenic potency, most angiogenesis research in glioblastoma multiforme has focused on IL10 and TGFB1 [273]. The process of angiogenesis involves a complex interplay of multiple factors [274]. Our findings highlight the importance of CXCL8 and their associated inflammatory markers cascade in GBM. Our study also revealed distinctive gene expression patterns of cytokines and their receptors in GBM compared to diffuse astrocytoma. The overexpression of IL6, TGFB1, IL 10 and their association with IL8 (CXCL8) in GBM demonstrates their potential contribution in an aggressive tumor, proliferation and survival [275, 276]. Our results are consistent with these findings and emphasized the relevance of CXCL8 as a possible therapeutic target for treating GBM. The IL8 (CXCL8) chemokine promotes cell proliferation and endothelial cell survival [277]. GBM and other hyper-vascular tumors have been found to exhibit a different mode known as vascular mimicry (VM) [278]. VM involves the formation of cell-lined channels of tumors facilitating the phenotypic and molecular reprogramming of tumor cells into endothelial-like cells [279]. Anti-angiogenic therapies such as avastin have been ineffective in reducing VM, which may explain their limited efficacy [280]. Recent studies have revealed the role of CXCL8 in the invasion and migration of glioblastoma through the NF-κB/AP-1 pathway [281]. It has also been shown to promote a synergistic interaction between cancer stem cells and endothelial cells in GBM [282]. Autocrine and paracrine signaling of CXCL8 plays a critical role in maintaining stem-like traits in glioblastoma stem cells (GSCs) [283]. The mitogenic effect of IL8 (CXCL8) has been observed in various cancers, including ovarian, melanoma, prostate, colon, and lung cancers [284]. Several signaling pathways have been implicated in CXCL8 signal transduction. Activation of PI3K/Akt (Phosphatidylinositol-3'-kinase/Akt), PLC/PKC (phospholipase C/protein-kinase-C), and Erk1/2 (Ras/Raf,/extracellular signal-regulated-protein-kinases 1 and 2) cascades has been observed upon stimulation of

CXCR1/2 by CXCL8. Additionally, Rho, focal adhesion kinase, Rac, and JAK/-STAT (Janus kinase/signal transducers and activators of transcription) pathways have been shown to be activated by IL8 (CXCL8) [285]. Therefore these findings highlighted the significant role of CXCL8 in glioblastoma. Inhibition of the CXCL8 may serve as a promising strategy to suppress GBM growth.

Previous studies reported the correlation of IL8 with the over expression of IL6 and TGFB1 for promoting angiogenesis in glioblastoma. IL-6 is a pleiotropic cytokine known for the acute-phase reaction caused by injury and infection, encouraging the development of VEGF in different cell types[286]. IL-6 can recruit myeloid-derived suppressor cells (MDSCs) and Polarize-myeloid cells into an M2-phenotype in multiple malignancies [287]. The vascular-endothelial-cells within the GBM microenvironment have identified as sources of IL-6 to induce alternative activation of tumor-infiltrating macrophages [288]. Our findings align with clinical observations of increased IL-6 expression in GFAP-positive GBM patients (figure 4.4, 4.5). Moreover, our biopsy-based results are supported by TCGA analysis revealing an association between tumor IL-6 expression and poor survival (figure 4.15,4.16). Previous studies have indicated IL-6 overexpression in the mesenchymal GBM subtype. The elevated expression of IL-6 in glioblastoma is characterized by Immunological Infiltrates and Immuno-suppressive indicators [289, 290]. GBM-derived IL-6 may play a role in directing systemic and local immunosuppression. Acting as the primary STAT3 Activator, IL-6 binds with the (PD-L1) promoter and upregulates immunosuppressive cytokines [291]. GBM-derived IL-6/STAT3 signaling implicated in tumor cell proliferation, angio-genesis, invasion, autophagy, and maintenance of glioma stem cell [292]. These findings highlight the multifaceted role of IL-6 in glioblastoma. The development of neovascularity in GBM is a complex process influenced by various growth factors [293]. Similarly TGF-β1 plays a crucial role in tumor growth and angio-genesis in gliomas via interacting with other cytokines and macrophages in the tumor micro-environment [294]. In this study, we performed expression profilling and mutational analysis of TGF-β1 and the pathway enrichment showed the interaction of TGFB1 with interleukins and chemokines (Figure 4.19B) Our findings revealed its significance in the diagnosis of glioblastoma, as depicted in Figure 4.25 and 4.26.

In our study, we demonstrated the upregulation of cytokines expression in glioma cells possibly orchestrated through NF-κB pathway. It is important to note that other genes and pathways may also be involved in these regulatory processes. Moreover, our results suggest that anti-inflammatory agents have the potential to inhibit inflammatory genes expression in glioma cells and tumor microenvironment mediated through the NF-κB pathway. These insights contribute the highlights of the complex interplay between immune cells and glioblastoma cancer cells.

The NF-κB p65 (RelA) family of pleiotropic transcription factors is sequestered in the cytoplasm of most normal cells by noncovalent interaction [295]. Recent investigations have demonstrated that various tumor cells express NF-κB p65 (Rela) constitutively activated. Interestingly, in glioblastoma, TNF α induces tumor cell motility and invasion via activating NF-κB [296].

The NF-κB pathway transcription factor NF-κB p65 (RelA) and its related TNF α were found to be prospective targets in GBM by our comprehensive integrated approach through bioinformatics and clinical sample analysis (as mentioned in result section 4.2.3 and 4.5.2). In this study NF-κB p65 (RelA) and TNF α were found highly expressed in many tumor types, including GBM from global databases (figure 4.15). Additionally, we used qRT-PCR to reanalyze the NF-κB p65 (RelA) and TNF α gene expression levels and transcript in the samples from GBM patients and discovered higher levels (figure 4.4, 4.5). In vitro glioblastoma's ability to invade and infiltrate, NF-κB p65 (RelA) and TNF α play crucial roles. Therefore, we investigated a variety of datasets, including the Oncomine, GEPIA, and TIMER databases, to study the relationship between NF-κB p65 (RelA) and TNF-α expression in GBM. Previous findings revealed that in the case of GBM, a various proteins and signaling pathways are dysregulated, which could lead to NF-κB p65 (RelA) activation [297]. TNF α is an extremely potent NF-κB p65 (RelA) activator. In the CNS, astrocytes, microglia, and certain neurons all release the pro-inflammatory chemical TNF α. TNF α may indeed, exhibited its effects through two receptors, TNF α receptors TNFR1 and TNFR2. The majority of cells typically express TNFR1, although oligodendrocytes and immune cells, particularly microglia, express TNFR2. Also, it was discovered that GBM and

its associated endothelial cells expressing higher TNFR1 as compared to normal brain tissues and gliomas with low-grade [298]. It is suggested that TNF α may be possible diagnostic markers for GBM in response of that NF-κB signaling cascade [299]. The dysregulation of numerous signaling pathways or growth factors and triggering of pro-inflammatory microenvironment, in gliomas may lead to the activation of NF-κB p65 (RelA).High constitutive NF-κB p65 (RelA) activity, is characteristic of GBM [300]. The impact of NF-κB p65 (RelA) and TNF α expression on the survival time of GBM patients were then assessed utilizing the GEPIA databases (Figure 4.16A - 4.16B). These results from GEPIA revealed that low NF-κB p65 (RelA) and TNF α expressions were independent predictors of OS for GBM. As in the previous studies, patients with GBM had shorter survival times due to upregulation of NF-κB p65 (RelA) and TNF α [301]. Nevertheless, constitutive NF-κB p65 (RelA) activation appears to promote the growth and metastasis of tumors by a range of mechanisms, including tumor metastasis, apoptosis, cell proliferation, angiogenesis, and metabolic reprogramming. It has been established that NF-κB p65 (RelA) stimulates the development of an inflammatory milieu that is conducive to the establishment of cancer. According to GBM, constitutive NF-κB p65 (RelA) activation promotes survival and development [301].

Interestingly, TNF α also induces tumor cell motility and invasion via activating NF-κB [296].Therefore our findings imply that these two genes can serve as a significant predictive marker for people with GBM. As anticipated, These genes (NF-κB p65 (RelA) andTNF α) increased SF-767 cell invasion because of other metabolic stimulus due to presence of LDL protein and receptors, which increases the cell proliferation turnover of growing tumor cells, these findings are also consistent with this study and caused NF-κB p65 (RelA) activation. As SF-767 cells revealed high-affinity LDL binding and maximum binding capacity [302, 303]. Our results were categorically established in GBM SF-767 cells with NF-κB p65 (RelA) overexpression and silencing as a positive modulator of NF-κB signaling by enhancing the translation of p65 transcript. Temozolomide (TMZ), an oral alkylating cytostatic medication, is frequently used to treat GBM, Therefore, the SF-767 glioblastoma cell line was used for invitro analysis in the current study (figure 4.10). According to the data, when the SF-767 cell line was exposed to 10 μM

TMZ, the inhibition was 33.1%. A higher concentration of TMZ (200 M) proved to be lethal in GBM cells, resulting in 89% cell death after the treatment. Due to the heterogeneity of the GBM tumor and its highly angiogenic and metastatic characteristics, combination therapies are now regarded as an essential component of anticancer therapy. Cancer monotherapy has become a rare chemotherapeutic treatment choice. The standard treatment for GBM is temozolomide therapy combined with surgery and radiation therapy, but because this approach has minimal effect on patients' overall survival, it is crucial to create drugs that can maximize their advantages and prevent tumor resistance. The combination of TMZ with celecoxib would be a workable strategy to treat GBM, even though TMZ has been successful in treating GBM [304]. However, mounting evidence pointing to NSAIDs' wide variety of COX-dependent targets, such as the presence of NF-κB, B-CATENIN, PPAR DELTA, NAG-1, and BCL-2, suggests that various molecular pathways are implicated in the anticancer effect of these medications [305]. In this study, we offer evidence that celecoxib inhibits NF-κB activation while inhibiting the development of GBM cells. The effectiveness of TMZ and COX-2 inhibitors in treating GBM in vivo and in vitro has been demonstrated in earlier research, but the underlying molecular mechanism has not been clarified. However, it has recently been found that the NSAIDs indomethacin and flurbiprofen suppress the growth of glioma cells [306]. Celecoxib, a medication used to treat inflammation, is now also used to treat cancer [307]. There is growing evidence that despite being a selective inhibitor of COX-2, it exerts anti-tumor effects on cancer cells that do not contain the COX-2 enzyme. In order to determine if celecoxib alone or in conjunction with other drugs is beneficial at treating glioblastomas, several researchers are now engaged in Phase II clinical studies [308, 309].Celecoxib and temozolomide were also used to treat a rat orthotropic glioma model, proving that both medications work well together to treat gliomas [310]. Our research supports the in vitro findings, but mounting evidence pointing to NSAIDs' wide spectrum of COX-independent targets, such as NF-κB p65 (RelA) and TNF α, indicates that a number of molecular pathways may be involved to the inhibit-neoplastic action of these drugs. In the present research, we analyzed the suppressive effect of celecoxib to the growth of GBM cells by inhibiting NF-κB activation and its

signaling pathway. Additionally, individuals with glioblastoma receiving temozolomide, dexamethasone, and cranial radiation therapy for peritumoral brains edema could take celecoxib without any danger [308]. Celecoxib use has increased due to these trials, offering a desirable anti-glioma treatment plan. In summary, our findings showed that celecoxib suppressed TNF α induced NF-κB activation, which is known to limit proliferation and trigger apoptosis in GBM cells. In the current investigation, we showed the anti-inflammatory role of potential drug candidate to suppress the NF-κB transcriptional activity.

In order to investigated the potential contribution and mechanism of inflammatory genes profiling, the PPI network by GeneMANIA and STRING and Pathway enrichment has been investigated, and the biological processes associated with inflammatory genes from GFAP positive and GFAP negative group **(IL-1 β, IL-6, IL-8, IL-10, TGF-β, and TNF-α, NF-κB)** were analyzed with Metascape and g:profiler in order to understand the molecular mechanism in the result section 4.9 and 4.10 . However, cytokines with elevated expression levels IL8 (CXCL8) and GCSF (CSF3) were found from both groups significantly correlated with the other genes interactions through STRING (Figure 4.18I, 4.18J). Therefore, our results demonstrated the important biological processes involving the cytokines interacting genes in Metascape. We hypothesized that the biological functions of inflammatory genes related to immunological processes, resulting in poor prognosis with elevated expression levels in GBM. Based on this presumption, TIMER was employed to investigate the correlation between the highly expressed genes found in the GBM clinical samples with the immune cells of GBM microenvironment. It is demonstrated in the previous studies that TGFB1, NF-κB p65 (RelA) and TNF α are the signaling molecules and showed significant contribution in the progression of cancer. Numerous studies highlighted TGFB1,NF-κB p65 (RelA) and TNF α mediated exacerbation of inflammation in the tumor microenvironment via interacting cytokines and macrophages. Similarly in our analysis these three genes are significantly correlated with the expression of other inflammatory genes (Figure 4.20). Hence these genes have been selected for immune infiltration analysis in the current study.

Previous literature evident that the microenvironment around gliomas is rich in chemotactic and inflammatory agents. These include colony-stimulating factors (CSFs), glial cell-derived neurotrophic factor (GDNF), and monocyte chemoattractant proteins (MCPs). These factors are responsible for the recruitment of tumor-associated macrophages (TAMs). They polarize TAMs from M1 to M2 phenotypes to promote tumorigenesis [311**?**]. These findings were also consistent with the immune infiltration analysis of CSF3 with GBM (Figure 4.21). It is reported that in GBM tissue samples, higher levels of IL-6 in the cerebrospinal fluid have been linked to a larger population of TAMs [312]. Our GBM analysis revealed the presence of nine immune cell types associated with patient survival. Previous research has indicated that tumor-associated macrophages interact with tumor cells through direct contact or various signaling pathways [313].These findings indicate the possibility that GCSF (CSF3) signaling and the preservation of the tumor microenvironment (TME) are associated. Co-expression of GCSF and IL-6 reported to have co-augmenting effects on neutrophils. This phenomenon causes elevation of STAT3 expression and decreased JAK/STAT pathway activation [314]. Moreover, our study revealed enrichment of differential immune-related genes in the JAK/STAT signaling pathway.

Consequently, Immune-suppression is a defining aspect of the patho-physiology of cancer [315]. The activation of NF-κB-signaling is also necessary for tumor-associated macrophage (TAM) immune suppression and polarization in glioblastoma multiforme [316]. GM-CSF enhances the immunosuppressive activity of myeloid-derived suppressor cells. It activated the interleukin-4 receptor-α (IL-4R α) [317]. These observations strongly suggested the crucial role of TAMs in the development and progression of GBM proposing them therapeutic targets in GBM.

Neutrophils are recruited in response of inflammation to chemotactic agents including GM-CSF, CXCL1, IL-6 and IL-8. As a result, neutrophils secrete various Pro-Inflammatory Mediators, including IL-1 β, IL-6, TNF-α, IL-12, MMP-9, arginase-1, and VEGF. These mediators promote angiogenesis and establish Immuno-suppressive State [318]. Pro-Inflammatory Mediators like LPS, IL2 and G-CSF protect neutrophils from programmed cell death [319].

Numerous cell types, including endothelium, epithelial, fibroblasts, astrocytic, microglial cells and monocytic, release MCP-1 (Monocyte Chemoattractant Protein-1). It revealed as the primary chemotactic factor responsible in TAM recruitment [320]. A strong correlation has been observed between increased expression of MCP-1 and infiltrating microglial cells in a rat glioma model.Previous study revealed an increase of ten-fold in the cells of microglia in GBM as compared to control samples [266]. Similarly, TAMs in human glioblastoma multiforme cells recruited by glioma-derived MCP-3 [142].

Tumor-derived M-CSF (macrophage colony-stimulating factor/CSF1) and GM-CSF (granulocyte macrophage colony-stimulating factor/CSF2) , play significant roles in microglia accumulation, activation, progression of glioma and activation [321, 322]. These factors also interact with other pro-inflammatory cytokines, including TNF (tumor necrosis factor) and IL-1 β (interleukin-1 beta).

Increased expression of M-CSF(CSF1) has been associated with angiogenesis in various tumors. M-CSF stimulates microglia to secret IGFBP1 (insulin-like growth factor-binding protein 1), promoting angiogenesis in glioma [323]. GM-CSF/CSF2 triggers microglial cells to enhance the infiltration capacity of tumor cells in human glioma. The presence of CSF2/GM-CSF has been shown to increase the migration capacity of glioma cells. As a result, it confers resistance to apoptosis [324].

Glioblastoma (GBM) is characterized by its genomic heterogeneity which reflects the intricate molecular landscape of this tumor [325]. Our study also aimed to investigate the role of Granulocyte-Colony-Stimulating-Factor (GCSF) in glioblastoma in GFAP-negative cells to validate the correlation of GCSF with GFAP positive and GFAP negative glioblastoma samples. Previous research revealed that With the exception of glioblastomas, all GFAP-Positive tumors exhibited G-CSF expression. G-CSF expression was significantly reduced in recurrent tumors that had grown more dedifferentiated than their initial equivalents. In some GFAP-Negative tumors, such as Oligodendro-gliomas, G-CSF expression could not be seen [326]. Whereas Our IHC results clearly demonstrated that positive GFAP expression in Grade IV gliomas because of presence GFAP isoform variant (GFAP-δ) in glioblastoma (Figure 4.3).

We carried out the the analysis of GCSF, GCSFR, and STAT3 gene expressions in tumor-associated normal tissue (TANT) and grade-IV glioma. We observed statistically significant differences in their expression levels. The co-expression of GCSF and GCSFR suggests the potential for heightened autocrine and paracrine signaling in GBM [327]. Our RT-PCR-based study on glioblastoma patient biopsy samples revealed that GCSF functions as a tumor-promoting factor (Figure 4.7). It modulates the malignant biological properties of glioma cells. The increased expression of GCSF, GCSFR, and STAT3 genes was further validated by quantifying their respective proteins using ELISA (Figure 4.8). It was discovered in earlier studies that the granulocytosis typical of malignant disease may be associated to the production of G-CSF by (brain) tumor cells.Previous research described peripheral blood glioblastoma multiforme with severe granulocytosis [328].Constitutive activation of STAT3 suppresses host anti-tumor immune responses. As a result, it orchestrates unregulated tumorigenesis, angiogenesis, and the induction of immune evasion mechanisms. The increased expression of GCSF appears to facilitate STAT3 activation. STAT3 activation contributes to GBM immune evasion through a reduction in activated circulating lymphocytes and regulatory T cells (Tregs) [329]. We conducted a meta-analysis of RNA-seq datasets to identifying differentially expressed genes . Our results demonstrated that molecular mechanisms differ distinctly based on the expression patterns of specific genes in glioblastoma. Our findings revealed that high expressions of GCSF and GCSFR independently predicted decreased overall survival (OS) for GBM patients. Our research confirmed that both genes expression were significantly correlated with patient survival as disscussed in result section 4.8 . Multiple studies have highlighted the role of GCSF in exacerbating inflammation within the tumor microenvironment [330]. Our study validated the upregulated expression of GCSF in GBM and these findings were also consistant with in various cancer types [331]. Our study advances knowledge of the tumor-promoting characteristics connected to this aggressive brain malignancy.

Oncogenic mechanisms underlying GBM progression often involve genetic alterations and karyotype changes [332]. In our study through Insilico mutational analysis, we observed various genetic alterations in the inflammatory genes and

their associated driver genes due to their significant up regulated expression in GBM. In order to analyze the aberrant shift and changes in the gene expression of highly expressed genes, DriverDBV3 and cBIO Portal were applied in the current study.

DriverDBV3 imparts the extensive exome-seq data set published recently by combining driver gene analysis from various approaches and visualizing mutation data according to many factors. Based on various presumptions and characteristics, various bioinformatics techniques have been employed to discover driver genes, each offering a different perspective. Gene-Ontology, Pathway analysis and Protein/Genetics Interaction are the three levels of biological interpretation offered by driverDBV3, which integrates the study results of one or multiple methods [217]. The results of this visualization will help analyze the links between the driver genes. This study illustrates a driver gene found in glioblastoma multiforme (GBM). The 20 driver genes discovered were TP53, EGFR, IDH1, PIK3CA, PIK3R1, PTEN, LRRC37A, GSTM1, SIRPB1, SLC24A3, OS9, MELK, ZBTB42, UGT2B17, ENHO, and CDKN2B (each gene by at least 7 methods by driverDBV3). The important six genes listed (EGFR, TP53, PTEN, PIK3CA, PIK3R1, IDH1) are recognized as crucial in developing GBM tumors due to harmful mutations [333]. Therefore, through integrated analysis 12 mutations reported in the EGFR gene, 12 in the TP53 gene, 11 in the PTEN gene, 9 in the PIK3CA gene, 9 in the PIK3R1 gene, and 7 in the IDH1 gene. The 20 genes have been identified by our functional analysis as being involved in cell cycle-related categories, including phosphatidylinositol 3-kinase complex, cytoplasmic part, region of cytosol, cytoplasm, and apical plasma membrane, as well as in the molecular functions of driver genes of glioblastoma in relation to natural killer cell lectin-like receptor, insulin substrate insulin binding, and cyclin-dependent protein serine-threonine. A few abnormalities that cause primary glioblastoma (GBM) to proliferate and invade angiogenetically are EGFR Overexpression, PTEN (MMAC-I) Mutation, CDKN2A (p16) Deletion, and, less commonly, MDM2-Amplification [334]. In secondary GBM, TP53 mutations are typically the first genetic changes found [335]. Moreover, the IDH mutation was linked to the G-CIMP (Glioma CpG

Island Methylation Phenotype) of enhanced DNA methylation [336]. Somatic mutations in the iSH2 domain of PIK3R1, which encodes P85, provide a different way for tumors to downregulate the PI3K signaling cascade. This mutation also promotes the development of GBM [337]. In engineered mouse models and primary human cell systems, activation of PI3K signaling through PTEN loss or AKT overexpression has also been shown to promote the development of GBM tumors , validating the clinical significance of changes in this pathway that have been discovered in GBM patients [338]. Similarly, EGFR gene amplification and mutations play a significant genetic role in GBM, increasing the expression of both the wild-type (EGFRwt) and mutant oncogenic versions of the EGFR [339]. It has been shown that the mutant receptor may activate PI3K without PTEN loss because EGFRvIII strongly correlates with the activation of mTOR in vivo [340].Due to genetic modifications in the PTEN tumor suppressor gene on 10q23, such as LOH, Methylation and Mutation, and, 60% of GBMs have unregulated PI3K Signaling Pathways [332]. As reported poor survival in Anaplastic-Astrocytoma patients and GBM pateints are correlated with PTEN gene function loss caused by polymorphism or LOH,indicating that PTEN is involved in patient outcome [341]. TP53 mutations have been discovered to directly reduce overall survival in glioma patients [342]. The DNA-binding domain has missense mutations, accounting for 75% of p53 mutations [343]. The components of this pathway (PTEN, p110, p85, and probably receptor tyrosine kinases like EGFR) are the starting locations for signaling accelerated invasion among the prevalent alterations that promote GBM development and progression. Given that 46% of GBM patients have mutually exclusive mutations in PIK3CA, PIK3R1, and PTEN, the PI3K pathway is a promising therapeutic target [344]. Poor survival effects were identified for the other three genes, CRISP2, DCSTAMP, and MLPH. Many physiological and pathological processes, such as immunology, venom toxicity, reproduction, and cancer biology, have been linked to the CAP family of proteins [345]. Cell-cell adhesion, a crucial step in establishing and maintaining tissue patterns during development and a crucial mechanism during invasion and metastasis, one of the hallmarks of cancer, is mediated by DCSTAMP and MLPH [346].

In the current study TGF-β1 was found upregulated in the clinical GBM samples

and globally available GBM datasets as discussed. Similarly immune infiltration analysis also validate these findings. Previous studies reported TGF-β1 importance in respect to cell invasion, angiogenesis, and the inhibition of the immune system and making it a known driver of GBM invasion [311]. Hence, in addition to its varied roles in the formation of GBM, TGF- β1 adds a new function as a result of our findings. Due to its effects on cell proliferation, tumor invasion, angiogenesis, immunosuppression, and the preservation of the steaminess of glioma stem cells (GSCs), the TGFB1 pathway has been recognized as a mediator in the initiation and progression of gliomas [347].We analyzed the degree of expression of TGFB1 in the current study, to evaluate the mutational status of the protein in GBM. It was found that the protein expression was markedly elevated in GBM biopsy samples. Human investigations have shown that malignant glioma tissues overexpress TGFB1 while normal brain tissues are undetectable, further demonstrating that TGFB1 is involved in the growth of gliomas [348]. TGFB1 driver gene mutation data were visualized using driverDBV3 through Insilco analysis. Hotspot mutation sites (in the protein's center and end), particularly in the "Mutation Percentage of TGFB1" were identified and computed (Figure 4.25, 4.26). It was noted in earlier studies, missense and deep deletion mutations of TGFBI were the most prevalent in GBM [349]. This has been identified as the cause of the suboptimal response to TGFB1 inhibitors in GBM with mutations in the Extracellular-Domain.Additionally to EGFR mutations at the kinase domain (KD), mutations at the extracellular domain activate EGFR in GBM. This has been observed as the cause of the poor response of GBM to EGFR Inhibitors e.g "erlotinib" that targeting the active-kinase conformation in GBM with mutations in the extracellular domain [350]. Our calculations successfully simulated this pattern, also visible in the 'Mutation Profile' of TGFB1 in DriverDBV3. Study showed that miRNA expression is aberrant in cancer due to miRNA gene amplification, loss, translocation, epigenetic silencing, Dysregulation of Transcription Factors such as "p53 and c-Myc", and flaws in the "enzymatic machinery" involved in synthesis [351]. The TGFB1 exhibited a 638.2k median expression copy number gain, while the segment means 0.489 at 0 to 0.5. Similarly, the bar chart's colors represent a functional impact of mutation. Similar to the theTGFB1, the segment

means for the TGFB1 ranges from median -0.66 at -1 to -0.5 and 320.7k median expression copy number loss. When DriverDBV3 determined the segment mean from 0.0480, TheTGFB1 displayed 580.4k expression copy number none. Finding mutations that cause cancer still poses a considerable difficulty, according to several studies that evaluated the effectiveness of current techniques for predicting harmful mutations.Therefore, we used the "Driver-Score" to highlight the Hotspot Mutation Zone and explain the detrimental intensity of a mutation through the driverDBV3 which incorporates the data from seven computational techniques to examine the mutational data focused on one or more specific protein positions, locus enrichment, domains, exons, or cancers.

Similarly from GFAP negative group we found high expression of GCSF (CSF3), so in order to investigate the possible mechanism and changes in the genomic landscape causing mutations, the CBioPortal online tool has been applied. In the current study GCSF gene observed deep deletions (0.34%), mutations (0.51%), amplifications (0.84%), high mRNA expression (1.86%), low mRNA expression (1.01%), and multiple alterations (0.17%). These genetic alterations were directly correlated with significantly upregulated mRNA expression. The findings highlight the potential functional impact of these changes [352]. However the GBM heterogeneity remains poorly understood.

In the current study we identified intricate interconnectedness between potential drug targets and associated proteins. The normal expression patterns of differentially expressed genes (DEGs) influence the expression of these biomolecules. The disruptions in their regulation can lead to dysregulation of the pathways. Previous investigations have demonstrated that GCSF enhances STAT3 phosphorylation and JAK2 overexpression by binding to G-CSFR. As a result, it promotes GBM cell migration and proliferation [353]. Filgrastim (rhG-CSF) is administered parenterally. It is used to mitigate chemotherapy-induced neutropenia [354]. Our study revealed that GCSF can upregulate GCSFR and STAT3 in glioblastoma patients. Importantly, we found that GCSF is highly expressed in high-grade glioblastoma. Th results suggest a strong association between GCSF, GCSFR,

and STAT3 activation through increased phosphorylation. Cationic peptides possess unique characteristics that make them capable of inducing tumor cell apoptosis process [355].They are more often acknowledged as having potential drug candidates for enhancing anticancer therapies. When considering ligands, a Low-Binding Score is favored. It shows direct correlations with higher binding affinity. In our docking study, Nisin was docked with the GCSF (5GW9) protein. It resulted in the identification of 33 docked clusters, with 7 clusters exhibiting the most favorable hydrophobic interactions. Cluster 0 displayed the lowest energy-weighted score of -554.7 kcal/mol. It was the most stable complex. Notably, the anticancer peptide Nisin exhibited potent hydrogen bond interactions with amino acid residues in both clusters. In current investigation, Nisin induced significant apoptosis in the SF-767 cell line compared to the normal CHO cell line. This may be attributed to electrostatic interactions between the negative-charged cell membranes and cationic nature of Nisin the cationic Nisin of tumor cells, which contain anionic substances like phosphatidylserine. Moreover, our findings revealed a direct relationship between Nisin concentration and cell viability. Previous studies have reported that Nisin induces programmed cell death, and inhibits cell growth in various cancer types including colorectal cancer [356].

This study inferred that these inflammatory genes might be an early diagnostic markers for GBM patients since the expression trend of these genes was essentially compatible with the transcript. The retrospective nature of this study also represents a significant limitation. In future, in vivo experiments may warranted to unravel the molecular mechanisms underlying the interactions between inflammatory genes and the therapeutic potential of repurposed drugs and anti-cancer peptides/Bacteriocins i.e., “Nisin” against glioblastoma.

Chapter 6

Conclusion and Future Work

Glioblastoma (GBM), the most malignant subtype of glioma, remains a major challenge in terms of pharmacological treatment. Molecular characterization based on genomic, transcriptomic, and epigenetic profiling has provided a better understanding of glioma subtypes and the individual paths of glioma evolution. The study aimed to identify robust inflammatory gene signatures and molecular mechanisms underlying GBM to facilitate the development of novel and more effective therapeutic strategies. The study involved the profiling of inflammatory gene expression and in vitro drug response in high-grade gliomas, combining GBM and tumor-associated normal tissue samples from multiple studies. Chemokines, cytokines, and chemotactic agents were found to play crucial roles in GBM development, angiogenesis, immune suppression, and inflammation. Inflammatory gene signatures, including interleukins, NF-κB p65, GCSF and TGFB1, were identified as important players in inducing angiogenesis and resisting apoptosis in GBM. Celecoxib was found to reduce the viability and proliferation of glioblastoma cells and inhibit NF-κB p65 and TNFα expression in a dose-dependent manner. Driver genes and TGFB1 mutation were identified as significant factors in GBM, showing differential regulation concerning distinct cellular pathways. Tumor-associated macrophages (TAMs) and neutrophils were implicated in establishing an inflammatory and immunosuppressive state in GBM.GCSF, GCSFR, and STAT3 were found to be associated with GFAP-negative expression in high-grade gliomas. Integrated analysis of transcriptomic and proteomic profiling revealed enrichment

in disease-related pathways and identified potential therapeutic targets for GBM. Computational docking analysis suggested that Nisin, an anticancer bacteriocin peptide, could inhibit the growth and metastasis of glioblastoma by targeting GCSF. The study highlights the importance of multi-parametric approaches, personalized profiling, and the integration of genomic and functional levels in glioma research. The identified robust DEGs (differentially expressed genes) have the potential to serve as diagnostic markers and therapeutic targets for GBM. The study suggests that understanding the pharmacogenomic features of inflammatory biomarkers in brain cancer, particularly glioma emphasizes the need for personalized treatment strategies and the linking of genotypes to functional phenotypes in order to identify therapeutic options for specific glioma subpopulations. This understanding can lead to more effective, individualized treatments, thereby enhancing outcomes for individuals dealing with this challenging condition.

6.1 Future Work

Future work recommendations include additional investigation of identified gene signatures and molecular mechanisms, validation of therapeutic targets through preclinical and clinical studies, investigation of personalized treatment plans based on patient characteristics, integration of various profiling approaches, development of targeted therapies, and investigation of combination therapies for improving our understanding of and treating glioblastoma (GBM) and its subtypes. Longitudinal profiling, *In vitro* study validation in relation to the anti-inflammatory roles of the genes and monitoring of glioma patients to understand the dynamics of molecular changes, CNV identifications during treatment and disease progression. The study's findings could be strengthened by considering the potential influence of age, gender, ethnicity, and environmental factors in glioblastoma. These factors may contribute to variations in treatment response and outcomes, and exploring their impact could provide valuable insights for personalized medicine approaches.

Bibliography

[1] R. Visone and C. M. Croce, "Mirnas and cancer," *The American Journal of Pathology*, vol. 174, no. 4, pp. 1131–1138, 2009.

[2] H. Sung, J. Ferlay, R. L. Siegel, M. Laversanne, I. Soerjomataram, A. Jemal, and F. Bray, "Global cancer statistics 2020: Globocan estimates of incidence and mortality worldwide for 36 cancers in 185 countries," *CA: a Cancer Journal for Clinicians*, vol. 71, no. 3, pp. 209–249, 2021.

[3] F. Danish, H. Salam, M. A. Qureshi, and M. Nouman, "Comparative clinical and epidemiological study of central nervous system tumors in pakistan and global database," *Interdisciplinary Neurosurgery*, vol. 25, pp. 101239–101239, 2021.

[4] P. Kalita-de Croft, H. Sadeghi Rad, H. Gasper, K. O?Byrne, S. R. Lakhani, and A. Kulasinghe, "Spatial profiling technologies and applications for brain cancers," *Expert Review of Molecular Diagnostics*, vol. 21, no. 3, pp. 323–332, 2021.

[5] A. Darlix, S. Zouaoui, V. Rigau, F. Bessaoud, D. Figarella-Branger, H. Mathieu-Daudé, B. Trétarre, F. Bauchet, H. Duffau, L. Taillandier, *et al.*, "Epidemiology for primary brain tumors: a nationwide population-based study," *Journal of Neuro-oncology*, vol. 131, pp. 525–546, 2017.

[6] Q. T. Ostrom, H. Gittleman, J. Xu, C. Kromer, Y. Wolinsky, C. Kruchko, and J. S. Barnholtz-Sloan, "Cbtrus statistical report: primary brain and other central nervous system tumors diagnosed in the united states in 2009–2013," *Neuro-oncology*, vol. 18, no. suppl_5, pp. v1–v75, 2016.

[7] D. N. Louis, A. Perry, G. Reifenberger, A. Von Deimling, D. Figarella-Branger, W. K. Cavenee, H. Ohgaki, O. D. Wiestler, P. Kleihues, and D. W. Ellison, "The 2016 world health organization classification of tumors of the central nervous system: a summary," *Acta Neuropathologica*, vol. 131, pp. 803–820, 2016.

[8] H. Yan, D. W. Parsons, G. Jin, R. McLendon, B. A. Rasheed, W. Yuan, I. Kos, I. Batinic-Haberle, S. Jones, G. J. Riggins, *et al.*, "Idh1 and idh2 mutations in gliomas," *New England Journal of Medicine*, vol. 360, no. 8, pp. 765–773, 2009.

[9] D. J. Aum, D. H. Kim, T. L. Beaumont, E. C. Leuthardt, G. P. Dunn, and A. H. Kim, "Molecular and cellular heterogeneity: the hallmark of glioblastoma," *Neurosurgical Focus*, vol. 37, no. 6, pp. E11–E11, 2014.

[10] L. Dirven, N. K. Aaronson, J. J. Heimans, and M. J. Taphoorn, "Health-related quality of life in high-grade glioma patients," *Chinese Journal of Cancer*, vol. 33, no. 1, pp. 40–40, 2014.

[11] N. Gabel, D. B. Altshuler, A. Brezzell, E. M. Briceno, N. R. Boileau, Z. Miklja, K. Kluin, T. Ferguson, K. McMurray, L. Wang, *et al.*, "Health related quality of life in adult low and high-grade glioma patients using the national institutes of health patient reported outcomes measurement information system (promis) and neuro-qol assessments," *Frontiers in Neurology*, vol. 10, pp. 212–212, 2019.

[12] N. Zahid, R. S. Martins, W. Zahid, W. Khalid, I. Azam, S. S. Bhamani, K. Ahmad, A. Jabbar, M. S. Shamim, R. J. Khan, *et al.*, "Resilience and its associated factors in brain tumor patients in karachi, pakistan: An analytical cross-sectional study," *Psycho-Oncology*, vol. 30, no. 6, pp. 882–891, 2021.

[13] S. Grochans, A. M. Cybulska, D. Simińska, J. Korbecki, K. Kojder, D. Chlubek, and I. Baranowska-Bosiacka, "Epidemiology of glioblastoma multiforme–literature review," *Cancers*, vol. 14, no. 10, pp. 2412–2412, 2022.

[14] T. Siegal, "Clinical impact of molecular biomarkers in gliomas," *Journal of Clinical Neuroscience*, vol. 22, no. 3, pp. 437–444, 2015.

[15] T. Komori, "Grading of adult diffuse gliomas according to the 2021 who classification of tumors of the central nervous system," *Laboratory Investigation*, vol. 102, no. 2, pp. 126–133, 2022.

[16] A. L. Garton, C. J. Kinslow, A. I. Rae, A. Mehta, S. C. Pannullo, R. S. Magge, R. Ramakrishna, G. M. McKhann, M. B. Sisti, J. N. Bruce, *et al.*, "Extent of resection, molecular signature, and survival in 1p19q-codeleted gliomas," *Journal of Neurosurgery*, vol. 134, no. 5, pp. 1357–1367, 2020.

[17] H. S. Marques, B. B. de Brito, F. A. F. da Silva, M. L. C. Santos, J. C. B. de Souza, T. M. L. Correia, L. W. Lopes, N. S. de Macêdo Neres, R. S. D. M. Dórea, A. C. S. Dantas, *et al.*, "Relationship between th17 immune response and cancer," *World Journal of Clinical Oncology*, vol. 12, no. 10, pp. 845–845, 2021.

[18] T. A. Gonda, S. Tu, and T. C. Wang, "Chronic inflammation, the tumor microenvironment and carcinogenesis," *Cell Cycle*, vol. 8, no. 13, pp. 2005–2013, 2009.

[19] C. I. Diakos, K. A. Charles, D. C. McMillan, and S. J. Clarke, "Cancer-related inflammation and treatment effectiveness," *The Lancet Oncology*, vol. 15, no. 11, pp. e493–e503, 2014.

[20] K. Haruki, T. Taniai, M. Yanagaki, K. Furukawa, M. Tsunematsu, S. Onda, Y. Shirai, M. Matsumoto, N. Okui, and T. Ikegami, "Sustained systemic inflammatory response predicts survival in patients with hepatocellular carcinoma after hepatic resection," *Annals of Surgical Oncology*, vol. 30, no. 1, pp. 604–613, 2023.

[21] J.-F. Rossi, Z. Y. Lu, C. Massart, and K. Levon, "Dynamic immune/inflammation precision medicine: the good and the bad inflammation in infection and cancer," *Frontiers in Immunology*, vol. 12, pp. 595722–595722, 2021.

[22] H. Zhao, L. Wu, G. Yan, Y. Chen, M. Zhou, Y. Wu, and Y. Li, "Inflammation and tumor progression: signaling pathways and targeted intervention," *Signal Transduction and Targeted Therapy*, vol. 6, no. 1, pp. 263–263, 2021.

[23] Q. Hao, J. V. Vadgama, and P. Wang, "Ccl2/ccr2 signaling in cancer pathogenesis," *Cell Communication and Signaling*, vol. 18, pp. 1–13, 2020.

[24] E. A. Comen, R. L. Bowman, and M. Kleppe, "Underlying causes and therapeutic targeting of the inflammatory tumor microenvironment," *Frontiers in Cell and Developmental Biology*, vol. 6, pp. 56–56, 2018.

[25] R. Baghban, L. Roshangar, R. Jahanban-Esfahlan, K. Seidi, A. Ebrahimi-Kalan, M. Jaymand, S. Kolahian, T. Javaheri, and P. Zare, "Tumor microenvironment complexity and therapeutic implications at a glance," *Cell Communication and Signaling*, vol. 18, pp. 1–19, 2020.

[26] F. R. Greten and S. I. Grivennikov, "Inflammation and cancer: triggers, mechanisms, and consequences," *Immunity*, vol. 51, no. 1, pp. 27–41, 2019.

[27] G. Landskron, M. De la Fuente, P. Thuwajit, C. Thuwajit, and M. A. Hermoso, "Chronic inflammation and cytokines in the tumor microenvironment," *Journal of Immunology Research*, vol. 2014, 2014.

[28] W. Yu, Y. Tu, Z. Long, J. Liu, D. Kong, J. Peng, H. Wu, G. Zheng, J. Zhao, Y. Chen, *et al.*, "Reactive oxygen species bridge the gap between chronic inflammation and tumor development," *Oxidative Medicine and Cellular Longevity*, vol. 2022, 2022.

[29] A. Mostofa, S. R. Punganuru, H. R. Madala, M. Al-Obaide, and K. S. Srivenugopal, "The process and regulatory components of inflammation in brain oncogenesis," *Biomolecules*, vol. 7, no. 2, pp. 34–34, 2017.

[30] F. Takata, S. Nakagawa, J. Matsumoto, and S. Dohgu, "Blood-brain barrier dysfunction amplifies the development of neuroinflammation: understanding of cellular events in brain microvascular endothelial cells for prevention and treatment of bbb dysfunction," *Frontiers in Cellular Neuroscience*, vol. 15, pp. 661838–661838, 2021.

[31] L. Muzio, A. Viotti, and G. Martino, "Microglia in neuroinflammation and neurodegeneration: from understanding to therapy," *Frontiers in Neuroscience*, vol. 15, pp. 742065–742065, 2021.

[32] D. Hambardzumyan, D. H. Gutmann, and H. Kettenmann, "The role of microglia and macrophages in glioma maintenance and progression," *Nature Neuroscience*, vol. 19, no. 1, pp. 20–27, 2016.

[33] H. S. Kwon and S.-H. Koh, "Neuroinflammation in neurodegenerative disorders: The roles of microglia and astrocytes," *Translational Neurodegeneration*, vol. 9, pp. 1–12, 2020.

[34] J. Qin, Z. Ma, X. Chen, and S. Shu, "Microglia activation in central nervous system disorders: A review of recent mechanistic investigations and development efforts," *Frontiers in Neurology*, vol. 14, 2023.

[35] M. Singh, A. Raghav, and K. A. Gautam, "Role of the circulatory interleukin-6 in the pathogenesis of gliomas: A systematic review," *World Journal of Methodology*, vol. 12, no. 5, pp. 428–428, 2022.

[36] A. E. Kartikasari, C. S. Huertas, A. Mitchell, and M. Plebanski, "Tumor-induced inflammatory cytokines and the emerging diagnostic devices for cancer detection and prognosis," *Frontiers in Oncology*, vol. 11, pp. 692142–692142, 2021.

[37] N. Lin, W. Yan, K. Gao, Y. Wang, J. Zhang, and Y. You, "Prevalence and clinicopathologic characteristics of the molecular subtypes in malignant glioma: a multi-institutional analysis of 941 cases," *PLoS One*, vol. 9, no. 4, pp. e94871–e94871, 2014.

[38] J. Han, C. A. Alvarez-Breckenridge, Q.-E. Wang, and J. Yu, "Tgf-β signaling and its targeting for glioma treatment," *American Journal of Cancer Research*, vol. 5, no. 3, pp. 945–945, 2015.

[39] S. Shalapour, M. Karin, *et al.*, "Immunity, inflammation, and cancer: an eternal fight between good and evil," *The Journal of Clinical Investigation*, vol. 125, no. 9, pp. 3347–3355, 2015.

[40] L. Antonioli, C. Blandizzi, P. Pacher, and G. Haskó, "Immunity, inflammation and cancer: a leading role for adenosine," *Nature Reviews Cancer*, vol. 13, no. 12, pp. 842–857, 2013.

[41] B. Huang, X. Lang, and X. Li, "The role of il-6/jak2/stat3 signaling pathway in cancers," *Frontiers in Oncology*, vol. 12, 2022.

[42] K. Masliantsev, B. Pinel, A. Balbous, P.-O. Guichet, G. Tachon, S. Milin, J. Godet, M. Duchesne, A. Berger, C. Petropoulos, *et al.*, "Impact of stat3 phosphorylation in glioblastoma stem cells radiosensitization and patient outcome," *Oncotarget*, vol. 9, no. 3, pp. 3968–3968, 2018.

[43] W. Fu, X. Hou, L. Dong, and W. Hou, "Roles of stat3 in the pathogenesis and treatment of glioblastoma," *Frontiers in Cell and Developmental Biology*, vol. 11, pp. 196–196, 2023.

[44] W. Li and M. B. Graeber, "The molecular profile of microglia under the influence of glioma," *Neuro-oncology*, vol. 14, no. 8, pp. 958–978, 2012.

[45] P. Sharma, S. Alsharif, A. Fallatah, and B. M. Chung, "Intermediate filaments as effectors of cancer development and metastasis: a focus on keratins, vimentin, and nestin," *Cells*, vol. 8, no. 5, pp. 497–497, 2019.

[46] E. J. van Bodegraven, J. V. van Asperen, P. A. Robe, and E. M. Hol, "Importance of gfap isoform-specific analyses in astrocytoma," *Glia*, vol. 67, no. 8, pp. 1417–1433, 2019.

[47] E. Kim, S.-U. Hwang, J. D. Yoon, H. Kim, G. Lee, and S.-H. Hyun, "Isolation and characterization of gfap-positive porcine neural stem/progenitor cells derived from a gfap-creert2 transgenic piglet," *BMC Veterinary Research*, vol. 14, no. 1, pp. 1–10, 2018.

[48] F. Jin, H. Jin-Lee, and A. Johnson, "Mouse models of experimental glioblastoma," *Exon Publications*, pp. 15–45, 2021.

[49] Z. Yang and K. K. Wang, "Glial fibrillary acidic protein: from intermediate filament assembly and gliosis to neurobiomarker," *Trends in Neurosciences*, vol. 38, no. 6, pp. 364–374, 2015.

[50] A. Kunchok, A. Zekeridou, and A. McKeon, "Autoimmune glial fibrillary acidic protein astrocytopathy," *Current Opinion in Neurology*, vol. 32, no. 3, pp. 452–452, 2019.

[51] E. J. van Bodegraven, J. V. van Asperen, J. A. Sluijs, C. B. van Deursen, M. E. van Strien, O. M. Stassen, P. A. Robe, and E. M. Hol, "Gfap alternative splicing regulates glioma cell–ecm interaction in a dusp4-dependent manner," *The FASEB Journal*, vol. 33, no. 11, pp. 12941–12959, 2019.

[52] R. Uceda-Castro, J. V. van Asperen, C. Vennin, J. A. Sluijs, E. J. van Bodegraven, A. S. Margarido, P. A. Robe, J. van Rheenen, and E. M. Hol, "Gfap splice variants fine-tune glioma cell invasion and tumour dynamics by modulating migration persistence," *Scientific Reports*, vol. 12, no. 1, pp. 424–424, 2022.

[53] S. Zhou, D. J. Skaar, P. A. Jacobson, and R. S. Huang, "Pharmacogenomics of medications commonly used in the intensive care unit," *Frontiers in Pharmacology*, vol. 9, pp. 1436–1436, 2018.

[54] C. Manzoni, D. A. Kia, J. Vandrovcova, J. Hardy, N. W. Wood, P. A. Lewis, and R. Ferrari, "Genome, transcriptome and proteome: the rise of omics data and their integration in biomedical sciences," *Briefings in Bioinformatics*, vol. 19, no. 2, pp. 286–302, 2018.

[55] M.-H. Yeh, H.-C. Wu, N.-W. Lin, J.-J. Hsieh, J.-W. Yeh, H.-P. Chiu, M.-C. Wu, T.-Y. Tsai, C.-C. Yeh, and T.-M. Li, "Long-term use of combined conventional medicine and chinese herbal medicine decreases the mortality risk of patients with lung cancer," *Complementary Therapies in Medicine*, vol. 52, pp. 102427–102427, 2020.

[56] A. Sochacka-Cwikla, M. Mkaczynski, and A. Regiec, "Fda-approved small molecule compounds as drugs for solid cancers from early 2011 to the end of 2021," *Molecules*, vol. 27, no. 7, pp. 2259–2259, 2022.

[57] J.-P. Jourdan, R. Bureau, C. Rochais, and P. Dallemagne, "Drug repositioning: a brief overview," *Journal of Pharmacy and Pharmacology*, vol. 72, no. 9, pp. 1145–1151, 2020.

[58] M. A. Qureshi, T. Mirza, S. Khan, B. Sikandar, M. Zahid, M. Aftab, S. Mohsin, S. Sharafat, L. Avesi, and S. Hassan, "Cancer patterns in karachi (all districts), pakistan: First results (2010–2015) from a pathology based cancer registry of the largest government-run diagnostic and reference center of karachi," *Cancer Epidemiology*, vol. 44, pp. 114–122, 2016.

[59] R. Idrees, S. Fatima, J. Abdul-Ghafar, A. Raheem, and Z. Ahmad, "Cancer prevalence in pakistan: meta-analysis of various published studies to determine variation in cancer figures resulting from marked population heterogeneity in different parts of the country," *World Journal of Surgical Oncology*, vol. 16, no. 1, pp. 1–11, 2018.

[60] F. Badar and S. Mahmood, "Cancer in lahore, pakistan, 2010–2019: an incidence study," *BMJ Open*, vol. 11, no. 8, pp. e047049–e047049, 2022.

[61] P. Kamarajan, T. Hayami, B. Matte, Y. Liu, T. Danciu, A. Ramamoorthy, F. Worden, S. Kapila, and Y. Kapila, "Nisin zp, a bacteriocin and food preservative, inhibits head and neck cancer tumorigenesis and prolongs survival," *PloS One*, vol. 10, no. 7, pp. e0131008–e0131008, 2015.

[62] D. Hanahan and R. A. Weinberg, "The hallmarks of cancer," *Cell*, vol. 100, no. 1, pp. 57–70, 2000.

[63] M. Preusser and C. Marosi, "Advances in brain tumour classification and therapy," *Nature Reviews Neurology*, vol. 13, no. 2, pp. 71–72, 2017.

[64] C. Press, "Cell press: Cell press." https://www.cell.com/action/showPdf. (Accessed on 06/20/2023).

[65] S. Muçaj, N. Ramadani, S. Kabashi-Muçaj, N. Jerliu, A. Rashiti-Bytyci, and S. Hoxha, "Epidemiological profile and incidence of brain tumors in kosovo," *South Eastern European Journal of Public Health (SEEJPH)*, 2022.

[66] A. R. Omram, "The epidemiologic transition: a theory of the epidemiology of population change," *Bulletin of the World Health Organization*, vol. 79, no. 2, pp. 161–170, 2001.

[67] S. R. L. M. S. I. J. A. B. F. G. c. s. . Sung H, Ferlay J, "Global cancer statistics 2020: Globocan estimates of incidence and mortality worldwide for 36 cancers in 185 countries - sung - 2021 - ca: A cancer journal for clinicians - wiley online library." https://acsjournals.onlinelibrary.wiley.com/doi/10.3322/caac.21660. (Accessed on 06/20/2023).

[68] E. J. Maile, I. Barnes, A. E. Finlayson, S. Sayeed, and R. Ali, "Nervous system and intracranial tumour incidence by ethnicity in england, 2001–2007: a descriptive epidemiological study," *PLoS One*, vol. 11, no. 5, pp. e0154347–e0154347, 2016.

[69] Q. T. Ostrom, M. Price, C. Neff, G. Cioffi, K. A. Waite, C. Kruchko, and J. S. Barnholtz-Sloan, "Cbtrus statistical report: Primary brain and other central nervous system tumors diagnosed in the united states in 2015–2019," *Neuro-oncology*, vol. 24, no. Supplement_5, pp. v1–v95, 2022.

[70] A.-L. Luger, S. König, P. F. Samp, H. Urban, I. Divé, M. C. Burger, M. Voss, K. Franz, E. Fokas, K. Filipski, *et al.*, "Molecular matched targeted therapies for primary brain tumors?a single center retrospective analysis," *Journal of Neuro-oncology*, vol. 159, no. 2, pp. 243–259, 2022.

[71] K. K. Jain, "A critical overview of targeted therapies for glioblastoma," *Frontiers in Oncology*, vol. 8, pp. 419–419, 2018.

[72] Z. Khazaei, E. Goodarzi, V. Borhaninejad, F. Iranmanesh, H. Mirshekarpour, B. Mirzaei, H. Naemi, S. M. Bechashk, I. Darvishi, R. Ershad Sarabi, *et al.*, "The association between incidence and mortality of brain cancer and human development index (hdi): an ecological study," *BMC Public Health*, vol. 20, no. 1, pp. 1–7, 2020.

[73] B. T. Whitfield and J. T. Huse, "Classification of adult-type diffuse gliomas: Impact of the world health organization 2021 update," *Brain Pathology*, vol. 32, no. 4, pp. e13062–e13062, 2022.

[74] R. L. Siegel, K. D. Miller, N. S. Wagle, and A. Jemal, "Cancer statistics, 2023," *CA: a Cancer Journal for Clinicians*, vol. 73, no. 1, pp. 17–48, 2023.

[75] A. Perry and P. Wesseling, "Histologic classification of gliomas," *Handbook of Clinical Neurology*, vol. 134, pp. 71–95, 2016.

[76] P. O. Valko, A. Siddique, C. Linsenmeier, K. Zaugg, U. Held, and S. Hofer, "Prevalence and predictors of fatigue in glioblastoma: a prospective study," *Neuro-oncology*, vol. 17, no. 2, pp. 274–281, 2015.

[77] A. P. Kyritsis, M. L. Bondy, and V. A. Levin, "Modulation of glioma risk and progression by dietary nutrients and antiinflammatory agents," *Nutrition and Cancer*, vol. 63, no. 2, pp. 174–184, 2011.

[78] K. R. Porter, B. J. McCarthy, S. Freels, Y. Kim, and F. G. Davis, "Prevalence estimates for primary brain tumors in the united states by age, gender, behavior, and histology," *Neuro-oncology*, vol. 12, no. 6, pp. 520–527, 2010.

[79] G. Minniti, G. Lombardi, and S. Paolini, "Glioblastoma in elderly patients: current management and future perspectives," *Cancers*, vol. 11, no. 3, pp. 336–336, 2019.

[80] C. Alifieris and D. T. Trafalis, "Glioblastoma multiforme: Pathogenesis and treatment," *Pharmacology & Therapeutics*, vol. 152, pp. 63–82, 2015.

[81] X. Dong, A. Noorbakhsh, B. R. Hirshman, T. Zhou, J. A. Tang, D. C. Chang, B. S. Carter, and C. C. Chen, "Survival trends of grade i, ii, and iii astrocytoma patients and associated clinical practice patterns between 1999 and 2010: a seer-based analysis," *Neuro-oncology Practice*, vol. 3, no. 1, pp. 29–38, 2016.

[82] K. P. Ohgaki H, "Genetic pathways to primary and secondary glioblastoma - pubmed." https://pubmed.ncbi.nlm.nih.gov/17456751/. (Accessed on 06/21/2023).

[83] N. Grech, T. Dalli, S. Mizzi, L. Meilak, N. Calleja, and A. Zrinzo, "Rising incidence of glioblastoma multiforme in a well-defined population," *Cureus*, vol. 12, no. 5, 2020.

[84] C. Adamson, O. O. Kanu, A. I. Mehta, C. Di, N. Lin, A. K. Mattox, and D. D. Bigner, "Glioblastoma multiforme: a review of where we have been and where we are going," *Expert Opinion on Investigational Drugs*, vol. 18, no. 8, pp. 1061–1083, 2009.

[85] P. Wesseling, M. van den Bent, and A. Perry, "Oligodendroglioma: pathology, molecular mechanisms and markers," *Acta Neuropathologica*, vol. 129, pp. 809–827, 2015.

[86] S. G. Berntsson, R. T. Merrell, E. S. Amirian, G. N. Armstrong, D. Lachance, A. Smits, R. Zhou, D. I. Jacobs, M. R. Wrensch, S. H. Olson, *et al.*, "Glioma-related seizures in relation to histopathological subtypes: a report from the glioma international case–control study," *Journal of Neurology*, vol. 265, pp. 1432–1442, 2018.

[87] A. Latysheva, K. E. Emblem, P. Brandal, E. O. Vik-Mo, J. Pahnke, K. Røysland, J. K. Hald, and A. Server, "Dynamic susceptibility contrast and diffusion mr imaging identify oligodendroglioma as defined by the 2016 who classification for brain tumors: histogram analysis approach," *Neuroradiology*, vol. 61, pp. 545–555, 2019.

[88] K. Leu, G. A. Ott, A. Lai, P. L. Nghiemphu, W. B. Pope, W. H. Yong, L. M. Liau, T. F. Cloughesy, and B. M. Ellingson, "Perfusion and diffusion mri signatures in histologic and genetic subtypes of who grade ii–iii diffuse gliomas," *Journal of Neuro-oncology*, vol. 134, pp. 177–188, 2017.

[89] M. Zulfiqar, N. Dumrongpisutikul, J. Intrapiromkul, and D. M. Yousem, "Detection of intratumoral calcification in oligodendrogliomas by susceptibility-weighted mr imaging," *American Journal of Neuroradiology*, vol. 33, no. 5, pp. 858–864, 2012.

[90] K. Mirchia and T. E. Richardson, "Beyond idh-mutation: emerging molecular diagnostic and prognostic features in adult diffuse gliomas," *Cancers*, vol. 12, no. 7, pp. 1817–1817, 2020.

[91] M. J. van den Bent, M. Weller, P. Y. Wen, J. M. Kros, K. Aldape, and S. Chang, "A clinical perspective on the 2016 who brain tumor classification and routine molecular diagnostics," *Neuro-oncology*, vol. 19, no. 5, pp. 614–624, 2017.

[92] S. Sharma and P. Deb, "Intraoperative neurocytology of primary central nervous system neoplasia: A simplified and practical diagnostic approach," *Journal of Cytology/Indian Academy of Cytologists*, vol. 28, no. 4, pp. 147–147, 2011.

[93] K. S. Lee, G. Choe, K. H. Nam, A. N. Seo, S. Yun, K. J. Kim, H. J. Cho, and S. H. Park, "Immunohistochemical classification of primary and secondary glioblastomas," *Korean Journal of Pathology*, vol. 47, no. 6, pp. 541–541, 2013.

[94] W. H. K.-T. C. Reifenberger, G., "Advances in the molecular genetics of gliomas — implications for classification and therapy — nature reviews clinical oncology." https://www.nature.com/articles/nrclinonc.2016.204. (Accessed on 06/21/2023).

[95] D. L. Pozzi, "Glioma classification and key molecular pathology - atlas antibodies." https://www.atlasantibodies.com/blog/glioma-classification-and-key-molecular-pathology/. (Accessed on 06/21/2023).

[96] A. Leibetseder, J. Leitner, M. J. Mair, S. Meckel, J. A. Hainfellner, M. Aichholzer, G. Widhalm, K. Dieckmann, S. Weis, J. Furtner, *et al.*, "Prognostic factors in adult brainstem glioma: a tertiary care center analysis and review of the literature," *Journal of Neurology*, pp. 1–17, 2022.

[97] M. K. Goel, P. Khanna, and J. Kishore, "Understanding survival analysis: Kaplan-meier estimate," *International Journal of Ayurveda Research*, vol. 1, no. 4, pp. 274–274, 2010.

[98] C. Fernandes, A. Costa, L. Osório, R. C. Lago, P. Linhares, B. Carvalho, and C. Caeiro, "Current standards of care in glioblastoma therapy," *Exon Publications*, pp. 197–241, 2017.

[99] M. P. La Quaglia, B. H. Kushner, W. Su, G. Heller, K. Kramer, S. Abramson, N. Rosen, S. Wolden, and N.-K. V. Cheung, "The impact of gross total resection on local control and survival in high-risk neuroblastoma," *Journal of Pediatric Surgery*, vol. 39, no. 3, pp. 412–417, 2004.

[100] A. Bex and B. Mathon, "Advances, technological innovations, and future prospects in stereotactic brain biopsies," *Neurosurgical Review*, vol. 46, no. 1, pp. 5–5, 2022.

[101] T. Noh, M. Mustroph, and A. J. Golby, "Intraoperative imaging for high-grade glioma surgery," *Neurosurgery Clinics*, vol. 32, no. 1, pp. 47–54, 2021.

[102] F. Dhermain, "Radiotherapy of high-grade gliomas: current standards and new concepts, innovations in imaging and radiotherapy, and new therapeutic approaches," *Chinese Journal of Cancer*, vol. 33, no. 1, pp. 16–16, 2014.

[103] J. S. Marra, G. P. Mendes, G. H. Yoshinari, F. da Silva Guimarães, S. C. Mazin, and H. F. de Oliveira, "Survival after radiation therapy for high-grade glioma," *Reports of Practical Oncology and Radiotherapy*, vol. 24, no. 1, pp. 35–40, 2019.

[104] G. Paolo Spinelli, E. Miele, G. Lo Russo, M. Miscusi, G. Codacci-Pisanelli, V. Petrozza, A. Papa, L. Frati, C. Della Rocca, A. Gulino, *et al.*, "Chemotherapy and target therapy in the management of adult high-grade gliomas," *Current Cancer Drug Targets*, vol. 12, no. 8, pp. 1016–1031, 2012.

[105] S. Braunstein, D. Raleigh, R. Bindra, S. Mueller, and D. Haas-Kogan, "Pediatric high-grade glioma: current molecular landscape and therapeutic approaches," *Journal of Neuro-oncology*, vol. 134, pp. 541–549, 2017.

[106] M. Z. Wojtukiewicz, M. M. Rek, K. Karpowicz, M. Górska, B. Polityńska, A. M. Wojtukiewicz, M. Moniuszko, P. Radziwon, S. C. Tucker, and K. V. Honn, "Inhibitors of immune checkpoints?pd-1, pd-l1, ctla-4?new opportunities for cancer patients and a new challenge for internists and general practitioners," *Cancer and Metastasis Reviews*, vol. 40, pp. 949–982, 2021.

[107] M. W. Yu and D. F. Quail, "Immunotherapy for glioblastoma: current progress and challenges," *Frontiers in Immunology*, pp. 1637–1637, 2021.

[108] M. W. Yu and D. F. Quail, "Frontiers — immunotherapy for glioblastoma: Current progress and challenges." https://www.frontiersin.org/articles/10.3389/fimmu.2021.676301/full. (Accessed on 06/21/2023).

[109] M. F. Almahariq, T. J. Quinn, P. Kesarwani, S. Kant, C. R. Miller, and P. Chinnaiyan, "Inhibition of colony-stimulating factor-1 receptor enhances the efficacy of radiotherapy and reduces immune suppression in glioblastoma," *In Vivo*, vol. 35, no. 1, pp. 119–129, 2021.

[110] Y. Guo, K. Lei, and L. Tang, "Neoantigen vaccine delivery for personalized anticancer immunotherapy," *Frontiers in Immunology*, vol. 9, pp. 1499–1499, 2018.

[111] N. Singh, D. Baby, J. P. Rajguru, P. B. Patil, S. S. Thakkannavar, and V. B. Pujari, "Inflammation and cancer," *Annals of African Medicine*, vol. 18, no. 3, pp. 121–121, 2019.

[112] T. Jayakumar, K.-C. Lin, C.-C. Chang, C.-W. Hsia, M. Manubolu, W.-C. Huang, J.-R. Sheu, and C.-H. Hsia, "Targeting mapk/nf-κb pathways in anti-inflammatory potential of rutaecarpine: Impact on src/fak-mediated macrophage migration," *International Journal of Molecular Sciences*, vol. 23, no. 1, pp. 92–92, 2021.

[113] S. Amor, L. A. Peferoen, D. Y. Vogel, M. Breur, P. van der Valk, D. Baker, and J. M. van Noort, "Inflammation in neurodegenerative diseases–an update," *Immunology*, vol. 142, no. 2, pp. 151–166, 2014.

[114] G. J. Harry, "Microglia: Neuroprotective and neurodestructive properties," in *Neurotoxicology*, pp. 185–212, CRC Press, 2016.

[115] T. Hirano, "Il-6 in inflammation, autoimmunity and cancer," *International Immunology*, vol. 33, no. 3, pp. 127–148, 2021.

[116] A. J. West, V. Tsui, S. S. Stylli, H. Nguyen, A. P. Morokoff, A. H. Kaye, and R. B. Luwor, "The role of interleukin-6-stat3 signalling in glioblastoma," *Oncology Letters*, vol. 16, no. 4, pp. 4095–4104, 2018.

[117] R. Al-Kharboosh, K. ReFaey, M. Lara-Velazquez, S. S. Grewal, J. Imitola, and A. Quiñones-Hinojosa, "Inflammatory mediators in glioma microenvironment play a dual role in gliomagenesis and mesenchymal stem cell homing: implication for cellular therapy," *Mayo Clinic Proceedings: Innovations, Quality & Outcomes*, vol. 4, no. 4, pp. 443–459, 2020.

[118] X. Liu, F. Ye, H. Xiong, D.-N. Hu, G. A. Limb, T. Xie, L. Peng, P. Zhang, Y. Wei, W. Zhang, *et al.*, "Il-1β induces il-6 production in retinal müller cells predominantly through the activation of p38 mapk/nf-κb signaling pathway," *Experimental Cell Research*, vol. 331, no. 1, pp. 223–231, 2015.

[119] M. Chen, H. Wang, W. Chen, and G. Meng, "Regulation of adaptive immunity by the nlrp3 inflammasome," *International Immunopharmacology*, vol. 11, no. 5, pp. 549–554, 2011.

[120] Q. He, Y. Fu, D. Tian, and W. Yan, "The contrasting roles of inflammasomes in cancer," *American Journal of Cancer Research*, vol. 8, no. 4, pp. 566–566, 2018.

[121] K. Fathima Hurmath, P. Ramaswamy, and D. N. Nandakumar, "Il-1β microenvironment promotes proliferation, migration, and invasion of human glioma cells," *Cell Biology International*, vol. 38, no. 12, pp. 1415–1422, 2014.

[122] X. Feng, F. Szulzewsky, A. Yerevanian, Z. Chen, D. Heinzmann, R. D. Rasmussen, V. Alvarez-Garcia, Y. Kim, B. Wang, I. Tamagno, *et al.*, "Loss

of cx3cr1 increases accumulation of inflammatory monocytes and promotes gliomagenesis," *Oncotarget*, vol. 6, no. 17, pp. 15077–15077, 2015.

[123] E. T. Ha, J. P. Antonios, H. Soto, R. M. Prins, I. Yang, N. Kasahara, L. M. Liau, and C. A. Kruse, "Chronic inflammation drives glioma growth: cellular and molecular factors responsible for an immunosuppressive microenvironment," *Neuroimmunology and Neuroinflammation*, vol. 1, pp. 66–76, 2014.

[124] M. A. Nengroo, A. Verma, and D. Datta, "Cytokine chemokine network in tumor microenvironment: Impact on csc properties and therapeutic applications," *Cytokine*, vol. 156, pp. 155916–155916, 2022.

[125] A. Mostofa, S. Punganuru, H. R. Madala, M. Al-Obaide, and K. Srivenugopal, "(pdf) the process and regulatory components of inflammation in brain oncogenesis." https://www.researchgate.net/publication/315663845_The_Process_and_Regulatory_Components_of_Inflammation_in_Brain_Oncogenesis. (Accessed on 06/21/2023).

[126] A. Ellert-Miklaszewska, M. Dabrowski, M. Lipko, M. Sliwa, M. Maleszewska, and B. Kaminska, "Molecular definition of the pro-tumorigenic phenotype of glioma-activated microglia," *Glia*, vol. 61, no. 7, pp. 1178–1190, 2013.

[127] D. Hambardzumyan, D. H. Gutmann, and H. Kettenmann, "The role of microglia and macrophages in glioma maintenance and progression," *Nature Neuroscience*, vol. 19, no. 1, pp. 20–27, 2016.

[128] R. E. Kast, Q. A. Hill, D. Wion, H. Mellstedt, D. Focosi, G. Karpel-Massler, T. Heiland, and M.-E. Halatsch, "Glioblastoma-synthesized g-csf and gm-csf contribute to growth and immunosuppression: Potential therapeutic benefit from dapsone, fenofibrate, and ribavirin," *Tumor Biology*, vol. 39, no. 5, pp. 97–97, 2017.

[129] T. N. Seyfried and L. M. Shelton, "Cancer as a metabolic disease," *Nutrition & Metabolism*, vol. 7, pp. 1–22, 2010.

[130] M. Preusser and C. Marosi, "Advances in brain tumour classification and therapy," *Nature Reviews Neurology*, vol. 13, no. 2, pp. 71–72, 2017.

[131] N. Cartier, C.-A. Lewis, R. Zhang, and F. M. Rossi, "The role of microglia in human disease: therapeutic tool or target?," *Acta Neuropathologica*, vol. 128, pp. 363–380, 2014.

[132] S. Guo, H. Wang, and Y. Yin, "Microglia polarization from m1 to m2 in neurodegenerative diseases," *Frontiers in Aging Neuroscience*, vol. 14, pp. 75–75, 2022.

[133] C. Lin, N. Wang, and C. Xu, "Glioma-associated microglia/macrophages (gams) in glioblastoma: Immune function in the tumor microenvironment and implications for immunotherapy," *Frontiers in Immunology*, vol. 14, 2023.

[134] J. K. Andersen, H. Miletic, and J. A. Hossain, "Tumor-associated macrophages in gliomas?basic insights and treatment opportunities," *Cancers*, vol. 14, no. 5, pp. 1319–1319, 2022.

[135] F. Szulzewsky, *Investigating the properties of glioma-associated microglia/-macrophages*. PhD thesis, 2015.

[136] S. Roesch, C. Rapp, S. Dettling, and C. Herold-Mende, "(pdf) when immune cells turn bad—tumor-associated microglia/macrophages in glioma." https://www.researchgate.net/publication/322893985_When_Immune_Cells_Turn_Bad-Tumor-Associated_MicrogliaMacrophages_in_Glioma. (Accessed on 06/21/2023).

[137] A. Gieryng, D. Pszczolkowska, K. A. Walentynowicz, W. D. Rajan, and B. Kaminska, "Immune microenvironment of gliomas," *Laboratory Investigation*, vol. 97, no. 5, pp. 498–518, 2017.

[138] E. C. Yeo, M. P. Brown, T. Gargett, and L. M. Ebert, "The role of cytokines and chemokines in shaping the immune microenvironment of glioblastoma: implications for immunotherapy," *Cells*, vol. 10, no. 3, pp. 607–607, 2021.

[139] M. D. Caverzán, L. Beaugé, P. M. Oliveda, B. Cesca González, E. M. Bühler, and L. E. Ibarra, "Exploring monocytes-macrophages in immune microenvironment of glioblastoma for the design of novel therapeutic strategies," *Brain Sciences*, vol. 13, no. 4, pp. 542–542, 2023.

[140] S. Roesch, C. Rapp, S. Dettling, and C. Herold-Mende, "Ijms — free full-text — when immune cells turn bad—tumor-associated microglia/macrophages in glioma." https://www.mdpi.com/1422-0067/19/2/436. (Accessed on 06/21/2023).

[141] A. Bianconi, G. Aruta, F. Rizzo, L. F. Salvati, P. Zeppa, D. Garbossa, and F. Cofano, "Systematic review on tumor microenvironment in glial neoplasm: From understanding pathogenesis to future therapeutic perspectives," *International Journal of Molecular Sciences*, vol. 23, no. 8, pp. 4166–4166, 2022.

[142] S. Roesch, C. Rapp, S. Dettling, and C. Herold-Mende, "When immune cells turn bad?tumor-associated microglia/macrophages in glioma," *International Journal of Molecular Sciences*, vol. 19, no. 2, pp. 436–436, 2018.

[143] G. Liu and H. Yang, "Modulation of macrophage activation and programming in immunity," *Journal of Cellular Physiology*, vol. 228, no. 3, pp. 502–512, 2013.

[144] S. Li, C. Wang, J. Chen, Y. Lan, W. Zhang, Z. Kang, Y. Zheng, R. Zhang, J. Yu, and W. Li, "Signaling pathways in brain tumors and therapeutic interventions," *Signal Transduction and Targeted Therapy*, vol. 8, no. 1, pp. 8–8, 2023.

[145] R. Kim, A. Mahta, and S. Kesari, "(pdf) glioma stem cells." https://www.researchgate.net/publication/221914086_Glioma_Stem_Cells. (Accessed on 06/21/2023).

[146] S. O. Rahaman, P. C. Harbor, O. Chernova, G. H. Barnett, M. A. Vogelbaum, and S. J. Haque, "Inhibition of constitutively active stat3 suppresses

proliferation and induces apoptosis in glioblastoma multiforme cells," *Oncogene*, vol. 21, no. 55, pp. 8404–8413, 2002.

[147] A. P. See, J. E. Han, J. Phallen, Z. Binder, G. Gallia, F. Pan, D. Jinasena, C. Jackson, Z. Belcaid, S. J. Jeong, *et al.*, "The role of stat3 activation in modulating the immune microenvironment of gbm," *Journal of Neuro-oncology*, vol. 110, pp. 359–368, 2012.

[148] G. Zhang, S. Tanaka, S. Jiapaer, H. Sabit, S. Tamai, M. Kinoshita, and M. Nakada, "Rbpj contributes to the malignancy of glioblastoma and induction of proneural-mesenchymal transition via il-6-stat3 pathway," *Cancer Science*, vol. 111, no. 11, pp. 4166–4176, 2020.

[149] M. Wu, D. Song, H. Li, Y. Yang, X. Ma, S. Deng, C. Ren, and X. Shu, "Negative regulators of stat3 signaling pathway in cancers," *Cancer Management and Research*, vol. 11, pp. 4957–4957, 2019.

[150] M. Khabibov, A. Garifullin, Y. Boumber, K. Khaddour, M. Fernandez, F. Khamitov, L. Khalikova, N. Kuznetsova, O. Kit, and L. Kharin, "Signaling pathways and therapeutic approaches in glioblastoma multiforme," *International Journal of Oncology*, vol. 60, no. 6, pp. 1–18, 2022.

[151] J. Seoane and R. R. Gomis, "Tgf-β family signaling in tumor suppression and cancer progression," *Cold Spring Harbor Perspectives in Biology*, vol. 9, no. 12, pp. a022277–a022277, 2017.

[152] Y. Chao, Y. Wang, X. Liu, P. Ma, Y. Shi, J. Gao, Q. Shi, J. Hu, R. Yu, and X. Zhou, "Mst1 regulates glioma cell proliferation via the akt/mtor signaling pathway," *Journal of Neuro-oncology*, vol. 121, pp. 279–288, 2015.

[153] T. Zhang, C. Ma, Z. Zhang, H. Zhang, and H. Hu, "Nf-κb signaling in inflammation and cancer," *MedComm*, vol. 2, no. 4, pp. 618–653, 2021.

[154] T.-H. Yen, C.-L. Hsieh, T.-T. Liu, C.-S. Huang, Y.-C. Chen, Y.-C. Chuang, S.-S. Lin, and F.-T. Hsu, "Amentoflavone induces apoptosis and inhibits nf-κb-modulated anti-apoptotic signaling in glioblastoma cells," *In Vivo*, vol. 32, no. 2, pp. 279–285, 2018.

[155] M. Zuccarini, P. Giuliani, S. Ziberi, M. Carluccio, P. Di Iorio, F. Caciagli, and R. Ciccarelli, "The role of wnt signal in glioblastoma development and progression: a possible new pharmacological target for the therapy of this tumor," *Genes*, vol. 9, no. 2, pp. 105–105, 2018.

[156] J. Polivka Jr and F. Janku, "Molecular targets for cancer therapy in the pi3k/akt/mtor pathway," *Pharmacology & Therapeutics*, vol. 142, no. 2, pp. 164–175, 2014.

[157] A. Barzegar Behrooz, Z. Talaie, F. Jusheghani, M. J. Łos, T. Klonisch, and S. Ghavami, "Wnt and pi3k/akt/mtor survival pathways as therapeutic targets in glioblastoma," *International Journal of Molecular Sciences*, vol. 23, no. 3, pp. 1353–1353, 2022.

[158] K. P. Ohgaki H, "Genetic pathways to primary and secondary glioblastoma - pubmed." https://pubmed.ncbi.nlm.nih.gov/17456751/. (Accessed on 06/21/2023).

[159] Y. Zhang, M. Xia, K. Jin, S. Wang, H. Wei, C. Fan, Y. Wu, X. Li, X. Li, G. Li, *et al.*, "Function of the c-met receptor tyrosine kinase in carcinogenesis and associated therapeutic opportunities," *Molecular Cancer*, vol. 17, no. 1, pp. 1–14, 2018.

[160] Y. Kwak, S.-I. Kim, C.-K. Park, S. H. Paek, S.-T. Lee, and S.-H. Park, "C-met overexpression and amplification in gliomas," *International Journal of Clinical and Experimental Pathology*, vol. 8, no. 11, pp. 14932–14932, 2015.

[161] A. Ardizzone, S. A. Scuderi, D. Giuffrida, C. Colarossi, C. Puglisi, M. Campolo, S. Cuzzocrea, E. Esposito, and I. Paterniti, "Role of fibroblast growth factors receptors (fgfrs) in brain tumors, focus on astrocytoma and glioblastoma," *Cancers*, vol. 12, no. 12, pp. 3825–3825, 2020.

[162] Y. Chen and D. Gutmann, "The molecular and cell biology of pediatric low-grade gliomas," *Oncogene*, vol. 33, no. 16, pp. 2019–2026, 2014.

[163] K. Szklener, M. Mazurek, M. Wieteska, M. Wacławska, M. Bilski, and S. Mańdziuk, "New directions in the therapy of glioblastoma," *Cancers*, vol. 14, no. 21, pp. 5377–5377, 2022.

[164] A. K. Sisakht, M. Malekan, F. Ghobadinezhad, S. N. M. Firouzabadi, A. Jafari, S. M. A. Mirazimi, B. Abadi, R. Shafabakhsh, and H. Mirzaei, "Cellular conversations in glioblastoma progression, diagnosis and treatment," *Cellular and Molecular Neurobiology*, vol. 43, no. 2, pp. 585–603, 2023.

[165] W. Ji, Y. Liu, B. Xu, J. Mei, C. Cheng, Y. Xiao, K. Yang, W. Huang, J. Jiao, H. Liu, *et al.*, "Bioinformatics analysis of expression profiles and prognostic values of the signal transducer and activator of transcription family genes in glioma," *Frontiers in Genetics*, vol. 12, pp. 625234–625234, 2021.

[166] W. Zhang, J. Zhang, W. Yan, G. You, Z. Bao, S. Li, C. Kang, C. Jiang, Y. You, Y. Zhang, *et al.*, "Whole-genome microrna expression profiling identifies a 5-microrna signature as a prognostic biomarker in chinese patients with primary glioblastoma multiforme," *Cancer*, vol. 119, no. 4, pp. 814–824, 2013.

[167] C. Vastrad and B. Vastrad, "Bioinformatics analysis of gene expression profiles to diagnose crucial and novel genes in glioblastoma multiform," *Pathology-Research and Practice*, vol. 214, no. 9, pp. 1395–1461, 2018.

[168] A. Burska, K. Roget, M. Blits, L. Soto Gomez, F. Van De Loo, L. Hazelwood, C. Verweij, A. Rowe, G. Goulielmos, L. Van Baarsen, *et al.*, "Gene expression analysis in ra: towards personalized medicine," *The pharmacogenomics Journal*, vol. 14, no. 2, pp. 93–106, 2014.

[169] R. Mehrian Shai, J. K. Reichardt, and T. C. Chen, "Pharmacogenomics of brain cancer and personalized medicine in malignant gliomas," 2008.

[170] J. Li, C. Di, A. K. Mattox, L. Wu, and D. C. Adamson, "The future role of personalized medicine in the treatment of glioblastoma multiforme," *Pharmacogenomics and Personalized Medicine*, pp. 111–127, 2010.

[171] H. Van Thuijl, B. Ylstra, T. Würdinger, D. van Nieuwenhuizen, J. Heimans, P. Wesseling, and J. Reijneveld, "Genetics and pharmacogenomics of diffuse gliomas," *Pharmacology & Therapeutics*, vol. 137, no. 1, pp. 78–88, 2013.

[172] J. S. Young, M. D. Prados, and N. Butowski, "Using genomics to guide treatment for glioblastoma," *Pharmacogenomics*, vol. 19, no. 15, pp. 1217–1229, 2018.

[173] L. F. Coelho, N. Bernardes, and A. M. Fialho, "Prospective therapeutic applications of bacteriocins as anticancer agents," in *Microbial Infections and Cancer Therapy*, pp. 339–366, Jenny Stanford Publishing, 2019.

[174] J.-W. Yoon and S.-S. Kang, "In vitro antibiofilm and anti-inflammatory properties of bacteriocins produced by pediococcus acidilactici against enterococcus faecalis," *Foodborne Pathogens and Disease*, vol. 17, no. 12, pp. 764–771, 2020.

[175] N. Zainodini, G. Hassanshahi, M. Hajizadeh, S. K. Falahati-Pour, M. Mahmoodi, and M. R. Mirzaei, "Nisin induces cytotoxicity and apoptosis in human asterocytoma cell line (sw1088)," *Asian Pacific Journal of Cancer Prevention: APJCP*, vol. 19, no. 8, pp. 2217–2217, 2018.

[176] T. M. Karpiński and A. Adamczak, "Anticancer activity of bacterial proteins and peptides," *Pharmaceutics*, vol. 10, no. 2, pp. 54–54, 2018.

[177] L. S. Biswaro, M. G. da Costa Sousa, T. M. Rezende, S. C. Dias, and O. L. Franco, "Antimicrobial peptides and nanotechnology, recent advances and challenges," *Frontiers in microbiology*, vol. 9, pp. 855–855, 2018.

[178] P. Kamarajan, T. Hayami, B. Matte, Y. Liu, T. Danciu, A. Ramamoorthy, F. Worden, S. Kapila, and Y. Kapila, "Nisin zp, a bacteriocin and food preservative, inhibits head and neck cancer tumorigenesis and prolongs survival," *PloS One*, vol. 10, no. 7, pp. e0131008–e0131008, 2015.

[179] S. M. Patil and N. K. Kunda, "Nisin zp, an antimicrobial peptide, induces cell death and inhibits non-small cell lung cancer (nsclc) progression in vitro

in 2d and 3d cell culture," *Pharmaceutical Research*, vol. 39, no. 11, pp. 2859–2870, 2022.

[180] M. D. Siegelin, E. Schneider, M.-A. Westhoff, C. R. Wirtz, and G. Karpel-Massler, "Current state and future perspective of drug repurposing in malignant glioma," in *Seminars in cancer biology*, vol. 68, pp. 92–104, Elsevier, 2021.

[181] C. Seliger, J. Schaertl, M. Gerken, C. Luber, M. Proescholdt, M. J. Riemenschneider, M. F. Leitzmann, P. Hau, and M. Klinkhammer-Schalke, "Use of statins or nsaids and survival of patients with high-grade glioma," *PloS One*, vol. 13, no. 12, pp. e0207858–e0207858, 2018.

[182] S. B. Lyne and B. Yamini, "An alternative pipeline for glioblastoma therapeutics: a systematic review of drug repurposing in glioblastoma," *Cancers*, vol. 13, no. 8, pp. 1953–1953, 2021.

[183] A. Vamvakas, S. Williams, K. Theodorou, E. Kapsalaki, K. Fountas, C. Kappas, K. Vassiou, and I. Tsougos, "Imaging biomarker analysis of advanced multiparametric mri for glioma grading," *Physica Medica*, vol. 60, pp. 188–198, 2019.

[184] D. Sturm, B. A. Orr, U. H. Toprak, V. Hovestadt, D. T. Jones, D. Capper, M. Sill, I. Buchhalter, P. A. Northcott, I. Leis, *et al.*, "New brain tumor entities emerge from molecular classification of cns-pnets," *Cell*, vol. 164, no. 5, pp. 1060–1072, 2016.

[185] J. Kim, H. Kim, M.-S. Lee, H. Lee, Y. J. Kim, W. Y. Lee, S. H. Yun, H. C. Kim, H. K. Hong, S. Hannenhalli, *et al.*, "Transcriptomes of the tumor-adjacent normal tissues are more informative than tumors in predicting recurrence in colorectal cancer patients," *Journal of Translational Medicine*, vol. 21, no. 1, pp. 1–15, 2023.

[186] L.-B. Wang, A. Karpova, M. A. Gritsenko, J. E. Kyle, S. Cao, Y. Li, D. Rykunov, A. Colaprico, J. H. Rothstein, R. Hong, *et al.*, "Proteogenomic and metabolomic characterization of human glioblastoma," *Cancer Cell*, vol. 39, no. 4, pp. 509–528, 2021.

[187] Z. Liu, M. Rao, T. Poiret, S. Nava, Q. Meng, A. von Landenberg, J. Bartek Jr, S. Xie, G. Sinclair, I. Peredo, *et al.*, "Mesothelin as a novel biomarker and immunotherapeutic target in human glioblastoma," *Oncotarget*, vol. 8, no. 46, pp. 80208–80208, 2017.

[188] G. Högnäs, K. Kivinummi, H. M. Kallio, R. Hieta, P. Ruusuvuori, A. Koskenalho, J. Kesseli, T. L. Tammela, J. Riikonen, J. Ilvesaro, *et al.*, "Feasibility of prostate paxgene fixation for molecular research and diagnostic surgical pathology," *The American Journal of Surgical Pathology*, vol. 42, no. 1, pp. 103–115, 2018.

[189] D. N. Louis, A. Perry, P. Wesseling, D. J. Brat, I. A. Cree, D. Figarella-Branger, C. Hawkins, H. Ng, S. M. Pfister, G. Reifenberger, *et al.*, "The 2021 who classification of tumors of the central nervous system: a summary," *Neuro-oncology*, vol. 23, no. 8, pp. 1231–1251, 2021.

[190] J. Litlekalsoy, V. Vatne, J. G. Hostmark, and O. D. Laerum, "Immunohistochemical markers in urinary bladder carcinomas from paraffin-embedded archival tissue after storage for 5–70 years," *BJU International*, vol. 99, no. 5, pp. 1013–1019, 2007.

[191] T. M. Alicea-Reyes, *The Role of the Endocannabinoid System in Prostate Cancer Perineural Invasion*. PhD thesis, University of Puerto Rico Medical Sciences (Puerto Rico), 2020.

[192] B. M. Osrah, *The 18kDa translocator protein in human glioma*. The University of Manchester (United Kingdom), 2021.

[193] W. Xu, W. Liang, and Y. Dai, "A three-mirna signature as a potential biomarker for the diagnosis of glioma," *Int J Clin Exp Pathol*, vol. 10, no. 3, pp. 2814–2823, 2017.

[194] H. Anderson, G. P. Takacs, C. Kreiger, D. Luo, L. Rong, J. K. Harrison, and T. Stepien, "A cts team approach to modeling migration and suppression of ccr2+/cx3cr1+ myeloid cells in glioblastoma," 2022.

[195] Z. Tu, C. Wang, Q. Hu, C. Tao, Z. Fang, L. Lin, K. Lei, M. Luo, Y. Sheng, X. Long, *et al.*, "Protein disulfide-isomerase a4 confers glioblastoma angiogenesis promotion capacity and resistance to anti-angiogenic therapy," *Journal of Experimental & Clinical Cancer Research*, vol. 42, no. 1, pp. 1–19, 2023.

[196] M. J. Reese, D. W. Knapp, K. M. Anderson, J. A. Mund, J. Case, D. R. Jones, and R. A. Packer, "In vitro effect of chlorambucil on human glioma cell lines (sf767 and u87-mg), and human microvascular endothelial cell (hmvec) and endothelial progenitor cells (ecfcs), in the context of plasma chlorambucil concentrations in tumor-bearing dogs," *Plos One*, vol. 13, no. 9, pp. e0203517–e0203517, 2018.

[197] H. K. Rooprai, P. Lawrence, S. Keshavarz, P. Yashod, R. W. Gullan, R. P. Selway, and D. Davies, "Draq7 as an alternative to mtt assay for measuring viability of glioma cells treated with polyphenols," *Anticancer Research*, vol. 40, no. 10, pp. 5427–5436, 2020.

[198] L. Wei, F. Yin, C. Chen, and L. Li, "Expression of integrin α-6 is associated with multi drug resistance and prognosis in ovarian cancer," *Oncology Letters*, vol. 17, no. 4, pp. 3974–3980, 2019.

[199] S. Babichev, B. Durnyak, V. Senkivskyy, O. Sorochynskyi, M. Kliap, and O. Khamula, "Exploratory analysis of neuroblastoma data genes expressions based on bioconductor package tools.," in *IDDM*, pp. 268–279, 2019.

[200] P. Dhamodharan and M. Arumugam, "Multiple gene expression dataset analysis reveals toll-like receptor signaling pathway is strongly associated with chronic obstructive pulmonary disease pathogenesis," *COPD: Journal of Chronic Obstructive Pulmonary Disease*, vol. 17, no. 6, pp. 684–698, 2020.

[201] Y. Taguchi, "Principal component analysis based unsupervised feature extraction applied to budding yeast temporally periodic gene expression," *BioData Mining*, vol. 9, no. 1, pp. 1–23, 2016.

[202] Y. Zhou, B. Zhou, L. Pache, M. Chang, A. H. Khodabakhshi, O. Tanaseichuk, C. Benner, and S. K. Chanda, "Metascape provides a biologist-oriented resource for the analysis of systems-level datasets," *Nature Communications*, vol. 10, no. 1, pp. 1523–1523, 2019.

[203] A. P. Davis, C. J. Grondin, R. J. Johnson, D. Sciaky, R. McMorran, J. Wiegers, T. C. Wiegers, and C. J. Mattingly, "The comparative toxicogenomics database: update 2019," *Nucleic Acids Research*, vol. 47, no. D1, pp. D948–D954, 2019.

[204] C.-C. Wang, W.-J. Shen, G. Anuraga, Y.-H. Hsieh, H. D. Khoa Ta, D. T. M. Xuan, C.-F. Shen, C.-Y. Wang, and W.-J. Wang, "Penetrating exploration of prognostic correlations of the fkbp gene family with lung adenocarcinoma," *Journal of Personalized Medicine*, vol. 13, no. 1, pp. 49–49, 2022.

[205] S. Nomiri, H. Karami, B. Baradaran, D. Javadrashid, A. Derakhshani, N. S. Nourbakhsh, M. A. Shadbad, A. G. Solimando, N. J. Tabrizi, O. Brunetti, *et al.*, "Exploiting systems biology to investigate the gene modules and drugs in ovarian cancer: A hypothesis based on the weighted gene co-expression network analysis," *Biomedicine & Pharmacotherapy*, vol. 146, pp. 112537–112537, 2022.

[206] S. Kumari and P. Kumar, "Design and computational analysis of an mmp9 inhibitor in hypoxia-induced glioblastoma multiforme," *ACS Omega*, vol. 8, no. 11, pp. 10565–10590, 2023.

[207] S. U. Kumar, D. T. Kumar, R. Siva, C. G. P. Doss, and H. Zayed, "Integrative bioinformatics approaches to map potential novel genes and pathways involved in ovarian cancer," *Frontiers in Bioengineering and Biotechnology*, vol. 7, pp. 391–391, 2019.

[208] A. Marco-Ramell, M. Palau-Rodriguez, A. Alay, S. Tulipani, M. Urpi-Sarda, A. Sanchez-Pla, and C. Andres-Lacueva, "Evaluation and comparison of bioinformatic tools for the enrichment analysis of metabolomics data," *BMC Bioinformatics*, vol. 19, pp. 1–11, 2018.

[209] M. Burnett, V. Rodolico, F. Shen, R. Leng, M. Zhang, D. D. Eisenstat, and C. Sergi, "Pathvisio analysis: An application targeting the mirna network associated with the p53 signaling pathway in osteosarcoma," *Biocell*, vol. 45, no. 1, pp. 17–17, 2021.

[210] L. Liu, C. Wang, S. Li, Y. Qu, P. Xue, Z. Ma, X. Zhang, H. Bai, and J. Wang, "Ero1l is a novel and potential biomarker in lung adenocarcinoma and shapes the immune-suppressive tumor microenvironment," *Frontiers in Immunology*, vol. 12, pp. 677169–677169, 2021.

[211] A. Salavaty, Z. Rezvani, and A. Najafi, "Survival analysis and functional annotation of long non-coding rnas in lung adenocarcinoma," *Journal of Cellular and Molecular Medicine*, vol. 23, no. 8, pp. 5600–5617, 2019.

[212] X. Yang, Y. Wen, X. Song, S. He, and X. Bo, "Exploring the classification of cancer cell lines from multiple omic views," *PeerJ*, vol. 8, pp. e9440–e9440, 2020.

[213] T. Das, G. Andrieux, M. Ahmed, and S. Chakraborty, "Integration of online omics-data resources for cancer research," *Frontiers in Genetics*, vol. 11, pp. 578345–578345, 2020.

[214] M. Usman, M. K. Okla, H. M. Asif, G. AbdElgayed, F. Muccee, S. Ghazanfar, M. Ahmad, M. J. Iqbal, A. M. Sahar, G. Khaliq, *et al.*, "A pan-cancer analysis of gins complex subunit 4 to identify its potential role as a biomarker in multiple human cancers," *American Journal of Cancer Research*, vol. 12, no. 3, pp. 986–986, 2022.

[215] H. Wu, H. Wang, Z. Jiang, and Y. Chen, "Identification of three core secretome genes associated with immune infiltration in high tumor mutation

burden across 14 major solid tumors," *International Journal of General Medicine*, pp. 6755–6767, 2021.

[216] Y. Liu, D. Wang, Z. Li, X. Li, M. Jin, N. Jia, X. Cui, G. Hu, T. Tang, and Q. Yu, "Pan-cancer analysis on the role of pik3r1 and pik3r2 in human tumors," *Scientific Reports*, vol. 12, no. 1, pp. 5924–5924, 2022.

[217] M. F. I. Faruque, "Identification of dephosphorylated sites in the proximity of recurrent mutations in pp2a targets," 2018.

[218] M. Soudy, A. M. Anwar, E. A. Ahmed, A. Osama, S. Ezzeldin, S. Mahgoub, and S. Magdeldin, "Uniprotr: Retrieving and visualizing protein sequence and functional information from universal protein resource (uniprot knowledgebase)," *Journal of Proteomics*, vol. 213, pp. 103613–103613, 2020.

[219] J. Gao and H. Zheng, "Illuminating the lipidome to advance biomedical research: peptide-based probes of membrane lipids," *Future Medicinal Chemistry*, vol. 5, no. 8, pp. 947–959, 2013.

[220] K. Surachat, U. Sangket, P. Deachamag, and W. Chotigeat, "In silico analysis of protein toxin and bacteriocins from lactobacillus paracasei sd1 genome and available online databases," *PloS One*, vol. 12, no. 8, pp. e0183548–e0183548, 2017.

[221] S. S. Qawoogha and A. Shahiwala, "Identification of potential anticancer phytochemicals against colorectal cancer by structure-based docking studies," *Journal of Receptors and Signal Transduction*, vol. 40, no. 1, pp. 67–76, 2020.

[222] A. Pavlopoulou and I. Michalopoulos, "State-of-the-art bioinformatics protein structure prediction tools," *International Journal of Molecular Medicine*, vol. 28, no. 3, pp. 295–310, 2011.

[223] O. V. Sobolev, P. V. Afonine, N. W. Moriarty, M. L. Hekkelman, R. P. Joosten, A. Perrakis, and P. D. Adams, "A global ramachandran score identifies protein structures with unlikely stereochemistry," *Structure*, vol. 28, no. 11, pp. 1249–1258, 2020.

[224] S. Cheng and M. Y. Niv, "Molecular dynamics simulations and elastic network analysis of protein kinase b (akt/pkb) inactivation," *Journal of Chemical Information and Modeling*, vol. 50, no. 9, pp. 1602–1610, 2010.

[225] P. Mahzouni, E. Aghili, and B. Sabaghi, "An immunohistochemical study of vascular endothelial growth factor expression in meningioma and its correlation with tumor grade," *Middle East Journal of Cancer*, vol. 9, no. 4, pp. 288–294, 2018.

[226] A. A. Hashmi, N. Faridi, B. Malik, M. M. Edhi, A. Khurshid, and M. Khan, "Morphologic spectrum of glial tumors: an increased trend towards oligodendroglial tumors in pakistan," *International Archives of Medicine*, vol. 7, no. 1, pp. 1–6, 2014.

[227] S. Zaman, F. Jahangir, Z. Rathore, M. Khalid, M. Hussain, M. Nasir, S. Shafqat, and A. Naseem, "Histologic spectrum of brain tumors at children hospital and institute of child health, lahore," *Pakistan Journal of Medical & Health Sciences*, vol. 12, no. 2, pp. 567–569, 2018.

[228] D. N. Louis, P. Wesseling, K. Aldape, D. J. Brat, D. Capper, I. A. Cree, C. Eberhart, D. Figarella-Branger, M. Fouladi, G. N. Fuller, *et al.*, "cimpact-now update 6: new entity and diagnostic principle recommendations of the cimpact-utrecht meeting on future cns tumor classification and grading," 2020.

[229] Y. Ahmadipour, O. Gembruch, D. Pierscianek, U. Sure, and R. Jabbarli, "Does the expression of glial fibrillary acid protein (gfap) stain in glioblastoma tissue have a prognostic impact on survival?," *Neurochirurgie*, vol. 66, no. 3, pp. 150–154, 2020.

[230] H. Lassmann and M. Bradl, "Multiple sclerosis: experimental models and reality," *Acta Neuropathologica*, vol. 133, pp. 223–244, 2017.

[231] E. M. Hol and M. Pekny, "Glial fibrillary acidic protein (gfap) and the astrocyte intermediate filament system in diseases of the central nervous system," *Current Opinion in Cell Biology*, vol. 32, pp. 121–130, 2015.

[232] Z. Yang and K. K. Wang, "Glial fibrillary acidic protein: from intermediate filament assembly and gliosis to neurobiomarker," *Trends in Neurosciences*, vol. 38, no. 6, pp. 364–374, 2015.

[233] J. Li and S. Qin, "Activation of astrocytes in neurodegenerative diseases," *Neurodegenerative Diseases Biomarkers: Towards Translating Research to Clinical Practice*, pp. 39–70, 2022.

[234] Y. Sawaishi, "Review of alexander disease: beyond the classical concept of leukodystrophy," *Brain and Development*, vol. 31, no. 7, pp. 493–498, 2009.

[235] K. Giannikou, Z. Zhu, J. Kim, K. D. Winden, M. E. Tyburczy, D. Marron, J. S. Parker, Z. Hebert, A. Bongaarts, L. Taing, *et al.*, "Subependymal giant cell astrocytomas are characterized by mtorc1 hyperactivation, a very low somatic mutation rate, and a unique gene expression profile," *Modern Pathology*, vol. 34, no. 2, pp. 264–279, 2021.

[236] O. Okolie, J. R. Bago, R. S. Schmid, D. M. Irvin, R. E. Bash, C. R. Miller, and S. D. Hingtgen, "Reactive astrocytes potentiate tumor aggressiveness in a murine glioma resection and recurrence model," *Neuro-oncology*, vol. 18, no. 12, pp. 1622–1633, 2016.

[237] D. Rohle, J. Popovici-Muller, N. Palaskas, S. Turcan, C. Grommes, C. Campos, J. Tsoi, O. Clark, B. Oldrini, E. Komisopoulou, *et al.*, "An inhibitor of mutant idh1 delays growth and promotes differentiation of glioma cells," *Science*, vol. 340, no. 6132, pp. 626–630, 2013.

[238] H. Takeuchi, T. Kubota, K. Sato, J. F. Llena, and A. Hirano, "Epithelial differentiation and proliferative potential in spinal ependymomas," *Journal of Neuro-oncology*, vol. 58, pp. 13–19, 2002.

[239] S. Berendsen, E. van Bodegraven, T. Seute, W. G. Spliet, M. Geurts, J. Hendrikse, L. Schoysman, W. B. Huiszoon, M. Varkila, S. Rouss, *et al.*, "Adverse prognosis of glioblastoma contacting the subventricular zone: Biological correlates," *PloS One*, vol. 14, no. 10, pp. e0222717–e0222717, 2019.

[240] F. M. Brehar, D. Arsene, L. A. Brinduse, and M. R. Gorgan, "Immunohistochemical analysis of gfap-δ and nestin in cerebral astrocytomas," *Brain Tumor Pathology*, vol. 32, pp. 90–98, 2015.

[241] I. Jovčevska, "Genetic secrets of long-term glioblastoma survivors," *Bosnian Journal of Basic Medical Sciences*, vol. 19, no. 2, pp. 116–116, 2019.

[242] N. Gagliano, F. Costa, C. Cossetti, L. Pettinari, R. Bassi, M. Chiriva-Internati, E. Cobos, M. Gioia, and S. Pluchino, "Glioma-astrocyte interaction modifies the astrocyte phenotype in a co-culture experimental model," *Oncology Reports*, vol. 22, no. 6, pp. 1349–1356, 2009.

[243] R. Godbout, D. A. Bisgrove, D. Shkolny, and R. S Day, "Correlation of b-fabp and gfap expression in malignant glioma," *Oncogene*, vol. 16, no. 15, pp. 1955–1962, 1998.

[244] L. Martinian, K. Boer, J. Middeldorp, E. Hol, S. Sisodiya, W. Squier, E. Aronica, and M. Thom, "Expression patterns of glial fibrillary acidic protein (gfap)-delta in epilepsy-associated lesional pathologies," *Neuropathology and Applied Neurobiology*, vol. 35, no. 4, pp. 394–405, 2009.

[245] C. Lind, C. Gray, A. Pearson, R. Cameron, S. O'Carroll, P. Narayan, J. Lim, and M. Dragunow, "The mitogen-activated/extracellular signal-regulated kinase kinase 1/2 inhibitor u0126 induces glial fibrillary acidic protein expression and reduces the proliferation and migration of c6 glioma cells," *Neuroscience*, vol. 141, no. 4, pp. 1925–1933, 2006.

[246] J. van Asperen, R. Uceda-Castro, C. Vennin, J. Sluijs, E. J. van Bodegraven, A. S. Margarido, P. A. Robe, J. van Rheenen, and E. M. Hol, "Gfap splice variants fine-tune glioma cell invasion and and tumour dynamics by modulating migration persistence," *BioRxiv*, pp. 2021–08, 2021.

[247] S. S. Rao, J. DeJesus, A. R. Short, J. J. Otero, A. Sarkar, and J. O. Winter, "Glioblastoma behaviors in three-dimensional collagen-hyaluronan composite hydrogels," *ACS Applied Materials & Interfaces*, vol. 5, no. 19, pp. 9276–9284, 2013.

[248] C. Leduc and S. Etienne-Manneville, "Intermediate filaments in cell migration and invasion: the unusual suspects," *Current Opinion in Cell Biology*, vol. 32, pp. 102–112, 2015.

[249] S. Seetharaman and S. Etienne-Manneville, "Cytoskeletal crosstalk in cell migration," *Trends in Cell Biology*, vol. 30, no. 9, pp. 720–735, 2020.

[250] E. J. Van Bodegraven and S. Etienne-Manneville, "Intermediate filaments against actomyosin: the david and goliath of cell migration," *Current Opinion in Cell Biology*, vol. 66, pp. 79–88, 2020.

[251] M. Moeton, O. M. Stassen, J. A. Sluijs, V. W. van der Meer, L. J. Kluivers, H. van Hoorn, T. Schmidt, E. A. Reits, M. E. van Strien, and E. M. Hol, "Gfap isoforms control intermediate filament network dynamics, cell morphology, and focal adhesions," *Cellular and Molecular Life Sciences*, vol. 73, pp. 4101–4120, 2016.

[252] R. Radu, G. E. Petrescu, R. M. Gorgan, and F. M. Brehar, "Gfapδ: A promising biomarker and therapeutic target in glioblastoma," *Frontiers in Oncology*, vol. 12, 2022.

[253] J. V. van Asperen, P. A. Robe, and E. M. Hol, "Gfap alternative splicing and the relevance for disease–a focus on diffuse gliomas," *ASN Neuro*, vol. 14, pp. 2065–2065, 2022.

[254] E. J. van Bodegraven, J. V. van Asperen, P. A. Robe, and E. M. Hol, "Importance of gfap isoform-specific analyses in astrocytoma," *Glia*, vol. 67, no. 8, pp. 1417–1433, 2019.

[255] E. Fasterius, M. Uhlén, and C. Al-Khalili Szigyarto, "Single-cell rna-seq variant analysis for exploration of genetic heterogeneity in cancer," *Scientific Reports*, vol. 9, no. 1, pp. 1–11, 2019.

[256] M. Qazi, P. Vora, C. Venugopal, S. Sidhu, J. Moffat, C. Swanton, and S. Singh, "Intratumoral heterogeneity: pathways to treatment resistance and relapse in human glioblastoma," *Annals of Oncology*, vol. 28, no. 7, pp. 1448–1456, 2017.

[257] O. M. Stassen, E. J. van Bodegraven, F. Giuliani, M. Moeton, R. Kanski, J. A. Sluijs, M. E. van Strien, W. Kamphuis, P. A. Robe, and E. M. Hol, "Gfapδ/gfapα ratio directs astrocytoma gene expression towards a more malignant profile," *Oncotarget*, vol. 8, no. 50, pp. 88104–88104, 2017.

[258] A. C. Fuentes-Fayos, M. C. Vázquez-Borrego, J. M. Jimenez-Vacas, L. Bejarano, S. Pedraza-Arevalo, F. L.-López, C. Blanco-Acevedo, R. Sánchez-Sánchez, O. Reyes, S. Ventura, *et al.*, "Splicing machinery dysregulation drives glioblastoma development/aggressiveness: oncogenic role of srsf3," *Brain*, vol. 143, no. 11, pp. 3273–3293, 2020.

[259] N. Kelly, J. Varga, E. Specker, C. Romeo, B. Coomber, and J. Uniacke, "Hypoxia activates cadherin-22 synthesis via eif4e2 to drive cancer cell migration, invasion and adhesion," *Oncogene*, vol. 37, no. 5, pp. 651–662, 2018.

[260] Z.-w. Liu, Y.-m. Zhang, L.-y. Zhang, T. Zhou, Y.-y. Li, G.-c. Zhou, Z.-m. Miao, M. Shang, J.-p. He, N. Ding, *et al.*, "Duality of interactions between tgf-β and tnf-α during tumor formation," *Frontiers in Immunology*, vol. 12, p. 5628, 2022.

[261] R. A. Kore and E. C. Abraham, "Inflammatory cytokines, interleukin-1 beta and tumor necrosis factor-alpha, upregulated in glioblastoma multiforme, raise the levels of cryab in exosomes secreted by u373 glioma cells," *Biochemical and Biophysical Research Communications*, vol. 453, no. 3, pp. 326–331, 2014.

[262] Y. Yeung, K. McDonald, T. Grewal, and L. Munoz, "Interleukins in glioblastoma pathophysiology: implications for therapy," *British Journal of Pharmacology*, vol. 168, no. 3, pp. 591–606, 2013.

[263] D. Jansson, J. Rustenhoven, S. Feng, D. Hurley, R. L. Oldfield, P. S. Bergin, E. W. Mee, R. L. Faull, and M. Dragunow, "A role for human brain pericytes in neuroinflammation," *Journal of Neuroinflammation*, vol. 11, no. 1, pp. 1–20, 2014.

[264] M. Yang, L. Wang, X. Wang, X. Wang, Z. Yang, and J. Li, "Il-6 promotes fsh-induced vegf expression through jak/stat3 signaling pathway in bovine granulosa cells," *Cellular Physiology and Biochemistry*, vol. 44, no. 1, pp. 293–302, 2018.

[265] M. Baggiolini, B. Dewald, and B. Moser, "lnterleukin-8 and related chemotactic cytokines—cxc and cc chemokines," *Advances in Immunology*, vol. 55, pp. 97–179, 1993.

[266] B. S. Qazi, K. Tang, and A. Qazi, "Recent advances in underlying pathologies provide insight into interleukin-8 expression-mediated inflammation and angiogenesis," *International Journal of Inflammation*, vol. 2011, 2011.

[267] K. Snoussi, W. Mahfoudh, N. Bouaouina, S. B. Ahmed, A. N. Helal, and L. Chouchane, "Genetic variation in il-8 associated with increased risk and poor prognosis of breast carcinoma," *Human Immunology*, vol. 67, no. 1-2, pp. 13–21, 2006.

[268] C. Jackson, J. Ruzevick, J. Phallen, Z. Belcaid, and M. Lim, "Challenges in immunotherapy presented by the glioblastoma multiforme microenvironment," *Clinical and Developmental Immunology*, vol. 2011, 2011.

[269] Y. Xiao, K. Yang, Z. Wang, M. Zhao, Y. Deng, W. Ji, Y. Zou, C. Qian, Y. Liu, H. Xiao, *et al.*, "Cd44-mediated poor prognosis in glioma is associated with m2-polarization of tumor-associated macrophages and immunosuppression," *Frontiers in Surgery*, vol. 8, pp. 785–785, 2022.

[270] K. R. Arya, R. P. Bharath Chand, C. S. Abhinand, A. S. Nair, O. V. Oommen, and P. R. Sudhakaran, "Identification of hub genes and key pathways associated with anti-vegf resistant glioblastoma using gene expression data analysis," *Biomolecules*, vol. 11, no. 3, pp. 403–403, 2021.

[271] J. K. Tiwari, S. Negi, M. Kashyap, S. Nizamuddin, A. Singh, and A. Khattri, "Pan-cancer analysis shows enrichment of macrophages, overexpression

of checkpoint molecules, inhibitory cytokines, and immune exhaustion signatures in emt-high tumors," *Frontiers in Oncology*, vol. 11, pp. 793881–793881, 2022.

[272] I. Sharma, A. Singh, F. Siraj, and S. Saxena, "Il-8/cxcr1/2 signalling promotes tumor cell proliferation, invasion and vascular mimicry in glioblastoma," *Journal of Biomedical Science*, vol. 25, no. 1, pp. 1–13, 2018.

[273] S. Bastola, *Molecular Regulation of Glioblastoma Spatial Heterogeneity and Therapeutic Resistance*. PhD thesis, The University of Alabama at Birmingham, 2020.

[274] N. Zheng, S. Zhang, W. Wu, N. Zhang, and J. Wang, "Regulatory mechanisms and therapeutic targeting of vasculogenic mimicry in hepatocellular carcinoma," *Pharmacological Research*, vol. 166, pp. 105507–105507, 2021.

[275] Y. Soda, C. Myskiw, A. Rommel, and I. M. Verma, "Mechanisms of neovascularization and resistance to anti-angiogenic therapies in glioblastoma multiforme," *Journal of Molecular Medicine*, vol. 91, pp. 439–448, 2013.

[276] S.-H. Ahn, H. Park, Y.-H. Ahn, S. Kim, M.-S. Cho, J. L. Kang, and Y.-H. Choi, "Necrotic cells influence migration and invasion of glioblastoma via nf-κb/ap-1-mediated il-8 regulation," *Scientific Reports*, vol. 6, no. 1, pp. 1–12, 2016.

[277] M. G. McCoy, D. Nyanyo, C. K. Hung, J. P. Goerger, W. R. Zipfel, R. M. Williams, N. Nishimura, and C. Fischbach, "Endothelial cells promote 3d invasion of gbm by il-8-dependent induction of cancer stem cell properties," *Scientific Reports*, vol. 9, no. 1, pp. 9069–9069, 2019.

[278] H. Motaln and T. Lah Turnsek, "Cytokines play a key role in communication between mesenchymal stem cells and brain cancer cells," *Protein and Peptide Letters*, vol. 22, no. 4, pp. 322–331, 2015.

[279] Q. Liu, A. Li, Y. Tian, J. D. Wu, Y. Liu, T. Li, Y. Chen, X. Han, and K. Wu, "The cxcl8-cxcr1/2 pathways in cancer," *Cytokine & Growth Factor Reviews*, vol. 31, pp. 61–71, 2016.

[280] D. J. Waugh and C. Wilson, "The interleukin-8 pathway in cancer," *Clinical Cancer Research*, vol. 14, no. 21, pp. 6735–6741, 2008.

[281] S. Kaur, Y. Bansal, R. Kumar, and G. Bansal, "A panoramic review of il-6: Structure, pathophysiological roles and inhibitors," *Bioorganic & Medicinal Chemistry*, vol. 28, no. 5, pp. 115327–115327, 2020.

[282] J.-I. Youn and D. I. Gabrilovich, "The biology of myeloid-derived suppressor cells: the blessing and the curse of morphological and functional heterogeneity," *European Journal of Immunology*, vol. 40, no. 11, pp. 2969–2975, 2010.

[283] K. Li, H. Shi, B. Zhang, X. Ou, Q. Ma, Y. Chen, P. Shu, D. Li, and Y. Wang, "Myeloid-derived suppressor cells as immunosuppressive regulators and therapeutic targets in cancer," *Signal Transduction and Targeted Therapy*, vol. 6, no. 1, pp. 362–362, 2021.

[284] R. Sun and A. H. Kim, "The multifaceted mechanisms of malignant glioblastoma progression and clinical implications," *Cancer and Metastasis Reviews*, vol. 41, no. 4, pp. 871–898, 2022.

[285] J. Erbani, M. Boon, and L. Akkari, "Therapy-induced shaping of the glioblastoma microenvironment: Macrophages at play," in *Seminars in Cancer Biology*, Elsevier, 2022.

[286] X. Jiang, J. Wang, X. Deng, F. Xiong, J. Ge, B. Xiang, X. Wu, J. Ma, M. Zhou, X. Li, *et al.*, "Role of the tumor microenvironment in pd-l1/pd-1-mediated tumor immune escape," *Molecular Cancer*, vol. 18, no. 1, pp. 1–17, 2019.

[287] A. J. West, V. Tsui, S. S. Stylli, H. Nguyen, A. P. Morokoff, A. H. Kaye, and R. B. Luwor, "The role of interleukin-6-stat3 signalling in glioblastoma," *Oncology Letters*, vol. 16, no. 4, pp. 4095–4104, 2018.

[288] M. Groblewska and B. Mroczko, "Pro-and antiangiogenic factors in gliomas: Implications for novel therapeutic possibilities," *International Journal of Molecular Sciences*, vol. 22, no. 11, pp. 6126–6126, 2021.

[289] J. Han, C. A. Alvarez-Breckenridge, Q.-E. Wang, and J. Yu, "Tgf-β signaling and its targeting for glioma treatment," *American Journal of Cancer Research*, vol. 5, no. 3, pp. 945–945, 2015.

[290] G. K. Gray, B. C. McFarland, S. E. Nozell, and E. N. Benveniste, "Nf-κb and stat3 in glioblastoma: therapeutic targets coming of age," *Expert Review of Neurotherapeutics*, vol. 14, no. 11, pp. 1293–1306, 2014.

[291] S. Raffaele, M. Lombardi, C. Verderio, and M. Fumagalli, "Tnf production and release from microglia via extracellular vesicles: impact on brain functions," *Cells*, vol. 9, no. 10, pp. 2145–2145, 2020.

[292] Y. Jiang, J. Zhou, J. Zhao, D. Hou, H. Zhang, L. Li, D. Zou, J. Hu, Y. Zhang, and Z. Jing, "Mir-18a downregulated rora inhibits the proliferation and tumorigenesis of glioma through tnf-α-mediated nf-κb signaling pathway," *Available at SSRN 3466978*, 2019.

[293] T.-X. Xie, Z. Xia, N. Zhang, W. Gong, and S. Huang, "Constitutive nf-κb activity regulates the expression of vegf and il-8 and tumor angiogenesis of human glioblastoma," *Oncology reports*, vol. 23, no. 3, pp. 725–732, 2010.

[294] L. Hai, C. Zhang, T. Li, X. Zhou, B. Liu, S. Li, M. Zhu, Y. Lin, S. Yu, K. Zhang, *et al.*, "Notch1 is a prognostic factor that is distinctly activated in the classical and proneural subtype of glioblastoma and that promotes glioma cell survival via the nf-κb (p65) pathway," *Cell Death & Disease*, vol. 9, no. 2, pp. 158–158, 2018.

[295] M. K. Shanmugam, A. P. Kumar, B. K. Tan, and G. Sethi, "Role of nf-κb in tumorigenesis," *Onco Therapeutics*, vol. 4, no. 2, 2013.

[296] T. Yan, Y. Tan, G. Deng, Z. Sun, B. Liu, Y. Wang, F. Yuan, Q. Sun, P. Hu, L. Gao, *et al.*, "Tgf-β induces gbm mesenchymal transition through upregulation of cldn4 and nuclear translocation to activate tnf-α/nf-κb signal pathway," *Cell Death & Disease*, vol. 13, no. 4, pp. 339–339, 2022.

[297] E. Malchinkhuu, K. Sato, T. Muraki, K. Ishikawa, A. Kuwabara, and F. Okajima, "Assessment of the role of sphingosine 1-phosphate and its receptors

in high-density lipoprotein-induced stimulation of astroglial cell function," *Biochemical Journal*, vol. 370, no. 3, pp. 817–827, 2003.

[298] S. Wang, Y. Meng, C. Li, M. Qian, and R. Huang, "Receptor-mediated drug delivery systems targeting to glioma," *Nanomaterials*, vol. 6, no. 1, pp. 3–3, 2015.

[299] D. Yin, G. Jin, H. He, W. Zhou, Z. Fan, C. Gong, J. Zhao, and H. Xiong, "Celecoxib reverses the glioblastoma chemo-resistance to temozolomide through mitochondrial metabolism," *Aging (Albany NY)*, vol. 13, no. 17, pp. 21268–21268, 2021.

[300] E. Kaduševičius, "Novel applications of nsaids: Insight and future perspectives in cardiovascular, neurodegenerative, diabetes and cancer disease therapy," *International Journal of Molecular Sciences*, vol. 22, no. 12, pp. 6637–6637, 2021.

[301] A. Kardosh, M. Blumenthal, W. J. Wang, T. C. Chen, and A. H. Schonthal, "Differential effects of selective cox-2 inhibitors on cell cycle regulation and proliferation of glioblastoma cell lines," *Cancer Biology & Therapy*, vol. 3, no. 1, pp. 55–62, 2004.

[302] G. R. Sareddy, K. Geeviman, C. Ramulu, and P. P. Babu, "The nonsteroidal anti-inflammatory drug celecoxib suppresses the growth and induces apoptosis of human glioblastoma cells via the nf-κb pathway," *Journal of Neuro-oncology*, vol. 106, pp. 99–109, 2012.

[303] G. R. Sareddy, D. Kesanakurti, P. B. Kirti, and P. P. Babu, "Nonsteroidal anti-inflammatory drugs diclofenac and celecoxib attenuates wnt/β-catenin/tcf signaling pathway in human glioblastoma cells," *Neurochemical Research*, vol. 38, pp. 2313–2322, 2013.

[304] J. Qiu, Z. Shi, and J. Jiang, "Cyclooxygenase-2 in glioblastoma multiforme," *Drug Discovery Today*, vol. 22, no. 1, pp. 148–156, 2017.

[305] M. Penas-Prado, K. R. Hess, M. J. Fisch, L. W. Lagrone, M. D. Groves, V. A. Levin, J. F. De Groot, V. K. Puduvalli, H. Colman, G. Volas-Redd, *et al.*,

"Randomized phase ii adjuvant factorial study of dose-dense temozolomide alone and in combination with isotretinoin, celecoxib, and/or thalidomide for glioblastoma," *Neuro-oncology*, vol. 17, no. 2, pp. 266–273, 2015.

[306] A. Buonfiglioli and D. Hambardzumyan, "Macrophages and microglia: The cerberus of glioblastoma," *Acta Neuropathologica Communications*, vol. 9, no. 1, pp. 1–21, 2021.

[307] R. Al-Kharboosh, K. ReFaey, M. Lara-Velazquez, S. S. Grewal, J. Imitola, and A. Quiñones-Hinojosa, "Inflammatory mediators in glioma microenvironment play a dual role in gliomagenesis and mesenchymal stem cell homing: implication for cellular therapy," *Mayo Clinic Proceedings: Innovations, Quality & Outcomes*, vol. 4, no. 4, pp. 443–459, 2020.

[308] T. Sasayama, K. Tanaka, T. Hori, M. Nishihara, M. Maeyama, S. Nakamizo, H. Tanaka, and E. Kohmura, "Tmic-40. interleukin-6 in cerebrospinal fluid as a prognostic marker for glioblastoma patients," *Neuro-oncology*, 2018.

[309] S. Singh, D. Anshita, and V. Ravichandiran, "Mcp-1: Function, regulation, and involvement in disease," *International Immunopharmacology*, vol. 101, pp. 107598–107598, 2021.

[310] A. S. Basheer, F. Abas, I. Othman, and R. Naidu, "Role of inflammatory mediators, macrophages, and neutrophils in glioma maintenance and progression: mechanistic understanding and potential therapeutic applications," *Cancers*, vol. 13, no. 16, p. 4226, 2021.

[311] I. Ushach and A. Zlotnik, "Biological role of granulocyte macrophage colony-stimulating factor (gm-csf) and macrophage colony-stimulating factor (m-csf) on cells of the myeloid lineage," *Journal of Leucocyte Biology*, vol. 100, no. 3, pp. 481–489, 2016.

[312] G. Wang, K. Zhong, Z. Wang, Z. Zhang, X. Tang, A. Tong, and L. Zhou, "Tumor-associated microglia and macrophages in glioblastoma: From basic insights to therapeutic opportunities," *Frontiers in Immunology*, vol. 13, 2022.

[313] S. A. Richard, "The pivotal immunoregulatory functions of microglia and macrophages in glioma pathogenesis and therapy," *Journal of Oncology*, vol. 2022, 2022.

[314] K. Abou-El-Ardat, M. Seifert, K. Becker, S. Eisenreich, M. Lehmann, K. Hackmann, A. Rump, G. Meijer, B. Carvalho, A. Temme, *et al.*, "Comprehensive molecular characterization of multifocal glioblastoma proves its monoclonal origin and reveals novel insights into clonal evolution and heterogeneity of glioblastomas," *Neuro-oncology*, vol. 19, no. 4, pp. 546–557, 2017.

[315] A. C. Stan, G. F. Walter, K. Welte, B. Schneider, C. A. Bona, and T. Pietsch, "Expression of granulocyte colony-stimulating factor in recurrent glial tumors is inversely correlated with tumor progression," *Journal of Neuroimmunology*, vol. 94, no. 1-2, pp. 66–73, 1999.

[316] J. Wang, L. Yao, S. Zhao, X. Zhang, J. Yin, Y. Zhang, X. Chen, M. Gao, E.-A. Ling, A. Hao, *et al.*, "Granulocyte-colony stimulating factor promotes proliferation, migration and invasion in glioma cells," *Cancer Biology & Therapy*, vol. 13, no. 6, pp. 389–400, 2012.

[317] R. Q. Hintzen, J. Voormolen, P. Sonneveld, and S. G. van Duinen, "Glioblastoma causing granulocytosis by secretion of granulocyte-colony-stimulating factor," *Neurology*, vol. 54, no. 1, pp. 259–259, 2000.

[318] A. P. See, J. J. Parker, and A. Waziri, "The role of regulatory t cells and microglia in glioblastoma-associated immunosuppression," *Journal of Neuro-oncology*, vol. 123, pp. 405–412, 2015.

[319] P. Jeannin, L. Paolini, C. Adam, and Y. Delneste, "The roles of csf s on the functional polarization of tumor-associated macrophages," *The FEBS Journal*, vol. 285, no. 4, pp. 680–699, 2018.

[320] W. Fu, G. Zhu, L. Xu, J. Liu, X. Han, J. Wang, X. Wang, J. Hou, H. Zhao, and H. Zhong, "G-csf upregulates the expression of aquaporin-9 through

cebpb to enhance the cytotoxic activity of arsenic trioxide to acute myeloid leukemia cells," *Cancer Cell International*, vol. 22, no. 1, pp. 195–195, 2022.

[321] I. Crespo, A. L. Vital, M. Gonzalez-Tablas, M. del Carmen Patino, A. Otero, M. C. Lopes, C. de Oliveira, P. Domingues, A. Orfao, and M. D. Tabernero, "Molecular and genomic alterations in glioblastoma multiforme," *The American Journal of Pathology*, vol. 185, no. 7, pp. 1820–1833, 2015.

[322] F. Rücker, A. Russ, S. Cocciardi, H. Kett, R. Schlenk, U. Botzenhardt, C. Langer, J. Krauter, S. Fröhling, B. Schlegelberger, *et al.*, "Altered mirna and gene expression in acute myeloid leukemia with complex karyotype identify networks of prognostic relevance," *Leukemia*, vol. 27, no. 2, pp. 353–361, 2013.

[323] Y. Komohara, M. Jinushi, and M. Takeya, "Clinical significance of macrophage heterogeneity in human malignant tumors," *Cancer Science*, vol. 105, no. 1, pp. 1–8, 2014.

[324] B. Yan, J.-J. Wei, Y. Yuan, R. Sun, D. Li, J. Luo, S.-J. Liao, Y.-H. Zhou, Y. Shu, Q. Wang, *et al.*, "Il-6 cooperates with g-csf to induce protumor function of neutrophils in bone marrow by enhancing stat3 activation," *The Journal of Immunology*, vol. 190, no. 11, pp. 5882–5893, 2013.

[325] F. Skoulidis, L. A. Byers, L. Diao, V. A. Papadimitrakopoulou, P. Tong, J. Izzo, C. Behrens, H. Kadara, E. R. Parra, J. R. Canales, *et al.*, "Co-occurring genomic alterations define major subsets of kras-mutant lung adenocarcinoma with distinct biology, immune profiles, and therapeutic vulnerabilitiesco-occurring genomic alterations define kras subgroups," *Cancer Discovery*, vol. 5, no. 8, pp. 860–877, 2015.

[326] A. Heidari, P. M. Sharif, and N. Rezaei, "The association between tumor-associated macrophages and glioblastoma: a potential target for therapy," *Current Pharmaceutical Design*, vol. 27, no. 46, pp. 4650–4662, 2021.

[327] G. Kohanbash, K. McKaveney, M. Sakaki, R. Ueda, A. H. Mintz, N. Amankulor, M. Fujita, J. R. Ohlfest, and H. Okada, "Gm-csf promotes

the immunosuppressive activity of glioma-infiltrating myeloid cells through interleukin-4 receptor-αil-4rα+ suppressive myeloid cells in gliomas," *Cancer Research*, vol. 73, no. 21, pp. 6413–6423, 2013.

[328] A. Herrero-Cervera, O. Soehnlein, and E. Kenne, "Neutrophils in chronic inflammatory diseases," *Cellular & Molecular Immunology*, vol. 19, no. 2, pp. 177–191, 2022.

[329] P. Hofman, "Molecular regulation of neutrophil apoptosis and potential targets for therapeutic strategy against the inflammatory process," *Current Drug Targets-Inflammation & Allergy*, vol. 3, no. 1, pp. 1–9, 2004.

[330] W.-R. Schabitz, R. Kollmar, M. Schwaninger, E. Juettler, J. Bardutzky, M. Scholzke, C. Sommer, and S. Schwab, "Neuroprotective effect of granulocyte colony–stimulating factor after focal cerebral ischemia," *Stroke*, vol. 34, no. 3, pp. 745–751, 2003.

[331] A. Theyab, K. F. Alsharif, K. J. Alzahrani, A. A. A. Oyouni, Y. M. Hawsawi, M. Algahtani, S. Alghamdi, and A. F. Alshammary, "New insight into strategies used to develop long-acting g-csf biologics for neutropenia therapy," *Frontiers in Oncology*, vol. 12, 2022.

[332] B. E. Oyinloye, A. F. Adenowo, and A. P. Kappo, "Reactive oxygen species, apoptosis, antimicrobial peptides and human inflammatory diseases," *Pharmaceuticals*, vol. 8, no. 2, pp. 151–175, 2015.

[333] Z. Norouzi, A. Salimi, R. Halabian, and H. Fahimi, "Nisin, a potent bacteriocin and anti-bacterial peptide, attenuates expression of metastatic genes in colorectal cancer cell lines," *Microbial Pathogenesis*, vol. 123, pp. 183–189, 2018.

[334] V. Patil, J. Pal, and K. Somasundaram, "Elucidating the cancer-specific genetic alteration spectrum of glioblastoma derived cell lines from whole exome and rna sequencing," *Oncotarget*, vol. 6, no. 41, pp. 43452–43452, 2015.

[335] G. Carrabba, D. Mukhopadhyay, and A. Guha, "Aberrant signalling complexes in gbms: prognostic and therapeutic implications," *Glioblastoma: Molecular Mechanisms of Pathogenesis and Current Therapeutic Strategies*, pp. 95–129, 2010.

[336] H. Ohgaki and P. Kleihues, "Genetic pathways to primary and secondary glioblastoma," *The American Journal of Pathology*, vol. 170, no. 5, pp. 1445–1453, 2007.

[337] T. M. Malta, C. F. de Souza, T. S. Sabedot, T. C. Silva, M. S. Mosella, S. N. Kalkanis, J. Snyder, A. V. B. Castro, and H. Noushmehr, "Glioma cpg island methylator phenotype (g-cimp): biological and clinical implications," *Neuro-oncology*, vol. 20, no. 5, pp. 608–620, 2018.

[338] M. Martini, M. C. De Santis, L. Braccini, F. Gulluni, and E. Hirsch, "Pi3k/akt signaling pathway and cancer: an updated review," *Annals of Medicine*, vol. 46, no. 6, pp. 372–383, 2014.

[339] F. A. Karreth, Y. Tay, D. Perna, U. Ala, S. M. Tan, A. G. Rust, G. DeNicola, K. A. Webster, D. Weiss, P. A. Perez-Mancera, *et al.*, "In vivo identification of tumor-suppressive pten cernas in an oncogenic braf-induced mouse model of melanoma," *Cell*, vol. 147, no. 2, pp. 382–395, 2011.

[340] Z. An, O. Aksoy, T. Zheng, Q.-W. Fan, and W. A. Weiss, "Epidermal growth factor receptor and egfrviii in glioblastoma: signaling pathways and targeted therapies," *Oncogene*, vol. 37, no. 12, pp. 1561–1575, 2018.

[341] J. L. Nakamura, "The epidermal growth factor receptor in malignant gliomas: pathogenesis and therapeutic implications," *Expert Opinion on Therapeutic Targets*, vol. 11, no. 4, pp. 463–472, 2007.

[342] O. O. Kanu, B. Hughes, C. Di, N. Lin, J. Fu, D. D. Bigner, H. Yan, and C. Adamson, "Glioblastoma multiforme oncogenomics and signaling pathways," *Clinical Medicine. Oncology*, vol. 3, pp. CMO–S1008, 2009.

[343] G. F. Reis, M. Pekmezci, H. M. Hansen, T. Rice, R. E. Marshall, A. M. Molinaro, J. J. Phillips, H. Vogel, J. K. Wiencke, M. R. Wrensch, *et al.*, "Cdkn2a

loss is associated with shortened overall survival in lower-grade (world health organization grades ii–iii) astrocytomas," *Journal of Neuropathology & Experimental Neurology*, vol. 74, no. 5, pp. 442–452, 2015.

[344] A. Petitjean, E. Mathe, S. Kato, C. Ishioka, S. V. Tavtigian, P. Hainaut, and M. Olivier, "Impact of mutant p53 functional properties on tp53 mutation patterns and tumor phenotype: lessons from recent developments in the iarc tp53 database," *Human Mutation*, vol. 28, no. 6, pp. 622–629, 2007.

[345] K. Holand, F. Salm, and A. Arcaro, "The phosphoinositide 3-kinase signaling pathway as a therapeutic target in grade iv brain tumors," *Current Cancer Drug Targets*, vol. 11, no. 8, pp. 894–918, 2011.

[346] G. M. Gibbs, K. Roelants, and M. K. O'bryan, "The cap superfamily: cysteine-rich secretory proteins, antigen 5, and pathogenesis-related 1 proteins—roles in reproduction, cancer, and immune defense," *Endocrine Reviews*, vol. 29, no. 7, pp. 865–897, 2008.

[347] Y. Yao, X. Cai, F. Ren, Y. Ye, F. Wang, C. Zheng, Y. Qian, and M. Zhang, "The macrophage-osteoclast axis in osteoimmunity and osteo-related diseases," *Frontiers in Immunology*, vol. 12, p. 664871, 2021.

[348] J. V. Joseph, V. Balasubramaniyan, A. Walenkamp, and F. A. Kruyt, "Tgf-β as a therapeutic target in high grade gliomas–promises and challenges," *Biochemical Pharmacology*, vol. 85, no. 4, pp. 478–485, 2013.

[349] J. V. Joseph, C. R. Magaut, S. Storevik, L. H. Geraldo, T. Mathivet, M. A. Latif, J. Rudewicz, J. Guyon, M. Gambaretti, F. Haukas, *et al.*, "Tgf-β promotes microtube formation in glioblastoma through thrombospondin 1," *Neuro-oncology*, vol. 24, no. 4, pp. 541–553, 2022.

[350] S. Darmanis, S. A. Sloan, D. Croote, M. Mignardi, S. Chernikova, P. Samghababi, Y. Zhang, N. Neff, M. Kowarsky, C. Caneda, *et al.*, "Single-cell rna-seq analysis of infiltrating neoplastic cells at the migrating front of human glioblastoma," *Cell Reports*, vol. 21, no. 5, pp. 1399–1410, 2017.

[351] H. K. Gan, A. H. Kaye, and R. B. Luwor, "The egfrviii variant in glioblastoma multiforme," *Journal of Clinical Neuroscience*, vol. 16, no. 6, pp. 748–754, 2009.

[352] V. Shah and J. Shah, "Recent trends in targeting mirnas for cancer therapy," *Journal of Pharmacy and Pharmacology*, vol. 72, no. 12, pp. 1732–1749, 2020.

[353] I. Solaroglu, T. Tsubokawa, J. Cahill, and J. H. Zhang, "Anti-apoptotic effect of granulocyte-colony stimulating factor after focal cerebral ischemia in the rat," *Neuroscience*, vol. 143, no. 4, pp. 965–974, 2006.

[354] A. Theyab, K. F. Alsharif, K. J. Alzahrani, A. A. A. Oyouni, Y. M. Hawsawi, M. Algahtani, S. Alghamdi, and A. F. Alshammary, "New insight into strategies used to develop long-acting g-csf biologics for neutropenia therapy," *Frontiers in Oncology*, vol. 12, pp. 1026377–1026377, 2023.

[355] B. E. Oyinloye, A. F. Adenowo, and A. P. Kappo, "Reactive oxygen species, apoptosis, antimicrobial peptides and human inflammatory diseases," *Pharmaceuticals*, vol. 8, no. 2, pp. 151–175, 2015.

[356] Z. Norouzi, A. Salimi, R. Halabian, and H. Fahimi, "Nisin, a potent bacteriocin and anti-bacterial peptide, attenuates expression of metastatic genes in colorectal cancer cell lines," *Microbial Pathogenesis*, vol. 123, pp. 183–189, 2018.